



HAL
open science

Omics of human plasma lipoproteins : role in cardiometabolic diseases

Emil Zakiev

► **To cite this version:**

Emil Zakiev. Omics of human plasma lipoproteins : role in cardiometabolic diseases. Human health and pathology. Sorbonne Université, 2019. English. NNT : 2019SORUS436 . tel-03001290

HAL Id: tel-03001290

<https://theses.hal.science/tel-03001290>

Submitted on 12 Nov 2020

HAL is a multi-disciplinary open access archive for the deposit and dissemination of scientific research documents, whether they are published or not. The documents may come from teaching and research institutions in France or abroad, or from public or private research centers.

L'archive ouverte pluridisciplinaire **HAL**, est destinée au dépôt et à la diffusion de documents scientifiques de niveau recherche, publiés ou non, émanant des établissements d'enseignement et de recherche français ou étrangers, des laboratoires publics ou privés.

Sorbonne Université

Ecole Doctorale Physiologie, Physiopathologie et Thérapeutique (ED394)

INSERM-UMR-S 1166/Equipe 4

Omics of human plasma lipoproteins: Role in cardiometabolic diseases

Par Emile ZAKIEV

Thèse de Doctorat de Physiopathologie

Dirigée par Dr. Anatol KONTUSH

Présentée et soutenue publiquement le 28 Juin 2019

Devant un jury composé de :

Dr. Philippe LESNIK	Directeur de Recherche INSERM Sorbonne Université	Président du Jury
Dr. Anne NEGRE-SALVAYRE	Directeur de Recherche CNRS Université Toulouse III	Rapporteur
Prof. Dominique BONNEFONT-ROUSSELOT	PU-PH de l'Hôpital Pitié Salpêtrière Université Paris Descartes - Paris 5	Rapporteur
Dr. Mikael CROYAL	Ingénieur d'études Université de Nantes	Examineur
Dr. Boris HANSEL	MCU-PH de l'Hôpital Bichat - Claude Bernard Université Paris Diderot – USPC	Examineur
Dr. Anatol KONTUSH	Directeur de Recherche INSERM Sorbonne Université	Directeur de thèse



TABLE OF CONTENTS

ACKNOWLEDGMENTS	1
LIST OF ABBREVIATIONS	5
RESUME	8
ABSTRACT	11
INTRODUCTION.....	14
1. Introduction to lipoproteins	14
1.1 LDL	16
1.2 HDL	16
1.3 Other lipoprotein classes	17
2. Epidemiology of lipoproteins	18
2.1 LDL	18
2.2 HDL	19
2.3 Other lipoprotein classes	20
3. HDL.....	20
3.1 Structure	20
3.2 Composition.....	22
3.2.1 Classic techniques	22
3.2.2 Omics approaches	24
3.2.2.1 Proteome	25
3.2.2.2 Lipidome	27
3.2.2.3 Glycome	31
3.3 Heterogeneity.....	31
3.4 Metabolism	35
3.4.1 Biosynthesis	35
3.4.2 Remodelling	36
3.4.3 Catabolism	36
3.5 Biological activities and structure-function relationships	37
3.6 Dysfunctional HDL	41
3.6.1 Cardiometabolic diseases and atherosclerosis.....	41
3.6.2 Altered composition and impaired biological function.....	43
3.6.3 Altered metabolism.....	45
3.7 Therapeutic targeting of abnormal HDL metabolism	45
3.7.1 CETP inhibition	45
3.7.2 rHDL infusion	46

3.7.3	LPL activation	48
3.7.4	Nicotinic acid	49
3.7.5.	Other agents	50
4.	LDL	51
4.1	Structure and composition	51
4.1.1	Proteome	51
4.1.2	Lipidome	52
4.1.3	Glycome	52
4.2	Metabolism	52
4.2.1	Biosynthesis	52
4.2.2	Catabolism	54
4.3	Altered composition and metabolism in cardiometabolic diseases	54
4.4	Therapeutic targeting of abnormal LDL metabolism	56
	WORKING HYPOTHESIS AND OBJECTIVE	59
	METHODS	61
1.	Subjects	61
2.	Blood samples	62
3.	Isolation of lipoproteins	62
4.	Chemical analysis of lipoproteins	64
5.	Heterogeneity and mean size of HDL	64
6.	Lipidomic analysis	65
6.1	Lipid standards	66
6.2	Lipid extraction	67
6.3	LC/MS analysis	68
6.4	Quantification	68
6.5	Sphingosine-1-phosphate	69
7.	Glycomic analysis	70
8.	Functional assays	71
8.1	Cholesterol efflux	72
8.2	Antioxidative activity of HDL	72
8.3	Anti-apoptotic activity of HDL	74
8.4	Cellular cholesterol accumulation induced by LDL	74
9.	Statistical analysis	75
	RESULTS	79
1.	HDL lipidome and functionality in normolipidemic controls	79

1.1 Lipidome	79
1.2 Function	83
2. HDL lipidome and functionality in cardiometabolic diseases	83
2.1 Familial apoA-I deficiency	83
2.1.1. Abundances of individual lipid species	85
2.1.2. PCA	92
2.1.3. Heatmaps	92
2.1.4. Bubble plots	92
2.1.5. Structural plots.....	96
2.1.6. Network analysis	100
2.1.7. Metabolic pathways affected by apoA-I deficiency.....	105
2.1.8. Lipid-related genes affected by apoA-I deficiency	105
2.2 ST-elevated myocardial infarction	108
2.2.1. Characteristics of subjects and overall abundances of lipid classes and species.....	108
2.2.2. PCA	116
2.2.3. Heatmaps	116
2.2.4. Bubble plots.....	116
2.2.5. Structural plots.....	117
2.2.6. Network maps.....	123
2.2.7. Metabolic pathways affected by STEMI.....	126
3. HDL and LDL glycome in normolipidemic controls	127
3.1. Glycomic profiling of LDL and HDL	127
3.2. Role of glycome in biological activities of lipoproteins	135
3.2.1. Cholesterol efflux capacity of HDL	135
3.2.2. Cellular cholesteryl ester accumulation induced by LDL	136
3.2.3. Heterogeneity, mean size and LCAT activity of HDL	137
3.2.4. Relationships between the glycome and biological properties of LDL & HDL...	138
DISCUSSION AND CONCLUSIONS	142
1. Lipidome of normolipidemic HDL particles	142
2. Lipidome of HDL particles in CMD.....	145
2.1 Lipidome of HDL particles isolated from apoA-I-deficient patients	145
2.2. Lipidome of HDL particles isolated from STEMI patients.....	150
3. Glycome of normolipidemic HDL and LDL	154
4. General conclusions	158
REFERENCES.....	162

ACKNOWLEDGMENTS

My PhD project has been developed at the UMRS 1166 Research Unit of the French National Institute for Health and Medical Research (INSERM) and the University of Sorbonne (Doctoral School ED394 "Physiology, physiopathology and therapeutic"). Here I would like to acknowledge people who have supported me during this process.

First, I would like to express my sincere gratitude towards my supervisor, Dr. Anatol Kontush, a persistent and rigorous scientist with an unrivaled expertise in his field. His optimism, practicality and wisdom saved the day for me for too many times to count. Without his constant support I would certainly have not been able to finish this project. He taught me all the intricacies of being a scientist in a modern world – a knowledge not to be underestimated. I am profoundly grateful for his kindness for giving me the opportunity to perform my PhD in his team.

I would also like to thank Dr. Isabelle Guillas-Baudouin, who is an honored professional in her field, humble, energetic and appealing. Isabelle was always there when I needed help, be it a theoretical or a practical question, even if she was extremely busy with her own research or teaching. Her mere presence was comforting; during my project her advices were often stalemate-breaking.

I would also like to thank Dr. Maryam Darabi-Amin, with whom we became good friends, and who also helped me with my project considerably. She was always helpful in my project even though, being a postdoc at the time, she had a lot of other important things to do.

During these years, I also befriended another PhD student, now Dr. Feng Ma, and I thank him for his constant moral support and good company. I will remember our giggles during lunch breaks and those good times spent together during the free time of scientific conferences.

I owe Mr. Vasily Sukhorukov and Ms. Emilie Tubeuf a debt of gratitude for teaching me how to perform the experiments the first time when I came to the lab, it was a really nice memory of their careful guidance. Dr. Eric Frisdal and Dr. Wilfried Le Goff were always there to teach me the lab techniques as well, and I am sincerely grateful to them too.

I would like to thank Dr. Marie Lhomme and Dr. Fabiana Rached for helping me to perform the measurements in the lipidomics. I am also grateful for substantial support from Professors Raul Santos and Carlos Serrano from the University of Sao Paulo, Professor Gordan Lauc and Dr. Maja Pučić Baković and Dr. Ivan Gudelj from the University of Zagreb, and Professor Patrice Therond from the Hospital of Le Kremlin-Bicetre. Without their input, my thesis would not have happened.

Many thanks to all the members of Teams 4 and 5 of UMRS 1166. I would like to thank all the scientists in the team, especially Dr. Philippe Lesnik, Dr. Maryse Guerin, Dr. Philippe Couvert, Dr. Thierry Huby, Dr. Emmanuel Gautier and Ms. Martine Moreau for their help and constructive criticism in the development of my project.

I would equally like to express my gratitude to the members of my thesis committee, Dr. Philippe Lesnik, Dr. Anne Negre-Salvayre, Prof. Dominique Bonnefont-Rousselot, Dr. Boris

Hansel and Dr. Mikael Croyal, whose helpful participation was essential for this project to become fruitful.

I send my special thanks to Mme Severine Lowinski, Dr. Isabelle Cremer and Dr. Catherine Monnot of the Doctoral School ED394 for their constant support and care. Also big thanks to the secretary staff of our department, especially to Mme Natalie Abiola, Mme Olga Nobel, Mme Roberte Le-Galleu, Mme Angelique Riquelme, and Mme Martine Duquesne for their constant work on making our work possible.

Furthermore, I would like to acknowledge the financial support which was provided by the Ministry of Foreign Affairs of the French Republic (Vernadski scholarship) and support provided by the Institute for Atherosclerosis Research, Skolkovo, and its director, Prof. Alexander Orekhov. Thanks to these means of support I was able to do my project in France. Our team also gratefully acknowledges continuous financial support from French National Institute for Health and Medical Research (INSERM).

I would like to conclude with thanking one special person for her continuous support and endless love. I am deeply grateful to her for enduring my whims. She would always make me believe in myself when I felt like the world had me down on my knees and support me in every crucial decision in my life. "Behind every great man, there is a great woman", they say. While I certainly have not achieved grandiosity by any means, I would not be even at this level without the Great Woman of My Life - Adele.

Finally, I would also like to express my gratitude to my lovely parents Roustem and Dilyara,

to my dear sister Galiya, to my kind cousins Renat and Nailya, to my cool uncle Ildar, and to my awesome grandparents Mirfatyh and Elena for their unconditional love and support in good and hard times during my sometimes-stormy PhD process.

LIST OF ABBREVIATIONS

A

A1AT	α 1-antitrypsin
AAPH	Azo-initiator 2,2'-azo-bis-(2-amidinopropane) hydrochloride
ABCA1	ATP binding cassette transporter A1
ABCG1	ATP binding cassette transporter G1
ACN	Acetonitrile
ACS	Acute Coronary Syndrome
AMI	Acute myocardial infarction
ApoA	Apolipoprotein A
ApoB	Apolipoprotein B
ApoC	Apolipoprotein C
ApoD	Apolipoprotein D
ApoE	Apolipoprotein E
ApoF	Apolipoprotein F
ApoJ	Apolipoprotein J
ApoL	Apolipoprotein L
ApoM	Apolipoprotein M

B

BET	Bromodomain and extra-terminal domain
-----	---------------------------------------

C

CAD	Coronary artery disease
CCHS	Copenhagen City Heart Study
CDS	Phosphatidate cytidiltransferase
CE	Cholesteryl ester
Cer	Ceramide
CETP	Cholesteryl ester transfer protein
CM	Chylomicron
CMD	Cardiometabolic disease
CHD	Coronary heart disease
CVD	Cardiovascular disease

D

E

EDTA	Ethylenediaminetetraacetic acid
EL	Endothelial lipase
eNOS	Endothelial nitric oxide synthase
ER	Endoplasmic reticulum

F

FA	Formic acid
FAID	Familial apoA-I deficiency
FC	Free cholesterol
FDR	False discovery rate
FH	Familial hypercholesterolemia
FXR	Farnesoid X receptor

G	GC	Gas chromatography
	GLTP	Glycolipid Transfer Protein
	GP	Glycerophospholipid
H	HDL	High-density lipoprotein
	HDL-C	High-density lipoprotein-cholesterol
	HILIC-SPE	hydrophilic interaction liquid chromatography solid-phase extraction
	HILIC-UHPLC-FLD	Hydrophilic-interaction ultra-high-performance liquid chromatography with fluorescence detection
	HPLC	High-performance liquid chromatography
	HL	Hepatic lipase
	hsCRP	High-sensitivity C-reactive protein
	HUVEC	Human umbilical vein endothelial cells
	I	ICAM-1
IDL		Intermediate-density lipoprotein
L	LA	Linoleic acid
	lbLDL	Large buoyant LDL
	LC	Liquid chromatography
	LC-MS	Liquid chromatography – mass spectrometry
	LC/MS/MS	Liquid chromatography–tandem MS
	LC-ESI-MS/MS	Liquid chromatography–electrospray ionization–tandem MS
	LCAT	Lecithin-cholesterol acyltransferase
	LDL	Low-density lipoprotein
	LDL-C	Low-density lipoprotein-cholesterol
	LDLR	Low-density lipoprotein receptor
	Lp(a)	Lipoprotein(a)
	LpA-I	apoA-I-containing particle
	LpA-I:A-II	apoA-I- and apoA-II-containing particle
	LPC	Lysophosphatidylcholine
	LPL	Lipoprotein lipase
	LpPLA2	Lipoprotein-associated phospholipase A2
	LPS	Lipopolysaccharide
	LRP1	LPLR-related protein-1
	LXR	Liver X receptor
M	MALDI-TOF-MS	Matrix-assisted laser desorption ionization time-of-flight MS
	MI	Myocardial infarction
	miRNAs, miR	MicroRNAs
	MPO	Myeloperoxidase
	MS	Mass-spectrometry
N	NO	Nitric oxide
	NMR	Nuclear magnetic resonance
P		

	PA	Phosphatidic acid
	PAF-AH	Platelet-activating factor-acetyl hydrolase
	PBS	Phosphate-buffered saline
	PC	Phosphatidylcholine
	PCA	Principal component analysis
	PCSK7/9	Proprotein convertase subtilisin/kexin type 7/9
	PE	Phosphatidylethanolamine
	PG	Phosphatidylglycerol
	PGI ₂	Prostacyclin
	PI	Phosphatidylinositol
	PI3K	Phosphatidylinositol 3-kinase
	PL	Phospholipid
	PLOOH	Phospholipid hydroperoxide
	PLA2G1B	Group IB Phospholipase 2
	PLTP	Phospholipid transfer protein
	PNGase F	Peptide:N-glycosidase F
	PON1	Paraoxonase 1
	PPAR α	Peroxisome proliferator-activated receptor α
	PS	Phosphatidylserine
R		
	RCT	Reverse cholesterol transport
	rHDL	Reconstituted HDL
	RXR	Retinoid X receptor
S		
	S1P	Sphingosine-1-phosphate
	SAA	Serum amyloid A
	sdLDL	Small dense LDL
	SM	Sphingomyelin
	SL	Sphingolipid
	SNPs	Single-nucleotide polymorphisms
	sPLA ₂	Secretory phospholipase A2
	SR-B1	Scavenger receptor class B type 1
	STEMI	ST-segment elevation myocardial infarction
T		
	T2D	Type 2 diabetes
	TC	Total cholesterol
	TG	Triglyceride
	TGRL	Triglyceride-rich lipoprotein
	TOF	Time-of-flight
U		
	UC	Ultracentrifugation
V		
	VLDL	Very low-density lipoprotein
	VLDLR	VLDL-receptor

RESUME

Omics vise à la caractérisation et à la quantification collectives de pools de molécules biologiques qui traduisent notre compréhension de la structure et de la fonction d'un organisme ou d'une partie de celui-ci. Les lipoprotéines plasmatiques humaines jouent un rôle important dans le développement de la résistance à l'insuline, de la dyslipidémie, de l'hypertension, de l'adiposité centrale et de maladie cardiovasculaire (MCV), le tout collectivement appelé maladie cardiometabolique (MCM). En effet, on sait que la diminution des taux de cholestérol lipoprotéine de haute densité (LHD) et l'augmentation des taux de cholestérol lipoprotéine de basse densité (LBD) sont associées à un risque accru de MCM. En dépit des succès enregistrés dans le développement de médicaments normalisant les taux de cholestérol-LBD (C-LBD), les MCM représentent toujours la majorité de morbidité et des décès dans les pays développés. Nos nouvelles tentatives de réduction du risque de MCM ne réussissent pas toujours, reflétant parmi d'autres notre méconnaissance de biologie des lipoprotéines qui inclut, comme éléments clés, la fonction biologique et les caractéristiques de composition des particules de lipoprotéine lequel les rendent distinctement indispensables pour les conditions métaboliques saines. Notre compréhension du protéome des LHD et des LBD a beaucoup progressé, alors que leur lipidome et leur glycome n'ont guère retenu l'attention de la communauté scientifique ces dernières années. Ce travail porte sur la lipidomique et la glycomique des LHD et LBD plasmatiques chez l'humain en ce qui concerne leurs fonctions biologiques chez les sujets sains et les patients atteints de MCM, comprenant déficit familial en apoA-I (DFAI) - dyslipidémie déterminée génétiquement entraînant un risque cardiovasculaire (RV) élevé, et infarctus du myocarde avec élévation du segment ST (IMEST), une présentation aiguë des MCV.

Dans la section Introduction du manuscrit, connaissances existantes sur la structure, la fonction et le métabolisme des LBD et des LHD est discuté, tout en abordant brièvement d'autres classes de lipoprotéines, avec un accent particulier sur les approches omiques. La section Méthodes décrit comment le recherche a été accompli, décrivant les méthodes de recrutement de patients, de prélèvements sanguins, d'analyses chimiques des lipoprotéines, de dosages fonctionnels, de détermination par chromatographie en phase liquide-spectrométrie de masse en tandem de la composition en lipoprotéines et d'aboutir aux méthodes statistiques utilisées. La section suivante Résultats décrit les résultats sur le lipidome des lipoprotéines chez les sujets normolipidémiques, le lipidome des lipoprotéines dans le MCM et le glycome des lipoprotéines chez les sujets normolipidémiques. Le lipidome de lipoprotéines, isolé de sujets normolipidémiques et MCM, a été caractérisé et quantifié en environ 160 espèces lipidiques individuelles, appartenant à 9 sous-classes lipidiques: la phosphatidylcholine (PC), la sphingomyéline (SM), la lysophosphatidylcholine (LPC), la phosphatidyléthanolamine (PE), le céramide (Cer), la phosphatidylsérine (PS), l'acide phosphatidique (PA) et le phosphatidylglycérol (PG). Le lipidome normolipidémique a révélé une forte hétérogénéité parmi les principales sous-populations de HDL (2b, 2a, 3a, 3b et 3c), de petites denses HDL3b et HDL3c présentant un potentiel plus élevé en termes de propriétés anti-athérogènes et enrichies en LPC, PI, PS et PA. En MCM, des perturbations du lipidome des espèces affectées par les LHD de toutes les classes de lipides. Notamment, les LHD DFAI manquaient de nombreuses espèces lipidiques polyinsaturées, telles que PC 34:2 et PC 40:8, tout en possédant des quantités accrues d'espèces saturées telles que PC 32:0 et PC 34:0, alors que IMEST LHD possédait des quantités réduites d'espèces lipidiques polyinsaturées, notamment PC 36:2 et PC 38:5, tout en possédant des quantités accrues d'espèces pro-inflammatoires lysophospholipidiques saturées, telles que LPC 16:0, LPC 18:0 et PA 32:0. Des altérations du lipidome dans le MCM ont été associées à des

voies de fonctionnement incorrect du métabolisme de l'acide linoléique et des glycérophospholipides.

Quand les glycomes des LHD et LBD normolipidémiques ont été caractérisés, plus de 17 pics chromatographiques distincts ont été identifiés, présentant une diversité élevée. Structurellement, la composition comprenait des fractions du complexe, du mannose élevé aux hybrides N-glycanes. Les fonctions biologiques des HDL, à savoir la capacité d'efflux de cholestérol cellulaire, les activités antioxydantes et anti-apoptotiques, se sont avérées diminuées dans le MCM comparativement aux témoins sains. Les lipidomes et les glycomes ont montré des associations avec les fonctions biologiques des lipoprotéines, établissant ainsi des relations structure-fonction distinctes pour les deux MCM étudiés. Le manuscrit est fini par une discussion des résultats et des conclusions générales, au cours desquelles on suppose les applications potentielles des résultats obtenus. Nous proposons notamment un concept de normalisation de la fonction LHD en les exposant à des perfusions de certains lipides qui ont montré des associations avec la fonctionnalité LHD dans nos tests.

Ces études ont été publiées dans le *Journal of Clinical Lipidology* [1] et *Biochimica et Biophysica Acta - Molecular and Cell Biology of Lipids* [2].

ABSTRACT

Omics aims at the collective characterization and quantification of pools of biological molecules that translate into our understanding of the structure and function of an organism and/or its components. Human plasma lipoproteins play important roles in the development of insulin resistance, dyslipidemia, hypertension, central adiposity and cardiovascular disease (CVD), all collectively referred to as cardiometabolic disease (CMD). Indeed, decreased levels of high-density lipoprotein (HDL)-cholesterol (HDL-C) and increased levels of low-density lipoprotein (LDL)-cholesterol (LDL-C) are known to be associated with an increased risk of CMD. Despite successes in the development of drugs normalizing LDL-C levels, CMD still account for the majority of morbidity and mortality in developed countries. Our further attempts in decreasing CMD risk do not always succeed reflecting among others our poor grasp of lipoprotein biology which includes, as key elements, biological function and compositional features of lipoprotein particles that make them distinctly indispensable for healthy metabolic conditions. Major advances have been made in our understanding of the proteome of HDL and LDL, while their lipidome and glycome has not enjoyed much attention of scientific community. This thesis focuses on lipidomics and glycomics of human plasma HDL and LDL in respect to their biological functions in healthy subjects and in patients with CMD, including familial apoA-I deficiency (FAID), a genetically determined dyslipidemia resulting in elevated cardiovascular (CV) risk, and ST-elevated myocardial infarction (STEMI), an acute presentation of CVD.

In the Introduction section of the manuscript, existing knowledge about LDL and HDL structure, function and metabolism is discussed, while briefly touching upon other lipoprotein classes, with a particular emphasis on the omics methods. The Methods section describes how this research was accomplished, detailing approaches to patient recruitment, blood sampling, chemical analysis

of lipoproteins, functional assays, liquid chromatography-tandem mass-spectrometry determination of lipoprotein composition and statistical methods employed. The following Results section describes findings on the lipidome of HDL in normolipidemic subjects, lipidome of HDL in CMD, and glycome of LDL and HDL in normolipidemic subjects. Lipidome of HDL, isolated from normolipidemic and CMD subjects, was characterized and quantified into ~160 individual lipid species belonging to 9 lipid subclasses, including phosphatidylcholine (PC), sphingomyelin (SM), lysophosphatidylcholine (LPC), phosphatidylinositol (PI), phosphatidylethanolamine (PE), ceramide (Cer), phosphatidylserine (PS), phosphatidic acid (PA), and phosphatidylglycerol (PG). Normolipidemic lipidome revealed high heterogeneity among major HDL subpopulations (2b, 2a, 3a, 3b and 3c), with small, dense HDL3b and HDL3c showing enhanced anti-atherogenic properties and being enriched in LPC, PI, PS, and PA relative to large, light HDL. In CMD, perturbations of the lipidome of HDL affected species from all lipid classes. Notably, FAID HDLs lacked numerous polyunsaturated lipid species, including PC 34:2 and PC 40:8, while possessing increased amounts of saturated species, including PC 32:0 and PC 34:0, while STEMI HDL possessed decreased amounts of polyunsaturated lipid species, including PC 36:2 and PC 38:5, while possessing increased amounts of saturated lysophospholipid pro-inflammatory species, such as LPC 16:0, LPC 18:0 and PA 32:0. Alterations of the HDL lipidome in CMD were associated with improperly functioning pathways of linoleic acid and glycerophospholipid metabolism.

When glycomes of normolipidemic HDL and LDL were characterized, more than 17 distinct moieties were identified and quantified, revealing high compositional diversity. Structurally, lipoprotein glycans varied from complex, high-mannose to hybrid N-glycans. Biological functions of HDL, namely cellular cholesterol efflux capacity, antioxidative and anti-apoptotic

activities, were found to be diminished in CMD as compared to healthy normolipidemic controls. Both lipidome and glycome revealed multiple associations with biological functions of lipoproteins, thereby establishing distinct structure-function relationships for the two CMD studied. The manuscript is completed with discussion of the results and general conclusions, suggesting potential applications of the results obtained. Notably, we propose a concept of normalizing HDL function through intravenous infusions of certain lipids that showed associations with HDL functionality in our in analysis.

These studies were published in *Journal of Clinical Lipidology* [1] and *Biochimica et Biophysica Acta - Molecular and Cell Biology of Lipids* [2].

INTRODUCTION

1. Introduction to lipoproteins

Lipids provide structural, signaling (steroid hormones), and energetic functions (bile acids, nutritional fatty acids). The structural function of lipids involves formation and sustaining of membranes, and this is important in separation of water-soluble and water-insoluble media of the human organism. Since our blood is water-based, lipids need to be compartmentalized in order to be transported through such polar milieu. Here is where lipoproteins come into play: they form micellar structures, engulfing lipids into ready-transportable “packages” with special apolipoproteins being attached to them, serving as ever-vigilant “courier”.

These packages have hydrophobic lipids, including triglyceride (TG) and cholesterol esters (CE), as their major “cargo”. The package is wrapped around with a monolayer of phospholipids (PL) and free cholesterol (FC). Proteins, primarily apolipoproteins and enzymes, serve as an all-in-one transportation company courier: they “pack” the lipids inside, ensuring their safety, and then “knock on the door” of a cell, delivering the lipid cargo to the cell, or from the cell.

Lipoproteins are distinguished by their structural, biological, chemical and physical properties. Differences in physical properties allows separating lipoproteins according to their density, charge and size. In the order of increasing density, major lipoproteins in human plasma are chylomicron (CM), very low-density lipoprotein (VLDL), intermediate-density lipoprotein (IDL), low-density lipoprotein (LDL) and high-density lipoprotein (HDL).

Table 1. Density, size, molecular weight and apolipoprotein contents of different human plasma lipoproteins [3, 4]

Lipoproteins	Density (g/ml)	Diameter (nm)	Molecular mass (Da)	Major apolipoproteins
CM	0.93	75-1200	50-1000×10 ⁶	B48, E, C, A-I
VLDL	0.93-1.006	30-800	10-80×10 ⁶	B100, E, C
IDL	1.006-1.019	27-35	5-10×10 ⁶	B100, E
LDL	1.019-1.063	18-27	2.3×10 ⁶	B100
HDL2	1.063-1.125	9-12	360×10 ³	A-I, A-II, C
HDL3	1.125-1.210	7-9	175×10 ³	A-I, A-II, C
Pre-β HDL	1.210-1.240	<7 (discoidal)	28-70×10 ³	A-I

Lipoprotein(a) (Lp(a)) forms additional lipoprotein subpopulation which consists of an LDL-like particle and the specific apolipoprotein (a) [5]. Density, size and major apolipoproteins of these lipoproteins are listed in Table 1 and Figure 1. LDL and HDL particles play key roles in the development of cardiometabolic disease (CMD), which is a term encompassing insulin resistance, dyslipidemia, hypertension, central adiposity and cardiovascular disease (CVD) [6]; therefore, we initially focus on these two lipoproteins.

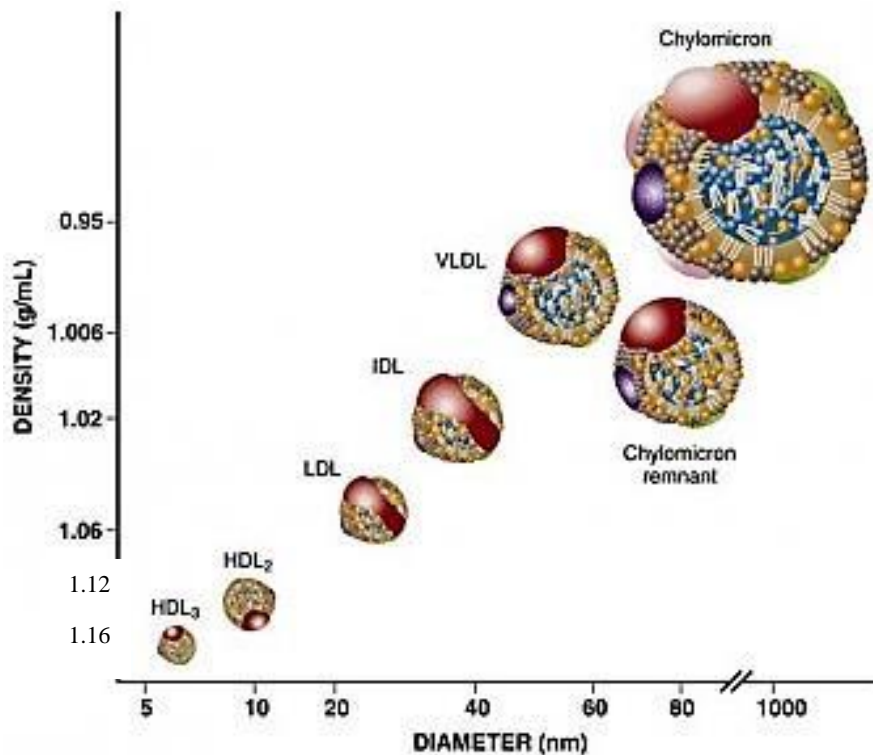


Figure 1. Density and diameter of human plasma lipoproteins[7]

1.1 LDL

LDL particles possess a hydrophobic core predominantly comprised of CE with a minor amount of TG, packaged into PL-FC coat with a single apoB100 molecule and some other minor proteins embedded into it. LDL particles display size of 18-27 nm and density of 1.019-1.063 g/ml. LDL perform their lipid transporting actions with a various degree of lipid capacity [8] and they deliver lipid to cells via receptor-mediated endocytosis [9, 10].

1.2 HDL

HDL are lipoproteins with a diameter of 7-12 nm and density of 1.063-1.21 g/ml. As LDL, HDL carry CE, TG and other lipids in its hydrophobic core, but the core/surface ratio is much smaller in HDL. The coating is made of a monolayer of PL and FC, with apolipoproteins embedded into it.

The most abundant of these apolipoproteins are apolipoprotein A-I (apoA-I) and apolipoprotein A-II (apoA-II), which are crucial to HDL metabolism [11, 12].

HDL pool in the circulation is highly heterogeneous and can be separated according to size and density using ultracentrifugation, gel electrophoresis, and FPLC or on the basis of apolipoprotein composition into three classes: apoA-I-only HDL (LpA-I), apoA-I- and apoA-II-containing HDL (LpA-I:A-II), or apolipoprotein E (apoE)-containing HDL [13]. HDL possess multiple antiatherogenic properties which primarily include cellular cholesterol efflux capacity together with antioxidative, anti-inflammatory, antithrombotic, anti-infectious and vasodilatory activities.

1.3 Other lipoprotein classes

CMs are secreted by the intestine after a meal. These are large and light (75-1200 nm, mean density of 0.93 g/ml) spherical particles [14, 15], predominantly consisting of TG with minor amounts of CE, covered by a monolayer of PL and FC, with proteins residing in the monolayer [16-20]. ApoB48 is the main structural protein of CM. CM levels in the circulation surge shortly after a fatty meal and rapidly decrease in normolipidemic individuals [21, 22]. CMs are formed in the endoplasmic reticulum (ER) of enterocytes and are released into the circulation via the lymphatic system [23, 24]. Elevated CM production is associated with dyslipidemia and increased CVD risk in metabolic disorders, such as in Type 2 diabetes (T2D).

VLDLs are large (30-800 nm, 0.93-1.006 g/ml) particles produced by the liver from TG, FC, and apolipoproteins and let off into the circulation [25]. Unlike CM, VLDL transports endogenous liver-derived lipids to peripheral tissues, making it the key transport vehicle for endogenous lipids. Apolipoprotein B100 (apoB100) is the main structural protein of VLDL which ensures its proper assembly and secretion [26]. Newly produced VLDL particles contain apoB100, apolipoprotein C (apoC)-I, apoE, PL, FC, CE, and TG. During maturation in the circulation, they acquire apoC-II

and apoE from HDL. VLDL is converted in the circulation to IDL and LDL and is a metabolic precursor of LDL [27]. Both IDLs and LDL are recognized by receptors in the liver and endocytosed by the hepatocytes. Once cholesterol level inside IDLs exceeds the level of TG, IDL finally becomes LDL.

Term “TG-rich lipoproteins (TGRL)” encompasses lipoproteins that display a high content of TG, such as CM and VLDL, secreted by the intestine and the liver, respectively. TG in TGRL is hydrolyzed by lipoprotein lipase (LPL), producing free fatty acids and glycerol. Similarly to LDL, remnants of CM and VLDL produced by lipolysis may enter the arterial wall and provoke formation of atherosclerotic lesions [28-30].

2. Epidemiology of lipoproteins

2.1 LDL

Our interest to LDL is primarily derived from the fact that elevated LDL-cholesterol (LDL-C) levels are associated with an increased risk of coronary heart disease (CHD), as shown in multiple large-scale epidemiological studies. Framingham Heart Study, for example, explicitly specified LDL-C as an independent risk factor for CHD after multivariate adjustments [31].

According to this study, circulating LDL-C levels of higher than 130 mg/dl are associated with an increased risk of CHD, reaching values of approximately +70% for the relative likelihood of the development of CHD in patients with LDL-C levels higher than 160 mg/dl. The Atherosclerosis Risk in Communities Study estimated increase in relative risk of CHD as approximately 40% for every 38.8 mg/dl (1 mmol/l) increase from the median values of LDL-C of 88 mg/dl and 95 mg/dl for women and men, respectively [32]. A meta-analysis revealed that single nucleotide polymorphisms (SNPs) of genes associated with increased LDL-C levels were implicated in increased risk of coronary artery disease (CAD) [33]. These genes were coding for the apoB and

apoE protein families, proprotein convertase subtilisin/kexin type 9 (PCSK9) and LDL receptor (LDLR). Other epidemiological studies produced similar results [34-37]. On the other hand, the opposite is also true: naturally occurring SNPs that reduce circulating LDL-C levels are associated with decreased risk of CHD [38]. The risk decrease is stronger than in patients with statin treatment started later in life reaching similar reduction in LDL-C levels, implying cumulative effect of the exposure to high levels of LDL-C [39, 40]. All these observations made LDL-C to be colloquially known as “bad cholesterol”.

2.2 HDL

CHD patients typically display reduced circulating levels of HDL-cholesterol (HDL-C) as compared to healthy controls [41, 42]. In the 60s [43] and 70s [44], low concentrations of HDL-C were implicated in the poor clearance of excessive plasma cholesterol and, as a corollary, were proposed to represent the main cause of CHD development. Combined with the observation of 2-3 % decrease of CHD risk for each additional 1 mg/dl increase of HDL-C [45, 46], and additionally reinforced by a multitude of large-scale epidemiological studies, reporting an inverse relationship between levels of HDL-C and the risk of CHD [47-52], HDL-C earned itself a moniker “good cholesterol”.

A whole plethora of factors is known to affect HDL-C levels: race [53-55], gender (with women displaying higher levels than men) [56, 57], conditions with compromised metabolism, including familial dyslipidemias [58], T2D [59, 60] or obesity [57].

There is however no consensus on the exact role of HDL subclasses in CVD [61, 62]. It has been reported that small, dense particles, such as HDL3c, are more efficient in performing their biological roles, than large, light HDL2 [63], while at the same time levels of small dense HDL

particles are increased in patients with CHD and levels of large, light HDL are decreased [62], adding to the controversy.

2.3 Other lipoprotein classes

Role of TGRL particles in the atherosclerosis is not particularly straightforward. Indeed, atherosclerosis and CVD do not preferentially affect individuals with extremely high plasma TG, while those with high LDL-C levels develop premature atherosclerosis [64, 65]. This observation can be explained by large TGRLs not being able to penetrate the arterial wall to lay a harmful lipid deposition there [66, 67]. On the other hand, moderately elevated TG levels most probably feature TGRL particles small enough to enter the arterial wall, yet big enough to cause all sorts of atherosclerotic mayhem there [68-70]. Copenhagen City Heart Study (CCHS), Women's Health Study and Emerging Risk Factors Collaboration consistently associated increased risks of myocardial infarction (MI), CHD, stroke and all-cause mortality with raised levels of TG [71-74]. Furthermore, increased fasting triglycerides were associated with elevated risk of ischaemic stroke. Other studies demonstrated that the concentration of non-HDL-cholesterol rather than raised plasma TG was associated with CHD [75-77].

3. HDL

3.1 Structure

ApoA-I is a major component of HDL, accounting for approximately 70% of HDL protein mass [78]. Depending on the presence or absence of a lipid cargo in an HDL particle and this cargo's composition, apoA-I can occur in multiple forms which include lipid-free apoA-I, a "belt" of discoid HDL (also known as pre- β HDL) [79], or a structural component of spherical HDL particles [78].

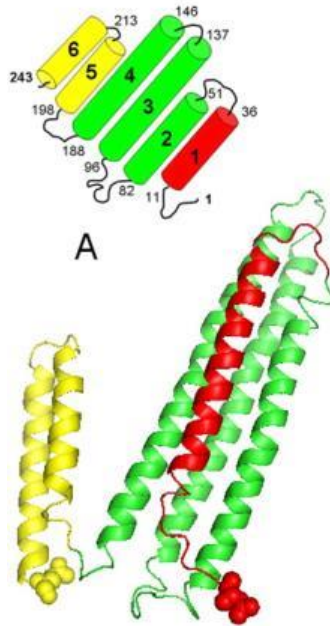


Figure 2. X-ray crystal structure of lipid-free apoA-I [78]

The lipid-free apoA-I most probably does not exist in plasma as the protein avidly interacts, trace amounts of lipids. Resulting lipid-poor apoA-I accounts for only 5–10% of total plasma apoA-I yet is believed to possess a crucial role in the HDL metabolism. ApoA-I is a 243-amino acid, 28-kDa single polypeptide organized into eight α -helical segments of 22 amino acids and two 11-mer repeats, leaving only 44 N-terminal amino acids not pertaining to any tertiary structure (

Figure 2). Another element in the process of HDL maturation (see section 3.4.2) is represented by discoidal HDL which contains small amounts of amphipathic lipids, such as PL and FC, alongside the apoA-I itself. The apoA-I in the discoidal HDL particles is thought to form a double-belt around the amphipathic lipid bilayer (Figure 3A). Double-belt in this model is formed by two apoA-I molecules wrapped beltwise around a small patch of bilayer containing 160 lipid molecules with each monomer having a ringlike C-terminal domain, with a curved, planar amphipathic alpha helix with an average of 3.67 residues per turn, and with the hydrophobic surface curved toward the lipids [80]. The next and last incarnation of the HDL lifecycle involves

spherical HDL (Figure 3A). Compared to discoidal HDL, spherical HDL additionally contains hydrophobic lipid core formed by TG and CE. In this configuration apoA-I becomes embedded into the surface lipid layer of the particle, while keeping contact with the lipid core [78].

Arrangement of the three apoA-I chains in the spherical HDL particle was proposed by Silva et al. [81] in which the three apoA-I chains are paired with each other for half of their length to form a symmetric construct made of three folded rings coined the Trefoil model [82].

3.2 Composition

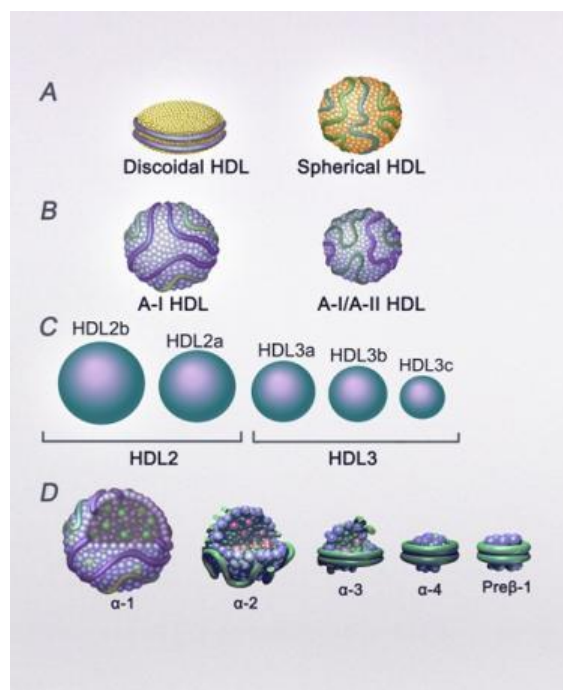


Figure 3. Different means of HDL subpopulation classification: A) by maturation step B) by protein content C) by size D) by charge [83, 84]

3.2.1 Classic techniques

As mentioned above, HDL particles possess a surface coat and a lipid core. The surface coat consists of apolipoproteins (approximately 50-55% of total HDL mass), unesterified cholesterol (4%) and PL (20-30%). The core consists primarily of CE (14-18%) and TG (3-6%). PL subclasses present in HDL include phosphatidylcholine (PC), sphingomyelin (SM),

lysophosphatidylcholine (LPC), phosphatidylinositol (PI), phosphatidylethanolamine (PE), ceramide (Cer), phosphatidylserine (PS), phosphatidic acid (PA), and phosphatidylglycerol (PG) [85] (Figure 4).

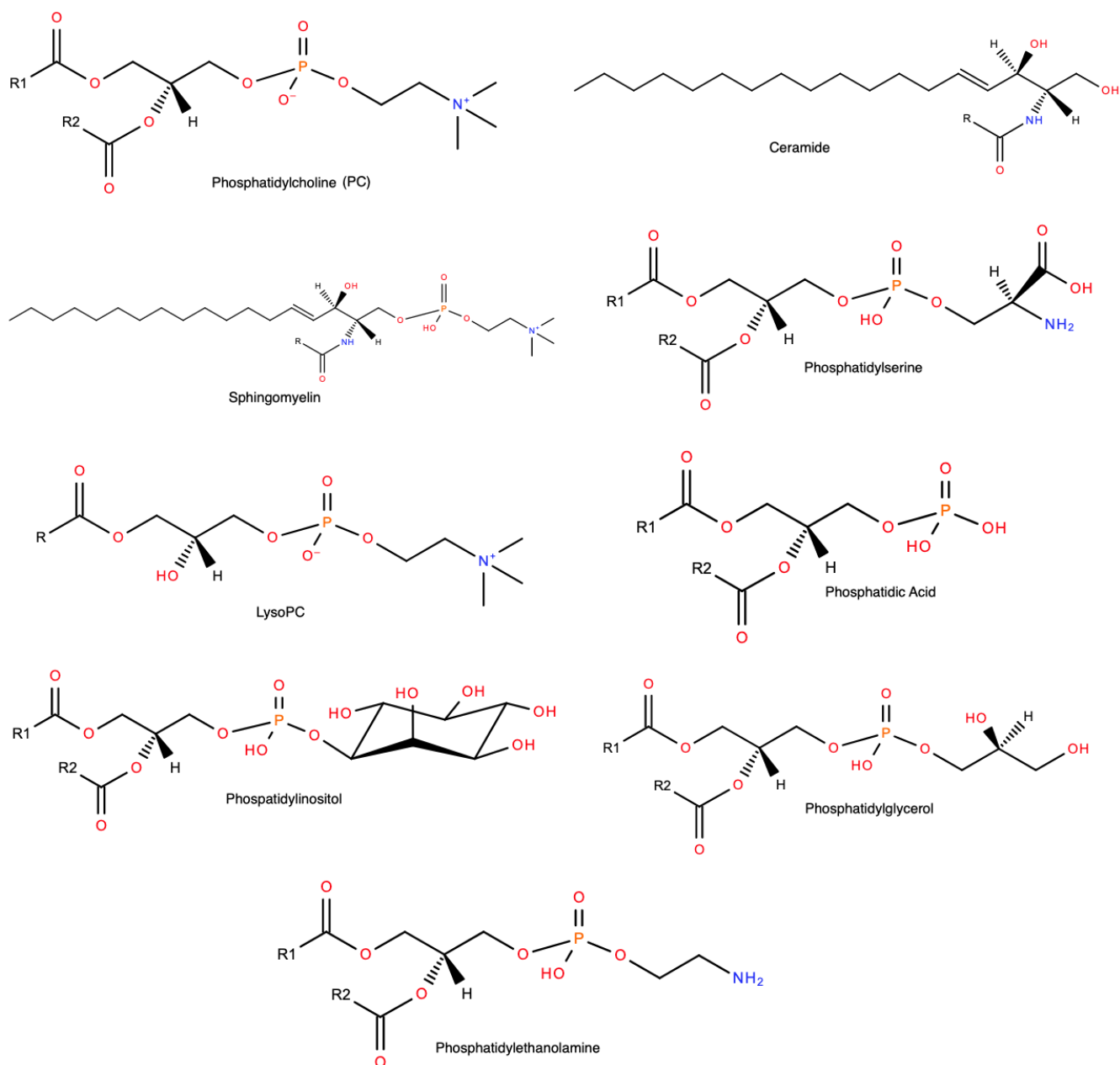


Figure 4. Structure of the major lipid subclasses studied, source: lipidmaps.org

Generally, before the arrival of proteomic techniques all HDL proteins identified by classic techniques were attributed to one of the three categories which involved apolipoproteins, lipid transfer proteins, and enzymes. Apolipoproteins included apoA-I, apoA-II, apoA-IV C-I, C-II, C-III and apoE, with apoA-I being the most prominent of them in terms of the abundance (70% of the protein mass of HDL), while apoA-II was found to account for about 20% of total HDL protein, which rendered it a second-major protein component of HDL [86]. Lipid transfer proteins included phospholipid transfer protein (PLTP) and cholesteryl ester transfer protein (CETP). Enzymes of HDL encompassed lecithin:cholesterol acyltransferase (LCAT), paraoxonase-1 (PON1), PON3 and platelet-activating factor-acetyl hydrolase (PAF-AH). Among these proteins identified by classic biochemical assays, many play important biological roles: for example, LCAT converts FC into CE, while PAF-AH and PON1 exert plausible antioxidative activities [87-91].

In order to successfully realize the qualitative and quantitative analysis of lipid components of HDL in the past, many analytical methods had to be employed, including thin-layer chromatography (TLC), gas chromatography (GC), liquid chromatography (LC), enzyme-linked immunosorbent assays (ELISA) and nuclear magnetic resonance (NMR) which allowed characterizing major lipid classes [92]. However, analysis of molecular lipid species was either impossible or highly laborious using these techniques.

Lest we forget about the glycan part of the HDL. Indeed, it has been long known that in addition to lipids and proteins, lipoproteins contain carbohydrates as a minor component (e.g. 3.3 wt% in HDL) [93]. However, without qualitative and quantitative analysis of HDL carbohydrates was not feasible using traditional methodology (see section 3.2.2.3 Glycome).

3.2.2 Omics approaches

Omics refers to a field of study in biology ending in *-omics*, such as genomics - study of genes and their function, proteomics - study of proteins, lipidomics - study of cellular lipids or glycomics - study of cellular carbohydrates.

3.2.2.1 Proteome

Advances in omics approaches allowed for a detailed molecular characterization of individual proteins present in HDL particles. Before the widespread arrival of liquid chromatography-mass spectrometry (LC-MS), the proteins had to be purified and subsequently exposed to Edman degradation – a slow and painful process, requiring the protein of interest to be broken into fragments of 50 amino acid long, with each such fragment taking up more than full three days of constant work from an automatic Edman sequencer to be analyzed [94]. On the other hand, liquid chromatography–electrospray ionization–tandem MS (LC-ESI-MS/MS), can detect more than 100 different proteins in HDL during a single run (Figure 5) [90]. Some of these proteins are cross-validated by classical methods yet revealing many previously undetected minor proteins representing less than 5% of HDL protein mass. Multiple complement-regulatory proteins and a diverse array of distinct serpins with serine-type endopeptidase inhibitor activity, as well as acute-phase response proteins were thereby detected, supporting the idea that HDL is of central importance in inflammation and immune response [90, 95]. More importantly, proteomics allowed not only to find minor yet crucial proteins in HDL, but also permitted a reliable quantification of their abundances across heterogeneous HDL subpopulations of HDL2 and HDL3 (see Figure 5; more details in section **3.3 Heterogeneity**) in both normolipidemic subjects and subjects with disorders of lipid metabolism and CAD. Example of such proteins, differentially presented in the control vs CAD subjects, may include acute-phase-response proteins, C4A/C4B, C9, and vitronectin [90]. Indeed, HDL from CAD patients was selectively

enriched in proteins that play critical roles in macrophage biology, lipid metabolism, and the inflammatory response (Figure 6) [90].

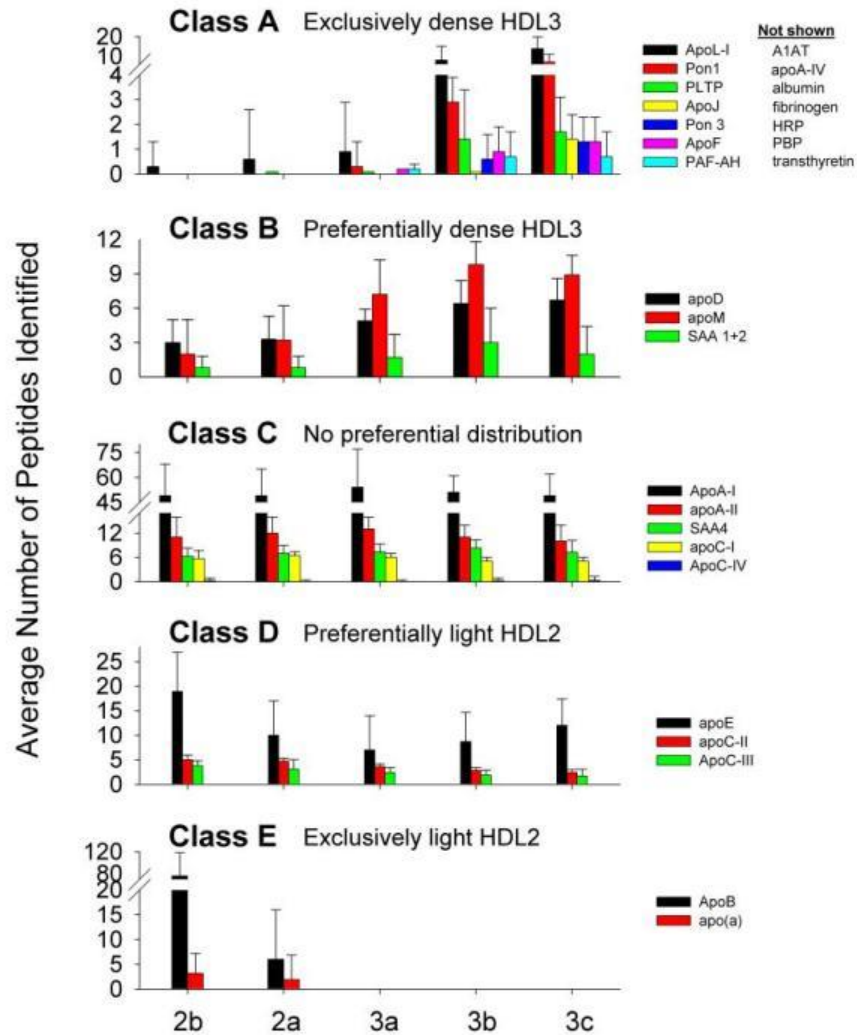


Figure 5. Abundance patterns of representative proteins across major HDL subpopulations. Class A — limited to dense HDL3, those listed showed the same pattern (not shown). Class B - prefer dense HDL3 but are in all subfractions. Class C - evenly distributed. Class D — prefer light HDL2 but are in all subfractions. Class E — limited to light HDL2. Error bars =1 S.D (n=9) [95].

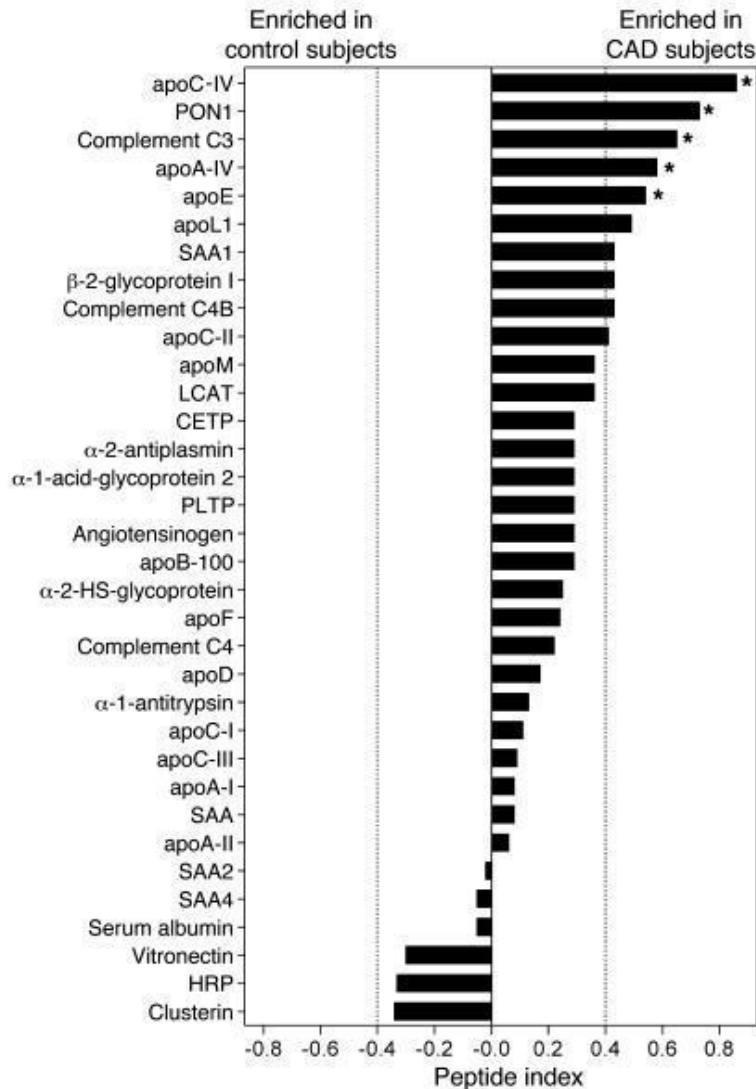


Figure 6. Relative abundance of proteins isolated from HDL3 of control and CAD subjects. HDL3 was isolated from plasma of 6 control subjects and 7 subjects with established CAD. The relative abundance of proteins in the CAD subjects versus the control subjects was assessed by the peptide index. * $P < 0.05$ by Student's t test (peptide number) or Fisher's exact test (subject number) [90].

3.2.2.2 Lipidome

Thanks to mass spectrometry, which bests the classic techniques in that it combines high sensitivity and specificity, high throughput and high accuracy [92], we can delve into lipidomics with a relative ease. Before the arrival of the omics technologies, analysis of individual lipid components of lipoproteins was probably even more cumbersome than the assessment of the composition of

their protein moieties. Indeed, lipids are an extremely diverse group of compounds consisting of tri-, di- and monoacylglycerols, free fatty acids, PL, sterols, carotenoids and vitamins A and D among others [96] and require a plethora of analytical techniques to be analyzed properly.

Although lipidomics is still considered to be in its early stages of development [92], lipidomic analysis already made significant progress in the determination of the lipoprotein composition. PC, the principal plasma phospholipid that accounts for 32-35 mol % of total lipids in HDL, is a structural lipid, consistent with its even distribution across HDL subpopulations (Figure 7) [97]. LPC is another important phospholipid subclass in HDL (1.4-8.1 mol % of total lipids) derived from regulated degradation of PC by phospholipases, including LCAT. PE is moderately abundant in HDL (0.7-0.9 mol % of total lipids). Plasmalogens are minor phospholipids which contain a vinyl ether linked fatty acid essential for their antioxidative properties [98]. PI, PS, PG, PA and cardiolipin are negatively charged minor (0.8 mol % of total lipids) PL present in HDL which may impact its net surface charge and modulate lipoprotein interactions with lipases, extracellular matrix and other protein components [97].

SM, a structural lipid which enhances surface rigidity, is the major HDL sphingolipid (SL) (5.6-6.6 mol % of total lipids), which largely originates from TGRL [98]. Cer is a minor (<0.1 mol % of total lipids) sphingolipid intermediate implicated in cell signalling, apoptosis, inflammatory responses, mitochondrial function and insulin sensitivity. Both SM and Cer are enriched in large, light relative to small, dense HDL [97]. Among lysosphingolipids, sphingosine-1-phosphate (S1P) is particularly interesting, reflecting its key role in vascular biology [99]. S1P is associated preferentially with small, dense HDL particles [98], consistent with their elevated content of apoM [95], a carrier for S1P [100].

Unesterified (free) sterols are located in the surface monolayer of HDL particles and regulate its fluidity. HDL sterols are dominated by cholesterol, reflecting the pivotal role of lipoproteins in

the cholesterol transport through the body. CE are largely (up to 80%) produced in HDL and form its lipid core [101]. Most of HDL CE is accounted for by cholesteryl linoleate. HDL-associated TG are dominated by species containing oleic, palmitic and linoleic acid moieties [101]. Minor HDL lipids include diacylglycerides, monoacylglycerides and free fatty acids.

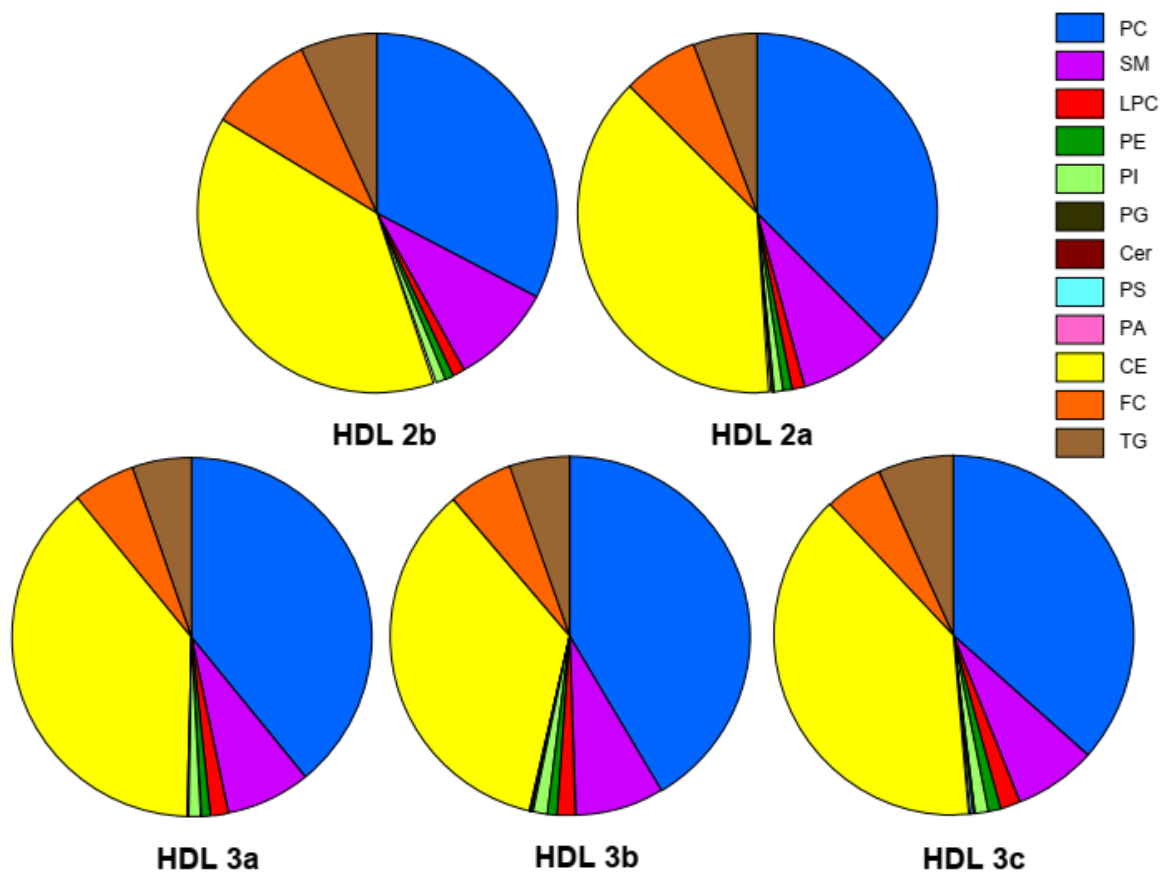


Figure 7. Differential representation of the major glycerosphingolipid classes in five major HDL subpopulations [97].

Akin to the discoveries of the newfangled proteomics, lipidomics readily reveals differences between HDL subpopulations, as well as between HDL obtained from normolipidemic controls and from metabolically compromised patients. An example of the first would be the report of Camont and colleagues documenting differences between major HDL subpopulations in normolipidemic patients [97]. As it can be seen in Figure 7, differences between the five major

HDL subpopulations (HDL2b, 2a, 3a, 3b and 3c) were observed in the contents of PC, SM, LPC, PI, PE, PS, Cer, PA and PG. Concentrations of PS, PC, LPC and PA generally increased in parallel with increase in hydrated density from HDL2b to HDL3c. Indeed, small, dense HDL were enriched in PC, PS, and PA relative to large, light HDL ($P=0.01$, $P=0.003$, and $P<0.001$ for trend, respectively). HDL3c was enriched in LPC (+48%; $P=0.05$) and PS (17-fold; $P<0.01$) relative to HDL2b. Similarly, PE, PI, and PG tended to concentrate in small, dense HDL; these trends did not, however, attain significance. Proportion of SM and Cer decreased progressively in parallel with HDL density from 20% and 0.19% of total PL+SL in HDL2b to 14% and 0.11% in HDL3c. Another report details lipid classes of HDL that are most affected by ST-elevated myocardial infarction (STEMI) [102], and which include LPC and PA (Figure 8). Many if not all of these lipids are biologically active and play either signalling role (LPC and PA), or are believed to be involved in anti-apoptotic and anti-inflammatory features of HDL (PS, Cer and PA) [103-109]. However, all reports known to date do not provide a detailed representation of the contents of molecular lipid species, although more than 200 species of lipids are known to be present in the lipidome of HDL [97, 110].

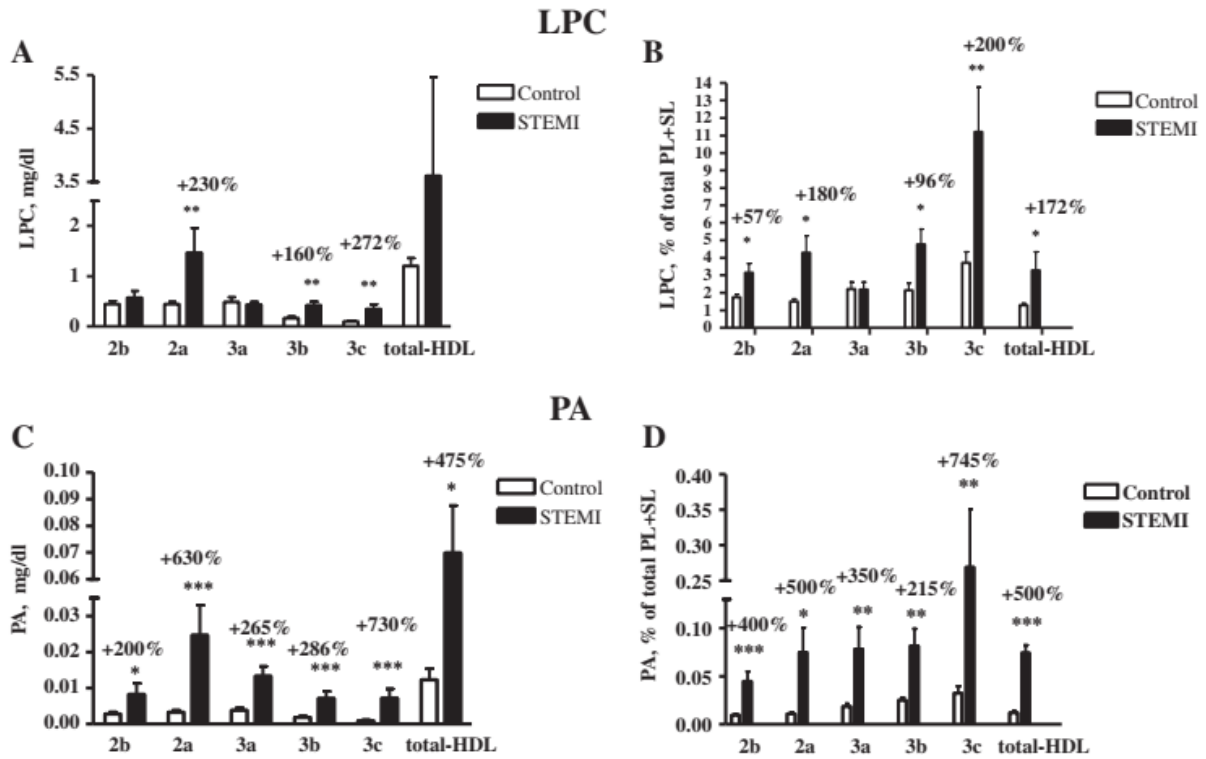


Figure 8. Levels (A, C) and content (B, D) of LPC (A, B) and PA (C, D) in HDL subpopulations and in total HDL, expressed as mg/dl (A, C) and % of total PL + SL (B, D), in STEMI patients and control subjects; * $p < 0.05$ vs. controls [102].

3.2.2.3 Glycome

HDLs are highly sialylated particles in which most of the glycans contain one or two sialic acid residues [111]. Several HDL proteins, including LCAT, CETP, apoCs, fetuin A and α -1-antitripsin, are glycosylated, while the glycosylation of apoA-I remains controversial [112-114]. Remarkably, carbohydrate residues are specifically associated with distinct HDL proteins, such as apoC-III which contains O-linked glycans [115]. Glycans, attached not to proteins, but rather to lipids directly with a covalent bond (glycolipids), contain sialic acids as well [116].

3.3 Heterogeneity

HDL particles are heterogeneous in size, charge, protein content or by biological activities they exert.

Ultracentrifugation (~200 000 g for 48 h) allows HDL particles to be subfractionated by density into light, large, lipid-rich HDL2 particles with a density of 1.063-1.125 g/ml and small, dense, protein-rich HDL3 particles with a density of 1.125-1.21g/ml [13]. HDL2 and HDL3 are two major subpopulations of spherical HDL. HDL2 particles contain PL, FC, CE and TG at approximately 25, 6, 18 and 9 wt %, respectively, while HDL3 contains PL, FC, CE and TG at approximately 23, 3, 14, and 7 wt %, respectively [117]. Further fractionation of HDL2 and HDL3 into five increasing-density subpopulations of HDL2b, HDL2a, HDL3a, HDL3b, and HDL3c can be achieved by density gradient ultracentrifugation (Figure 3C) [13, 118].

It is also possible to subfractionate HDL particles by their charge and size (Figure 3D). Namely, 2D gel electrophoresis separates plasma HDL particles into: (a) very small discoidal precursor HDL of pre- β mobility (pre- β -1 HDL, diameter about 5.6 nm), which contains apoA-I and PL; (b) very small discoidal HDL of α mobility (α -4 HDL, diameter about 7.4 nm), which contains apoA-I, PL, and free cholesterol; (c) small spherical HDL of α mobility (α -3 HDL, diameter about 8.0 nm), which contains apoA-I, apoA-II, phospholipid, free cholesterol, cholesteryl ester, and triglyceride; (d) medium-sized spherical HDL of α mobility (α -2 HDL, diameter about 9.2 nm), which contains the same constituents as α 3 HDL; and (e) large spherical HDL of α mobility (α -1 HDL), which contains the same constituents as α -3 and α -2 HDL, except for the near absence of apoA-II (Figure 9) [13].

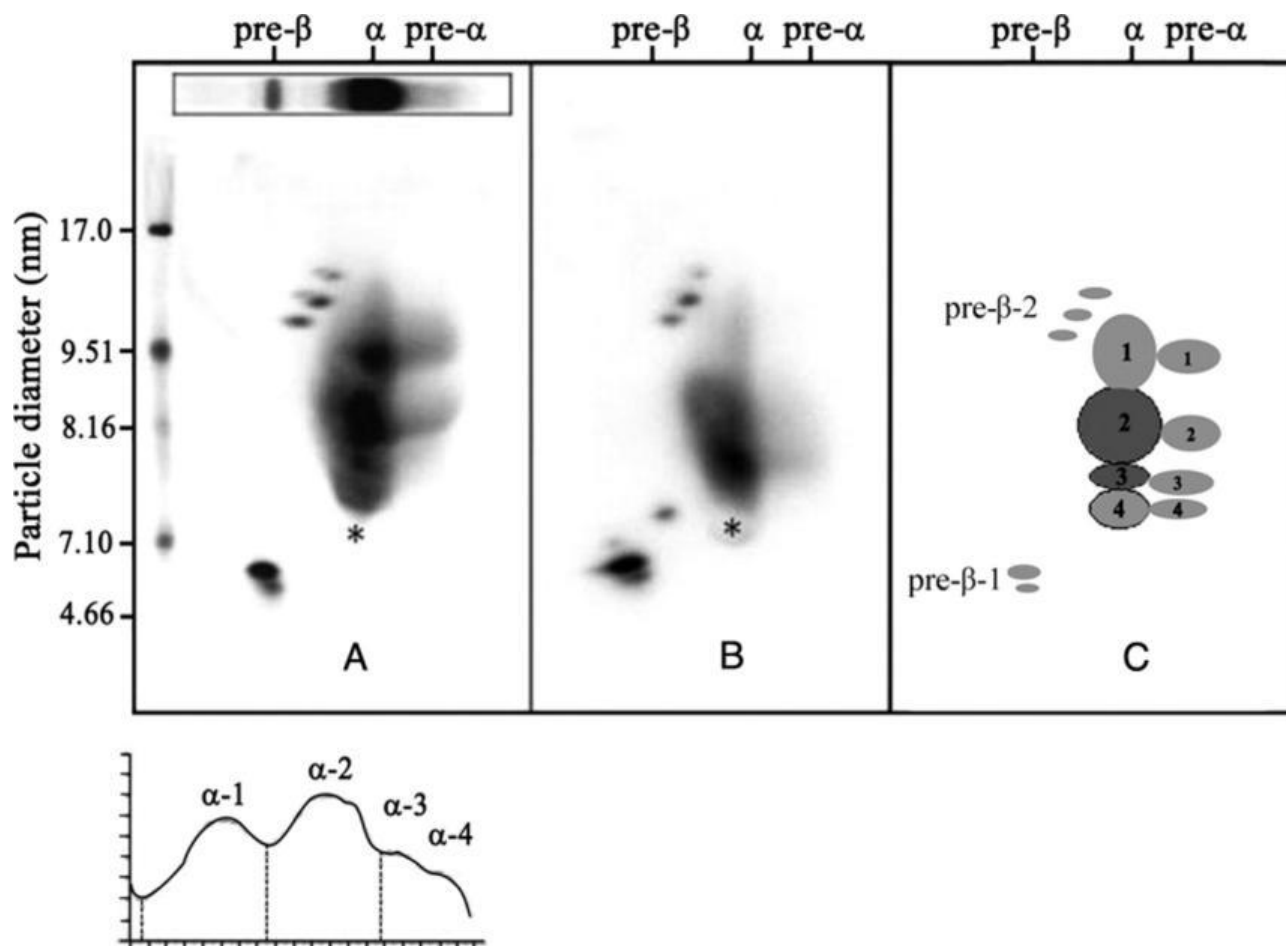


Figure 9. The apoA-I-containing HDL subpopulation profiles of a CHD patient (A) and a healthy individual (control) (B), with a schematic diagram of all of the apoA-I-containing HDL particles shown on the right (C). Below panel (A) is a plot of a densitometric scan across the α -migrating HDL-particle region indicating the presence of 4 α -migrating HDL particles ranging in mean particle diameter from very large α -1 HDL (11.0-nm diameter) to very small pre- β -1 HDL (5.6-nm diameter). In the schematic diagram α -migrating apoA-I-containing particles in the α -2 region (9.2-nm diameter) and in the α -3 region (8.1-nm diameter) contain both apoA-I and apoA-II (more heavily shaded), whereas all other particles containing apoA-I, including small α -4 HDL (7.4-nm diameter), do not contain appreciable amounts of apoA-II (less heavily shaded). The asterisk marks the serum albumin or α front. Based on their composition, very small pre- β -1 HDL and small α -4 HDL are discoidal particles that do not contain cholesteryl ester or triglyceride, whereas medium, large, and very large α -3, -2, and -1 HDL are spherical and contain cholesteryl ester and triglyceride in their cores. CHD patients in general in the untreated state tend to have significant decreases in the levels of apoA-I in very large and large α -migrating HDL and modest increases in apoA-I in very small pre- β -1 HDL and small α -4 HDL. In (C), 1, 2, 3, and 4 refer to α -1, -2, -3, and -4, respectively [119].

Plasma HDL can also be subfractionated and classified on the basis of their apolipoprotein composition into particles containing apoA-I (LpA-I) and those containing apoA-I *and* apoA-II (LpA-I:A-II) (Figure 3B). LpA-I and LpA-I:A-II are the major HDL subpopulations accounting for approximately 35% and 65% of plasma apoA-I, respectively. The cardioprotective roles of LpA-I and LpA-I:A-II are however controversial. A general conclusion resulting from these studies is that increased HDL-C concentrations involving an increase in the large HDL subclasses containing both LpA-I and LpA-I:A-II is associated with decreased CHD risk, whereas the reduction in lipid-poor LpA-I and pre- β HDL is associated with increased CHD risk [13].

Finally, NMR can quantify three distinct HDL subclasses differing in size, notably large (8.8-13.0 nm), medium (8.2-8.8 nm) and small (7.3-8.2 nm) HDL [13]

HDL heterogeneity is also observed at the level of the proteome, lipidome and glycome. For example, proteins, exclusively present in HDL3, but not present in HDL2, include apoL-I, apoF, PON1/2, PLTP, apoJ, PON3, α 1-antitrypsin (A1AT), apoA-IV, albumin, fibrinogen, Hrp, PBP and transthyretin [95]. In a similar fashion, PS is predominantly associated with the more biologically active HDL3 particle pool and thus, its HDL content is positively correlated with all metrics of HDL functionality [97]. In contrast, SM and Cer are preferentially found in large, light HDL [97]. Potential heterogeneity of the HDL glycome however remains undetermined.

3.4.2 Remodelling

Discoidal pre- β HDL particles are subjected to LCAT, which forms CE from FC, and mature into a full-fledged spherical HDL which constitutes a majority of plasma HDL pool [78]. Plasma CETP primarily transfers CE from mature spherical HDL to apoB-containing particles, particularly VLDL, in exchange for TG [122]. As a result of CETP activity, HDL becomes depleted of CE and enriched in TG, which accelerates HDL catabolism. PLTP is involved in the interconversion of HDL2 and HDL3 and that conversion generates small nascent HDL [123].

Both surface and core lipids of HDL are extensively modified by lipases. Hepatic lipase (HL) breaks down primarily tri- and diglycerides but also phospholipids of HDL, resulting in the reduction of HDL particle size. Endothelial lipase (EL) primarily hydrolyses HDL phospholipids but also triglycerides. Lastly, further remodeling of HDL occurs through particle fusion or PLTP-mediated transfer of surface remnants such as PL from LPL-hydrolyzed CMs of VLDL, eventually producing mature HDL [123]. Mature spherical HDL can further grow via effluxing cellular cholesterol and phospholipid through ATP-binding cassette transporter G1 (ABCG1) [124].

Selective uptake of HDL-C via SR-B1 includes apoA-I-dependent binding of HDL to SR-B1, transfer of HDL-CE to the cell membrane and intracellular hydrolysis of CE by cholesterol esterase to FC, with a release of small cholesterol-depleted HDL particles [125].

3.4.3 Catabolism

In healthy individuals, LpA-I is catabolized at a faster rate than LpA-I:A-II. The major sites of catabolism of the protein components of LpA-I and LpA-I:A-II are the liver and kidney, and the majority of HDL cholesterol is transported to the liver. Kinetic models incorporating the different rates of catabolism of LpA-I and LpA-I:A-II have been developed. The differential rates of metabolism of LpA-I and LpA-I:A-II have been proposed to be related to the decreased ability of apoA-I-containing lipoproteins to reassociate with HDL particles following cholesteryl ester

delivery to the liver via the SR-B1 receptors. This process includes apoA-I-dependent binding of HDL to SR-B1, transfer of HDL-CE to the cell membrane and intracellular hydrolysis of CE by cholesterol esterase to FC, with a release of small cholesterol-depleted HDL particles [125]. Intracellular FC is subsequently excreted into the bile or converted to bile acids for excretion [11, 125].

CETP also plays a role in the catabolism of HDL: CETP mediates the transfer of CE from HDL to apoB-containing lipoproteins (VLDL and LDL) in exchange for TG from the latter, thereby forming CE-depleted and TG-enriched HDL. CE-enriched TGRL transport CE to the liver and bind to the LDL receptor for subsequent particle uptake [125, 126]. TG-enriched HDLs are hydrolyzed by HL and EL to reduce particle size and release apoA-I, which interacts with ABCA1 in the next lipidation cycle [11, 127, 128].

HDL particles can be removed from the circulation by holoparticle HDL receptors, such as cubulin present in kidney proximal tubules and the ectopic β -chain of ATP synthase at the surface of hepatocytes [129, 130].

3.5 Biological activities and structure-function relationships

Beneficial effects of HDL are not limited to their influence on lipid metabolism. HDL equally possess cellular cholesterol efflux, antioxidative, anti-inflammatory, anti-apoptotic, cytoprotective, vasodilatory, anti-infectious and anti-thrombotic activities (Figure 11) [120, 131].

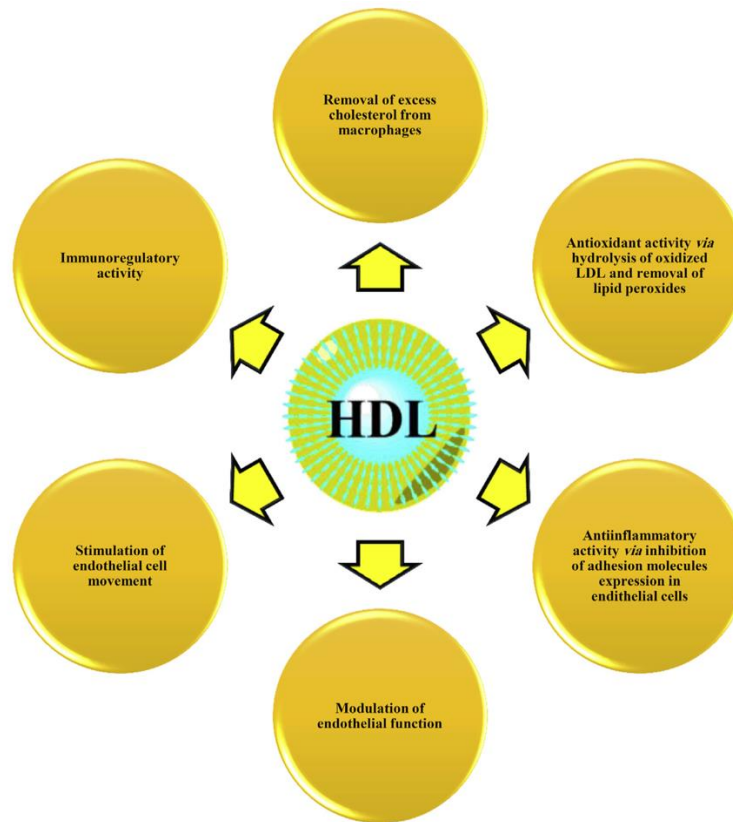


Figure 11. Biological activities of HDL [132]

Since several decades, the major biological role of HDL is thought to involve the removal of excess cholesterol from peripheral tissues to the liver for subsequent biliary excretion [133, 134]. Lipid-loaded macrophages that acquired cellular debris and modified or aggregated lipoproteins and are unable to metabolize nor to get rid of them, form foam cells. These foam cells are always found in the atherosclerotic lesions, implying their key role in atherogenesis. Cholesterol efflux from macrophages can be mediated through (a) one-directional, ATP-dependent pathways involving ABCA1 and ABCG1 transporters; (b) a bi-directional, ATP-independent pathway mediated by SR-B1; and (c) passive diffusion according to the gradient of cholesterol concentration [135, 136]. Mutations in ABCA1 lead to severe HDL deficits, manifesting as Tangier disease or other forms of familial hypoalphalipoproteinemia [137]. Highlighting the role of ABCA1 in cholesterol metabolism is the observation that any type of modulation (over- or under-representation) of this

transporter impacts the capacity of apoA-I to perform cholesterol efflux [138]. Nuclear liver X receptors (LXRs) type α and β and retinoid X receptor (RXR) regulate the expression of ABCA1 [139]. LXRs expression is modulated by cellular concentrations of oxysterols, a product of enzymatic modification of cholesterol. Therefore, LXR agonists and oxysterols can modulate the transcription of ABCA1 in macrophages, thereby enhancing cholesterol efflux to lipid-poor HDL particles. However, it is challenging to isolate lipid-poor apoA-I from the bloodstream, because after being secreted, it rapidly matures into spherical HDLs. Such mature, spherical HDLs can also perform cellular cholesterol efflux through ABCG1 transporter pathway [140, 141]. SR-B1 mediates another pathway of cholesterol efflux from macrophages to mature HDL [142], and in knockout mice models was shown to be atheroprotective [143, 144].

ApoA-I and apoA-II are the primary acceptors in the cholesterol efflux process, while apoA-IV, apoC-I, apoE and apoM can efficiently accept cellular cholesterol, too [122, 145-148]. Enzymes also exert major functions in cellular cholesterol efflux and reverse cholesterol transport (RCT). Thus, LCAT participates in the transfer of cholesterol from peripheral cells to the liver, ensuring formation of CE which is subsequently taken up by the liver via SR-B1. HDL lipids are also relevant in its cholesterol efflux capacity; thus, HDL containing liquid-crystal unsaturated PLs is a more efficient cholesterol acceptors than HDL containing gel-state saturated PLs [149, 150].

ApoA-I and S1P of HDL can inhibit expression of pro-inflammatory adhesion molecules in the cells, thereby diminishing inflammation [151]. These adhesion molecules include vascular cell adhesion molecule-1, endothelial-leukocyte adhesion molecule 1 and intracellular adhesion molecule-1 [152, 153]. HDL promotes proliferation of endothelial cell and attenuates apoptosis of the endothelial cells [12, 121, 153], inhibits monocyte activation, inhibits secretion of pro-inflammatory cytokines and chemokines and decreases activation of neutrophils in the arterial wall [124, 154].

Furthermore, HDL can inhibit one-electron and two-electron oxidation of LDL, two most common types of LDL oxidation to occur in vivo [155, 156]. The mechanisms of such actions are well understood: one-electron oxidants generate phospholipid hydroperoxides, which are sequestered by HDL and reduced by the redox-active methionine residues of apoA-I into redox-inactive PL hydroxides and methionine sulphoxides [157, 158]. Two-electron oxidation of LDL can be intercepted by direct oxidant scavenging of HDL [159]. ApoA-I, apoA-II, apoA-IV, apoE, apoJ, apoM as well as PON1, PAF-AH and LCAT exert antioxidative activities [120, 131, 160-167]. As mentioned in section **3.3 Heterogeneity**, HDL subpopulations are not equally potent in their key biological functions, antioxidative function being one them: small, dense HDL are more potent in their antioxidative activity than large, light HDL [168].

ABCG1-mediated efflux can serve as a mediator in the removal of oxidized lipids from the cells to HDL, with the latter exerting cytoprotective function. Oxidized lipids activate apoptotic caspases and may compromise the integrity of mitochondria [151]. HDL stimulates release of nitric oxide (NO) mediated by endothelial nitric oxide synthase (eNOS), and production of prostacyclin (PGI₂) in endothelial cells to maintain normal function of vascular endothelium [169]. Endothelial NO beneficially regulates inflammatory response of endothelium, platelet activity and proliferation of vascular smooth muscle cells [133]. Studies show that HDL promotes expression and activity of eNOS, which increases production of NO [170-173]. Activation of eNOS mediated by HDL includes HDL binding to the endothelial SR-B1, which triggers cell signaling pathways of phosphatidylinositol 3-kinase (PI3K)/Akt and the phosphorylation of eNOS [172, 173]. Moreover, NO production mediated by eNOS can be promoted by HDL-associated S1P via S1P1/S1P3 receptors [173, 174]. The eNOS activation can also be mediated by HDL-associated PON1 [170]. HDL possesses anti-coagulation activity, namely it inhibits activation of platelets and coagulation-promoting factors X, Va, VIIIa and tissue factor [169, 175, 176]. HDL is also known

to possess strong ability to quench infection by eliminating lipopolysaccharides (LPS), should they infiltrate the bloodstream. For example, apoA-I-overexpressing mice subjected to systemic inflammation by LPS show reduced CD14 expression on monocytes as compared to their wild-type counterparts [177].

Content-wise, there is no clear unanimity about the components with the most significant role. Abundances of specific lipids, such as sphingosine-1-phosphate (S1P) [178], or groups of lipids, such as PS [97, 179, 180] may modulate HDL's efficiency to reduce risk of CHD. Recent studies demonstrated that miRNAs, associated with CVD, can be exported or released by cells and circulate with the blood in a remarkably stable form, namely bound to apolipoproteins of HDL, and modulated in the CVD [181, 182], but this assumption was not confirmed by others [183]. Finally, the activity of myeloperoxidase (MPO), and PON1 - both HDL-associated enzymes, were also found to be associated with CVD [184-186]

Measurements of HDL biological performance could have potentially presented a viable alternative to the largely obsolete HDL-C metric, if they themselves were free of controversies: in one study cellular cholesterol efflux capacity of HDL was negatively correlated with the development of CHD [187], while another showed that enhanced cholesterol efflux was associated with elevated CVD risk [188].

3.6 Dysfunctional HDL

3.6.1 Cardiometabolic diseases and atherosclerosis

Metabolic conditions associated with elevated CHD risk, such as dyslipidemia, insulin resistance, obesity and inflammation, are collectively called cardiometabolic diseases (CMD). Alterations in the composition, structure, and metabolism of HDL particles under such conditions lead to the loss

of their atheroprotective functions, rendering them “dysfunctional” [189]. In addition, CMD are frequently characterized by low plasma HDL-C.

Several genetically determined conditions feature low HDL-C, accelerated CHD and dysfunctional HDL. Thus, homozygous or compound heterozygous apoA-I deficiency is a rare condition which results in complete absence of apoA-I from plasma accompanied by a marked decrease in HDL-C and increased risk of premature CVD [190]. Subjects with heterozygous forms of apoA-I deficiency feature plasma HDL-C and apoA-I levels that are about 50% of normal. HDL biogenesis is disrupted in apoA-I deficiency as a result of abnormal HDL production and deficient LCAT activation by apoA-I. Remarkably, some rare variants of apoA-I, including apoA-I Milano and apoA-I Paris, are paradoxically associated with low HDL-C levels and reduced risk of CVD paralleled by greater longevity [191].

Most known ABCA1 mutations result in Tangier disease associated with the deficiency in cellular cholesterol efflux to lipid-free and lipid-poor apolipoproteins [192]. Low HDL-C is a common characteristic of ABCA1 deficiency, frequently resulting in elevated CV risk [192]. Naturally occurring mutations in LCAT are another common cause of low plasma HDL-C (Figure) [193]. Familial LCAT deficiency results from the complete loss of LCAT activity, while fish-eye disease is associated with a change in the substrate specificity of LCAT that becomes inactive towards HDL, while retaining its CE-generating activity towards apoB-containing lipoproteins. The latter property can be important in accelerating atherosclerosis in fish-eye disease relative to familial LCAT deficiency [194]. In these diseases, plasma HDL-C and apoA-I levels are reduced, while plasma FC is elevated.

Genetic defects of LPL may lead to hypertriglyceridemia and low HDL-C [195]. Thus, familial LPL deficiency is a rare disorder characterised by severe hypertriglyceridemia and marked

reductions in HDL-C and LDL-C levels. Reduced LPL activity contributes to HDL-C lowering by reducing the availability of surface constituents of TGRL, primarily FC [196].

Genetically-determined elevated CETP activity leads to decreased concentrations of HDL-C and hypertriglyceridemia [197]. In addition, HDL metabolism is substantially altered in dyslipidemic states of hypertriglyceridemia and insulin resistance, reflecting rapid removal from the circulation of small HDL particles which result from the intravascular lipolysis of TG-enriched HDL. In hypercholesterolemia, abnormalities in HDL metabolism are primarily observed as moderate reductions in plasma apoA-I and HDL-C levels.

Finally, decrease in circulating HDL-C levels, increase in triglyceride levels and HDL enrichment in serum amyloid A (SAA) at the expense of apoA-I are typical components of inflammatory states and the acute phase reaction [198].

3.6.2 Altered composition and impaired biological function

The capacity of the plasma HDL pool to remove cholesterol from peripheral cells can be reduced as a result of diminished circulating levels of HDL particles (i.e., diminished HDL quantity). The link between reduction in plasma HDL levels, impairment of normal clearance of cholesterol from the arterial wall and acceleration of atherosclerosis was proposed by Miller and Miller in 1975 [44]. An assay that quantifies clinically relevant functional properties of HDL (i.e., diminished HDL quality) rather than its plasma concentrations can however be more appropriate for the evaluation of CV risk. A considerable body of evidence points to cellular cholesterol efflux from macrophages as a biomarker of beneficial effects of HDL on CV health [187, 199]. The negative relationship between cholesterol efflux capacity of HDL and both the presence of CVD and the risk of future CV events is frequently independent of HDL-C concentrations [187, 199], additionally suggesting that low levels of HDL-C can represent a crude biomarker of impaired HDL function rather than be causally related to CVD.

Monogenetic forms of low HDL-C dyslipidemia, such as apoA-I or LCAT deficiency, can be equally characterised by the presence of HDL with defective intrinsic cholesterol efflux capacity. HDL particles are also deficient in antioxidative activity in dyslipidemic states involving low HDL-C levels, often in association with insulin resistance [200].

Altered composition of HDL, primarily depletion of apoA-I paralleled by its oxidation and glycation as well as alterations in the HDL lipidome, typically underlies functional deficiency of HDL [201]. Furthermore, functionally relevant alterations in the HDL proteome occur under pro-atherogenic conditions [202], while inflammation-induced modifications of HDL composition may further contribute to HDL dysfunction [203]. In particular, SAA can replace apoA-I in HDL, attenuating anti-inflammatory properties of the lipoprotein, whereas deficiency in PON1, PAF-AH and/or LCAT can contribute to the impairment of HDL capacity to reduce inflammation [203]. In addition, HDL glycome can be altered under pathological conditions, bearing a potential to aggravate functional HDL deficiency. Such alterations may include desialylation which decreases size and negative charge of HDL and alters interactions with lipases and cellular proteins, resulting in diminished cholesterol efflux capacity and reduced LCAT activity [112]. HDL desialylation may be proatherogenic, diminishing both HDL-promoted cellular cholesterol efflux and cholesteryl esterification rate mediated by LCAT [204]. Desialylated HDL might be internalized via scavenger receptors without provoking cholesteryl ester accumulation in macrophages [205]. Furthermore, desialylation of apoE, a protein HDL component, decreases its binding to HDL, potentially leading to impaired RCT function [206]. Interestingly, patients with CAD display distinct HDL glycosylation pattern that distinguishes them from non-CAD controls [112]. Similar differences were found between patients with metabolic syndrome and healthy subjects [207]. Furthermore, HDL glycoprotein composition differentiates between clinical groups, correlating with immunomodulatory capacity of HDL [113].

Importantly, clinical relevance of impaired antiatherogenic activities of HDL in cardiometabolic diseases largely remains indeterminate. Indeed, the very concept of HDL dysfunction has been developed using *ex vivo* assays; it is unclear whether HDL particles are also dysfunctional in a setting of a living organism.

3.6.3 Altered metabolism

The alterations of HDL proteome and lipidome are intimately linked to altered HDL metabolism, which can involve defective HDL formation and/or remodeling. The common pathways of altered HDL formation include reduced production and deficient lipidation of apoA-I upon interaction with ABCA1 reflecting the presence of defective apoA-I and/or ABCA1, which results in the decreased levels of HDL-C. Cholesterol esterification in HDL can be diminished in the presence of deficient LCAT. When hepatic SAA production is increased, apoA-I is replaced by SAA in HDL. Altered HDL remodelling include increased hepatic production of VLDL, formation of TG-enriched HDL reflecting elevated CETP activity, enhanced intravascular lipolysis of TG-enriched HDL particles by HL; accelerated HDL remodelling by PLTP and elevated hydrolysis of HDL-PL by EL and secretory phospholipase A2 (sPLA₂).

3.7 Therapeutic targeting of abnormal HDL metabolism

Reflecting growing knowledge of HDL, a concept of therapeutic normalisation of HDL metabolism was proposed in the 1990s. Development of HDL-targeting therapeutics has been concentrated around several major directions including inhibition of CETP, infusions of reconstituted HDL (rHDL, a form of small pre- β HDL), activation of LPL and use of nicotinic acid, in addition to a broad variety of other strategies.

3.7.1 CETP inhibition

The first clinical trial attempting to intervene into this pathway of HDL metabolism was conducted with torcetrapib which was administered to statin-treated patients prone to coronary events whose HDL-C levels were increased by +72% and LDL-C levels decreased by -25% [208]. Unexpectedly, both overall and CV mortality were significantly elevated in the treatment arm relative to placebo. This deleterious effect was proposed to reflect off-target hypertensive effects of the drug [209].

Dalcetrapib, the second CETP inhibitor which entered clinical trials, raised HDL-C by +35% without affecting LDL-C levels. The development of the drug was discontinued due to the lack of positive effects on overall and coronary events-associated mortality [210]. The increase in HDL-C was suggested to be too modest for potential clinical benefits. Evacetrapib, another CETP inhibitor, was investigated in high-risk patients with vascular disease and did not result in a lower rate of CV events, whilst showing large increases in HDL-C (+133%) and reductions in LDL-C (-31%) concentrations [211]. Anacetrapib, the most recent addition to the class of CETP inhibitors, was thoroughly tested for safety and was found to be clinically effective, decreasing incidence of major coronary events in the absence of increased risk of death, cancer, or other serious adverse events [212]. The beneficial effect of the drug was however modest (-9%) despite large increase in HDL-C (+104%); in addition, anacetrapib was found to accumulate in adipose tissue [213] and its development was stopped. The clinical benefit of anacetrapib could be accounted for by the reduction in non-HDL-C, and more specifically, small VLDL levels, suggesting little clinical role of the HDL-C raising [213]. Therefore, despite considerable initial promise, CETP inhibition provides insufficient CV benefit for clinical use in patients treated with statins.

3.7.2 rHDL infusion

The first drug of this class entering clinical trials was ETC-216 comprised of apoA-I Milano protein supplied with a phospholipid [214]. The infusions of ETC-216 were indeed able to decrease the mean atheroma volume in patients with acute coronary syndrome (ACS) [214]. However, the drug was not pushed into further clinical development primarily due to high production costs compared to its moderate clinical benefit. Furthermore, ETC-216 was responsible for a dose-dependent increase in neutrophils [215].

Seeking improvement in safety and efficacy, a formulation called **MDCO-216** comprised of apoA-I Milano and phosphatidylcholine was introduced [216] which did not induce adverse immunostimulation [215], but neither showed effectiveness in a clinical setting [217].

The initial success with the trials of ETC-216 was followed by the development of **CSL-111** consisting of normal human apoA-I combined with soybean phosphatidylcholine. Short-term infusions of CSL-111 did not reduce atheroma volume and were slightly hepatotoxic at high concentrations, but did improve the plaque characterization index and coronary score [218]. The drug was reformulated as **CSL-112** that did not contained hepatotoxic cholate and was essentially homogenous in the particle size. In a phase II trial, CSL-112 was well tolerated and acutely enhanced cholesterol efflux in patients with CVD [219], probably acting via remodeling the circulating HDL pool through formation of small particles possessing enhanced anti-atherogenic activities [220].

Another infusion agent named **CER-001**, a negatively charged rHDL containing human recombinant apoA-I, sphingomyelin and phosphatidylglycerol, was somewhat efficient in patients with extreme conditions including homozygous familial hypercholesterolemia [221] and extensive plaque-burdened ACS [222], but was eventually proven to be ineffective in statin-treated patients with more typical presentation of ACS [223, 224].

A modification of HDL infusion therapy involved reinfusion of autologous **delipidated HDL** after their selective delipidation *ex vivo* [225]. This approach converted large, lipid-rich HDL to small, lipid-poor particles with enhanced atheroprotective activities [97] and tended to reduce total atheroma volume after seven weekly injections in ACS patients undergoing cardiac catheterisation as compared to control plasma apheresis treatment [225].

ApoA-I-mimetic peptides structurally resemble apoA-I in a way that they all contain amphipatic α -helical structures albeit often do not share any sequence homology to apoA-I yet possessing similar biological function [226]. These agents can beneficially impact HDL metabolism upon infusion. Unlike recombinant or purified apoA-I proteins, apoA-I mimetics are short-chain and easy to produce. Moreover, they can be administered orally, though their oral bioavailability is limited [227]. Initial reports were promising on the effectiveness of these agents in animal models but a recent report of aggregated results shows inconsistencies between *in vitro* and *in vivo* functional properties of seven apoA-I mimetic peptides [228].

Another therapeutic strategy features infusions of **recombinant LCAT**, a single HDL protein. A formulation called **ACP-501** favorably modified HDL metabolism after a single intravenous infusion [229]; an approach involving multiple intravenous infusions is currently being assessed in a phase 2 trial.

To sum up, none of the HDL infusions has proven to be both effective and safe up to date; furthermore, intravenous infusions appeared to be too impractical for everyday therapy.

3.7.3 LPL activation

Up-regulation of LPL activity is normally considered as a means to reduce plasma TG but this approach is highly effective in elevating HDL-C levels and can be added to the list of HDL-targeting therapies. ApoC-III represents a promising therapeutic target for the treatment of

hypertriglyceridemia as it inhibits TGRL hydrolysis by LPL [230]. Recent phase I trial of the administration of **volanesorsen**, an apoC-III antisense oligonucleotide, in healthy subjects revealed reductions in plasma apoC-III and TG levels accompanied by elevated HDL-C [230]. This approach is currently entering clinical trials [231].

Fibrates is a class of compounds that work by activating peroxisome proliferator-activated receptor α (PPAR α). PPAR α is active in hepatocytes where it stimulates production of apoA-I and apoA-II and inhibits production of apoC-III, thereby enhancing LPL activity [232]. As a result, fibrates increase concentrations of HDL-C and small pre- β 1-HDL. Fibrates are normally considered for treatment of hypertriglyceridemia and provide moderate clinical benefits [233] but their side-effects include formation of cholesterol gallstones, rhabdomyolysis and myopathy. A novel member of this drug class, pemafibrate, did not show major adverse effects and recently passed phase 3 of clinical trials [234].

Another approach to combat hypertriglyceridemia employs an adenoviral vector **AMT-011** expressing human LPL, with an intent to replace a faulty LPL gene with a properly functioning copy [235]. If successful, this strategy should equally be able to increase HDL-C.

3.7.4 Nicotinic acid

In the pre-statin era, **nicotinic acid**, also known as niacin and vitamin B3, was considered as a promising candidate to prevent CVD, reflecting its ability to raise HDL-C, decrease TG, alleviate carotid intima-media thickening and reduce incidence of stenosis [232]. However, recent large-scale studies performed in patients on statins failed to demonstrate clinical benefits of niacin treatment [236, 237]. In addition, Cochrane meta-analysis of long-term clinical trials did not find evidence for niacin's efficiency in patients already treated with statins [238]. Prolonged exposure to niacin was also found to be associated with increased risk for onset of diabetes [238]. Despite

these limitations, nicotinic acid may still be helpful for individuals not tolerating statins. Indeed, a meta-analysis reveals that niacin is capable of reducing CV events in the absence of statin treatment [239].

3.7.5. Other agents

Other agents employed within the paradigm of HDL-targeting therapy can be classified into bromodomain and extra-terminal domain (BET) inhibitors, nuclear receptors agonists and miR inhibitors.

BETs are protein-interaction modules involved in chromatin organization and modulation of gene transcription. **Apabetalone (RVX-208)**, a small **BET inhibitor** designed to directly upregulate hepatic secretion of apoA-I, moderately raised HDL-C and showed promising results in the early stages of clinical trials [240], but later failed to present significant clinical benefits compared to placebo [241]. In recent trials, vulnerability of atherosclerotic plaques was however favorably modified by apabetalone [242]. Pooled together, results from available clinical trials of apabetalone reveal a reduction in CV events relative to placebo [243].

Nuclear receptor agonists are primarily represented by those acting LXR. **LXR agonists** raise HDL-C and exert a multitude of antiatherogenic actions, including beneficial effects on cholesterol metabolism, inflammation, proliferation and insulin sensitivity [244]. Major adverse effects of LXR agonists however involve hepatic steatosis and nervous system deficiency [245]. There are two LXR types, notably LXR α expressed in the liver, kidney, and several other organs, and LXR β expressed ubiquitously [246]. Importantly, specific activation of LXR α retains beneficial effects on HDL whilst lacking lipogenic effects and may represent a promising strategy of dyslipidemia treatment.

MiRs are small RNAs that do not code proteins, and, hence, were earlier considered as “junk RNA” to be later discovered to play important biological role in the development, repair and homeostasis. HDL transports miRs, one of which, miR-33, inhibits ABCA1 expression [247, 248]. Although animal models support the role of miR-33 as a potential therapeutic target for HDL biogenesis, the efficacy of this approach in humans remains to be established.

4. LDL

4.1 Structure and composition

Similarly to HDL, plasma LDL is not a structurally homogeneous entity but consists of different particles varying in size, density, charge, and lipid and protein content. Two distinct LDL phenotypes have been described: phenotype or pattern A, with a predominance of large buoyant LDL (lbLDL) particles, and phenotype or pattern B, with a predominance of small dense LDL (sdLDL) particles. An intermediate phenotype, A/B, has also been characterized [249].

4.1.1 Proteome

ApoB-100 is the major structural component of LDL, accounting for over 95% of the total protein mass. There are, however, a number of other plasma proteins which can temporarily bind to or be associated with LDL particles in the circulation. Using a global approach involving techniques such as ultracentrifugation, 2D gel electrophoresis, amino acid sequencing, and peptide mass fingerprinting by time-of-flight (TOF) or tandem mass spectrometry, proteomic analyses have identified over 50 proteins to date, in addition to apoB-100 [249]. They include apolipoproteins regulating apoB metabolism and lipid transport (apoC-II, apoC-III, apoE, apoA-I, apoA-IV, and apoF) as well as proteins associated with inflammation (apolipoprotein D (apoD), apoJ, apoM, SAA4, PON1, prenylcysteine oxidase 1, migration inhibitory factor-related protein 8, and retinol

binding protein), thrombosis (fibrinogen a chain), the complement system, and innate immunity and antimicrobial functions (lysozyme C, A1AT, apoL-1, and transthyretin) [249]. Comparisons of the LDL and VLDL proteomes have revealed, further, that the proteins are preferentially distributed, with a greater number of proteins associated with VLDL than LDL. Taken together, these findings suggest that LDL particles may acquire some proteins directly from plasma, HDL particles, or peripheral cells, and not only through the intravascular remodeling of VLDL. Thus, some of these proteins may have LDL-specific functions [249].

4.1.2 Lipidome

LDL is a CE-rich lipoprotein and displays high CE content of approximately 55% of total lipid. Overall, LDL shows a low phospholipid to cholesterol ratio of 0.35. In relation to the sum of all analyzed glycerophospholipids and sphingolipids, PC was by far the most abundant lipid class at around 70%. As compared to other lipoproteins, LDL displayed a high content of SM (25%). Moreover, LDL carried more than 5-fold more of Cer than HDL. PE and PE-based plasmalogen had approximately 1% share in LDL lipidome [250].

4.1.3 Glycome

LDL apoB carries 4.4 wt% of carbohydrate residues [251]. Sialic acids are present in LDL as terminal carbohydrates of biantennary carbohydrate chains in apoB and of carbohydrate chains in gangliosides [252, 253].

4.2 Metabolism

4.2.1 Biosynthesis

In the circulation, the endothelium-bound LPL hydrolyzes TG in VLDL and turns it into LDL particles. LPL is expressed in the peripheral vessels, especially in muscle and adipose tissues. In addition, VLDL TG may be exchanged for CEs of HDL by CETP. Therefore, size, density and

composition of LDL particles depend on LPL and CETP activities. LDL particles are rich in CEs and can be absorbed by the liver and peripheral tissues via interactions between apo-B100 and LDL receptor (LDLR) [254]. Despite the volume of research on LDL particle size and CHD risk, the origin of sdLDL particles is still not well understood. Studies assessing kinetics of apoB-containing lipoproteins with stable isotope methodology and multicompartmental modeling have proposed several metabolic pathways. Positive correlations between sdLDL and plasma TG concentrations suggest that sdLDL particles are derived directly from LDL precursor particles and largely produced independently of lbLDL particles. Packard et al. [255] observed that healthy individuals with elevated plasma TG levels and LDL phenotype B reveal delayed catabolism of apoB in large VLDL, higher production of apoB in small VLDL, delayed lipolysis of both large and small VLDL, a marked decrease in the catabolism of LDL apoB, and diminished de novo production of apoB in IDL and LDL. In contrast, Aguilar-Salinas et al. [256] concluded, based on data from a study of familial combined hyperlipidemia kindred, that the formation of sdLDL particles is due to a clear precursor-product relationship between apoB in lbLDL and sdLDL, which is promoted by the delipidation of lbLDL. To address the discordant findings of these tracer studies, Geiss et al. [257] studied sdLDL particle formation by measuring rebound apoB concentrations in LDL subfractions after LDL apheresis. Using this approach in a study of heterozygous familial hypercholesterolemic individuals on statin therapy, they determined that the data were best fit with a model in which there was direct apoB production into VLDL and IDL, followed by direct conversion into large, intermediate, and small dense LDL (58% of total sdLDL), as well as the simultaneous delipidation of lbLDL to sdLDL (42% of total sdLDL) [249].

Although the data are not conclusive, it can be argued that sdLDL particles most likely originate from multiple sources and, furthermore, that the contribution of each pathway to the total sdLDL apoB pool depends on underlying metabolic conditions. Support for this concept comes from a

study by Zheng et al [258], who assessed the production and catabolism of apoB-containing lipoproteins according to the apoE and apoC-III content of particles isolated by immunoaffinity chromatography and density ultracentrifugation. ApoE and apoC-III possess well-known functions as offsetting regulators of apoB lipoprotein metabolism, which help to clarify the metabolic origin of the particles. Zheng et al. reported that when plasma TG levels were normal [<150 mg/dl (1.7 mmol/l)], sdLDL particles were formed primarily from VLDL and lbLDL particles which were secreted directly by the liver and subsequently delipidated to the denser subfraction. In hypertriglyceridemia, however, more sdLDL particles than lbLDL particles were secreted by the liver, more VLDL particles were converted to particles of sdLDL density than were catabolized, and the fraction of lbLDL delipidated to sdLDL increased [249].

4.2.2 Catabolism

The LDLR is expressed in the liver cells and other tissues, so that about 70% of circulating LDL particles are transferred into the liver and 30% by other tissues [254]. Metabolic studies have demonstrated that sdLDL remains in circulation longer than lbLDL before being cleared by the LDLR. It is hypothesized that delayed catabolism results in the lipid composition and size of sdLDL being altered through the CETP-mediated exchange of CE and TG between LDL and VLDL and/or HDL and, subsequently, by the action of HL on core TG and surface phospholipids [249].

4.3 Altered composition and metabolism in cardiometabolic diseases

Patients with condition like familial hypercholesterolemia (FH) feature autosomal dominant disorder, which causes defects in the gene that encodes the LDLR, so their LDL-C levels are severely increased, leading to a major increase in the risk of CVD for these patients [259].

Epidemiological studies have documented that sdLDL cholesterol levels are elevated in cases of myocardial infarction, stroke, and overall CVD [249]. Evidence from in vitro studies underscores the enhanced atherogenicity of sdLDL and, in turn, the potential for increased CHD risk due to higher sdLDL concentrations. sdLDL particles have been shown to be more readily oxidized in vitro than lbLDL [249]. They have enhanced affinity for proteoglycans in the arterial wall, contain an increased percentage of glycated apoB, and are overall more susceptible to glycation, relative to larger LDL particles. A recent study of modified LDL has also revealed that the activity of the inflammatory marker lipoprotein-associated phospholipase A2 (LpPLA2) was increased in apoB-containing lipoproteins in phenotype B, but not in diabetic individuals with phenotype A or in normolipidemics [249].

A critical question pertaining to the function, metabolism, and atherogenicity of LDL subfractions is the complement of exchangeable proteins associated with a particular particle size. Davidsson et al. [260] used surface-enhanced laser adsorption/ionization and matrix-assisted laser-desorption ionization-TOF/TOF mass spectrometry techniques to compare the apolipoprotein composition of LDL subfractions in men with metabolic syndrome or T2D and manifesting LDL phenotype B with the apolipoprotein composition of LDL subfractions in healthy men having phenotype A. In this study, phenotype B was characterized by a predominance of LDL particles of d 1.040–1.060 g/ml (24.4–25.2 nm in diameter), whereas phenotype A referred to a predominance of particles of d 1.030–1.040 g/ml (25.2–26.5 nm). After the data were adjusted for apoB-100 content, the sdLDL particles in the individuals with LDL phenotype B were observed to be enriched in all isoforms of apoC-III and depleted, in descending order, in apoC-I, apoE, and apoA-I, whereas the sdLDL particles in normolipidemic individuals with phenotype A had more apoC-I, apoA-I, and apoE and less apoC-III. In addition, there was a significant correlation between the sdLDL apoC-III concentration and the affinity of

LDL to bind arterial proteoglycans. The analyses revealed no significant differences in the exchangeable apolipoprotein content of lbLDL in the study cohorts. These findings underscore the significant regulatory role that apoC-III has in sdLDL metabolism [249].

Alterations of LDL composition in CMD are largely undeterminate. LDL glycome can be altered in disease. Desialylation of LDL by neuraminidases (sialidases) and other glycoside hydrolases may occur *in vivo* under normal and, particularly, under pathological conditions [261]. As a result, sialic acid content is diminished in LDL isolated from plasma of patients with CVD and T2D relative to LDL from healthy donors [262-265]. Moreover, atherogenic immune complexes present in the circulation contain LDL that display modifications similar to those found in desialylated LDL [266]. When administered to a primary culture of human aortic intimal cells or to a culture of human monocyte-derived macrophages, desialylated LDL induce intracellular cholesterol accumulation [262, 265, 267, 268]. Native LDL desialylated with neuraminidase *in vitro* reveal similar biological activity [205, 269].

LDL can undergo *in vivo* modifications by glyco-oxidation [270], glycation [271], oxidation [272], and desialylation [273] that increase LDL atherogenicity. Such modified LDL is taken up by macrophages through scavenger receptors, leading to the formation of foam cells. More specifically, uptake of desialylated LDL by human and mouse macrophages can be mediated by both scavenger receptors [265] and galactose-specific lectin receptors which recognize terminal galactose residues of LDL exposed after desialylation [274]. LDL apoB can also be oxidized and glycated [271, 272] while alterations of other LDL-associated proteins were not studied.

Similarly, unclear remain alterations in the LDL lipidome in CMD.

4.4 Therapeutic targeting of abnormal LDL metabolism

Statins, or 3-hydroxy-methylglutaryl coenzyme A reductase inhibitors, decrease hepatic cholesterol biosynthesis and reduce serum LDL-C and triglyceride levels, acting via enhanced expression of hepatic LDLR. Landmark clinical trials have convincingly demonstrated the efficacy of statins for both primary and secondary prevention of CHD. It has been proposed that statins exert both LDL-C-dependent and LDL-C-independent (or pleiotropic) effects. In addition, clinical studies show statin benefits in diseases that are not clearly related to LDL-C elevation, but some of the outcomes may be due to direct cholesterol lowering. Thus, decreased gallstone formation could be related to decreased hepatic cholesterol formation, as decreased plasma cholesterol reduces platelet aggregation and could lead to diminished occurrence of deep vein thrombosis, and decreased LDL-C can affect the progression of renal disease by decreasing renal artery atherosclerosis [275].

Despite the long-term documented benefits of statin use, controversy exists over using statins for primary prevention as some believe that risks outweigh benefits for those without CVD.

Although many people tolerate statins without issue, reported side effects in as many as one in five people include severe muscle aches, memory disturbance, sexual dysfunction, cataracts, and diabetes. Statin therapy could also cause myopathy, rhabdomyolysis, and liver function abnormalities in some people. Therefore, in older adults, intensive statin regimens remain a debate. Statins have also been associated with cognitive impairment including memory loss, forgetfulness, and confusion as well as increased risk for elevated blood glucose and for developing T2D [276].

Statin therapy – whether pravastatin, atorvastatin, or rosuvastatin – in individuals with dyslipidemia, familial combined hyperlipidemia, metabolic syndrome, or T2D significantly decreased the pool size of apoB-containing lipoproteins in a dose-dependent manner by

increasing the fractional catabolic rate of apoB, as predicted by the inhibitory effects of statins on LDLR activity.

Other approaches to target elevated LDL-C involve ezetimibe, which helps reducing blood cholesterol by limiting the absorption of dietary cholesterol [277], and PCSK9 inhibitors that enhance hepatic LDLR expression by inhibiting PCSK9 involved in the degradation of LDLR and make liver absorb more LDL cholesterol, thus lowering the amount of cholesterol in the circulation, especially in individuals with hypercholesterolemia or in post-CHD patients who have intolerance to statins or other cholesterol medications [278].

WORKING HYPOTHESIS AND OBJECTIVE

Available data reveal that abnormal composition of HDL and LDL is associated with CMD. In parallel, in vitro assays of HDL particles isolated from metabolically compromised patients often show diminished anti-atherosclerotic activity, and LDL particles isolated from such patients display pro-atherogenic features in such tests, all the while simultaneously possessing altered physicochemical properties. These findings clearly indicate that structure and composition of these lipoproteins are important in their proper functioning.

With a decrease of cost and an increase in performance of mass-spectrometrical systems, protein moieties of lipoprotein particles have been extensively studied, while lipidomic and particularly, glycomic moieties remain less well investigated. There is however a large body of evidence documenting the importance of lipid and carbohydrate moieties in the procurement of biological functions of lipoproteins, primarily of HDL and LDL. It is therefore necessary to provide an appropriate insight into individual molecular components of lipid and glycan moieties of HDL and LDL that allow for a healthy performance of these particles.

We therefore hypothesize that certain molecular components of HDL and LDL might be enriched or depleted in CMD and that altered abundances of these components ought to be associated with deficient biological function of said lipoproteins. We further hypothesize that disturbances in certain metabolic pathways can be observed as a result of, or as a reason for, the deficient function of the lipoproteins.

To test our hypothesis, we employed protocols for the assessment of lipidomic composition of HDL, as well as glycomic composition of HDL and LDL using omics technology in parallel with the evaluation of their biological functionality. We deployed these protocols on HDL and LDL

particles isolated from healthy subjects and patients with CMD. We focused at apoA-I deficiency, a genetically determined dyslipidemia resulting in elevated CV risk, and at acute myocardial infarction, an acute presentation of CVD. Thus, in this body of work our objective was to reveal structure-function relationships in human plasma HDL and LDL in healthy subjects and in patients with CMD, putting an emphasis on the lipidome and the glycome. The data obtained were analysed using original data analysis scripts developed in-house.

METHODS

1. Subjects

In our studies we focused on the structure and function of human plasma lipoproteins in individuals with compromised lipid metabolism. We were interested in chronic (genetically-determined) and acute forms of dyslipidemia both well-known to be associated with CVD. As a chronic dyslipidemia, we chose familial apoA-I deficiency (FAID), and as acute one, we chose ST-elevated myocardial infarction. Subjects recruited for our studies were, thus, split into the following categories: subjects with a rare hereditary mutation in the *APOA1* gene, and recent survivors of ST-elevated myocardial infarction.

For the first cohort of subjects we recruited four Caucasian male and one female heterozygous patients from a family with a nonsense mutation at *APOA1* codon -2, Q[-2]X, genotyped according to Santos et al [58], and eight healthy male Caucasian normolipidemic, non-smoking age-matched controls with no signs of a known disease, all recruited at the Heart Institute (InCor) of the University of Sao Paulo Hospital in Sao Paulo, Brazil, as previously described [279]. None of the patients or controls had pathologies affecting lipid metabolism such as T2D Mellitus, kidney and thyroid diseases. All subjects were off lipid-lowering medication for at least 2 months at the time of assessment. Written informed consent was obtained from all subjects, and the project was approved by the Ethics Committee of the Heart Institute-InCor in accordance with local institutional guidelines conformed to the Declaration of Helsinki.

The second cohort consisted of twelve male patients presenting STEMI recruited at the Heart Institute-InCor University of Sao Paulo Medical School Hospital (São Paulo, Brazil). All patients were recruited within no later than 24 hours of ischaemic symptoms and clinical presentation in

the Emergency Room. The diagnosis of AMI was confirmed by clinical assessment by a cardiologist, including electrocardiography changes, troponin I elevation, and the presence of CAD on coronary angiography in accordance with the Braunwald criteria [280]. Exclusion criteria were: female gender, smoking, secondary causes of hyperlipidemia (e.g; thyroid dysfunction), presence of inflammatory or infectious diseases, AMI or stroke during last six months, use of anti-inflammatory drugs (except aspirin) or antioxidant vitamins and use of lipid-lowering drugs during the month preceding the clinical event. Importantly, alterations in lipid metabolism observed in this cohort were therefore unrelated to lipid lowering medication. Ten male healthy, non-smoking, normolipidemic, age-matched subjects were recruited as controls. Written informed consent was obtained from all study subjects and the project was approved by the Ethics Committee of InCor in accordance with local institutional guidelines conformed to the Declaration of Helsinki.

2. Blood samples

Venous blood was collected from the antecubital vein into sterile evacuated tubes (Vacutainer) in the presence or absence (to obtain serum) of ethylenediaminetetraacetic acid (EDTA) (final concentration, 1.8 mg/ml) after an overnight fast. After blood collection, EDTA plasma was immediately separated by centrifugation at 4°C (20 min at 2000 rpm followed by 5 min at 4500 rpm), while serum was obtained after incubating samples for 30 min at room temperature and centrifuging for 10 min at 3000 RPM. Sucrose (final concentration, 0.6%) was added as a cryoprotectant for lipoproteins [281, 282] and samples were aliquoted and stored at -80°C under nitrogen. Each aliquot was thawed only once directly before analyses.

3. Isolation of lipoproteins

An aliquot of 3 ml serum and an aliquot of plasma were thawed and subjected to a single step, isopycnic nondenaturing density gradient ultracentrifugation in a Beckman SW41 Ti rotor at 40,000 rpm for 44 h in a Beckman XL70 ultracentrifuge at 15°C as described previously [283, 284]. Briefly, plasma density was increased to 1.21 g/ml by adding dry solid KBr. A discontinuous density gradient was then constructed as follows: 2 ml of a NaCl/KBr solution (d=1.24 g/ml), 3 ml plasma (d=1.21 g/ml), 2 ml of a solution (d=1.063 g/ml), 2.5 ml of a solution (d=1.019 g/ml), and 2.5 ml of a NaCl solution (d=1.006 g/ml). All density solutions contained sodium azide (0.01%), EDTA (0.01%), and gentamicin (0.005%), pH 7.4. After the ultracentrifugation, gradient was fractionated in predefined volumes from the meniscus downwards with an Eppendorf precision pipette, yielding five major HDL subfractions: large, light HDL2b (d 1.063–1.087 g/ml) and HDL2a (d 1.088–1.110 g/ml), and small, dense HDL3a (d 1.110–1.129 g/ml), HDL3b (d 1.129–1.154 g/ml) and HDL3c (d 1.154–1.170 g/ml) (Figure 12). Lipoproteins were extensively dialysed against phosphate-buffered saline (PBS; pH 7.4) at 4°C in the dark, stored at 4°C and used within 8 days for lipidomic analysis and functional studies. The validity and reproducibility of this density gradient procedure, which facilitates preparative fractionation of HDL particle subspecies in a non-denaturated, native state, have been extensively documented [283, 285, 286].

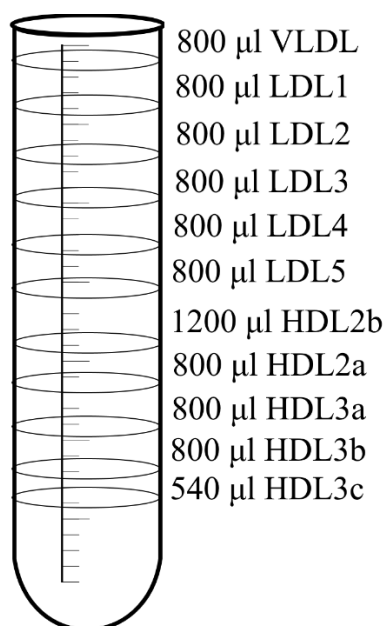


Figure 12. Density gradient distribution

4. Chemical analysis of lipoproteins

TC, FC, PL and TG contents of isolated lipoprotein subfractions were determined using commercially available assays (Diasys, France). CE was calculated by multiplying the difference between total and free cholesterol concentrations by 1.67. Total lipoprotein mass was calculated as the sum of total protein, CE, FC, PL and TG. ApoA-I and apoA-II content in HDL was quantified using commercially available kits (Diasys, France) [85].

LCAT activity of HDL was measured using a commercially available fluorescent kit for plasma LCAT activity from Roar Biochemical (New York, NY, USA) that evaluates accumulation of free cholesterol in the samples. The protocol was modified to include in the assay an amount of HDL similar to that employed in the measurement of LCAT activity in plasma. More specifically, a fixed amount of HDL protein of 50 μg was mixed with reagents according to the manufacturer's instructions. The coefficient of variation of the assay was 2.4%.

5. Heterogeneity and mean size of HDL

The heterogeneity of HDL was evaluated by native PAGE using precasted 4-12% gradient gels from Invitrogen (France) according to the manufacturer's instructions. This approach allowed detecting lipid-free/lipid-poor apoA-I by Western blotting and calculating mean HDL size as described elsewhere [287]. Briefly, 15 µg of HDL protein or 5 µg of lipid-free ApoA-I were applied to NuPAGE Tris-acetate 4-12% gels (Invitrogen, CA, USA) and the gels were run for 3h at 150V in the MOPS buffer according to the manufacturer's instructions. Following the transfer to nitrocellulose, goat anti-human apoA-I antibody (Merck) and donkey anti-goat IRDye 800CW antibody (LI-COR, Lincoln, NE, USA) were used as a primary and secondary antibody, respectively, to detect apoA-I.

The mean HDL size was calculated using the PageRuler Broad Range Unstained Protein Ladder as a calibration (Thermo Scientific, USA). Gels were scanned using Odyssey Imaging System for Western blots and gel imaging (LI-COR, Lincoln, NE, USA) and the mean position of each peak was identified using the system's software.

6. Lipidomic analysis

Lipidomic analysis in our laboratory is done through several major steps: extraction of lipids from the sample, their separation by high-performance liquid chromatographer, followed by detection using MS/MS, and finished with data aggregation and analysis (Figure 13).

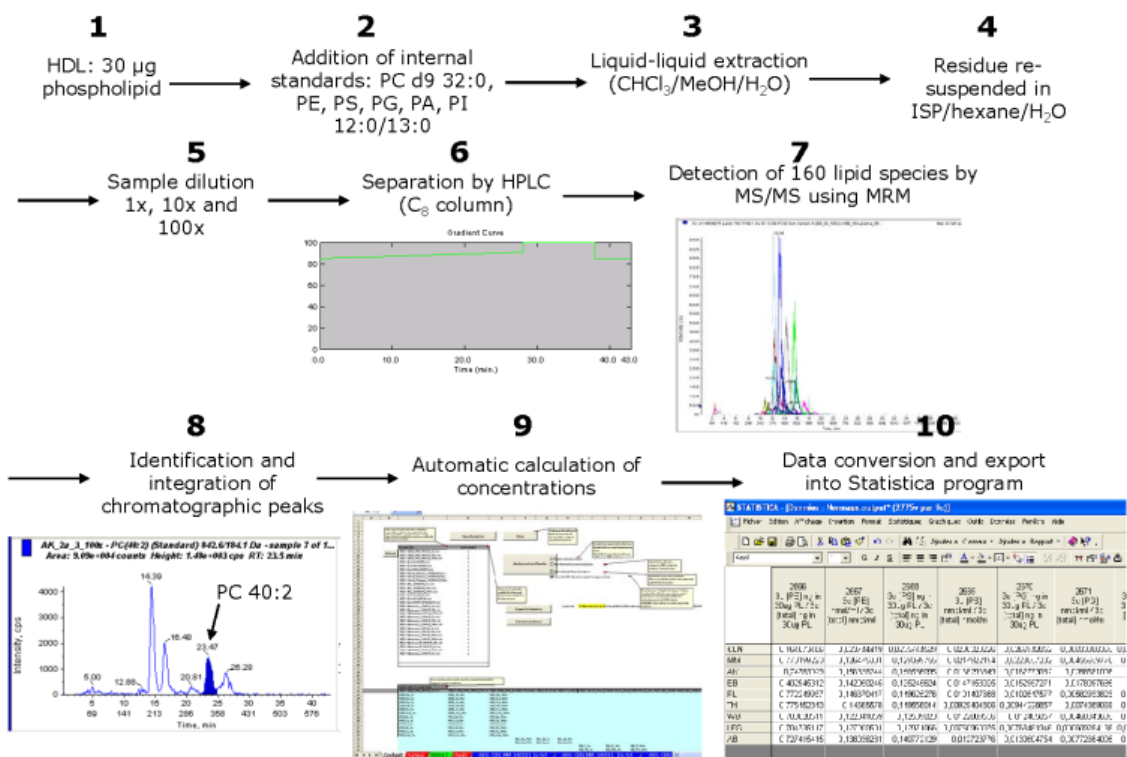


Figure 13. An in-house pipeline for extraction and separation of lipids, followed by detection using MS/MS and automated acquisition of the resulting data

6.1 Lipid standards

1,2-Dipalmitoyl-sn-glycero-3-phosphocholine-N,N,N-trimethyl-d9 (PC 16:0/16:0 d9), 1-lauroyl-2-tridecanoyl-sn-glycero-3-phospho-(1'-myo-inositol) (PI 12:0/13:0), 1-dodecanoyl-2-tridecanoyl-sn-glycero-3-phosphoethanolamine (PE 12:0/13:0), 1-dodecanoyl-2-tridecanoyl-sn-glycero-3-phospho-(1'-rac-glycerol) (PG 12:0/13:0), 1-dodecanoyl-2-tridecanoyl-sn-glycero-3-phosphate (PA 12:0/13:0), 1-dodecanoyl-2-tridecanoyl-sn-glycero-3-phospho-l-serine (PS 12:0/13:0), 1-pentadecanoyl-2-hydroxy-sn-glycero-3-phosphocholine (LPC 15:0), and N-heptadecanoyl-d-erythro-sphingosine (Cer d18:1/17:0) were used as internal standards. 1-Palmitoyl-2-hydroxy-sn-glycero-3-phosphocholine (LPC 16:0), 1-stearoyl-2-hydroxy-sn-glycero-3-phosphocholine (LPC 18:0), 1,2-dimyristoyl-sn-glycero-3-phosphocholine (PC 14:0/14:0), 1-myristoyl-2-palmitoyl-sn-glycero-3-phosphocholine (PC 14:0/16:0), 1,2-dipalmitoyl-sn-glycero-3-phosphocholine (PC 16:0/16:0), 1-palmitoyl-2-stearoyl-sn-glycero-3-phosphocholine (PC

16:0/18:0), 1-palmitoyl-2-oleoyl-sn-glycero-3-phosphocholine (PC 16:0/18:1), 1-palmitoyl-2-linoleoyl-sn-glycero-3-phosphocholine (PC 16:0/18:2), 1,2-distearoyl-sn-glycero-3-phosphocholine (PC 18:0/18:0), 1-stearoyl-2-oleoyl-sn-glycero-3-phosphocholine (PC 18:0/18:1), 1-stearoyl-2-linoleoyl-sn-glycero-3-phosphocholine (PC 18:0/18:2), 1-stearoyl-2-arachidonoyl-sn-glycero-3-phosphocholine (PC 18:0/20:4), 1-palmitoyl-2-docosahexaenoyl-sn-glycero-3-phosphocholine (PC 16:0/22:6), 1-stearoyl-2-docosahexaenoyl-sn-glycero-3-phosphocholine (PC 18:0/22:6), 1,2-distearoyl-sn-glycero-3-phosphoethanolamine (PE 18:0/18:0), 1-heptadecanoyl-2-(9Z-tetradecenoyl)-sn-glycero-3-phospho-(1'-myo-inositol) (PI 17:0/14:1), N-stearoyl-d-erythro-sphingosine (Cer d18:1/18:0), 1,2-distearoyl-sn-glycero-3-phosphate (PA 18:0/18:0), 1,2-distearoyl-sn-glycero-3-phospho-(1'-rac-glycerol) (PG 18:0/18:0), and 1-palmitoyl-2-linoleoyl-sn-glycero-3-phospho-l-serine (PS 16:0/18:2) were purchased from Avanti Polar Lipids (Alabaster, AL) to construct separate calibration curves as a function of the number of double bonds in fatty acid moieties and of their chain length.

6.2 Lipid extraction

HDL subpopulations were extracted according to a procedure adapted from Larijani et al [288]. Briefly, 30 µg of total PL mass determined using a commercially available assay was added to 4 ml of cold CHCl₃/acidified CH₃OH (5:2 v/v) containing 4 µg of PC d9 32:0, 100 ng of PI 25:0, 80 ng of PE 25:0, 80 ng of PA 25:0, 40 ng of PS 25:0, 20 ng of PG 25:0, and 20 ng of Cer 17:0. A blank (PBS) and a control (HDL2 obtained from a reference normolipidemic plasma) sample were extracted in parallel with each batch to ensure quality control; each sample was corrected for blank readings. K₄EDTA (200 mM) solution was added (1:5 v/v), and the mixture was vortexed for 1 min and centrifuged at 3,600 g for 10 min at 4°C. The organic phase was transferred into 5 ml Chromacol glass tubes and dried under nitrogen. Lipids were reconstituted

into 150 μ l isopropanol-hexane-water (10:5:2 v/v), transferred into LC/MS amber vials with inserts, dried under nitrogen, and resuspended in 40 μ l of isopropanol-hexane-water (10:5:2 v/v). Molecular lipid species were analyzed and quantified by LC/MS/MS.

6.3 LC/MS analysis

Seven principal phospholipid subclasses PC, LPC, PE, PI, PG, PS, PA and two principal sphingolipid (SL) subclasses SM and Cer, which together comprise approximately 160 individual molecular lipid species and account for >95% of total plasma glycerophospholipid (GP) and SM [289, 290], were assayed by LC/MS/MS. The lipid subclasses were divided into major (those whose content was >1% of total PL + SL, i.e., PC, SM, LPC, PE, and PI) and minor (those whose content was <1% of total GP + SL, i.e., PG, Cer, PS, and PA).

6.4 Quantification

Lipids were quantified by LC-ESI/MS/MS using a QTrap 4000 mass spectrometer (AB Sciex, Framingham, MA) equipped with a turbo spray ion source (300°C) combined with an LC20AD high-performance liquid chromatography (HPLC) system, a SIL-20AC autosampler (Shimadzu, Kyoto, Japan), and the Analyst 1.5 data acquisition system (AB Sciex). Quantification of GPs and SLs was performed in positive-ion mode, except for PI species that were detected in negative-ion mode.

Sample (4 μ l) was injected onto a Symmetry Shield RP8 3.5 μ m 2.1 \times 50 mm reverse phase column (Waters Corporation, Milford, MA) using a gradient from 85:15 to 91:9 (v/v) methanol-water containing 5 mM ammonium formate and 0.1% formic acid at a flow rate of 0.1 ml/min for 30 min. Lipid species were detected using multiple reaction monitoring reflecting the headgroup fragmentation of each lipid class. PC, LPC, and SM species were detected as product ions of m/z

184; PE, PS, PG, and PA as neutral losses of respectively m/z 141, 185, 189, and 115; and PI molecular species as product ions of m/z 241. Air was used as nebulizing gas and N_2 as collision gas. PE, PS, PG, PI, PA, and Cer species were monitored for 18 ms, while PC, LPC, and SM species were monitored for 30 ms at a unit resolution (0.7 amu at half peak height).

Lipids were quantified using calibration curves specific for the nine individual lipid classes with up to 12 component fatty acid moieties. Twenty-three calibration curves were generated in nondiluted and 10-fold diluted matrices to correct for matrix-induced ion suppression effects. More abundant lipid species that displayed a nonlinear response in nondiluted extracts were quantified from a 10- or 100-fold diluted sample. An in-house-developed Excel Macro script (Microsoft Office 2010, Redmond, WA) was used to compile data from the three successive injections.

6.5 Sphingosine-1-phosphate

S1P was determined in HDL subspecies as described by Nofer et al [173]. Methanol (1 ml) containing 2.5 μ l concentrated HCl was added to 100 μ L of HDL solution (0.5 to 2.0 mg HDL protein per ml buffer as a function of HDL subspecies). C17-S1P (15 pmol) was added as internal standard and lipids were extracted by addition of 1 ml chloroform, 200 μ l NaCl (4 M) and 100 μ l NaOH (3 M). The alkaline aqueous S1P-containing phase devoid of other sphingoid bases and of the majority of hydrophobic PL was transferred to a clean tube and the organic phase was re-extracted with 0.5 ml methanol, 0.5 ml of 1M NaCl and 3N NaOH (50 μ l). The alkaline aqueous phases were combined, acidified with 100 μ l concentrated HCl and extracted twice with 1.5 ml chloroform. The organic phases were evaporated and the dried lipids were dissolved in a mixture (50 μ l) of methanol and 0.07 M K_2HPO_4 (9:1 v/v). A derivatization mixture of 10 mg o-phthalaldehyde, 200 μ l ethanol, 10 μ l 2-mercaptoethanol and 10 ml boric

acid (3% wt/v) was prepared and adjusted to pH 10.5 with KOH. Five μ l of the derivatization mixture was added to the lipids and the solution incubated for 15 min at room temperature. The derivatives were analyzed with a Hewlett Packard HPLC system using an RP18 Kromasil column (2.1 mm i.d. x 150 mm) maintained at 45°C. Separation was performed with the isocratic eluent containing methanol: K_2HPO_4 (0.07 M) (78:22 v/v) at a flow rate of 0.25 ml/min. The derivatives were detected selectively using a Hewlett Packard spectrofluorometer with an excitation wavelength of 340 nm and an emission wavelength of 456 nm. S1P was quantified by comparison of its fluorescent signal with that of the derivative of the internal standard (coefficients of variation, <5%) [291].

7. Glycomic analysis

Lipoprotein samples were desalted using ice-cold methanol (Merck, Darmstadt, Germany). Briefly, dried lipoprotein samples were resuspended in 1 ml of ice-cold methanol and centrifuged for 15 min at 2200 g. The supernatant was carefully removed and the procedure was repeated. The remaining methanol was evaporated by drying down in the vacuum concentrator.

Dried samples were dissolved in 30 μ l of 1.33% SDS (w/v) and denatured by incubation at 65°C for 10 min. The following steps of N-glycan release and fluorescent labelling were essentially as described in [292]. After labelling, the free label and reducing agent were removed from the samples by hydrophilic interaction liquid chromatography solid-phase extraction (HILIC-SPE) using 0.2 μ m GHP filter plates and ice-cold 96% acetonitrile (ACN) [292].

Fluorescently labelled N-glycans were separated by hydrophilic-interaction ultra-high-performance liquid chromatography with fluorescence detection (HILIC-UHPLC-FLD) on a Waters Acquity Ultra HPLC (UHPLC) H-class system (Milford, MA, USA) as described previously [292].

Briefly, labelled N-glycans were separated on a Waters BEH Glycan chromatography column, 150 × 2.1 mm i.d., 1.7 µm BEH particles, with 100 mM ammonium formate, pH 4.4, as solvent A and ACN as solvent B. Separation method used linear gradient of 70–53% ACN (v/v) at flow rate of 0.56 ml/min in a 23 min analytical run. Samples were maintained at 10 °C before injection, and the separation temperature was 25 °C. The chromatograms obtained were all separated in the same manner into 22 and 18 chromatographic peaks for HDL and LDL, respectively, and the abundance of glycans in each peak was expressed as % of total integrated area.

The identity of N-glycans separated by HILIC-UHPLC-FLD was determined by matrix-assisted laser desorption ionization time-of-flight mass-spectrometry (MALDI-TOF-MS). Prior to MS analysis, fractions of each N-glycan chromatography peak were collected, dried down in a vacuum concentrator, resuspended in 10 µl of ultrapure water and stabilized by ethyl esterification as previously described [293]. Aliquots of 2 µl were spotted onto an MTP AnchorChip 384 BC MALDI target (Bruker Daltronics, Bremen, Germany), mixed on plate with 1 µl of matrix solution (5 mg/ml 2,5-DHB, 1 mM NaOH in 50 % ACN) and left to dry by air. Recrystallization was performed by adding 0.2 µl of ethanol to each spot. Analyses were performed in positive-ion reflectron mode on an UltrafleXtreme MALDI-TOF-MS equipped with a Smartbeam-II laser and FlexControl 3.4 software Build 119 (Bruker Daltonics). The instrument was calibrated using a plasma N-glycome standard. A 25 kV acceleration voltage was applied after a 140 ns extraction delay. A mass window of m/z 1000 to 5000 with suppression up to m/z 900 was used for N-glycan samples. For each spectrum, 10 000 laser shots were accumulated at a laser frequency of 2000 Hz, using a complete sample random walk with 200 shots per raster spot [2].

8. Functional assays

8.1 Cholesterol efflux

The cholesterol efflux capacity of HDL subpopulations were characterised in a human THP-1 monocytic cell system (ATCC, Manassas, VA, USA) as previously described [294]. In this assay, HDL particles were compared on the basis of their PL concentrations because PL was shown to represent the key component determining cholesterol efflux capacity of HDL [295]. In brief, THP-1 monocytes were cultured on 24-well tissue culture plates, grown in RPMI 1640 media with 10% fetal bovine serum and differentiated into macrophage-like cells with 50 ng/ml phorbol 12-myristate 13-acetate for 48 hours and 37°C. The cells were washed and loaded for 24 h with [³H]cholesterol-labelled acetylated LDL (acLDL, 1 µCi/ml) in serum-free RPMI 1640 culture medium supplemented with 50 mM glucose, 2 mM glutamine, 0.2% BSA, 100 µg/ml penicillin and 100 µg/ml streptomycin (further abbreviated as RGGB) to allow equilibration of cellular cholesterol pools. The labelling medium was removed and human macrophages were then equilibrated in RGGB for an additional 16-24 h period. Cellular cholesterol efflux to HDL was assayed at 15 µg/ml HDL-PL in serum-free medium for a 4- hour chase period. Finally culture media were harvested and cleared of cellular debris by brief centrifugation. Cell radioactivity was determined by extraction in hexane-isopropanol (3:2 v/v), evaporation of the solvent under nitrogen and liquid scintillation counting (Wallac Trilux 1450 Microbeta, Perkin Elmer, USA). The percentage of cholesterol efflux was calculated as (medium cpm) / (medium cpm + cell cpm) x 100%. Specific cholesterol efflux was determined by subtracting non-specific cholesterol efflux occurring in the absence of cholesterol acceptors.

8.2 Antioxidative activity of HDL

Antioxidative activity of serum-derived HDL subpopulations (final concentration of each, 10 mg total mass/dl) was assessed at a physiological HDL to LDL ratio of 2-6 mol/mol towards

reference LDL (d 1.019-1.063 g/ml; final concentration, 10 mg TC/dl) isolated from one healthy normolipidemic control subject [296-298]. In this assay, HDL particles were compared on the basis of their total mass concentrations because both protein and lipid components were shown to contribute to the capacity of HDL to inhibit LDL oxidation [157, 158].

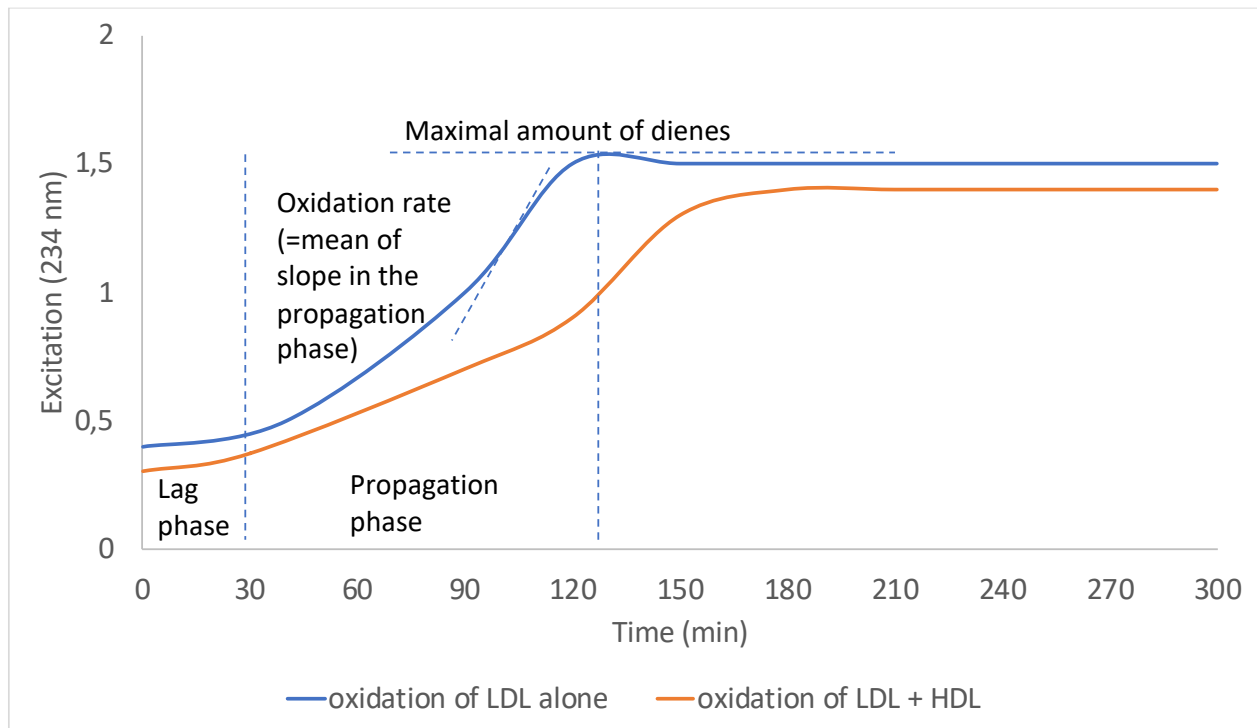


Figure 14. Schematic illustration of LDL oxidation curves and their characteristics

HDL subfractions were added to LDL directly before oxidation. Lipoprotein oxidation was induced by an azo-initiator 2,2'-azo-bis-(2-amidinopropane) hydrochloride (AAPH; final concentration 1 mmol/l) [296] as model of mild oxidation induced by free radicals in the arterial intima [299]. Serum was used as a source of HDL for this assay to ensure intact paraoxonase activity, which is inhibited by EDTA [300]. Thereby this assay employs mild oxidative conditions and integrates the antioxidative activities of several HDL components, i.e. apoA-I, antioxidative enzymes and lipophilic low-molecular-weight antioxidants [157].

Accumulation of conjugated dienes was measured as the increment in absorbance at 234 nm [296-298]. Absorbance kinetics were corrected for the absorbance of AAPH itself run in parallel as a blank. The kinetics of diene accumulation revealed two characteristic phases, the lag and propagation phases. For each curve, the duration of each phase, average oxidation rates within each phase and amount of dienes formed at the end of the propagation phase (maximal amount of dienes) were calculated [296-298] (Figure 14).

8.3 Anti-apoptotic activity of HDL

Anti-apoptotic activity of HDL was assayed as described elsewhere [301] with slight modifications. In brief, human umbilical vein endothelial cells (HUVEC) were purchased from PromoCell (Germany) and maintained in Endothelial Cell Basal Medium (C-22111, promocell) supplemented with fetal bovine serum (20%, v/v), and human basic fibroblast growth factor. Growth factor deprivation was induced by changing the media to Endothelial Cell Basal Medium (C-22111, promocell) without supplements. Floating endothelial cells were collected by centrifugation, while adherent cells were collected by trypsinization. For determination of the annexin V binding, combined cell populations (5×10^5 /ml) were resuspended in 140 mM NaCl, 10 mM Hepes, and 2.5 mM CaCl₂. Annexin V-FITC (BioLegend's FITC Annexin V Apoptosis Detection Kit with 7-AAD) was added for 15 min at room temperature. For determination of the cell membrane permeability, endothelial cells (5×10^5 /ml) were incubated for 30 min in phosphate-buffered saline. Flow cytometric measurements of annexin V binding were performed on a BD LSRFortessa flow cytometer (BD Biosciences, Franklin Lakes, New Jersey, USA).

8.4 Cellular cholesterol accumulation induced by LDL

THP-1 monocytes were cultured on 24-well tissue culture plates, grown in RPMI 1640 media with 10% FBS and differentiated into macrophage-like cells with 50 ng/ml phorbol 12-myristate 13-acetate (PMA) for 48 hours and 37 °C. The cells were washed and loaded for 48 h with desialylated LDL (100 µg protein/mL), or with native LDL (100 µg protein/mL) as a control, in serum-free RPMI 1640 culture medium supplemented with RGGB to allow equilibration of cellular metabolic processes. Control cells were prepared under identical conditions but without addition of LDL. Total cholesterol content of the THP-1 cells was determined by the Amplex Red cholesterol assay at the end of the incubations.

9. Statistical analysis

Between-group differences were analyzed using Mann-Whitney U -test. Pearson's product moment correlations were calculated to evaluate relationships between variables. For all statistical tests, a P value of less than 0.05 (Benjamini-Hochberg adjusted, otherwise known as false discovery rate [FDR] corrected) was considered statistically significant.

Principal component analysis (PCA) was performed to provide a broad view on a data set, emphasizing its most valuable informationwise subsets. PCA reduces intricate multiple-dimension data into several (usually two, less often three or more) most meaningful principal components in terms of information carried by them by maximizing the variance among the components. In this study, principal components (eigenvectors and eigenvalues) were calculated using R built-in *prcomp* function with *scale* parameter set *True*; corresponding charts were built using *ggbiplot* R package.

Heatmap is a graphical representation of data where individual values contained in a matrix are represented as colors. To create heatmaps, following rules were used: (i) abundance of each lipid species from the patient group was normalized to the mean value of the abundance of this species

in the control group; (ii) the given species was represented as a single colored bar; (iii) the bar color corresponded to the ratio of the abundance of this species between the patient and the control groups, varying from red (decreased abundance in the patient vs control group) through black (no difference) to green (increased abundance in the patient vs control group). All the charts were built using R, specifically the *heatmap.2* function from *gplots* package.

Bubble plots were used, which can be described as a more sophisticated variety of a heatmap with multiple additions, to provide a more in-depth view on the data as compared with heatmaps. As in the heatmaps, the main type of information conveyed in this plot type was the ratio of mean abundance of any given molecular species from the patient group to the mean abundances of the same species in the control group. In addition, the bubble plots provided quantitative information about mean abundance of molecular species in the patient group. Finally, the bubble plots contained P-values of the differences between abundances of lipid species in the patient vs control groups, thereby excluding from the plots all species, whose abundance was not significantly different between the groups. Every molecular species was presented as a colored circle (“bubble”), the color coded for phospholipid and sphingolipid class. The circle position along X axis represented the abundance of the species, and the position along the Y axis represented the ratio of the abundances in the patient vs control groups. The size of the bubble was inversely proportional to the P value mentioned above. All the axes as well as the size of the bubbles were plotted using logarithmic scale.

Structural 3D plots were built to convey information about the structure of fatty acid residues of affected lipid species, notably the number of double bonds and the length of carbon chains. Each dot represented a single molecular species, with a number of carbon atoms in the fatty acid chains displayed along the X axis and a number of double bonds displayed along the Y axis. The Z axis

enlisted all five HDL subfractions. Only molecular species whose abundances revealed statistically significant differences between the patient and control groups were shown in the plots.

Network maps offer a graph-type visual representation of all intrinsic correlations within a data set. Network maps were created to reveal relationships between the lipidome and function of HDL. In a given network community, a network map reveals all interconnections between the nodes of this community. Assuming the HDL lipidome and function representing the community, molecular species and functional metrics stood for the nodes of the graph. If there was a significant correlation between abundances of any two species of the lipidome or functional metrics (nodes), these species and metrics were assumed to have a connection (edge). The length of the vertices between the nodes was inversely proportional to the value of the correlation coefficient between the abundances of the lipid species represented by the nodes. Size of the node was proportional to the number of neighboring vertices connected to the node. Color of the node indicated lipid class each species belonged to, as for the bubble plots described above. All species from all HDL subpopulations were used to build network maps. To correlate the lipidomic data with the functional metrics, the species abundances were recalculated on the HDL concentration basis used to evaluate a given metric (phospholipid for cholesterol efflux capacity and total mass for antioxidative activity).

Affected metabolic pathways were identified and included in the classical pathway representation after identification using the MetExplore web-based tool [302]. The metabolic network *Homo sapiens* (strain: Global Network, source: KEGG Map, Version 24/08/2017) of human species was based on 88 metabolic pathways including 1572 metabolites [303]. Metabolic networks are directed graphs, so it is possible to calculate compound importance based on relative betweenness

centrality and out-degree centrality of any given compound from a pathway. Pathway impact is then calculated as a sum of the importance measures of the matched metabolites normalized by the sum of the importance measures of all metabolites in each pathway.

Affected genes were identified using MetaboAnalyst's Network Explorer tool [304].

Metaboanalyst uses Globaltest [305] and GlobalANCOVA [306], which are similar algorithms designed for testing differentially expressed genes or metabolites in functionally related groups.

Degree centrality and betweenness centrality are two measures to estimate the importance of a compound within a given gene-metabolic network and both are used to find the affected genes.

The former measures the number of connections, between the node of interest and other nodes, whereas the latter evaluates the number of shortest paths going through the node of interest.

RESULTS

This part focuses on lipidomics and glycomics of human plasma HDL and LDL in respect to their biological functions in healthy subjects and in patients with CMD. As examples of CMD were taken FAID and recent survivors of STEMI. FAID is a genetically determined condition resulting in elevated CV risk, signifying chronic dyslipidemia and STEMI represents an acute case of CVD. Parts of this work have been published [1, 2].

1. HDL lipidome and functionality in normolipidemic controls

Eight male normolipidemic control subjects (Table 2), whose lipidome is described in this subsection, were also employed as the control counterpart of the FAID segment of this study.

Table 2. Clinical and biological characteristics of control subjects (n=8) [85]

Age, y	51±14
BMI, kg/m ²	24±3
TC, mg/dl	183±24
LDL-C, mg/dl	113±27
HDL-C, mg/dl	53±10
TG, mg/dl	87±30
ApoB100, mg/dl	96±26
ApoA-I, mg/dl	133±18
ApoC-III, mg/dl	7.6±2.0
Fasting glucose, mg/dl	92±8
hsCRP, mg/l	0.62 (0.16; 4.87)

hsCRP is shown as a median (minimum; maximum) due to non-normal distribution

1.1 Lipidome

In short, we identified 157 individual molecular lipid species in 5 normolipidemic HDL subpopulations across 9 lipid subclasses, accounting for >95% of total plasma PL and SL [289,

290], including 23 PC, 21 SM, 9 LPC, 23 PE, 16 PI, 11 PG, 24 Cer, 17 PS, and 13 PA species.

PC species clearly predominated, accounting together for 68% to 81% of total PL+SL, followed by SM (12%–23%), LPC (0.9%–8.3%), PI (1.1%–2.8%), PE (0.8%–5.1%), Cer (0.07%–0.34%), PS (0.02%–3.11%), PG (0.001%–0.028%), and PA (0.004%–0.103%) species (Figure 15).

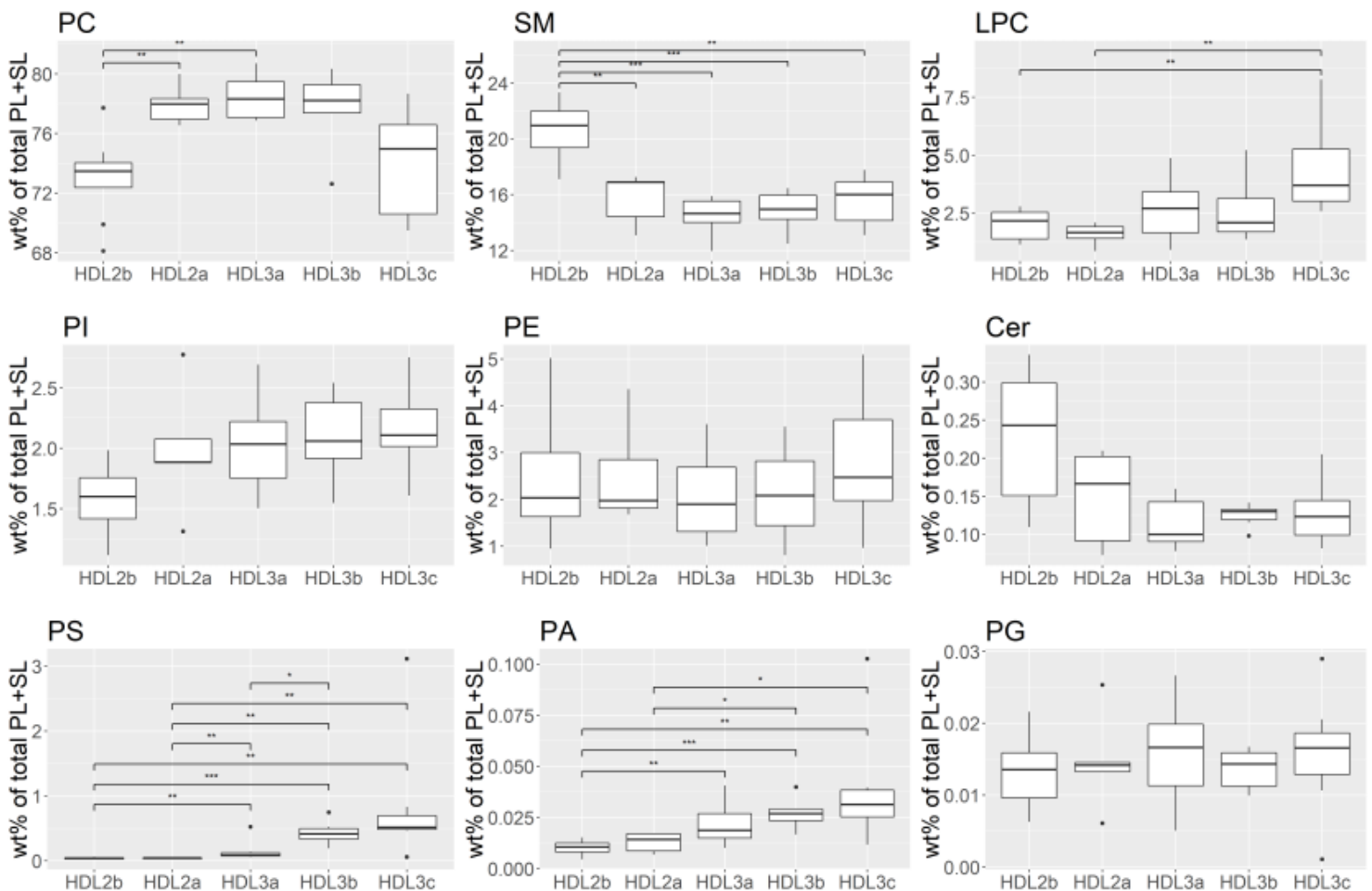


*Figure 15. Phosphosphingolipidome of HDL subpopulations in healthy normolipidemic subjects (n=8). HDL contents of PC, SM, LPC, PI, PE, Cer, PS, PA, and PG, expressed as wt% of total phosphosphingolipidome in each HDL subclass, are shown in the order of decreasing abundance; *P<0.05, **P<0.01, ***P<0.001. Whiskers represent the extremi of the abundances of given lipids in their appropriate HDL subpopulations (without the outliers).*

A high level of heterogeneity in lipid content was found across HDL subpopulations. Although absolute levels of the majority of lipid subclasses in HDL followed circulating concentrations of HDL particles (Table 3), SM and Cer tended to be enriched in large, light HDL2b, whereas PS

preferentially associated with small, dense HDL3 particles (Figure 15). As a result, when expressed as a wt% of PL+SL, PS, but also PI, LPC, and PA, showed a marked tendency to increase progressively in parallel with increase in hydrated density and reduction in size from HDL2b to HDL3c. Indeed, small, dense HDL were enriched in LPC, PS, and PA relative to large, light HDL ($p<0.05$; Figure 15). Similarly, PI and PG tended to concentrate in small, dense HDL; these trends did not, however, attain significance (Figure 15). Interestingly, lipid species of PS were localized almost exclusively in the densest HDL3c subfractions; PS content varied from 0.02 wt% of total PL+SL in HDL2b to 0.63 wt% in HDL3c. As a consequence, the percentage of negatively charged PLs PI, PS, PG, and PA increased with HDL density from HDL2b to HDL3c.

Table 3 Total mass (mg/dl) and % chemical composition of lipids and protein (wt/wt) of HDL subfractions from normolipidemic controls [85]

	HDL2b	HDL2a	HDL3a	HDL3b	HDL3c
Total mass (mg/dl)	75.3±33.9	89.0±12.7	73.8±18.7	33.2±9.1 ^{**§§§###}	14.2±4.4 ^{**§§§###/##}
PL	31.9±5.4	30.1±4.4 ^{**}	28.7±3.1 ^{**}	26.5±2.9 ^{**}	20.3±2.9 ^{**§§§###/##}
CE	27.1±5.5	22.3±3.9 ^{**}	20.8±3.7 ^{**}	17.8±3.6 ^{***§}	16.1±2.5 ^{***§§##}
FC	6.6±0.7	3.9±0.5 ^{***}	2.9±0.3 ^{***§§§}	2.5±0.2 ^{***§§§##}	2.0±0.4 ^{***§§§###/##}
TG	5.4±2.3	3.6±1.5 ^{***}	3.1±1.4 ^{***}	3.0±1.8 ^{***}	3.3±2 ^{***}
Total protein	29.0±5.4	40.0±5.8 [*]	44.5±5.1 [*]	50.2±6.6 ^{§§}	58.3±5.6 ^{§§§###/##}

* $p<0.05$, ** $p<0.01$, *** $p<0.001$ vs. HDL2b; § $p<0.05$, §§ $p<0.01$, §§§ $p<0.001$ vs. HDL2a; # $p<0.05$, ### $p<0.01$, ### $p<0.001$ vs. HDL3a; † $p<0.05$, †† $p<0.01$, ††† $p<0.001$ vs. HDL3b

Concomitant with such enrichment in PLs, the proportion of SM and Cer decreased progressively in parallel with HDL density from 21 wt% and 0.24 wt% of total PL+SL in HDL2b to 16 wt% and 0.13 wt% in HDL3c, respectively (Figure 15).

Consistent with published data [296, 307] HDL content of major lipid classes (PL, FC, CE, and TG) calculated on the basis of total HDL mass showed a distinct trend to decrease with increment in total protein content and particle density across the HDL particle spectrum (Table 3).

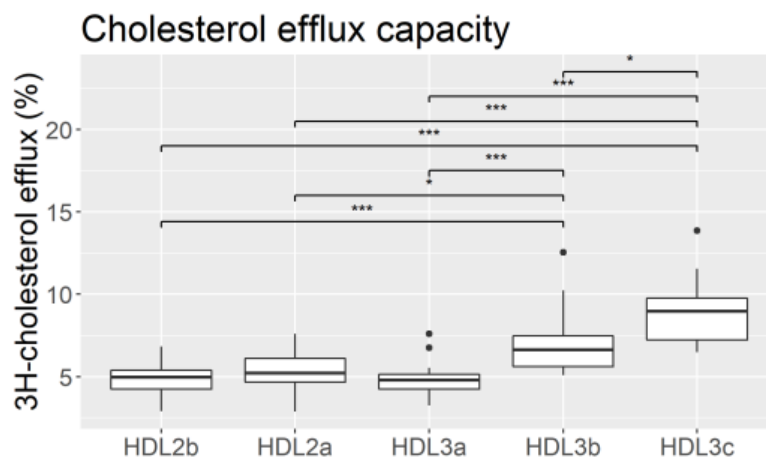


Figure 16 Cholesterol efflux capacity of normolipidemic HDL subpopulations compared on the basis of HDL PL. * $p < 0.05$, ** $p < 0.01$, *** $p < 0.001$

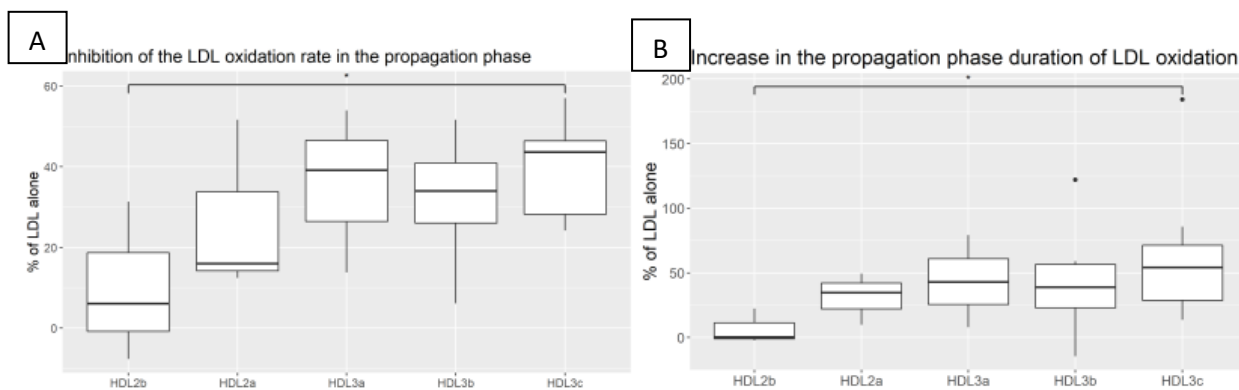


Figure 17. Antioxidative activity of HDL compared on the basis of total mass content toward LDL oxidation, expressed as a decrease in the LDL oxidation rate in the propagation phase (A) and an increase in the duration of this phase (B). * denotes significant difference $p < 0.05$ in HDL2b vs HDL3c.

1.2 Function

The capacity of individual HDL subpopulations to mediate cellular efflux of FC was evaluated in macrophage-like human THP-1 cells, which efflux cholesterol predominantly via the ABCA1-dependent pathway [294]. On the basis of unit PL mass content, both small, dense HDL3b and 3c particles displayed greater efficacy in removing cellular cholesterol as compared with other HDL subpopulations ($p < 0.05$; Figure 16). Thus, the cholesterol efflux capacity varied from 4.9% for HDL2b to 8.9% for HDL3c. Moreover, HDL3c exhibited higher cholesterol efflux capacity than HDL3b ($p < 0.05$).

Antioxidative activity of HDL particles was assessed as inhibition of free radical-induced LDL oxidation. Consistent with previous data [296], the inhibitory effects of small, dense HDL3c on LDL oxidation was superior relative to large, light HDL2b on the basis of total mass, with respect to both reduction in LDL oxidation rate in the propagation phase (4.1-fold; $P < 0.05$; Figure 17A) and increases in the duration of this phase (8.5-fold; $P < 0.05$ Figure 17B).

HDL capacity to efflux cellular cholesterol from THP-1 cells was positively associated with the contents of PS. Metrics of antioxidative activity of HDL toward LDL were correlated positively with the contents of PS and PA and negatively correlated with those of SM, Cer, CE, FC, and TG.

2. HDL lipidome and functionality in cardiometabolic diseases

2.1 Familial apoA-I deficiency

As reported earlier [279], heterozygous apoA-I-deficient patients featured atherogenic dyslipidemia with significantly reduced plasma apoA-I and HDL-C levels, while no difference between the groups in TG, TC, LDL-C, non-HDL-C, apoB-100, apoC-III, fasting glucose and

hsCRP levels was observed (Table 4). This section 2.1 on Familial apoA-I deficiency has been published in a peer-reviewed academic journal [1].

Table 4. Clinical and biological characteristics of FAID patients (n=5) and age-matched controls (n=8) [279].

	Controls (n=8)	Patients (n=5)
Age, years	51 ± 14	40 ± 27
BMI, kg/m ²	23.8 ± 2.8	28.7 ± 7.4
Male/female	8/0	4/1
Plasma parameters		
TC, mg/dl	183 ± 24	191 ± 8
LDL-C, mg/dl	113 ± 27	140 ± 27
HDL-C, mg/dl	53 ± 10	23 ± 4 *
TG, mg/dl	87 ± 30	127 ± 47
ApoB100, mg/dl	96 ± 26	116 ± 15
ApoA-I, mg/dl	133 ± 18	71 ± 14 *
ApoC-III, mg/dl	7.6 ± 2.0	5.7 ± 3.1
Fasting glucose, mg/dl	92 ± 8	86 ± 11
hsCRP, mg/l	0.62 (0.16; 4.87)	0.93 (0.63; 8.87)

* p<0.05 versus controls; hsCRP is shown as a median (minimum; maximum) due to non-normal distribution

2.1.1. Abundances of individual lipid species.

The HDL lipidome was markedly perturbed in apoA-I-deficient patients as reported earlier [279]. Among the nine PL- and SL subclasses studied, PA and PG were most strongly affected. Indeed, total PA and PG were significantly increased in apoA-I-deficient patients relative to controls in all five HDL subpopulations, including both large, light and small, dense HDLs [279]. Other lipid classes showed significant between-group differences in three (PC decreased in HDL2b, HDL3b, HDL3c; LPC elevated in HDL2b, HDL3b and HDL3c; PI elevated in HDL2b, HDL3a and HDL3c; PS increased in HDL2b, HDL2a and HDL3c), two (SM elevated in HDL2b and decreased in HDL3a) and one (PE decreased in HDL2b; Cer elevated in HDL2b) subpopulations [279].

When abundances of lipid species were analysed, all HDL subpopulations revealed significant between-group differences. However, the number of significantly differing (FDR-corrected) between the groups varied greatly across the HDL subpopulations for all lipid classes, including PC (from 1 to 6), SM (from 2 to 7), LPC (from 1 to 9), PI (from 1 to 3), PE (from 1 to 5), PS (from 2 to 8), Cer (from 1 to 19), PA (from 5 to 10) and PG (from 3 to 9) lipid species (Table 5 and Table 6). Significant between-group differences (FDR-corrected) were typically found in the abundances of unsaturated lipid species. Indeed, among molecular species significantly differing between apoA-I-deficient and control groups 92% (55 of 61), 95% (18 of 19), 94% (16 of 17), 91% (30 of 33) and 93% (51 of 55) possessed one or more double bond in their fatty acid carbon chain residues in HDL2b, 2a, 3a, 3b and 3c, respectively.

Table 5 Abundances of molecular lipid species of PL and SL in HDL2b, HDL2a and HDL3a subpopulations significantly differing between FAID patients and age-matched controls

HDL2b				HDL2a				HDL3a			
Class	Species	Controls	Patients	Class	Species	Controls	Patients	Class	Species	Controls	Patients
PC	32:0	0.82±0.14	1.09±0.13	PC	34:2	21.8±1.7	16.4±1.3	PC	34:2	22.0±2.3	17.0±1.1
	34:0	0.17±0.04	0.32 (0.30; 0.39)						38:3	1.50±0.41	3.49 (2.02; 3.71)
	34:2	20.2±2.1	15.7±2.3						40:5	0.34 (0.26; 0.56)	0.58±0.12
	38:3	1.33±0.42	2.69±0.52								
	40:4	0.10±0.04	0.19±0.05								
	40:8	0.05±0.01	0.03±0.01								
SM	36:1	1.00±0.19	1.34±0.16	SM	32:1	0.268±0.055	0.159±0.022	SM	32:1	0.23±0.03	0.12±0.01
	38:1	0.69±0.14	0.89±0.07						34:0	0.10±0.01	0.06±0.01
	40:1	1.61±0.46	2.37±0.26						34:1	3.62±0.62	2.23±0.33
	41:1	0.95±0.22	1.38±0.13						34:2	0.64±0.06	0.39±0.08
	42:1	1.12±0.36	1.78±0.25								
LPC	18:0	0.46±0.19	1.34±0.84	LPC	20:3	0.04±0.01	0.45±0.37	LPC			
	20:3	0.04±0.02	0.22±0.19								
PI	36:2	0.26±0.07	0.39±0.11	PI				PI	38:4	0.91±0.21	1.43±0.17
	38:3	0.08±0.02	0.13±0.03								
	38:4	0.73±0.18	1.03±0.11								
PE	34:2	0.183±0.107	0.047±0.023	PE	40:7	0.05±0.02	0.02±0.01	PE			
	36:2	0.654±0.372	0.293±0.060								
	36:3	0.244±0.172	0.094±0.009								
	38:6	0.351±0.243	0.080±0.034								
Cer	d18:0	0.0003±0.0002	0.0007±0.0002	Cer	d18:1	0.0002±0.0001	0.0005±0.0002	Cer			
	22:0				26:1						

d18:0 24:0	0.0004±0.0003	0.0010±0.0003
d18:1 14:0	0.0002±0.0001	0.0004±0.0001
d18:1 16:0	0.0047±0.0017	0.0086±0.0010
d18:1 18:0	0.0025±0.0010	0.0052±0.0009
d18:1 20:0	0.0034±0.0011	0.0054±0.0010
d18:1 22:0	0.0248±0.0110	0.0612±0.0208
d18:1 23:0	0.031±0.013	0.069±0.020
d18:1 24:0	0.074±0.035	0.171±0.038
d18:1 24:1	0.030±0.012	0.069±0.021
d18:1 25:0	0.005±0.003	0.015±0.005
d18:1 26:0	0.0012 (0.0010; 0.0023)	0.0038±0.0014
d18:1 26:1	0.0005±0.0002	0.0013±0.0004
d18:2 14:0	0.00011±0.00004	0.0002±0.0001
d18:2 16:0	0.0014±0.0004	0.0028±0.0008
d18:2 18:0	0.0006±0.0003	0.0013±0.0004

d18:2 20:0	0.0009±0.0004	0.0015±0.0003						
d18:2 24:1	0.0075±0.0028	0.0169±0.0066						
d18:2 24:2	0.0008±0.0004	0.0017±0.0006						
PS	36:2	0.0030±0.0008	0.0153±0.0125	PS	36:2	0.0035±0.0005	0.0089±0.0045	PS
	38:1	0.0005 (0.0004; 0.0009)	0.0020 (0.0016; 0.0080)		38:3	0.0017±0.0006	0.0045±0.0015	
	38:3	0.0013±0.0008	0.0090±0.0073					
	38:4	0.0087±0.0038	0.0424±0.0330					
	40:4	0.0018±0.0014	0.0095±0.0083					
	40:5	0.0019±0.0009	0.0085±0.0071					
PA	34:1	0.0013±0.0007	0.0174 (0.0016; 0.0565)	PA	34:1	0.0013±0.0011	0.0117 (0.0047; 0.0830)	PA
	34:2	0.0022±0.0008	0.0346±0.0325		34:2	0.003±0.001	0.037 (0.006; 0.117)	
	36:4	0.0003±0.0001	0.0043 (0.0002; 0.0148)			0.0005 (0.0004; 0.0011)	0.0027 (0.0013; 0.0194)	
	38:4	0.0008±0.0004	0.0082 (0.0010; 0.0239)		36:1	0.002 (0.002; 0.004)	0.030 (0.006; 0.103)	
					36:2	0.0014±0.0005	0.016 (0.005; 0.083)	
					36:3		0.0087 (0.0010; 0.0167)	
					36:4	0.0003±0.0002	0.0167)	
						0.0006 (0.0005; 0.0021)	0.0117±0.0089	
					38:4	0.0021)	0.0117±0.0089	
					38:6	0.0003±0.0001	0.0032±0.0019	
PG	34:1	0.0028 (0.0016; 0.0060)	0.0097±0.0034	PG	34:1	0.0034±0.0023	0.0174±0.0061	PG
	36:1	0.0034±0.0015	0.0070±0.0020		36:2	0.0044±0.0017	0.0177±0.0057	34:1
	36:2	0.0040±0.0014	0.0112±0.0024		36:3	0.0008±0.0003	0.0033±0.0006	0.0038±0.0015
	36:3	0.0007±0.0003	0.0020±0.0006					0.0186±0.0074
								0.0104±0.0025
								0.0167±0.0041
								0.0026±0.0006

38:2	0.0004±0.0002	0.0019±0.0010	36:4	0.0004±0.0001	0.0010±0.0005
38:3	0.0002±0.0001	0.0005 (0.0003; 0.0012)	38:2	0.0004±0.0003	0.0020±0.0006
38:4	0.0004±0.0002	0.0012±0.0003	38:5	0.0004±0.0002	0.0010±0.0004
38:5	0.0003±0.0001	0.0007±0.0001			

Data are shown as means ± SD and expressed as wt% of total PL+SL; only lipid species significantly (p<0.05) differing between the groups are shown; significantly elevated values are highlighted in bold.

Table 6 Abundances of molecular lipid species of PL and SL in small, dense HDL3b and HDL3c subpopulations significantly differing between apoA-I-deficient patients and age-matched controls

HDL3b				HDL3c			
Class	Species	Controls	Patients	Class	Species	Controls	Patients
PC	34:2	22.2±1.9	14.9±1.2	PC	34:1	6.70±0.77	3.95±1.59
	36:2	14.6±0.6	12.8±1.3		34:2	20.3±1.4	15.9±2.3
	36:5	1.42±0.61	0.54±0.18		38:3	1.68 (0.93; 1.88)	2.77±0.56
	38:3	1.36±0.48	2.85±0.74		38:6	4.11±1.27	2.57±0.49
	40:4	0.09±0.04	0.19±0.08		40:4	0.10±0.04	0.18 (0.15; 0.32)
	40:8	0.07±0.01	0.04±0.01		40:8	0.07±0.01	0.04±0.01
SM	32:1	0.25±0.04	0.14±0.02	SM	32:1	0.276±0.039	0.140±0.026
	34:0	0.12±0.03	0.07±0.01		32:2	0.013±0.002	0.007±0.002
					34:0	0.126±0.025	0.080±0.016
					34:1	3.99±0.52	2.61±0.44
					34:2	0.600 (0.573; 0.804)	0.415±0.081
					42:1	0.74±0.11	1.03±0.21
LPC	16:0	0.86±0.40	4.40±2.40	LPC	16:1	0.033±0.023	0.095±0.059
	16:1	0.02±0.01	0.13±0.08		18:0	0.93±0.35	2.53±1.00
	18:0	0.52±0.34	3.10±1.59		18:1	0.576±0.263	1.23±0.59
	18:1	0.35±0.18	1.62±0.99		18:2	0.72±0.45	1.83±0.72
	18:2	0.57±0.39	2.74±1.86		20:3	0.079 (0.031; 0.352)	0.499±0.287
	20:3	0.06±0.04	0.67±0.43		20:4	0.180 (0.085; 0.597)	0.805±0.338
	20:4	0.16±0.08	1.00±0.34		22:5	0.036±0.025	0.129±0.077
	22:5	0.03±0.02	0.16±0.08				
	22:6	0.05 (0.03; 0.19)	0.24±0.10				
PI				PI	38:3	0.10±0.03	0.17±0.04
					38:4	1.01±0.22	1.46±0.21

					34:0	0.0034±0.0031	0.0112±0.0061
PE			PE		38:3	0.04±0.03	0.08±0.03
					40:4	0.03±0.02	0.09±0.03
					36:2	0.033 (0.006; 0.196)	0.232±0.185
					38:1	0.011 (0.001; 0.156)	0.066±0.050
					38:2	0.010 (0.001; 0.056)	0.037±0.028
PS			PS		38:3	0.022 (0.005; 0.092)	0.121±0.088
					38:4	0.18 (0.01; 1.09)	0.57±0.32
					40:4	0.024±0.015	0.097±0.066
					40:5	0.029±0.026	0.083±0.050
	d18:1 24:0	0.031±0.006	0.046 (0.036; 0.110)		d18:0 22:0	0.00019 (0.00009; 0.00100)	0.00056±0.00031
Cer	d18:2 24:2	0.00058±0.00019	0.00103±0.00020	Cer	d18:0 24:0	0.00017 (0.00010; 0.00086)	0.00061±0.00036
					d18:1 25:0	0.00203±0.00051	0.00364±0.00140
	34:1	0.004±0.001	0.033 (0.013; 0.301)		34:1	0.005 (0.003; 0.018)	0.033 (0.020; 0.172)
	34:2	0.006±0.002	0.055 (0.025; 0.709)		34:2	0.006 (0.004; 0.024)	0.053 (0.040; 0.319)
	36:1	0.0022±0.0011	0.010 (0.004; 0.081)		36:1	0.0031±0.0017	0.0123 (0.005; 0.0611)
PA	36:3	0.002 (0.001; 0.005)	0.028 (0.016; 0.502)	PA	36:2	0.005 (0.001 ;0.020)	0.049 (0.041; 0.256)
	36:4	0.0009±0.0008	0.011 (0.004; 0.081)		36:3	0.002 (0.001; 0.015)	0.026 (0.023; 0.199)
	38:4	0.002 (0.002; 0.007)	0.021 (0.008; 0.125)		36:4	0.0009 (0.0005; 0.0045)	0.0106 (0.0057; 0.0589)
					38:4	0.0033±0.0023	0.0250 (0.0161; 0.0795)
					38:6	0.0010±0.0007	0.0043 (0.0025; 0.0212)
	34:1	0.0032±0.0008	0.0152±0.0045		36:1	0.0037±0.0027	0.0099±0.0018
	36:1	0.0031±0.0013	0.0098±0.0027		36:2	0.0051±0.0025	0.0175±0.0036
PG	36:2	0.004 (0.001; 0.005)	0.016±0.003	PG	36:3	0.0009±0.0005	0.0041±0.0004
	36:3	0.0009±0.0004	0.0047±0.0035		38:2	0.0004±0.0003	0.0028±0.0011
					38:4	0.0004±0.0003	0.0017±0.0007

Data are shown as means ± SD and expressed as wt% of total PL+SL; only lipid species significantly (p<0.05) differing between the groups are shown; significantly elevated values are highlighted in bold.

2.1.2. PCA

Control and patient groups were entirely separated for the lipidome of both small, dense and large, light HDL subpopulations on a plane of the first two Principal Components PC, indicating that individual components of the HDL lipidome were strongly altered in apoA-I-deficient subjects (Figure 18). Indeed, for all 5 HDL subpopulations, the variance explained by the first two PC was higher than 45%, consistent with marked between-group differences.

2.1.3. Heatmaps

A distinct pattern was observed across all HDL subpopulations between apoA-I-deficient and control subjects (Figure 19). Notably, abundances of LPC, PA, PG and, to a lesser extent, Cer species were typically elevated in apoA-I-deficient HDLs as compared to their counterparts from controls, whereas abundances of PE species were decreased. PC, SM, PS and PI profiles revealed mixed patterns, with species overrepresented and underrepresented in apoA-I-deficient HDLs making up approximately equal shares.

2.1.4. Bubble plots

Similar to the heatmaps, the bubble plots revealed that abundances of numerous molecular species of LPC, PA and PG, as well as some of Cer species were consistently increased in apoA-I-deficient HDLs (Figure 20). By contrast, PC, SM, PE and PI species revealed mixed patterns across HDL subpopulations, involving both elevated and reduced abundances. Importantly, a majority of lipid species significantly altered (FDR-corrected) by apoA-I deficiency were located in the middle-right part of the plots, indicating that they were moderately to highly abundant. Negative correlations between the magnitude of between-group difference for the species and their overall abundance in the HDL lipidome were observed for PC, LPC, PI, PA, PS, PG and

Cer lipids collectively ($r = -0.31, -0.61, \text{ and } -0.35$ for HDL2b, 3a, and 3c, respectively; $p < 0.05$ for all). On the contrary, PE and SM species collectively avoided this trend, presenting with a counter-trend of positive correlations between the magnitude of difference between the groups and overall abundance in HDL lipidome, reaching significance in HDL3a ($r = 0.94, p < 0.05$), subpopulation. Together with the heatmaps, the bubble plots thereby demonstrated that the LPC, PA and PG species were altered most when compared to the control group, while being moderately abundant, whilst moderately- to highly-abundant species of PC and SM revealed mixed patterns.

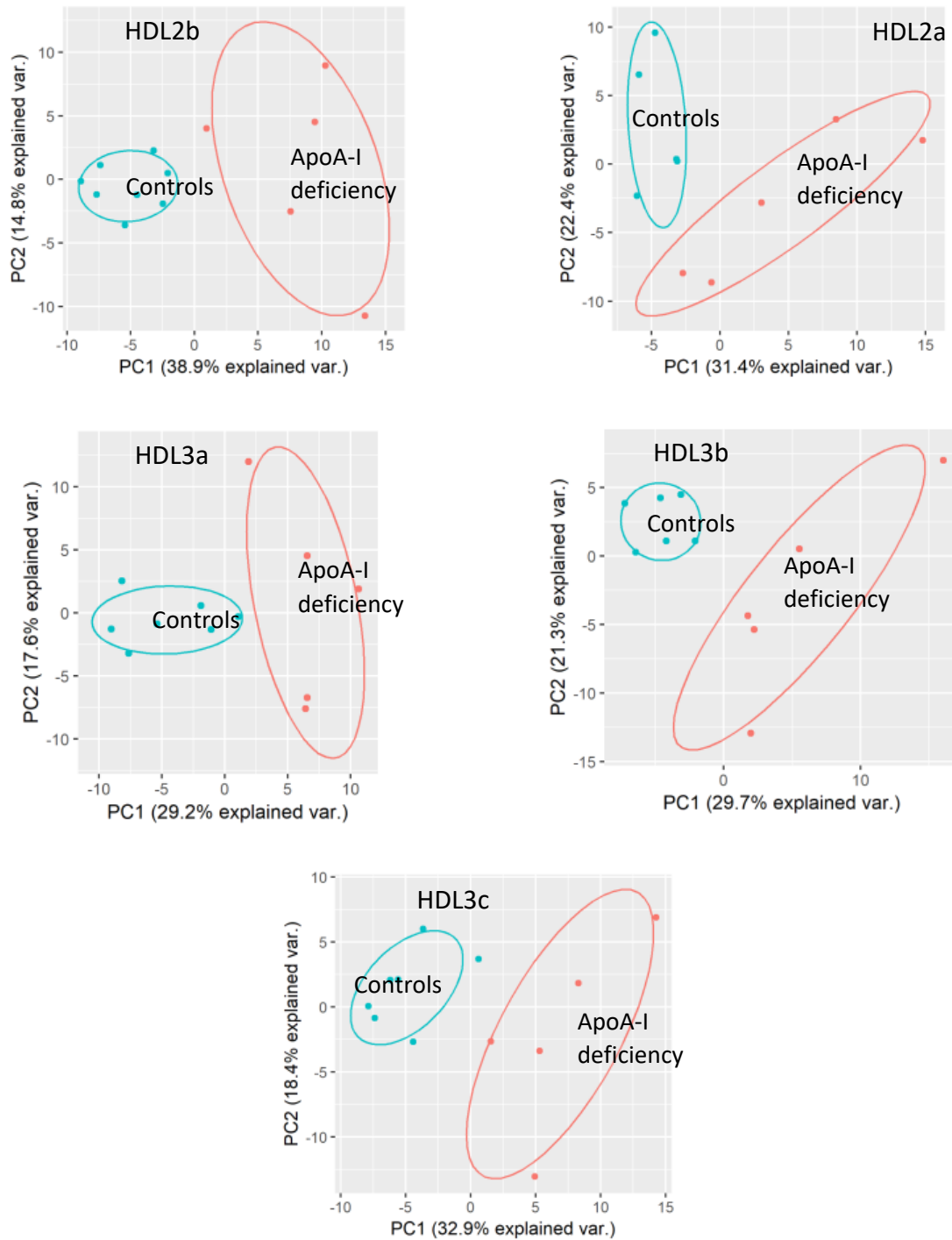


Figure 18. PCA plots for large, light HDL2b, HDL2a and small, dense HDL3a, HDL3b and HDL3c subpopulations. Blue and red ellipses represent the control and apoA-I-deficient groups, respectively. Total amounts of variance explained by the first two components is more than 45% for each chart.

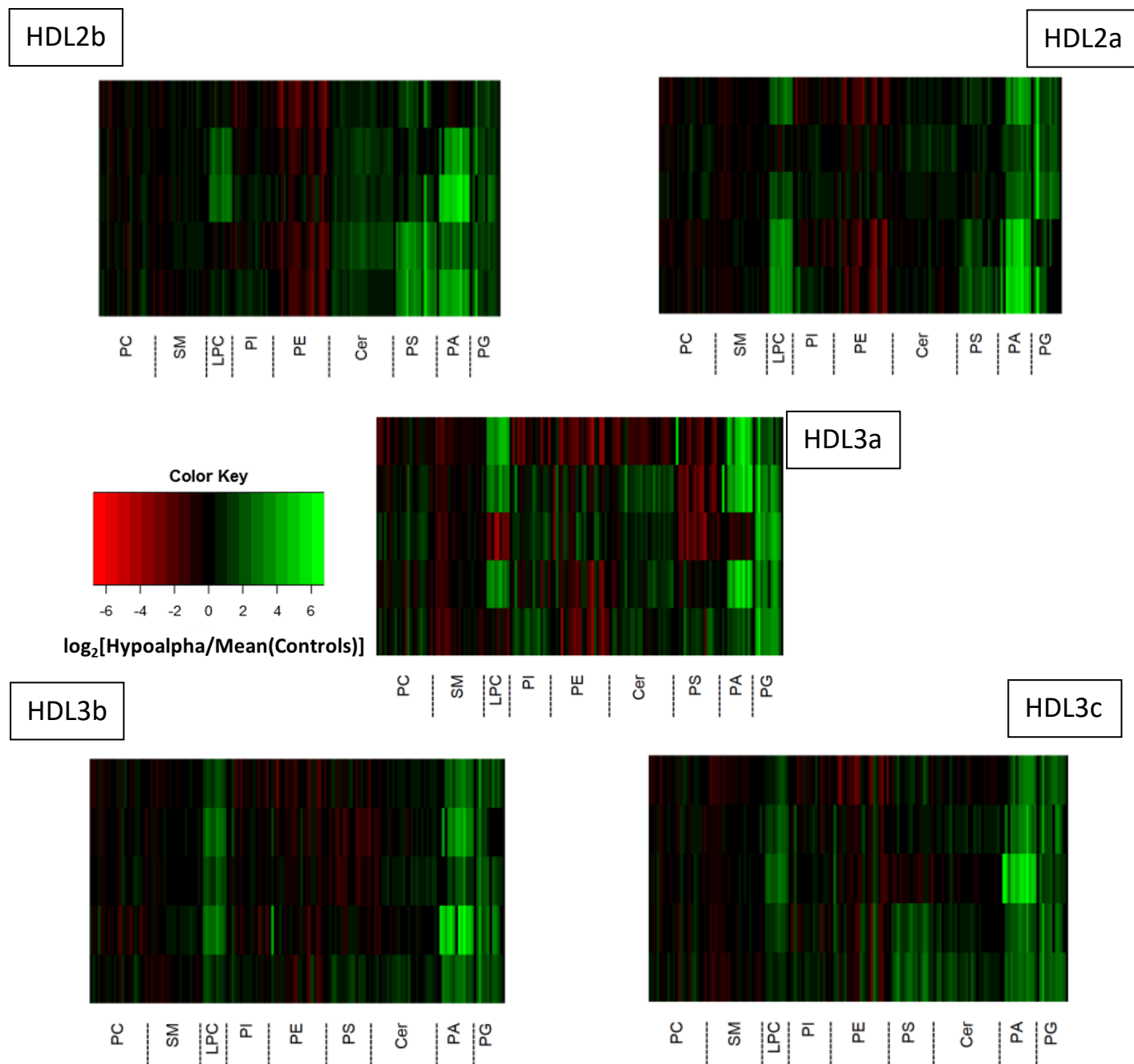


Figure 19. Heatmaps of molecular lipid species in the lipidome of HDL subpopulations of apoA-I-deficient patients and healthy controls. Abundance of every molecular species in apoA-I-deficient HDL is shown as a colored bar relative to its mean abundance in control HDL. The color represents the direction and the magnitude of the between-group differences: green color corresponds to increases in the abundance of molecular species in patients vs controls, whereas red color stays for their decreases. Within each lipid subclass, the species are presented in the order of increasing their backbone carbon chain length from left to right. Note that in HDL3b & 3c the order of Cer and PS species is inverted as compared to HDL2b, 2a & 3a, reflecting their different distribution in small, dense HDL3b & 3c.

2.1.5. Structural plots

This type of chart reveals the structure of lipid species significantly differing between the groups. Cornucopia of PC, LPC, PE, PA, and PG species with multiple double bonds in their fatty acid moieties showed significant differences (FDR-corrected) in their abundances between the patient and control groups, while differences in the species containing only saturated fatty acid residues did not reach significance (Figure 21). There were several significantly different (FDR-corrected) between the groups fully saturated species of PC, LPC and Cer classes, while the majority of the species shown in Figure 21 possessed one or several double bonds in their structure.

The most prominent and consistent differences (FDR-corrected) were found throughout HDL subpopulations for PC 34:2 (which was significantly decreased in apoA-I-deficient vs control subjects), SM 32:1 and 34:0 (which were decreased), LPC 20:3 (which was increased), PA 34:1, 36:3, 36:4 and 38:4 (which were increased), and PG 34:1, 34:2, 36:1, 36:2 and 36:3 (which were increased), revealing that unsaturated molecular species were most strongly affected by the apoA-I deficiency in the HDL lipidome. Of particular interest was the PC 34:2 species, which not only was underrepresented in all five apoA-I deficient HDL subpopulations, but was also highly abundant, representing the major HDL phospholipid species (~22 wt% of total PL+SL).

Intermediate- and long-chain species of SM and Cer were more strongly affected by FAID than their short-chain counterparts, resulting in positive correlations between their fold decrease in FAID and the carbon chain length ($r = 0.60$ and 0.38 , respectively; $p < 0.01$). The opposite was discovered for PG: short chains were most affected by FAID, judging by a negative correlation of $r = -0.41$ ($p < 0.05$) between its fold decrease in FAID and the carbon chain length. Significant negative correlation was observed between the fold decrease of PI in FAID and both carbon chain length and number of double bonds in it ($r = -0.61$ and -0.66 , respectively; both $p < 0.01$),

implying that PI with long-chain polyunsaturated species of PI took the blunt of the FAID impact. In addition, the fold decrease in PE, PG and PI species was positively correlated with the number of double bonds (e.g. $r = 0.40, 0.39$ and 0.34 for PE, PG and PI, respectively; all $p < 0.01$).

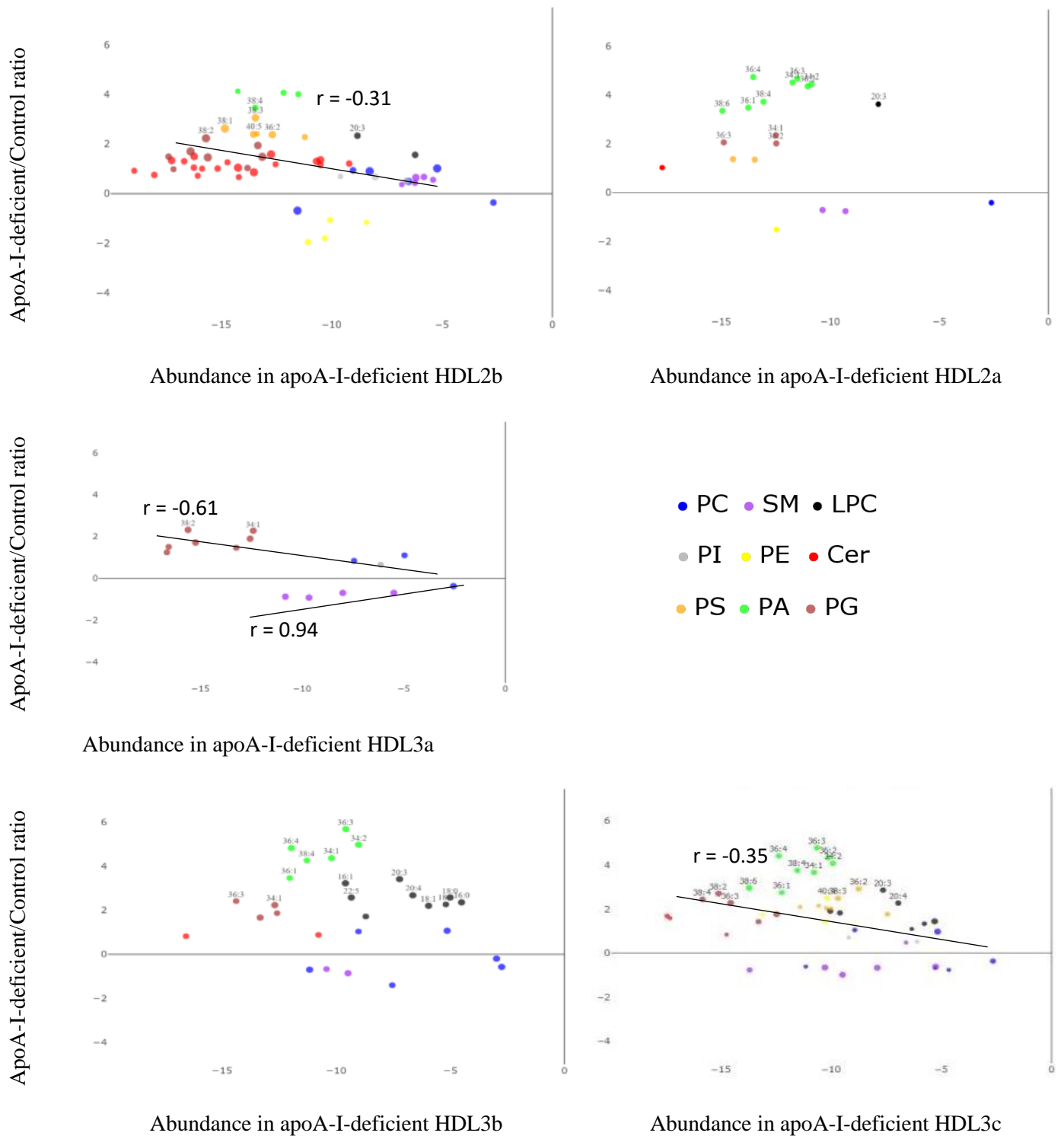
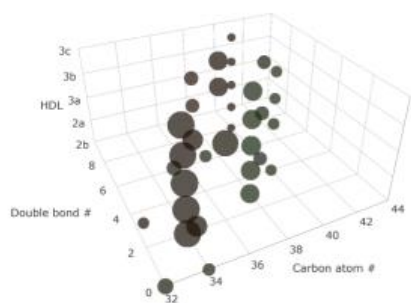
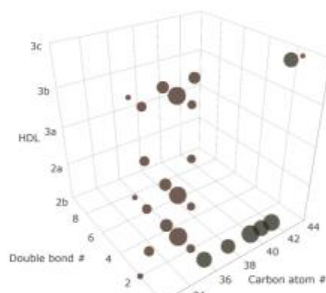


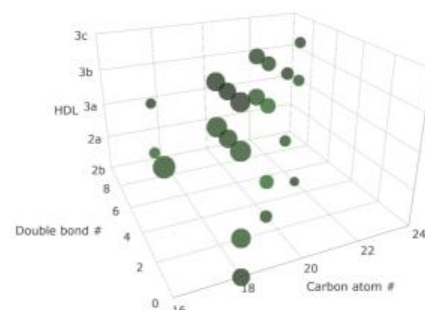
Figure 20. Bubble plots. Each colored bubble corresponds to a single molecular species. Horizontal axis represents a log₂ of the abundance of molecular species in the patient group (as wt%); vertical axis represents log₂ of the ratio of abundances of each molecular species in the patient and control groups. The $y = 0$ line separates the species that are increased in the patient group (above the line) from the species that are decreased (below the line) relative to controls. Size of each bubble is inversely proportional to the P value of the difference between the patient and control groups for a given molecular species. Only species with P values of < 0.05 for the between-group differences are shown. Species with between-group abundance ratio more than 2 or less than -2, and with between-group difference P value less than 0.01 are denoted by name tags showing their carbon backbone structure. Straight lines and corresponding r-values denote significant ($p < 0.05$) correlations between the abundance in FAID and FAID/ Control ratio



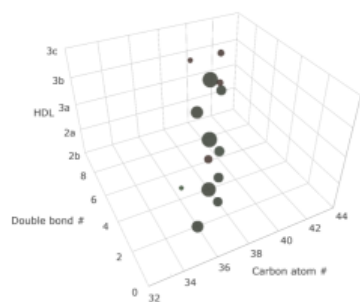
A. Phosphatidylcholines



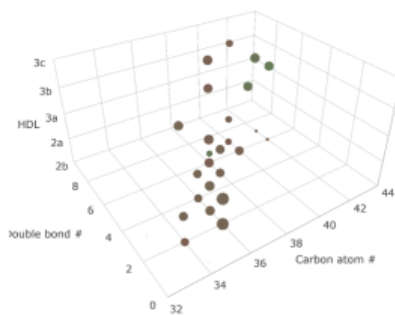
B. Sphingomyelins



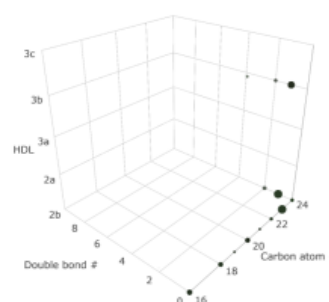
C. Lysophosphatidylcholines



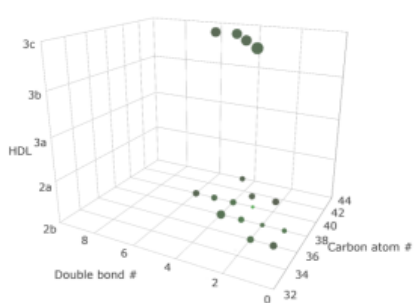
D. Phosphatidylinositols



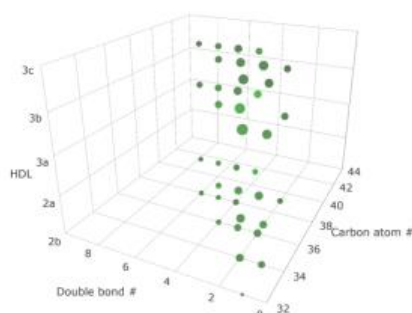
E. Phosphatidylethanolamines



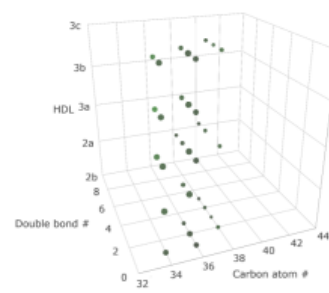
F. Ceramides



G. Phosphatidylserines



H. Phosphatidic acids



I. Phosphatidylglycerols

Color legend: $\log_2(\text{mean}[\text{ApoA-I-deficient}]/\text{mean}[\text{Control}])$

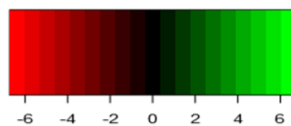


Figure 21 Structural double bond vs. carbon chain length plots of molecular species of PC (A), SM (B), LPC (C), PI (D), PE (E), Cer (F), PS (G), PA (H) and PG (I) in HDL subpopulations in apoA-I deficiency. The length of fatty acid carbon chains, their number of double bonds, and HDL subpopulation name are plotted along X, Y, and Z axes, respectively, in every single chart. Differences in lipid abundances relative to the control group expressed as $\log_2(\text{mean}[\text{ApoA-I-deficient}]/\text{mean}[\text{Control}])$ are color-coded. Red color denotes decreased abundance in comparison to controls, while green color accounts for increased abundance. The size of the dot is proportional to the mean abundance of a species in the patient group. Only species significantly differing ($p < 0.05$) in their abundance between the groups are shown.

2.1.6. Network analysis

To elucidate the role of compositional alterations for biological properties of HDL particles, network analysis was performed for all correlations between functional metrics and abundances of individual lipids in HDLs, as well as abundances of apoA-I and apoA-II proteins.

Compositional relationships revealed a systematic pattern across HDL subpopulations. Notably, SM, Cer and PS species formed three separate clusters, while LPC and PA species overlapped in another cluster. PC, PE and PI species were largely scattered around these clusters, with PG species on top (Figure 22 A). SM species were located next to those of Cer, while PS species appeared in the vicinity of those of LPC, PA and PG.

As earlier reported by us, biological properties of HDL differed significantly between the control and FAID groups for the majority of HDL subpopulations [279]. Indeed, cellular cholesterol efflux capacity was significantly reduced in the patient vs control group in all HDL subpopulations, except HDL3c. In addition, antioxidative activity of HDL, evaluated as LDL oxidation rate in the propagation phase and maximal concentration of dienes at the end of the propagation phase, showed significant decrease in the patient group for the HDL3c subpopulation, although no differences were found in HDL3b [279].

Cholesterol efflux capacity and antioxidative activity of HDLs were correlated with the abundances of multiple lipid species (Figure 22 B, C and D). Whereas cholesterol efflux capacity of HDLs was most closely associated with a single PC 34:2 as well as with numerous PS and PE species, the relationships between the HDL lipidome and antioxidative activity were less specific. Remarkably then, abundances of several species revealed significant correlations (FDR-corrected) with all the metrics of HDL functions assessed. The list of such species whose

abundances correlated with both cholesterol efflux capacity and antioxidative metrics contained 6 PC, 2 SM, 1 PI, 4 PE, 6 PS, and 5 Cer species (Table 7). Interestingly, this list contained only species with unsaturated fatty acid moieties. LPC, PA and PG species whose HDL content was markedly affected by apoA-I deficiency did not reveal significant associations with all the three functional metrics evaluated by us.

As expected, abundances of the species we observed to be positively correlated with the biological activities of HDL were significantly decreased (FDR-corrected) in apoA-I-deficient patients, while abundances of the species negatively correlated with those metrics were found to be increased (Table 7, green and red arrows). Abundances of 13 out of 24 species, linked to biological function of HDL did not show significant differences (FDR-corrected) between the groups in any HDL subpopulation. Strikingly, the abundance of PC 34:2 was decreased in apoA-I-deficient subjects throughout all five HDL subpopulations, while abundances of PC 40:4 and PC 40:8 differed in three HDL subpopulations. In addition, abundances of SM 42:1 and PS 38:4 differed in two HDL subpopulations, while abundances of PC 36:5, SM 41:1, PE 38:6, PE 40:7, Cer d18:2/14:0 and Cer d18:2/24:1 revealed differences in one HDL subpopulation only.

Table 7 Molecular lipid species whose abundance was significantly correlated with cholesterol efflux capacity and antioxidative activity of HDL subpopulations

Species significantly associated with HDL functions	HDL subpopulations in which species abundance revealed between-group differences
PC 34:2 ↓	HDL2b, HDL2a, HDL3a, HDL3b, HDL3c
PC 34:3	none
PC 36:3	none
PC 36:5 ↓	HDL3b
PC 40:4 ↑	HDL2b, HDL3b, HDL3c
PC 40:8 ↓	HDL2b, HDL3b, HDL3c
SM 41:1 ↑	HDL2b
SM 42:1 ↑	HDL2b, HDL3c
PI 40:6	none
PE 38:6 ↓	HDL2b
PE 40:6	none
PE 40:7 ↓	HDL2a
PE 42:7	none
PS 34:2	none
PS 36:1	none
PS 36:4	none
PS 38:4 ↑	HDL2b, HDL3c
PS 38:5	none
PS 40:6	none
Cer d18:2/14:0 ↑	HDL2b
Cer d18:2/22:0	none
Cer d18:2/23:0	none
Cer d18:2/24:0	none
Cer d18:2/24:1 ↑	HDL2b

Red and green arrows alongside the names of the species in the left column indicate their decreased and increased abundance respectively in apoA-I-deficient vs. control HDL subpopulations listed in the right column.

Finally, antiapoptotic activity of HDL particles assessed as inhibition of annexin V binding to starving HUVEC cells was not significantly correlated with abundances of any lipid species (Table 8).

Table 8 Antiapoptotic activity of control and apoA-I-deficient HDL

HDL2a		HDL3a		HDL3b	
Controls	Patients	Controls	Patients	Controls	Patients
39.4±13.2	62.0±23.4	50.2±18.2	48.1±7.3	58.6±17.2 [#]	39.3±27.8

Data are shown as means ± SD and expressed as % of inhibition compared to incubations in the absence of HDL. [#] significant difference from control HDL2a.

Given that S1P provides a key contribution to the capacity of HDL to reduce apoptosis [301], S1P content of HDL was evaluated to obtain additional insight into compositional determinants of this biological activity. No difference in S1P content of HDL subpopulations was observed between apoA-I-deficient and control subjects (Table 9). As reported by us earlier [291], S1P was more abundant in small, dense relative to large, light HDL in the both control and apoAI-deficient groups. Although no correlation between S1P abundance and biological activities of HDL was observed, there were significant (FDR-corrected) negative correlations of S1P content with the abundances of Cer d18:1/18:0, Cer d18:1/19:0, Cer d18:1/24:0, Cer d18:1/25:0, and Cer d18:2/23:0 in HDL2a as well as of S1P content with the abundances of PS 36:1 and PS 38:2 in HDL3a (data not shown)

Table 9 S1P content of control and apoA-I-deficient HDL

HDL2a		HDL3a		HDL3b	
Controls	Patients	Controls [#]	Patients	Controls	Patients
83.9±29.4	57.1±21.6	192.6±94.9	172±114	492±163	668±264 [§]

Data are shown as means ± SD and expressed as nmol S1P/g protein; [#] significant difference from control HDL2a; [§] significant difference from apoA-I-deficient HDL2a and 3a.

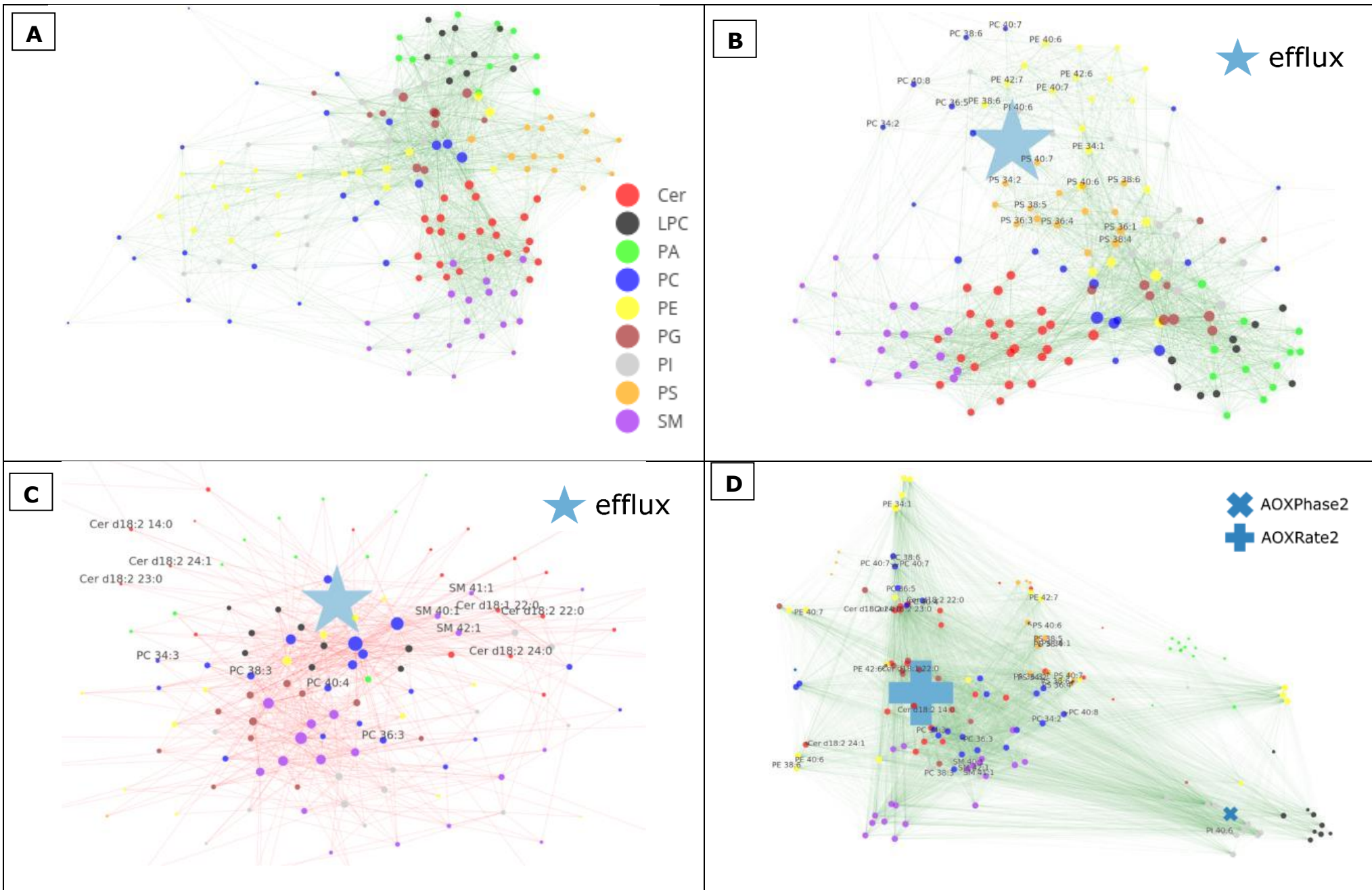


Figure 22. Network maps of molecular species abundances and functional metrics of HDL subpopulations. Positive correlations between abundances of lipid species (A), positive (B) and negative (C) correlations of cholesterol efflux capacity with the abundances of lipid species and positive correlations of metrics of antioxidative activity with the abundances of lipid species (D) are shown. Node size is proportional to the number of connections this particular node has with its neighbors. In this analysis, data obtained for all HDL subpopulations were combined. AOXPhase2, duration of the propagation phase; AOXRate2, oxidation rate in the propagation phase

2.1.7. Metabolic pathways affected by apoA-I deficiency

The list of lipid species whose abundances were correlated with the biological activities of HDL and were significantly differing between the groups was entered into the MetExplore web server [302] to identify metabolic pathways altered by apoA-I deficiency. The representation of the metabolic pathways identified was subsequently included in the classical pathway representation (Figure 23). The list of affected pathways included SL metabolism, GP metabolism, glycosylphosphatidylinositol-anchor biosynthesis, linoleic acid (LA) metabolism, and alpha-linoleic acid metabolism (Table 10). After Benjamini-Hochberg correction, significant metabolic alterations were only detected for SL, GP, and LA metabolism pathways.

Table 10 List of lipid metabolic pathways affected by apoA-I deficiency

Pathway name	Identifier	Number of reactions in the pathway	Nº of metabolites mapped onto the pathway	p-value	BH*-corrected p-value
alpha-Linolenic acid metabolism	hsa00592	9	1	0.040	0.071
Glycerophospholipid metabolism	hsa00564	49	3	0.0001	0.0009
Glycosylphosphatidylinositol -anchor biosynthesis	hsa00563	9	1	0.044	0.061
Linoleic acid metabolism	hsa00591	4	1	0.016	0.037
Sphingolipid metabolism	hsa00600	31	2	0.002	0.006

Green shading denotes significantly affected pathways. *BH, Benjamini-Hochberg

2.1.8. Lipid-related genes affected by apoA-I deficiency

The list of lipid species whose abundances were correlated with the biological activities of HDL and were significantly differing between the groups (FDR-corrected) was further used to identify lipid-related genes affected by apoA-I deficiency. For this purpose, the species names were converted to their corresponding Human Metabolome DataBase accessions and entered into the MetaboAnalyst Network Explorer tool. The analysis revealed seven genes being associated with impaired lipid metabolism in apoA-I deficiency, namely *APOA1*, *LCAT*, *Phosphatidate Cytidylyltransferase 1 (CDS1)*, *CDS2*, *Glycolipid Transfer Protein (GLTP)*, *Group IB Phospholipase A2 (PLA2G1B)*, and *Proprotein Convertase Subtilisin/Kexin Type 7 (PCSK7)* (Figure 24).

- Link
- ↔ Reversible link
- Reaction
- Metabolites

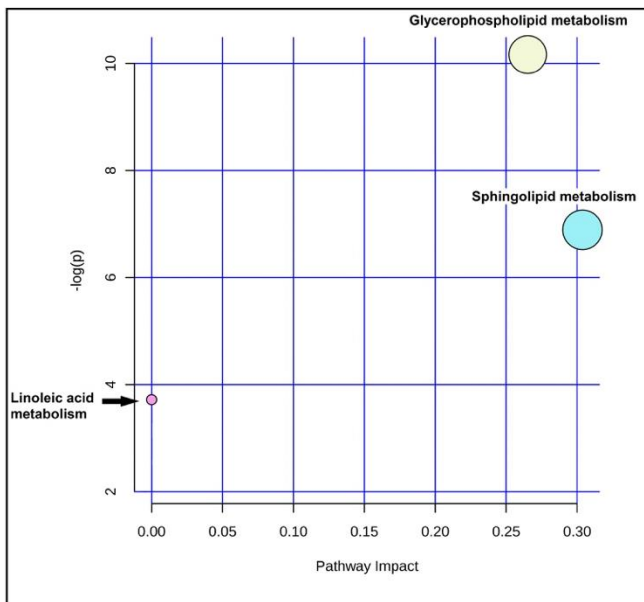
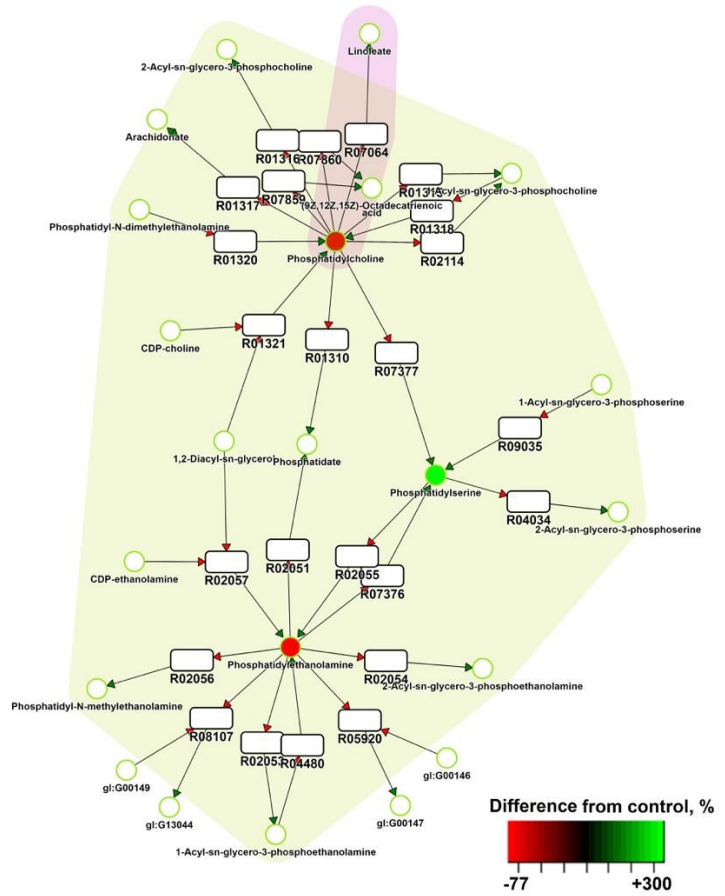
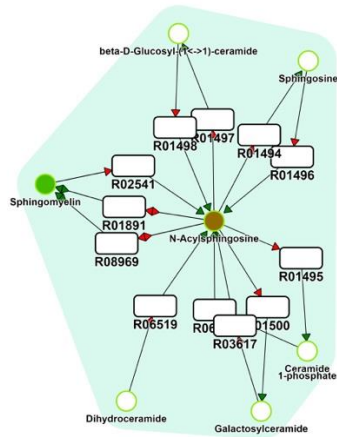


Figure 23. Metabolic pathways associated with alterations of the HDL lipidome in apoA-I deficiency, extracted using MetExplore. Inset denotes impact of identified pathways (X axis) in relationship to its significance (Y axis) produced using MetaboAnalyst. Colors in the graph highlight affected pathways and correspond to colors of circles in the inset. Green and red circles in the graph denote species whose abundances were respectively increased and decreased relative to control HDLs, with color scale at the bottom of the graph

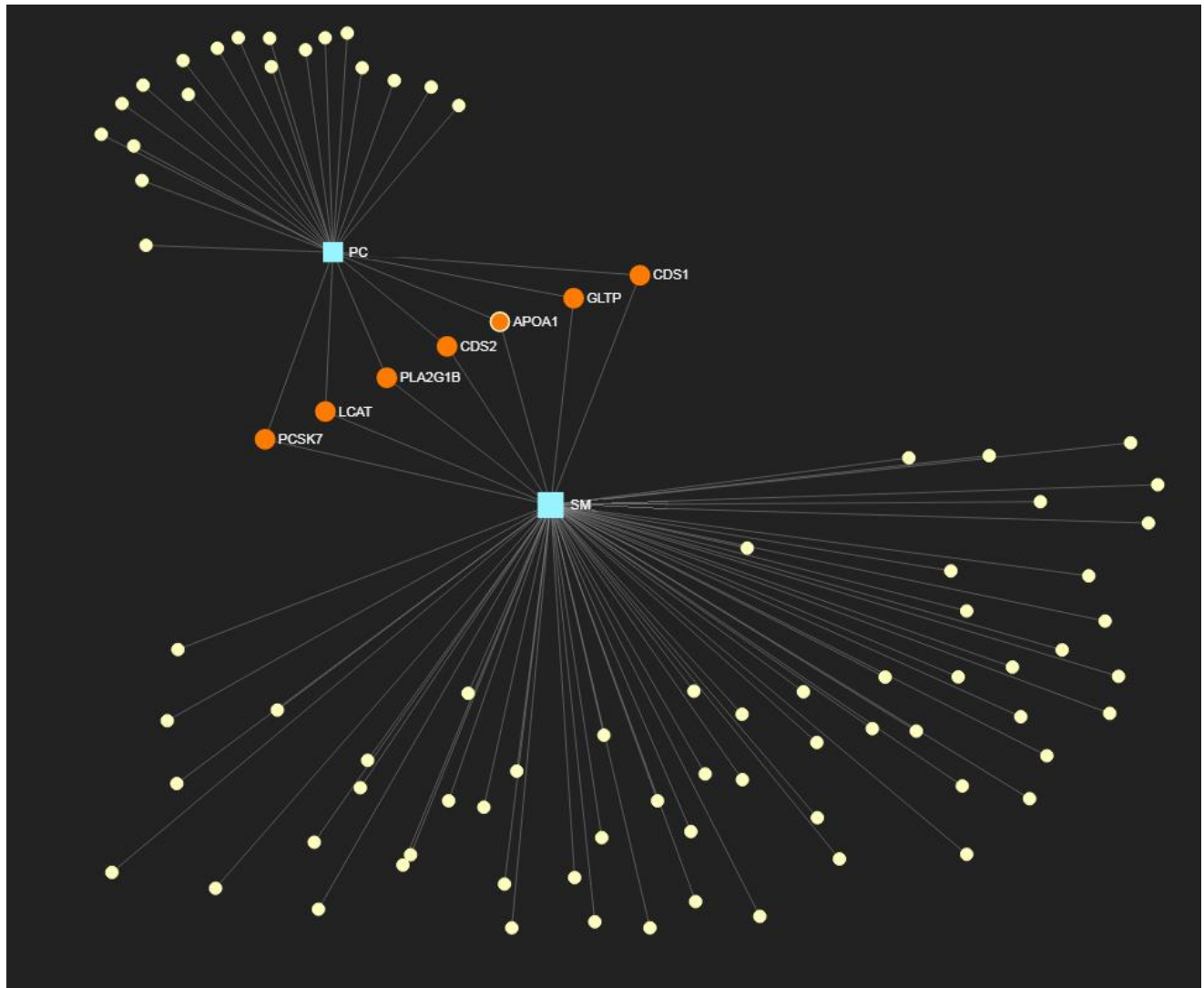


Figure 24. Genes associated with alterations of the HDL lipidome in apoA-I deficiency. Blue nodes depict molecular lipid species of phosphatidylcholine and sphingomyelin, both representatives of their lipid classes. Changes in the abundances of these species were significantly associated with seven genes shown as orange dots, notably APOA1, LCAT, Phosphatidate Cytidylyltransferase 1 (CDS1), CDS2, Glycolipid Transfer Protein (GLTP), Group IB Phospholipase A2 (PLA2G1B), and Proprotein Convertase Subtilisin/Kexin Type 7 (PCSK7). White dots denote genes significantly associated with the lipid species of phosphatidylcholine and sphingomyelin only separately, with their names therefore not provided. The analysis was performed using Metaboanalyst.

2.2 ST-elevated myocardial infarction

2.2.1. Characteristics of subjects and overall abundances of lipid classes and species

STEMI patients featured atherogenic dyslipidemia with significantly reduced HDL-C levels while no difference between the groups in age, body mass index, as well as in levels of triglycerides, LDL-C and non-HDL-C was observed as reported by us earlier (Table 11) [102].

Table 11 Clinical and biological characteristics of STEMI patients (n = 12) and control subjects (n = 10) [102].

	Controls	STEMI patients
Age, y	49±12	59±9
Body mass index, kg/m ²	23.7±2.3	26.5±2.7
Plasma parameters:		
Fasting glucose, mg/dl	78 (45–150)	124 (96–377)*
hsCRP, mg/l	0.5 (0.2–4.9)	5.6 (0.6–47.6)**
Total cholesterol, mg/dl	183±22	176±35
LDL-C, mg/dl	113±26	110±34
HDL-C, mg/dl	54±9	42±7*
Non-HDL-C, mg/dl	130±28	133±36
Triglycerides, mg/dl	93 (87-104)	125 (53–239)
ApoB100, mg/dl	92±24	89±26
ApoA-I, mg/dl	138±16	108±21*

** p < 0.01, * p < 0.05 vs. control subjects.

In terms of their overall abundance, PC predominated in the HDL lipidome (ranging from 71.3 wt% to 76.3 wt% in normolipidemic HDL3c and 2a, respectively), followed by SM, LPC, PI, PE, PS, Cer, PA and PG (ranging from 0.012 wt% to 0.015 wt% in normolipidemic HDL2b and 3c, respectively). The HDL lipidome was markedly perturbed in STEMI patients as reported earlier [102]. Interestingly, the pattern of these perturbations differed from that observed in familiar apoA-I deficiency. Among the nine phospho- and sphingolipid subclasses studied, PA was most strongly affected. Indeed, total PA was increased in STEMI patients relative to controls in all five HDL subpopulations, including both large, light and small, dense HDL subpopulations [102].

Other lipid classes showed significant between-group differences in four (LPC elevated in HDL2b, HDL2a, HDL3b and HDL3c) and one (Cer decreased in HDL3b; PC decreased in HDL3c) subpopulations [102]. No differences in the total content of SM, PE, PS, PI and PG was found in any HDL subfraction.

When abundances of lipid species were analyzed, all HDL subpopulations revealed significant between-group differences. However, the number of significantly differing between the groups species varied greatly across the HDL subpopulations for all lipid classes, including PC (from 7 to 9), SM (from 5 to 9), LPC (from 0 to 8), PI (from 0 to 5), PE (from 0 to 4), PS (from 0 to 2), Cer (from 1 to 11), PA (from 6 to 8) and PG (from 0 to 1) species (Table 12 and Table 13). The small, dense HDL3b subfraction was most affected presenting 53 species with significantly altered abundance, followed by HDL2a, 3c, 2b and 3a, presenting 50, 42, 34 and 23 such species, respectively. Significant between-group differences were typically found in the abundances of unsaturated lipid species. Indeed, among molecular species whose abundances significantly differed between the STEMI and control groups 91% (31 of 34), 92% (46 of 50), 100% (23 of 23), 94% (50 of 53) and 93% (39 of 42) possessed at least one double bond in their fatty acid carbon chain residues in HDL2b, 2a, 3a, 3b and 3c, respectively.

Table 12 Abundances of lipid species of PL and SL in HDL2b, HDL2a and HDL3a subpopulations significantly differing between STEMI patients and age-matched controls

HDL2b				HDL2a				HDL3a			
Class	Species	Controls	Patients	Class	Species	Controls	Patients	Class	Species	Controls	Patients
PC	(34:0)	0.171±0.035	0.112±0.037	PC	(32:2)	0.26±0.10	0.146±0.049	PC	(36:2)	14.3±1.1	11.4±1.8
	(36:2)	13.4±1.28	10.5±1.07		(34:0)	0.166±0.034	0.121±0.032		(36:4)	8.3±1.9	12.0±1.7
	(36:5)	1.34±0.58	0.77±0.29		(36:1)	1.84±0.33	1.24±0.22		(36:5)	1.41±0.69	0.791±0.217
	(38:5)	2.68±0.43	2.28±0.31		(36:2)	13.6±1.7	11.1±1.3		(38:4)	4.86±0.61	6.57±1.10
	(40:2)	0.00676±0.00119	0.00189±0.00089		(36:5)	1.30±0.62	0.74±0.17		(40:2)	0.0080±0.0012	0.0032±0.0028 0.135 (0.117; 0.256)
	(40:3)	0.00865±0.00248	0.00425±0.00180		(40:2)	0.00737±0.00102	0.00223±0.00145		(40:7)	0.291±0.090	
	(40:7)	0.242±0.074	0.149±0.072		(40:3)	0.0093±0.0020	0.00118±0.00049		(40:8)	0.066±0.012	0.0250±0.0098
	(40:8)	0.056±0.011	0.023±0.008		(40:8)	0.0672±0.0170	0.0275±0.0105				
SM	(32:2)	0.0189±0.0048	0.0103±0.0047	SM	(32:1)	0.285±0.048	0.197±0.057	SM	(32:1)	0.238±0.031	0.161±0.053
	(36:1)	1.01±0.17	1.29±0.16		(32:2)	0.0133 (0.0118; 0.0226)	0.00885±0.00528		(32:2)	0.0124±0.0023	0.0056±0.0014
	(37:1)	0.186±0.033	0.131±0.024		(36:1)	0.667±0.070	1.03±0.16		(38:2)	0.268±0.030	0.235±0.012
	(40:2)	1.28±0.16	0.98±0.23		(36:2)	0.47±0.04	0.55±0.07		(41:2)	0.57±0.06	0.41±0.07
	(41:2)	0.76±0.12	0.54±0.09		(37:1)	0.181±0.038	0.135±0.026		(43:2)	0.135±0.033	0.072±0.035
	(42:2)	2.91±0.34	2.38±0.44		(40:2)	1.17±0.13	0.81±0.14				
					(41:2)	0.617±0.067	0.509±0.121 1.079 (0.929; 1.467)				
					(42:3)	1.42±0.27	0.012 (0.041; 0.146)				
			(43:2)	0.139±0.032							
LPC	(16:0)	0.68±0.22	1.31±0.64	LPC	(16:0)	0.52±0.14	1.73±1.26	LPC			
	(20:3)	0.0333±0.0137	0.0819±0.0518		(16:1)	0.0105±0.0043	0.025±0.018				
	(20:4)	0.0829±0.0408	0.244±0.169		(18:2)	0.282±0.099	0.872±0.673				
					(20:3)	0.0351±0.0158	0.164±0.121				
					(20:4)	0.0886±0.0449	0.2495 (0.0929; 0.9764)				
					(22:5)	0.0128±0.0032	0.0276 (0.0132; 0.1056)				
			(22:6)	0.028±0.011	0.0903±0.0563						

PI	(34:0)	0.00182±0.00033	0.0073 (0.0011; 0.0238)	PI	(34:0)	0.00199±0.00083	0.00373 (0.00138; 0.02628)	PI	(36:1)	0.0992±0.0291	0.0555±0.0151
	(36:1)	0.078±0.013	0.0477±0.0207		(34:1)	0.108±0.020	0.072±0.027				
	(38:5)	0.0462±0.0117	0.0312±0.0108		(36:1)	0.0962±0.0231	0.0434±0.0089				
					(38:5)	0.0596±0.0192	0.0402±0.0093				
					(40:4)	0.0100 (0.0094; 0.0141)	0.0154±0.0046				
PE				PE	(34:1)	0.0342±0.0192	0.0761±0.0227	PE	(34:3)	0.00431 (0.00135; 0.00816) 0.00454 (0.00219; 0.02536)	0.0090±0.0032
					(34:3)	0.00494±0.00279 0.0166 (0.0103; 0.0568)	0.00845±0.00298		(40:4)		0.0206±0.0118
					(38:3)		0.0409±0.0154				
					(42:6)	0.00158±0.00060	0.00055±0.00032				
PS	(38:4)	0.0059 (0.0039; 0.0134)	0.0167±0.0082	PS	(38:1)	0.00144	0.00027±0.00007	PS			
					(38:4)	0.0072±0.0033	0.0128±0.0050				
Cer	(d18:1- 18:0)	0.00232±0.00086	0.00402±0.00114	Cer	(d18:0- 24:0)	0.00015±0.00004	0.00005 (0.00003; 0.00015)	Cer	(d18:1- 25:0)	0.00167±0.00070	0.00072±0.00051
	(d18:1- 26:1)	0.00054±0.00021	0.00183±0.00099		(d18:1- 18:0)	0.00150±0.00057	0.00269±0.00087				
	(d18:2- 14:0)	0.00010±0.00004	0.00005±0.00002		(d18:1- 26:1)	0.00023±0.00011	0.00092±0.00072				
					(d18:2- 14:0)	0.00009±0.00003	0.00004±0.00002 0.00070 (0.00043; 0.00192)				
					(d18:2- 16:0)	0.00118±0.00023					
					(d18:2- 22:0)	0.00594±0.00291	0.00285±0.00192 0.00154 (0.00084; 0.00497)				
					(d18:2- 23:0)	0.00472±0.00207					
PA	(34:1)	0.0014±0.0005	0.0055 (0.0022; 0.0137)	PA	(34:1)	0.0015±0.0009	0.0047 (0.0019; 0.0193)	PA	(34:1)	0.0025±0.0014 0.0033 (0.0024; 0.0099)	0.0084 (0.0035; 0.0355)
	(34:2)	0.0020±0.0007	0.0111±0.0076		(34:2)	0.0025±0.0005	0.0093 (0.0041; 0.0374)		(34:2)		0.029±0.027

(36:1)	0.0006±0.0002	0.0026±0.0012	(36:2)	0.0017±0.0004	0.0047 (0.0022; 0.0312)	(36:1)	0.0009±0.0003	0.0048±0.0033
(36:2)	0.0014±0.0007	0.0048±0.0020	(36:3)	0.0011±0.0005	0.0024 (0.0013; 0.0155)	(36:2)	0.0022 (0.0013; 0.0054)	0.0088±0.0058
(36:3)	0.0009±0.0005	0.0024 (0.0011; 0.0076)	(36:4)	0.0003±0.0001	0.0023 (0.0009; 0.0164)	(36:4)	0.0004 (0.0002; 0.0016)	0.0067±0.0058
(36:4)	0.0003±0.0001	0.0022±0.0013	(38:3)	0.00020±0.00009	0.00189±0.0017	(38:4)	0.0008 (0.0006; 0.0022)	0.0090±0.0052
(38:3)	0.00023±0.00016	0.00158±0.00102	(38:4)	0.00052±0.00011	0.00475±0.00308			
(38:4)	0.0008±0.0004	0.0059±0.0050						
(38:6)	0.00030±0.00016	0.00065±0.00022						
PG		0.00012 (0.00009; 0.00029)	PG					
(38:5)	0.00033±0.00013		(38:5)	0.00042±0.00013	0.00021±0.00013	(38:5)	0.00039±0.00017	0.00016±0.00004

Data are shown as means ± SD and expressed as wt% of total PL+SL; only lipid species whose abundances significantly (p<0.05) differed between the groups are shown; significantly elevated values are highlighted in bold;

Table 13. Abundances of molecular lipid species of PL and SL in small, dense HDL3b and HDL3c subpopulations significantly differing between STEMI patients and age-matched controls

HDL3b				HDL3c			
Class	Species	Controls	Patients	Class	Species	Controls	Patients
PC	(36:1)	1.94±0.33	1.29±0.24	PC	(32:2)	0.224±0.094	0.0999±0.0278
	(36:2)	14.3±1.0	11.1±1.4		(34:0)	0.186±0.039	0.136±0.020
	(36:4)	7.78±1.99	10.9±1.8		(36:1)	2.07±0.21	1.13 (1.01; 1.90)
	(36:5)	1.55±0.60	0.80±0.22		(36:2)	13.2±1.7	10.5±1.7
	(38:5)	3.08±0.38	2.67±0.23		(36:5)	1.49±0.55	0.62 (0.53; 0.92)
	(38:6)	4.37±1.09	3.05±1.26		(38:5)	3.11±0.47	2.58±0.31
	(40:2)	0.00640±0.00189	0.00291±0.00120		(40:2)	0.00652±0.00263	0.00143±0.00053
	(40:3)	0.00922±0.00261	0.00349±0.00195		(40:7)	0.32±0.058	0.158±0.107
(40:8)	0.0720±0.0129	0.0325±0.0081	(40:8)	0.0721±0.0157	0.0234±0.0134		
SM	(32:1)	0.25±0.0286	0.172±0.048	SM	(32:1)	0.272±0.0442	0.186±0.0577
	(36:2)	0.447±0.057	0.523±0.081		(32:2)	0.0149±0.00374	0.00676±0.0047
	(37:1)	0.194±0.054	0.127±0.033		(37:1)	0.195±0.0684	0.123±0.0319
	(40:2)	1.02±0.18	0.80±0.15		(40:2)	1.04±0.19	0.75±0.14
	(41:2)	0.56±0.07	0.42±0.06		(41:2)	0.61±0.11	0.44±0.07
	(42:3)	1.30±0.21	1.06±0.21		(43:2)	0.13±0.02	0.08±0.03
	(43:2)	0.13 (0.12; 0.18)	0.10±0.05				
LPC	(16:0)	0.63±0.25	1.53±0.77	LPC	(16:0)	1.26±0.69	2.82 (1.87; 7.41)
	(16:1)	0.0126±0.0065	0.0392±0.0301		(16:1)	0.02±0.01	0.04 (0.02; 0.19)
	(18:0)	0.33±0.14	0.71±0.38		(18:0)	0.69±0.30	1.13 (0.76; 3.79)
	(18:2)	0.336±0.191	0.73±0.40		(18:2)	0.496±0.311	1.51±0.91
	(20:3)	0.0265 (0.0168; 0.0855)	0.148±0.083		(20:3)	0.062±0.035	0.289±0.175
	(20:4)	0.125±0.077	0.399±0.219		(20:4)	0.154±0.083	0.622±0.282
	(22:5)	0.018±0.009	0.034 (0.020; 0.125)		(22:5)	0.026±0.0158	0.0926±0.0511
	(22:6)	0.0479±0.0244	0.0772 (0.0478; 0.2642)		(22:6)	0.0703±0.0427	0.19±0.11
PI	(34:1)	0.126±0.048	0.073±0.029	PI			
	(36:1)	0.103 (0.074; 0.210)	0.0479±0.0179				
	(38:5)	0.0591±0.0137	0.0403±0.0166				

	(38:6)	0.0179±0.008	0.00767 (0.00529; 0.01878)				
	(40:6)	0.053±0.023	0.0305±0.0116				
PE	(34:1)	0.0438±0.0254	0.0738±0.0291	PE	(36:5)	0.0071±0.0036	0.0029 (0.0022; 0.0069)
	(34:2)	0.107±0.076	0.186±0.034		(38:3)	0.0252±0.0135	0.0547±0.0236
	(38:3)	0.0177 (0.0086; 0.0375)	0.0379±0.0145				
	(42:6)	0.00132±0.00059	0.00048±0.00019				
PS	(40:7)	0.00205±0.00143	0.00083±0.00019	PS			
Cer	(d18:1-14:0)	0.00020±0.00007	0.00011±0.00005	Cer	(d18:1-18:0)	0.00181±0.00046	0.00305±0.00107
	(d18:1-18:0)	0.0017±0.0003	0.00222 (0.00146; 0.00403)		(d18:1-22:0)	0.013±0.003	0.00639 (0.00554; 0.01474)
	(d18:1-22:0)	0.0110 (0.0092; 0.0215)	0.0084 (0.0062; 0.0157)		(d18:1-24:0)	0.0283±0.0097	0.0131 (0.0098; 0.0333)
	(d18:1-24:0)	0.0273±0.0072	0.0182±0.0069		(d18:1-24:1)	0.0179 (0.0158; 0.0276)	0.0138±0.0056
	(d18:1-24:1)	0.0198±0.0034	0.0141±0.0043		(d18:1-25:0)	0.00178±0.00068	0.00073±0.00023
	(d18:1-25:0)	0.00147±0.00041	0.00085±0.00055		(d18:1-26:0)	0.00105±0.00030	0.00054±0.00033
	(d18:2-14:0)	0.00006±0.00002	0.00003±0.00002		(d18:2-22:0)	0.00392±0.00108	0.00190±0.00082
	(d18:2-22:0)	0.00469±0.00094	0.00243±0.00098		(d18:2-24:0)	0.0082 (0.0060; 0.0139)	0.00478±0.00209
	(d18:2-23:0)	0.00352±0.00138	0.00184±0.00096				
	(d18:2-24:0)	0.0104±0.0035	0.0067±0.0035				
	(d18:2-24:1)	0.00589±0.00177	0.00366±0.00144				
PA	(32:0)	0.00272±0.00218	0.01141 (0.00690; 0.03358)	PA	(34:1)	0.00439±0.00126	0.0226±0.0175
	(34:1)	0.00377±0.00127	0.01150±0.00716		(34:2)	0.00519±0.00172	0.0395±0.0277
	(34:2)	0.00562±0.00229	0.01294 (0.00365; 0.06088)		(36:2)	0.00364±0.00182	0.0270 (0.0048; 0.0317)
	(36:2)	0.00343±0.00149	0.00754±0.00472		(36:3)	0.00183±0.00091	0.01359 (0.00231; 0.01660)
	(36:3)	0.00178±0.00075	0.00471±0.00302		(36:4)	0.00078±0.00026	0.0096±0.0071
	(36:4)	0.0011±0.0009	0.0041±0.0028		(38:3)	0.0005±0.0001	0.0046±0.0039
	(38:3)	0.00044±0.00024	0.00233±0.00197		(38:4)	0.0022 (0.0008; 0.0078)	0.0137±0.0103
	(38:4)	0.00224±0.00113	0.00909±0.00605		(38:5)	0.00085±0.00048	0.00191 (0.00106; 0.00743)
PG				PG	(38:5)	0.00053±0.00029	0.00018±0.00009

Data are shown as means ± SD and expressed as wt% of total PL+SL; only lipid species whose abundances significantly ($p < 0.05$) differed between the groups are shown; significantly elevated values are highlighted in bold.

2.2.2. PCA

When PCA was applied to our dataset, the control and patient groups were entirely separated for the lipidome of both small, dense HDL3c and large, light HDL2b subpopulations, and largely separated for the lipidome of HDL2a, 3a & 3b (Figure 25), on planes of the first two Principal Components, indicating that individual components of the HDL lipidome were strongly altered in STEMI subjects. Indeed, for each of the five HDL subpopulations, the amount of variance explained by the first two principal components was higher than 38%, consistent with marked differences between the groups.

2.2.3. Heatmaps

When heatmaps were built for the differences in the abundances of lipid species between STEMI and control subjects, a distinct pattern was consistently observed across all HDL subpopulations (Figure 26). Notably, abundances of LPC and PA species were typically elevated in STEMI HDLs as compared to their counterparts from controls, while the content of PC and Cer species was decreased. Profiles of other five phospholipid subclasses revealed mixed patterns, with species overrepresented and underrepresented in STEMI HDLs making up comparable shares.

2.2.4. Bubble plots

Extending upon the information provided by the heatmaps, the bubble plots revealed that abundances of numerous species of PC and SM, as well as of some Cer species were consistently decreased in STEMI HDLs (Figure 27). By contrast, LPC and PA species were typically increased across HDL subpopulations. PE and PI species revealed mixed patterns involving both elevated and reduced abundances in STEMI HDL. Importantly, positive correlations between the magnitude of between-group difference for the species and their overall abundance in the HDL lipidome were observed for PC, SM and Cer lipids collectively ($r = 0.68, 0.61, 0.79, 0.66$ and

0.65 for HDL2b, 2a, 3a, 3b and 3c, respectively; $p < 0.005$ for all). On the contrary, LPC and PA species collectively avoided this trend, forming clusters in a seemingly random manner, or presenting with a counter-trend of negative correlations between the magnitude of difference between the groups and overall abundance in HDL lipidome, reaching significance in HDL2b ($r = -0.53$, $p < 0.05$), HDL3a ($r = -0.72$, $p < 0.05$) and HDL3b ($r = -0.49$, $p < 0.05$) subpopulations. Together with the heatmaps, the bubble plots thereby demonstrated that moderately and highly abundant, within their classes, PC, SM and Cer species were altered modestly, while low-abundant species of PC and PA, as well as moderately to highly-abundant species of LPC were affected more strongly in STEMI HDL.

2.2.5. Structural plots

Structural plots reveal the structure of lipid species whose abundances significantly differed between the groups. Cornucopia of PC, SM, LPC, PI, PE and PA species with multiple double bonds in their fatty acid moieties showed significant differences in their abundances between the patient and control groups, while differences in the HDL content of the species containing only saturated fatty acid residues typically did not reach significance (Figure 28). Indeed, there were only few significantly different between the groups fully saturated species of PC, SM, LPC and PI classes, while the majority of the species shown in Figure 28 possessed one or several double bonds in their structure. The most prominent and consistent differences were found throughout HDL subpopulations for PC 36:2, 36:5 and 40:8, SM 32:2, 41:2 (which were all significantly decreased in STEMI vs control subjects), as well as for LPC 16:0, 20:3 and 20:4, and PA 34:1, 34:2, 36:2, 36:4, and 38:4 (all increased vs controls) revealing that unsaturated molecular species were most strongly affected by STEMI in the HDL lipidome.

Intermediate- and long-chain species of PC, PI and PG were more strongly affected by STEMI than their short-chain counterparts, resulting in positive correlations between their fold decrease in STEMI and the carbon chain length (e.g. $r = 0.20, 0.27$ and 0.23 for PC, PG and PI classes, respectively; all $p < 0.05$). In addition, the fold decrease in PE, PG and PI species was positively correlated with the number of double bonds (e.g. $r = 0.40, 0.39$ and 0.34 for PE, PG and PI, respectively; all $p < 0.01$)

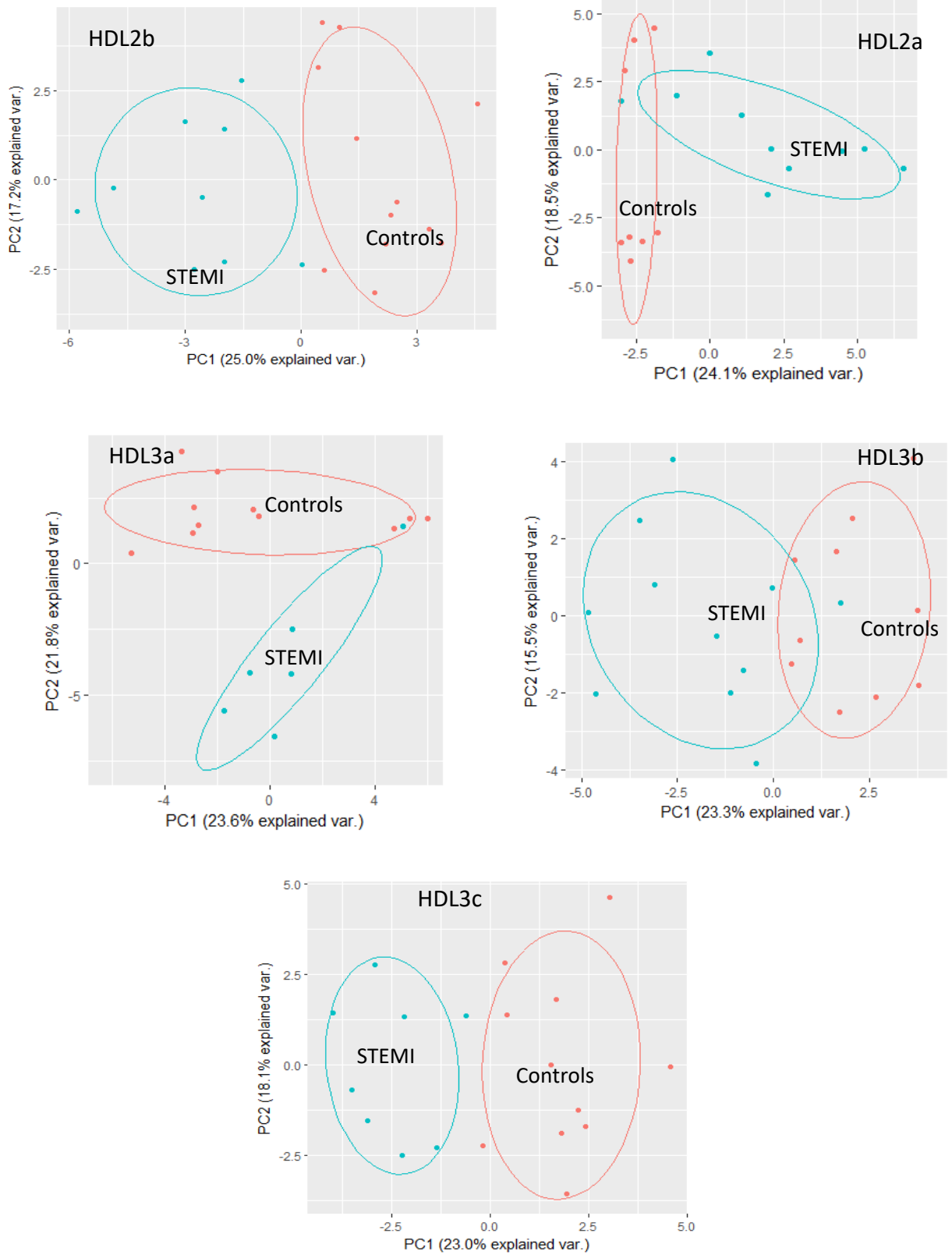


Figure 25 PCA plots for large, light HDL2b, HDL2a and small, dense HDL3a, HDL3b and HDL3c subpopulations. Blue and red ellipses represent the STEMI and control groups, respectively. Total amounts of variance explained by the first two components is more than 38% for each chart.

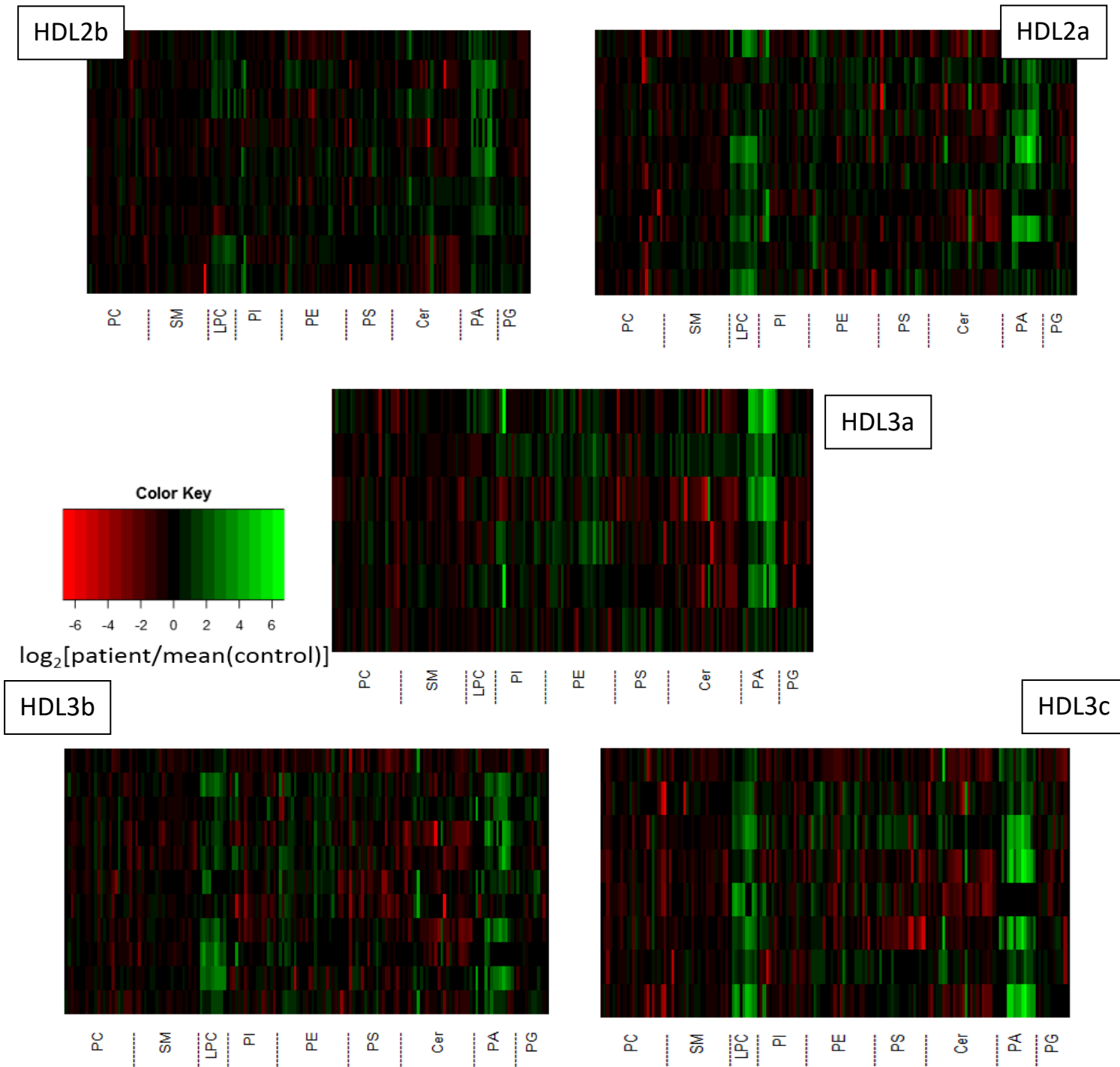


Figure 26 Heatmaps of molecular lipid species in the lipidome of HDL subpopulations of STEMI patients and healthy controls. Green color corresponds to increases in the abundance of molecular species in patients vs controls, whereas red color stays for their decreases. Within each lipid subclass, the species are presented in the order of increasing their backbone carbon chain length from left to right.

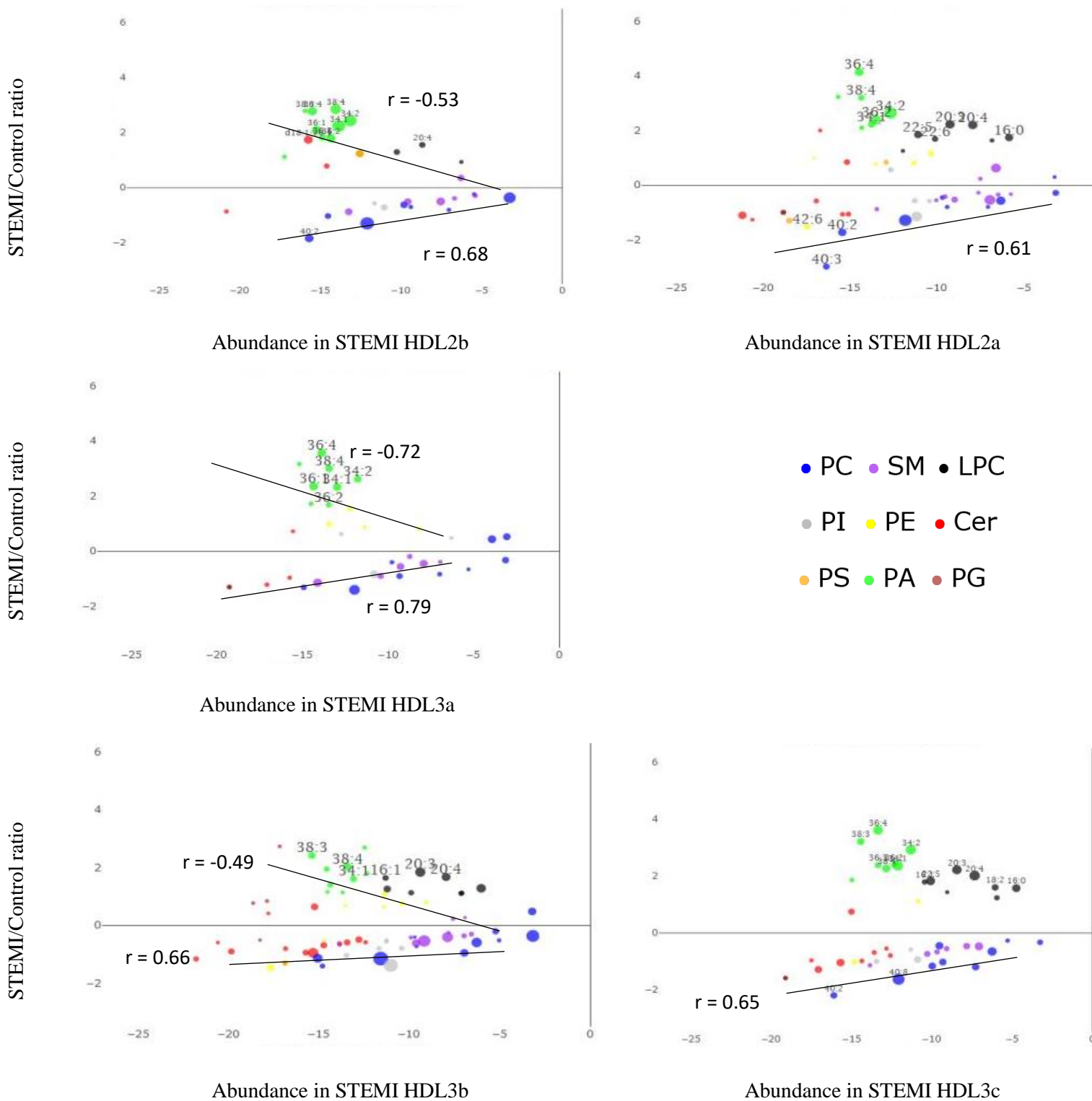
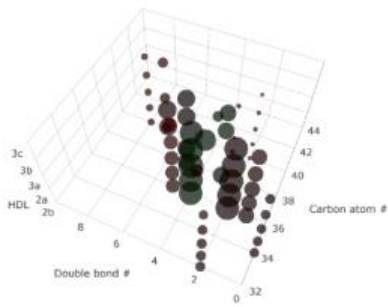
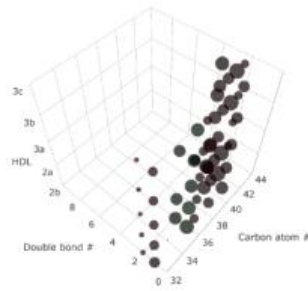


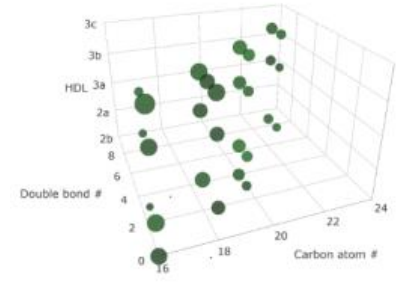
Figure 27. Bubble plots. Each colored bubble corresponds to a single molecular species. Horizontal axis represents a log₂ of the abundance of molecular species in the patient group (as wt%); vertical axis represents log₂ of the ratio of abundances of each molecular species in the patient and control groups. The y = 0 line separates the species that are increased in the patient group (above the line) from the species that are decreased (below the line) relative to controls. Size of each bubble is inversely proportional to the P value of the difference between the patient and control groups for a given molecular species. Only species with P values of < 0.05 for the between-group differences are shown. Species with between-group abundance ratio more than 2 or less than -2, and with between-group difference P value less than 0.01 are denoted by name tags showing their carbon backbone structure. Straight lines and corresponding r-values denote significant ($p < 0.05$) correlations between the abundance in STEMI and STEMI/Control ratio.



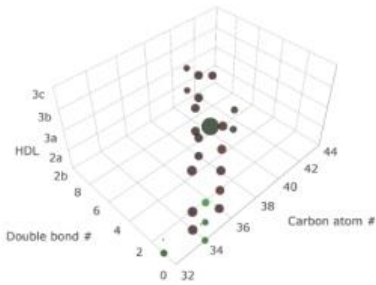
A. Phosphatidylcholines



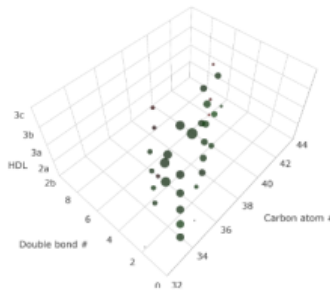
B. Sphingomyelins



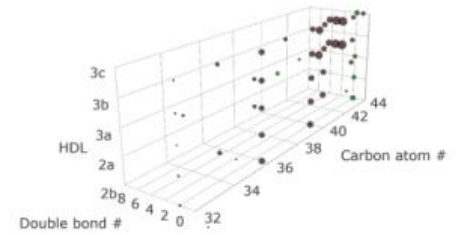
C. Lysophosphatidylcholines



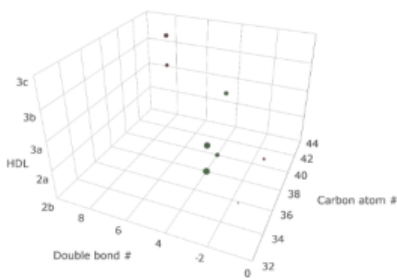
D. Phosphatidylinositols



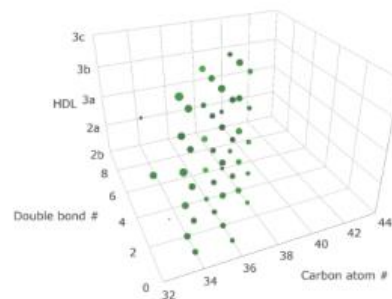
E. Phosphatidylethanolamines



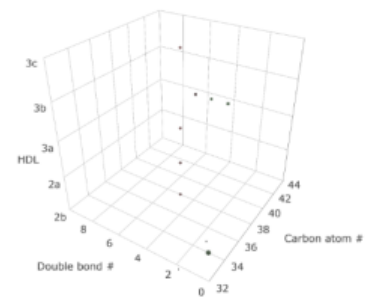
F. Ceramides



G. Phosphatidylserines



H. Phosphatidic acids



I. Phosphatidylglycerols

$\log_2(\text{mean[STEMI]}/\text{mean[Control]})$

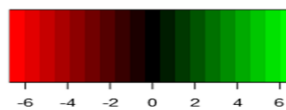


Figure 28. Structural double bond vs. carbon chain length plots of molecular species of PC (A), SM (B), LPC (C), PI (D), PE (E), Cer (F), PS (G), PA (H) and PG (I) in HDL subpopulations in STEMI patients in comparison to control subjects. The length of fatty acid carbon chains, their number of double bonds, and HDL subpopulation name are plotted along X, Y, and Z axes, respectively, in every single chart. Difference in lipid abundances relative to the control group expressed as $\log_2(\text{mean[STEMI]}/\text{mean[Control]})$ are color-coded. Red color denotes decreased abundance in comparison to controls, while green color accounts for increased abundance. The size of the dot is proportional to the mean abundance of a species in the patient group. Only species significantly differing ($p < 0.05$) in their abundance between the groups are shown.

2.2.6. Network maps

To elucidate the role of compositional alterations for biological properties of HDL particles, network analysis was performed for all correlations between functional metrics and individual lipid abundances in HDLs.

Compositional relationships revealed a systematic pattern across HDL subpopulations.

Interestingly, PC, PE and PS species formed three separate clusters, while LPC and PA, as well as SM and Cer species overlapped in two mixed clusters, respectively. PI and PG species were largely scattered around these clusters (Figure 29, A).

Cholesterol efflux capacity and antioxidative activity of HDLs were correlated with the abundances of multiple lipid species (Figure 29 B, C and D). Whereas cholesterol efflux capacity of HDLs was closely associated with a handful of PS, PI and PE species, the relationships between the HDL lipidome and antioxidative activity were less specific, involving species from multiple lipid classes, of which species of LPC revealed the most consistent associations.

Remarkably then, abundances of several species revealed significant correlations with all the metrics of HDL functionality assessed. The list of such species whose abundances correlated with both cholesterol efflux capacity and antioxidative metrics contained PC 38:5, PI 36:1 and PS 38:1 (Table 14) all of which possessed unsaturated fatty acid moieties. Intriguingly, none of SM, LPC, PA and Cer species whose HDL content was markedly affected by STEMI, revealed significant associations with all the functional metrics evaluated by us. As expected, abundances of the species we observed to be positively correlated with the biological activities of HDL were significantly decreased in STEMI patients (Table 14). The abundance of PI 36:1 species, linked to biological functions of HDL, was significantly decreased in STEMI subjects across all five

HDL subpopulations, while the abundance of PC 38:5 differed in four HDL subpopulations. By contrast, the abundance of PS 38:1 revealed differences in the HDL2a subpopulation only.

Table 14 Molecular lipid species whose abundance was significantly correlated with cholesterol efflux capacity and antioxidative activity of HDL subpopulations

Species significantly associated with HDL functions and direction of the differences in STEMI vs control HDL	HDL subpopulations in which the species revealed between-group differences in their abundance
PC 38:5 ↓	HDL2b, HDL3b, HDL3c
PI 36:1 ↓	HDL2b, HDL2a, HDL3a, HDL3b, HDL3c
PS 38:1 ↓	HDL2a

Red arrows alongside the names of the species in the left column indicate their decreased abundance respectively in STEMI vs. control HDL subpopulations listed in the right column.

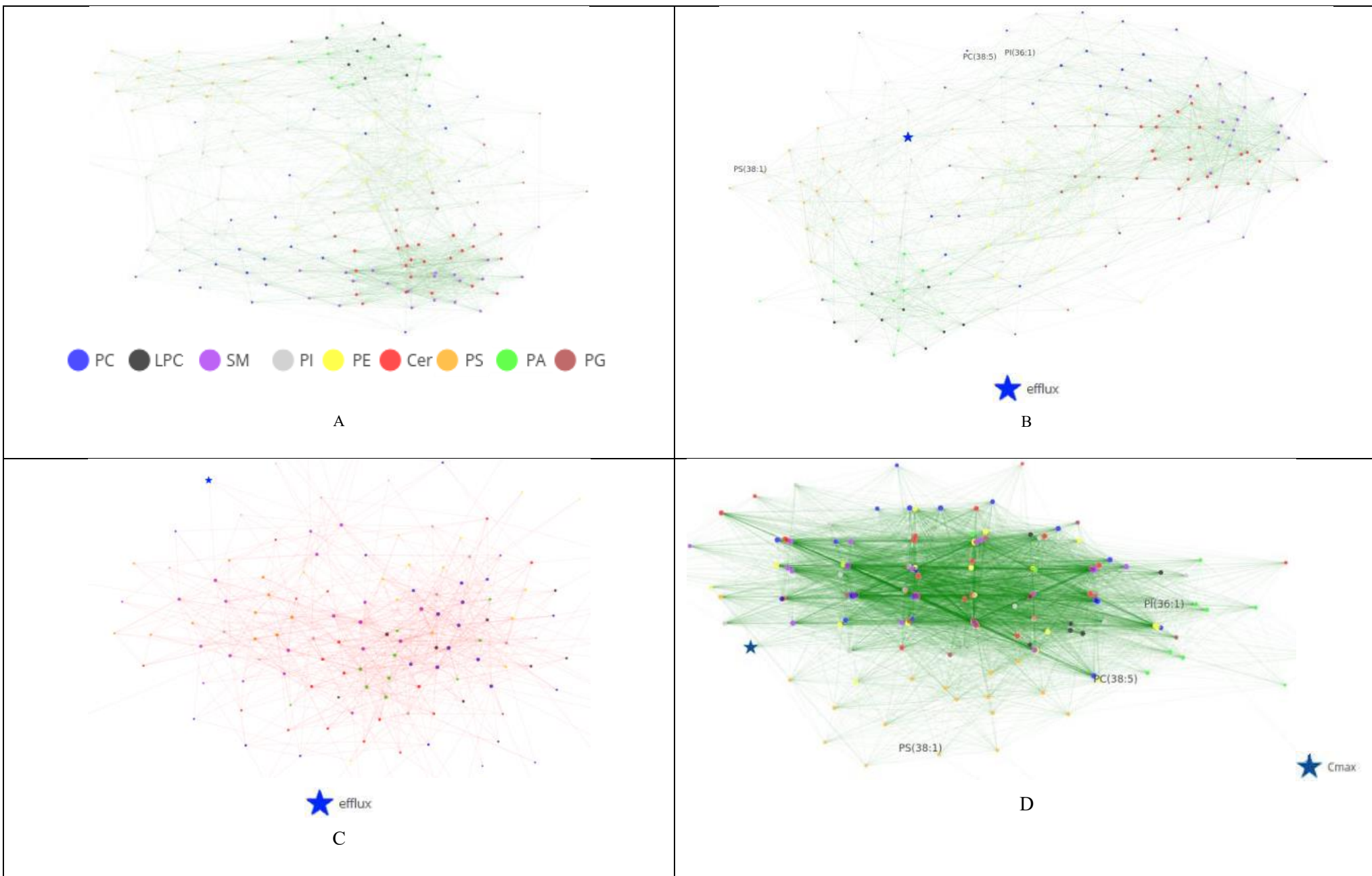


Figure 29 Network maps of molecular species abundances and functional metrics of HDL subpopulations. Positive correlations between abundances of lipid species (A) are shown. Positive correlations of cholesterol efflux capacity with the abundances of lipid species (B) are shown together with their negative correlations of cholesterol efflux capacity with the abundances of lipid species (C). Positive correlations of metrics of antioxidative activity and the abundances (D) are also represented. Node size is proportional to the number of connections this particular node displays with its neighbours. In this analysis, data obtained for all HDL subpopulations were combined.

2.2.7. Metabolic pathways affected by STEMI

The list of lipid species whose abundances were correlated with the biological activities of HDL and were significantly differing between the groups was entered into the MetExplore web server in order to identify metabolic pathways altered by STEMI. The representation of the metabolic pathways identified was subsequently included in the classical pathway representation (Figure 30). The list of affected pathways included inositol phosphate, GP, alpha-LA, GPIab and LA metabolism (Table 15). Following the BH-correction, significant metabolic alterations were only detected for glycerophospholipid and linoleic acid metabolism pathways.

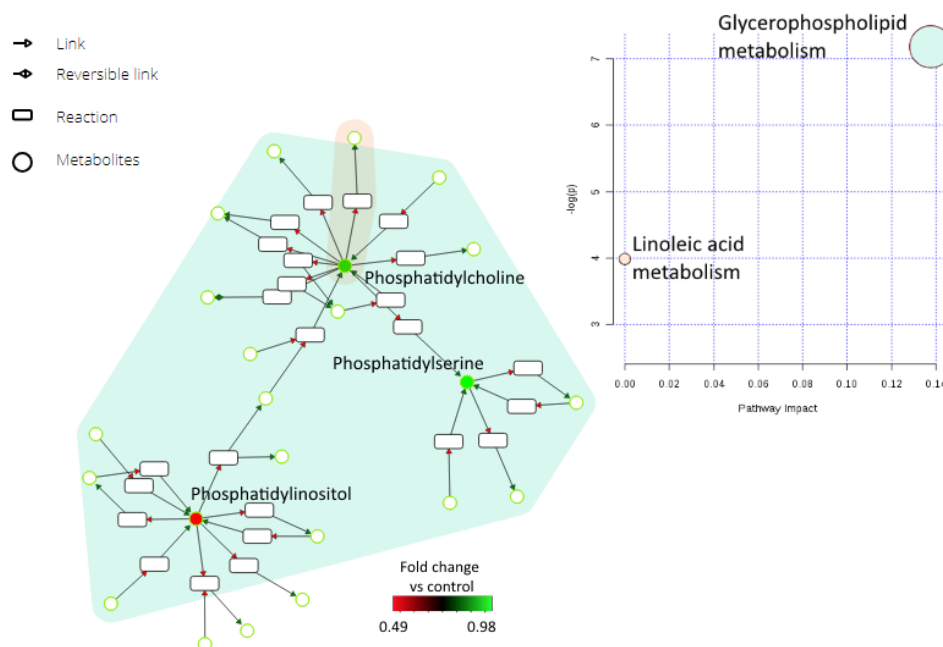


Figure 30. Metabolic pathways associated with alterations of the HDL lipidome in STEMI, extracted using MetExplore. Inset denotes the impact of identified pathways (X axis) in relationship to its significance (Y axis) produced using MetaboAnalyst. Colours in the graph highlight affected pathways and correspond to the colors of the circles in the inset. Green and red circles in the graph denote increased and decreased abundances vs. controls, respectively, with color scale shown at the bottom of the plot.

Table 15 List of lipid metabolic pathways affected by STEMI

Pathway name	Identifier	N ^o of reactions in the pathway	N ^o of metabolites, mapped onto the pathway	p-value	BH*-corrected p-value
Inositol phosphate metabolism	hsa00562	39	1	0.05620	0.0749
Glycerophospholipid metabolism	hsa00564	49	3	0.00001	0.0001
alpha-Linolenic acid metabolism	hsa00592	9	1	0.02462	0.0656
Glycosylphosphatidylinositol-anchor biosynthesis	hsa00563	9	1	0.02649	0.0529
Linoleic acid metabolism	hsa00591	4	1	0.00951	0.0380

Green shading denotes significantly affected pathways. *BH, Benjamini-Hochberg

3. HDL and LDL glycome in normolipidemic controls

3.1. Glycomic profiling of LDL and HDL

The following part of the thesis has been published [2]. Analysis of HDL (Figure 31, A) and LDL (Figure 31, B) N-glycans released after peptide:N-glycosidase F (PNGase F) treatment resulted in 22 and 18 distinct chromatographic peaks, respectively. Relative abundance of the peaks representing N-glycans was quantitatively assessed as a percentage of total integrated area. Identities of N-glycan structures present in each peak were determined by MALDI-TOF MS after ethyl esterification which chemically modifies sialylated glycans enabling distinction between α 2,3- and α 2,6-linked sialic acids.

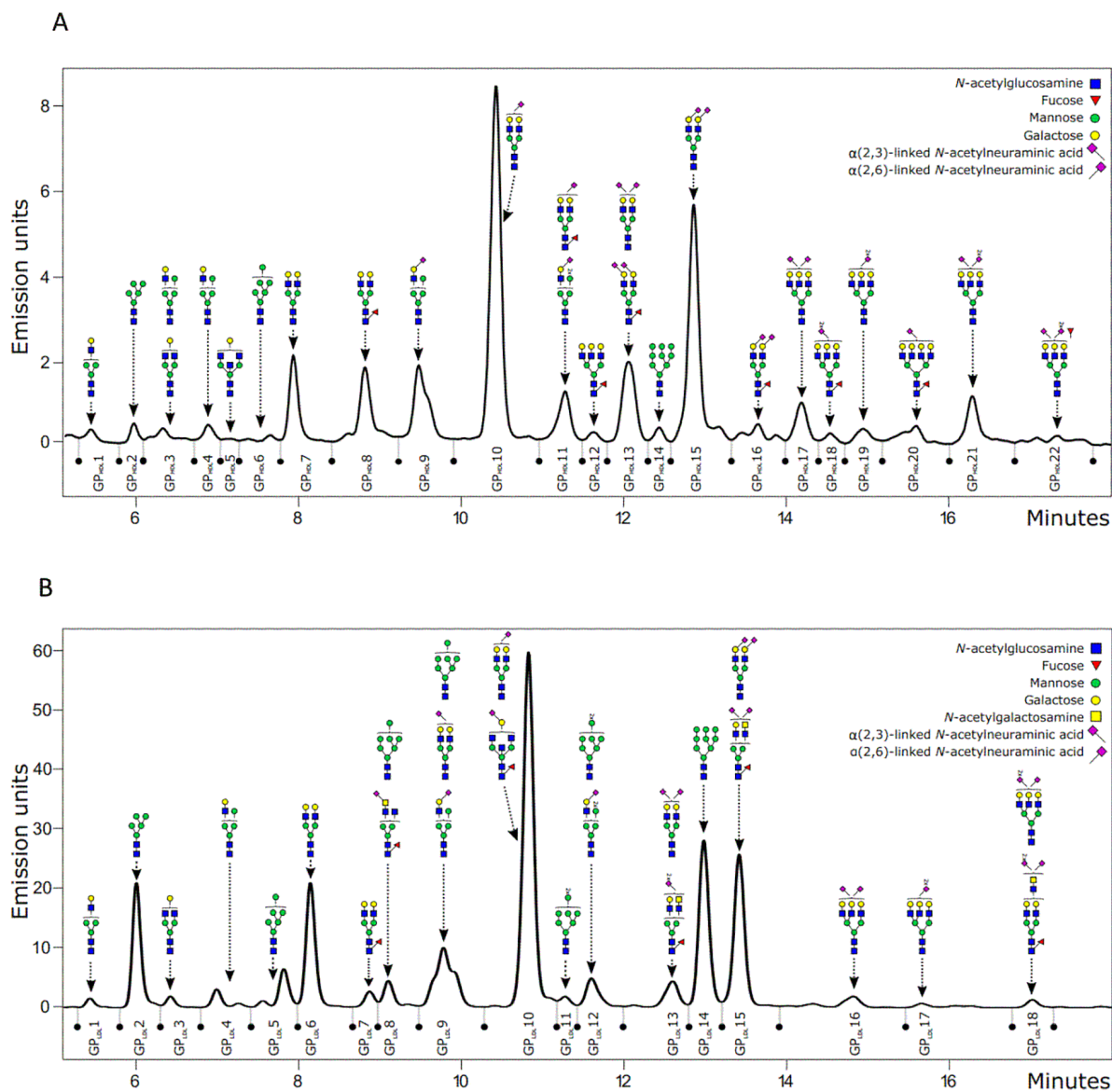


Figure 31 Representative chromatogram of 2-AB labeled N-linked glycans released from native HDL (A) and LDL (B) and separated by HILIC-UHPLC-FLD. The integration areas, together with major structures present in each chromatographic peak are shown.

The list of the most abundant HDL and LDL N-glycans in each peak with their m/z values, monosaccharide composition and proposed structures are given in Table 16 and Table 17, respectively. More than 20 glycan structures were characterized in both HDL and LDL, including complex, high-mannose and hybrid N-glycans. Most of the N-glycans present in HDL

(~70%) and LDL (~60%) were complex sialylated structures with one or two sialic acid residues. The most abundant HDL N-glycans were mono- and disialylated biantennary structures, A2G2S1 and A2G2S2. Similarly, A2G2S1 was the most abundant N-glycan in the LDL N-glycome, but in contrast to HDL, LDL revealed much higher prevalence of high-mannose N-glycans (~33% vs. ~3%).

Table 16 Composition of the HDL N-glycome.

Glycan peak	Registered m/z [M+Na]⁺	Composition¹	Proposed structure²
GP_{HDL}1	1418.954	H4N3	A1G1
GP_{HDL}2	1377.487	H5N2	M5
GP_{HDL}3	1580.740	H5N3	M4A1G1
	1621.754	H4N4	A2G1
GP_{HDL}4	1580.735	H5N3	M4A1G1
GP_{HDL}5	1824.958	H4N5	A2BG1
GP_{HDL}6	1539.900	H6N2	M6
GP_{HDL}7	1783.822	H5N4	A2G2
GP_{HDL}8	1929.743	H5N4F1	FA2G2
GP_{HDL}9	1899.789	H5N3E1	M4A1G1S[6]1
GP_{HDL}10	2102.970	H5N4E1	A2G2S[6]1
GP_{HDL}11	2249.204	H5N4F1E1	FA2G2S[6]1
	2062.102	H6N3E1	M5A1G1S[6]1
GP_{HDL}12	2294.788	H6N5F1	FA3G3
GP_{HDL}13	2376.184	H5N4E1L1	A2G2S[3,6]2

	2476.147	H5N4F1L2	FA2G2S[3,3]2
GP_{HDL14}	2026.124	H9N2	M9
GP_{HDL15}	2422.229	H5N4E2	A2G2S[6,6]2
GP_{HDL16}	2568.244	H5N4F1E2	FA2G2S[6,6]2
GP_{HDL17}	2741.402	H6N5E1L1	A3G3S[3,6]2
GP_{HDL18}	2841.466	H6N5F1L2	FA3G3S[3,3]2
GP_{HDL19}	2787.273	H6N5E2	A3G3S[6,6]2
GP_{HDL20}	2933.446	H7N6F1L1	FA4G4S[3]1
GP_{HDL21}	3060.590	H6N5E1L2	A3G3S[3,6,6]3
GP_{HDL22}	3206.680	H6N5F1E2L1	A3F1G3S[3,6,6]3

¹ H = hexose, N = N-acetylhexosamine, F = deoxyhexose (fucose), E = ethyl esterified N-acetylneuraminic acid (α 2,6-linked), L = lactonized N-acetylneuraminic acid (α 2,3-linked).

² Abbreviations used: all N-glycans possess a core sugar sequence consisting of two N-acetylglucosamines (GlcNAc) and three mannose residues; F at the start of abbreviation indicates a core fucose α 1-6 linked to the inner GlcNAc; M_x, number (x) of mannoses on core GlcNAc; A_x, number (x) of antennas (GlcNAc) on trimannosyl core; F_x, number (x) of fucose linked α 1-3 to antenna GlcNAc; G_x, number (x) of β 1-4 linked galactoses on antenna; S_x, number (x) of sialic acids linked to galactose; LacdiNAc(x), number (x) of lacdiNAc (GalNAc β 1-4GlcNAc) extensions.

HDL N-glycome was separated into 22 chromatographic peaks by HILIC-UHPLC-FLD and masses of individual glycan structures were detected by MALDI-TOF MS.

Table 17 Composition of the LDL N-glycome. LDL N-glycome was separated into 18 chromatographic peaks by HILIC-UHPLC-FLD and masses of individual glycan structures were detected by MALDI-TOF MS.

Glycan peak	Registered		
	m/z [M+Na] ⁺	Composition ¹	Proposed structure ²
GP_{LDL1}	1418.526	H4N3	A1G1
GP_{LDL2}	1377.596	H5N2	M5
GP_{LDL3}	1621.655	H4N4	A2G1

GPLDL4	1580.656	H5N3	M4A1G1
GPLDL5	1539.65	H6N2	M6
GPLDL6	1783.701	H5N4	A2G2
GPLDL7	1929.885	H5N4F1	FA2G2
GPLDL8	1701.661	H7N2	M7
	2081.946	H3N5F1L1	FA1LacdiNAcS[3]1
GPLDL9	1701.578	H7N2	M7
	2056.708	H5N4L1	A2G2S[3]1
	1899.659	H5N3E1	M4A1G1S[6]1
GPLDL10	2102.79	H5N4E1	A2G2S[6]1
	2244.025	H4N5F1L1	FA2BG1S[3]1
GPLDL11	1863.646	H8N2	M8
GPLDL12	1863.624	H8N2	M8
	2061.715	H6N3E1	M5A1G1S[6]1
GPLDL13	2375.82	H5N4E1L1	A2G2S[3,6]2
	2517.012	H4N5F1L2	FA1G1LacdiNAcS[3,3]2
GPLDL14	2025.825	H9N2	M9
GPLDL15	2421.876	H5N4E2	A2G2S[6,6]2
	2563.118	H4N5F1E1L1	FA1G1LacdiNAcS[3,6]2
GPLDL16	2740.958	H6N5E1L1	A3G3S[3,6]2
GPLDL17	2786.981	H6N5E2	A3G3S[6,6]2
GPLDL18	3060.109	H6N5E1L2	A3G3S[3,3,6]3
	3201.328	H5N6E1L2	FA2G2LacdiNAcS[3,3,6]2

¹ Composition and structures as in Table 16.

Treatment of HDL and LDL with neuraminidase, which selectively removes N-acetylneuraminic acid (sialic acid) residues, dramatically altered their N-glycomic profiles (Figure 32, A and B).

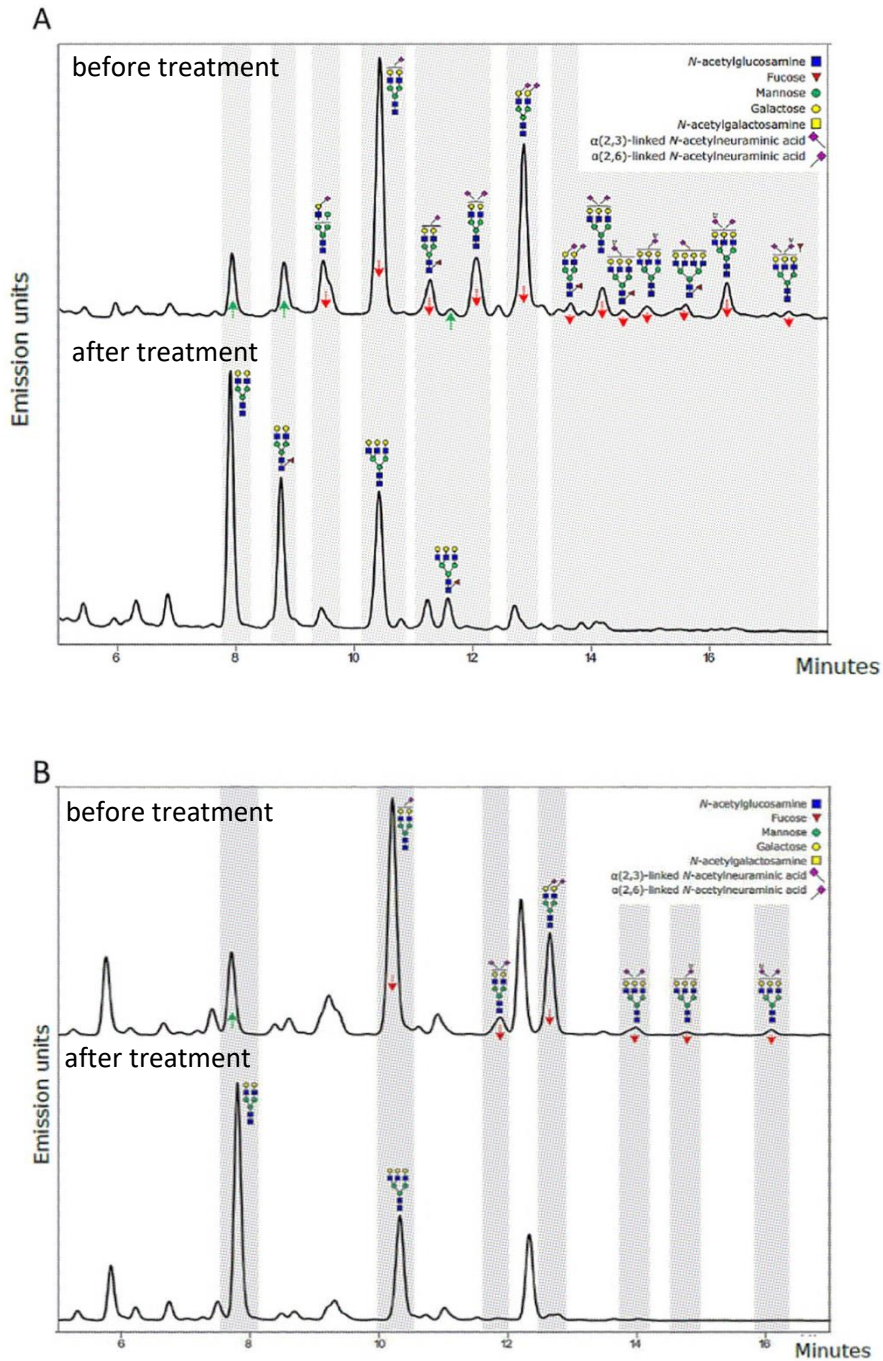


Figure 32. Representative HILIC-UHPLC-FLD chromatograms of 2-AB labeled N-linked glycans released from native and neuraminidase-treated human HDL (A) and LDL (B). Chromatographic peaks containing N-glycans affected by neuraminidase treatment are shaded in grey.

Notably, relative abundance of peaks representing sialylated structures was decreased upon the treatment (e.g. GPHDL13 and GPHDL15), while the abundance of peaks representing corresponding desialylated structures was increased (e.g. GPHDL7 and GPHDL8; Figure 33, A). Similarly, LDL peak GPLDL6 was increased, reflecting decrease of peaks GPLDL13 and GPLDL15 (Figure 33, B). This change in the relative abundance of sialylated N-glycans upon neuraminidase treatment was less evident in the case of GPHDL10 and GPLDL10 representing their most abundant N-glycan, A2G2S1, since besides causing a decrease in their abundances by shifting desialylated form of A2G2S1 to earlier elution times (GPHDL7 and GPLDL6), neuraminidase treatment also caused an increase in their abundances by shifting desialylated forms of triantennary N-glycans to elute at the retention time of GPHDL10 and GPLDL10 (e.g. A3G2S2 from GPHDL17 shifted to GPHDL10 after the desialylation).

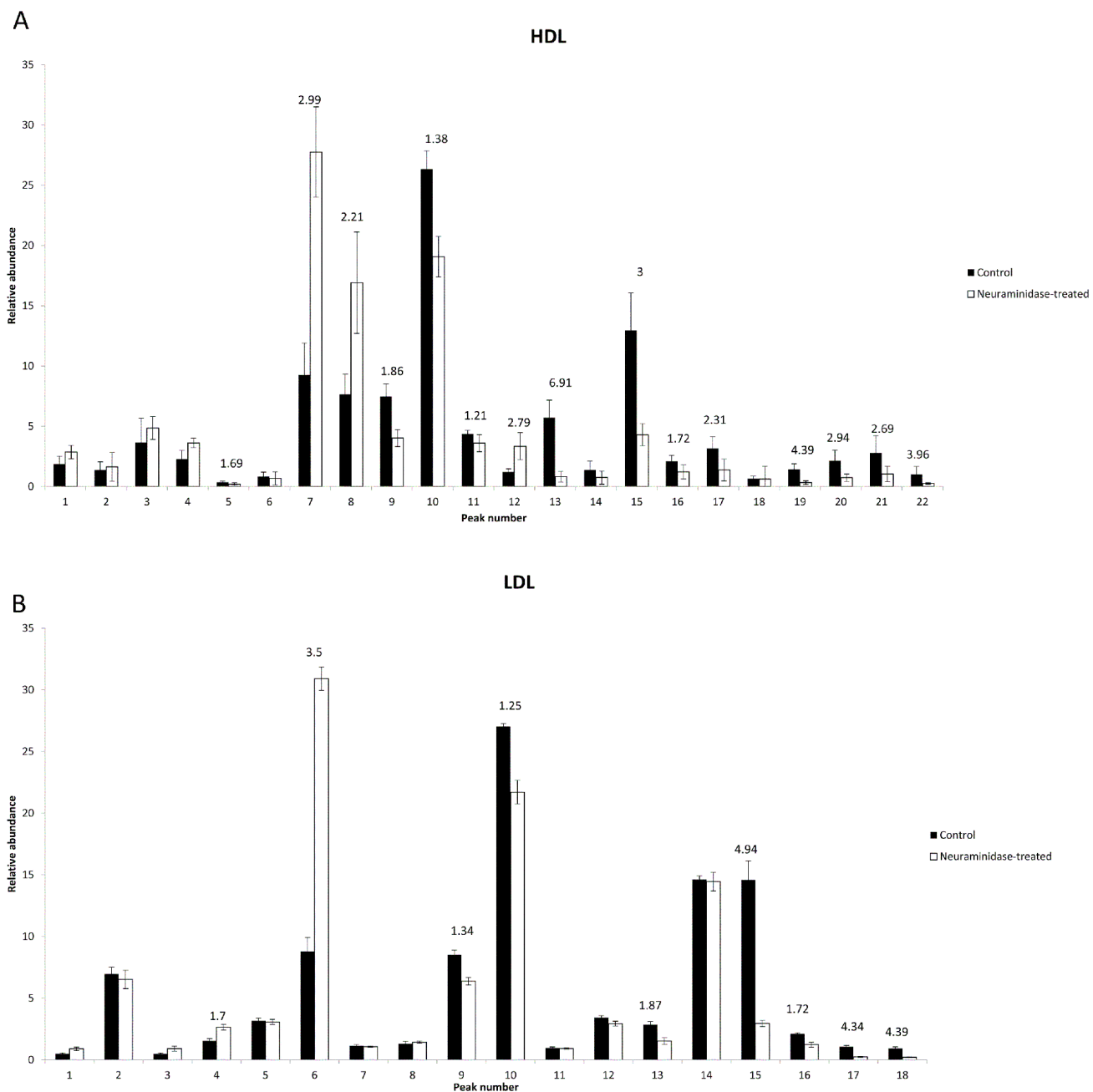


Figure 33 Relative abundance of individual glycan peaks in native and neuraminidase-treated human HDL (A) and LDL (B). Mean values \pm SDs obtained in six samples isolated from six healthy normolipidemic donors are shown; * $p < 0.05$ for differences between corresponding glycomic moieties from control vs. desialylated samples. The numbers at the bars represent the fold difference of mean values of two groups in peaks for which the difference of means is significant.

3.2. Role of glycome in biological activities of lipoproteins

3.2.1. Cholesterol efflux capacity of HDL

To address this biologically important question, the capacity of native and desialylated HDL particles to mediate cellular efflux of cholesterol was evaluated in macrophage-like human THP-1 cells, which efflux cholesterol predominantly via the ABCA1-dependent pathway. Native HDL displayed significantly greater efficacy (+16%) in removing cellular cholesterol as compared to desialylated HDL particles ($8.62 \pm 1.44\%$ for native vs $7.21 \pm 1.00\%$ for neuraminidase-treated samples, $p < 0.05$, Figure 34, A). By contrast, there was no significant difference in the capacity of native and desialylated HDL particles to remove cholesterol from human THP-1 cells in which *SCARB1* gene expression was knocked-down ($6.57 \pm 0.39\%$ vs. $6.09 \pm 0.47\%$, respectively; $p > 0.05$). Similarly, differences in cholesterol efflux capacity of native and desialylated HDL were absent in ABCA1 $-/-$ macrophagic cells ($4.19 \pm 0.18\%$ vs. $4.48 \pm 0.46\%$, respectively; $p > 0.05$).

When HDL was treated with beta-galactosidase following the treatment with neuraminidase, no further reduction in the cholesterol efflux capacity was observed (Figure 34, B). By contrast, a single treatment with PNGase F significantly diminished cholesterol efflux capacity of HDL (Figure 34, B).

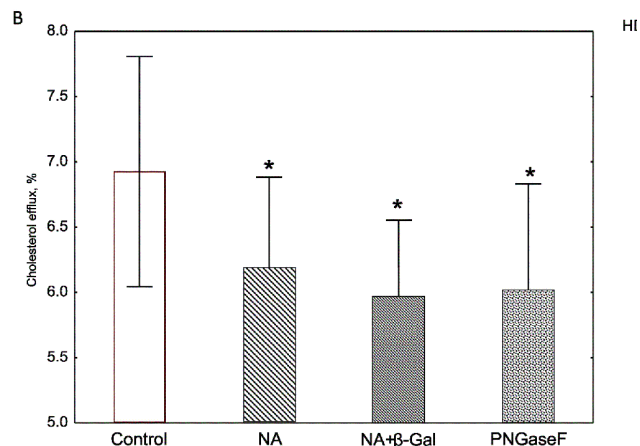
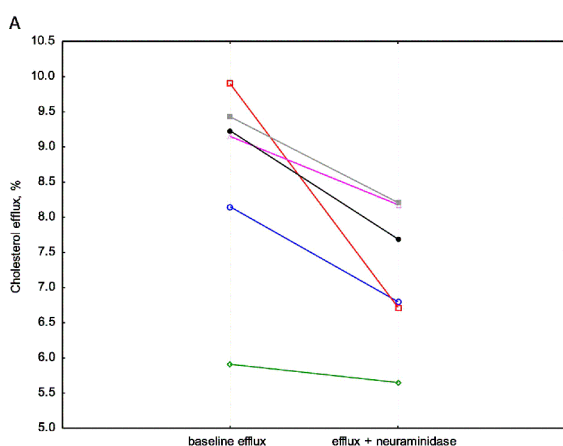
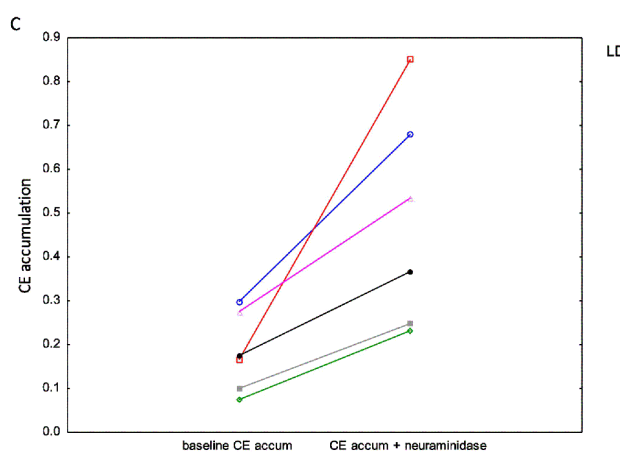


Figure 34 Influence of the treatment with neuraminidase and other enzymes on biological properties of human HDL and LDL. Cellular cholesterol efflux capacity of native and neuraminidase-treated human HDL in macrophagic THP-1 cells (A), cellular cholesterol efflux capacity of native, neuraminidase-, neuraminidase+β-galactosidase- and PNGaseF-treated human HDL in macrophagic THP-1 cells (B), and accumulation in THP-1 cells of cholesteryl ester derived from native and neuraminidase-treated human LDL (C) are shown. Mean values ± SDs obtained in six samples isolated from six healthy donors were as follows: (A) 8.63 ± 1.45 vs. 7.21 ± 1.00 % for native and neuraminidase-treated HDL, respectively ($p < 0.05$ for the difference); (B) 7.89 ± 3.16 % for control (baseline efflux), 6.99 ± 2.62 for neuraminidase-treated, 6.63 ± 2.18 for neuraminidase and β-galactosidase-treated, and 6.26 ± 1.76 for PNGaseF-treated HDL ($p < 0.05$ for control vs neuraminidase, control vs neuraminidase+β-galactosidase and control vs PNGaseF); (C) 0.49 ± 0.25 vs. 0.18 ± 0.09 % for native and neuraminidase-treated LDL, respectively ($p < 0.05$ for the difference).



3.2.2. Cellular cholesteryl ester accumulation induced by LDL

When native and desialylated LDL particles were incubated with macrophage-like human THP-1 cells, cellular accumulation of cholesteryl esters was significantly higher (2.7-fold) after

incubation with desialylated LDL as compared to incubations with native LDL (0.0242±0.0125% vs 0.0090±0.0045%, respectively; p<0.05, Figure 34, C).

3.2.3. Heterogeneity, mean size and LCAT activity of HDL

When HDL subpopulations were separated using native PAGE and apoA-I was detected by Western blotting, no release of the lipid-free/lipid-poor apoA-I from desialylated HDL was observed (Figure 35). Interestingly, the mean HDL size was slightly but significantly reduced from 9.5 ± 0.1 to 9.0 ± 0.1 nm (-5.3%, p<0.01, n=3) by the desialylation.

LCAT activity was markedly decreased (by -46%) after the desialylation as compared to HDL samples incubated in parallel in the absence of neuraminidase (925 ± 412 vs. 1702 ± 442 nmol/h/ml, respectively; p=0.10, n=3).

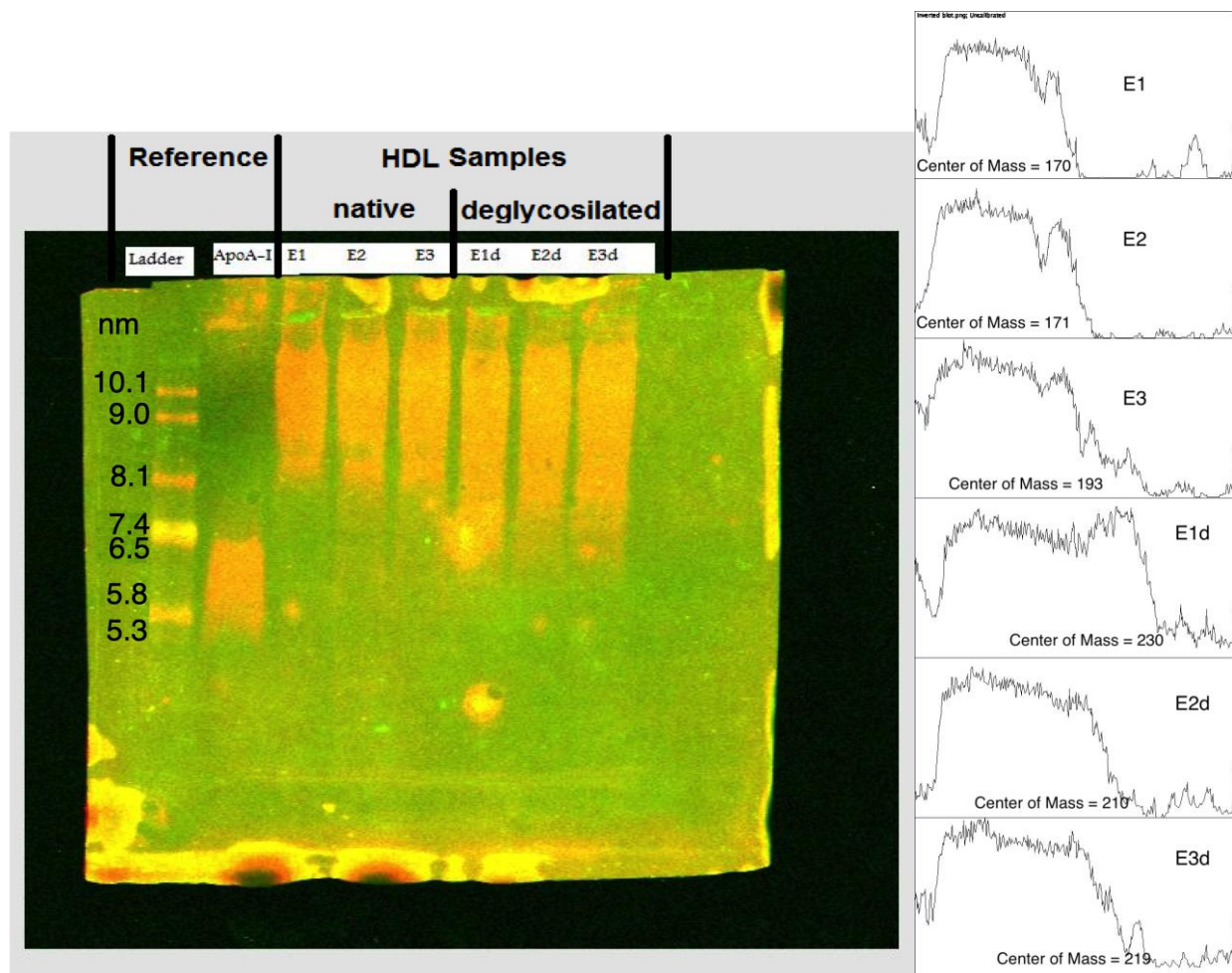


Figure 35 Influence of desialylation on HDL heterogeneity. Western blot (left): from left to right, the protein ladder; lipid-free/lipid-poor apoA-I standard; three HDL samples incubated in the absence of neuraminidase (E1, E2 and E3); the same samples incubated in the presence of neuraminidase (E1d, E2d and E3d). Histograms of color intensity of the gel bands in the blot (right): center of mass for each band is measured in pixels.

3.2.4. Relationships between the glycome and biological properties of LDL & HDL

Series of significant correlations was observed between N-glycomic composition and cellular cholesterol efflux capacity of HDL (Figure 36, A; Table 18). In native HDL samples, positive correlations were calculated for the peaks containing mono- and disialylated N-glycans (GPHDL11 and 13), while the level of a high-mannose N-glycan, M9 (GPHDL14) negatively correlated with HDL efflux capacity. Similarly, in neuraminidase-treated HDL samples, levels of

high-mannose and hybrid N-glycans (GPHDL2, 6 and 14) showed negative correlations with the efflux, while complex biantennary (GPHDL8) and triantennary (GPHDL22) N-glycans revealed a positive correlation.

As for the relationship between LDL N-glycomic profile and capacity to induce cellular cholesterol accumulation, only one significant correlation was found (Figure 36, B and Table 19). Notably, the peak GPLDL16, representing sialylated N-glycan A3G3S2, was positively correlated with the capacity of neuraminidase-treated LDL to induce cholesterol accumulation.

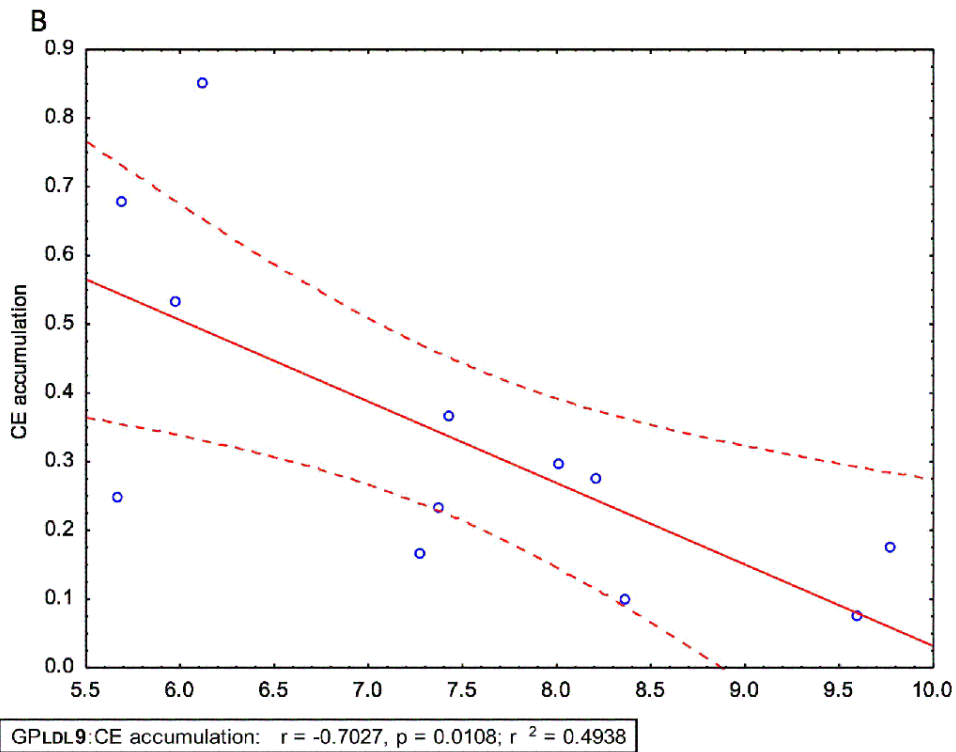
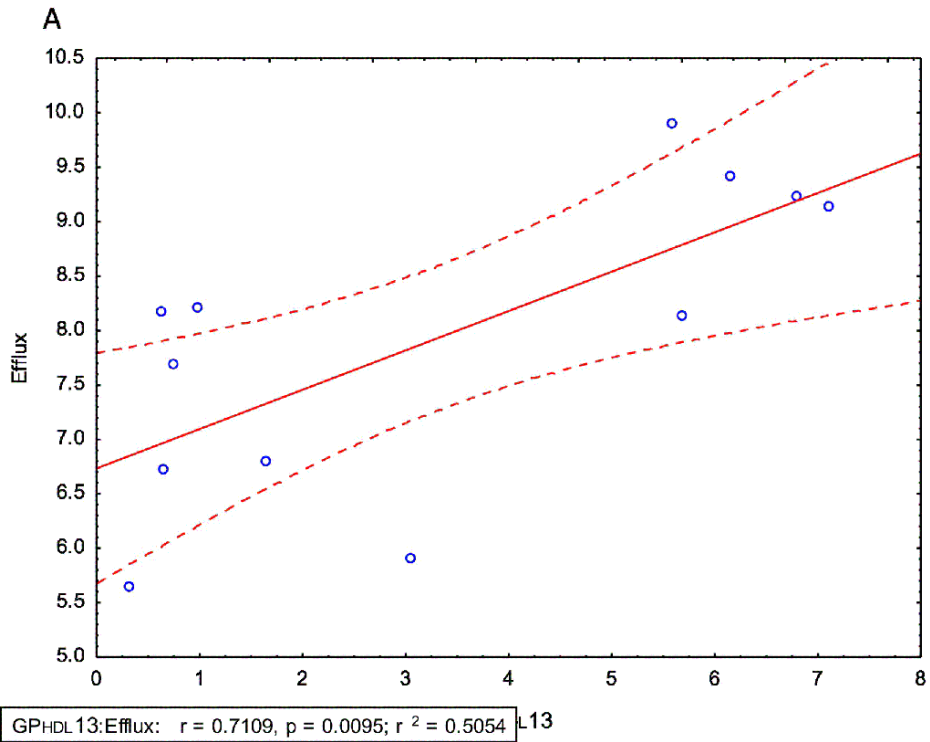


Figure 36. Correlations between cellular cholesterol efflux capacity of HDL and area of the peak 13 (A) and between cellular cholesteryl ester accumulation induced by LDL and area of the peak 9 (B).

Table 18. Correlation coefficients between N-glycomic composition and cellular cholesterol efflux capacity of HDL (both groups n = 6)

Peak	Controls	Neuraminidase-
GPHDL1	0.29	-0.1
GPHDL2	-0.72	-0.88
GPHDL3	-0.69	-0.55
GPHDL	0.25	-0.15
GPHDL5	0.06	0.71
GPHDL6	-0.69	-0.85
GPHDL7	-0.35	-0.66
GPHDL8	0.67	0.84
GPHDL9	0.55	-0.27
GPHDL10	-0.14	-0.55
GPHDL11	0.83	0.65
GPHDL12	0.15	0.78
GPHDL13	0.84	0.20
GPHDL14	-0.92	-0.89
GPHDL15	0.00	0.00
GPHDL16	0.20	0.08
GPHDL17	0.11	0.10
GPHDL18	0.59	0.57
GPHDL19	-0.27	0.30
GPHDL20	0.23	0.40
GPHDL21	0.05	0.43
GPHDL22	-0.15	0.82

Significant correlations are shown in bold;
p<0.05

Table 19. Correlation coefficients between glycomic composition and capacity of LDL to induce cellular cholesteryl esters accumulation (both group n = 6)

Peak	Controls	Neuraminidase-
GPLDL1	-0.71	-0.44
GPLDL2	-0.08	0.02
GPLDL3	-0.72	-0.58
GPLDL4	-0.79	-0.54
GPLDL5	-0.23	0.02
GPLDL6	-0.58	-0.22
GPLDL7	-0.45	-0.31
GPLDL8	-0.66	-0.80
GPLDL9	-0.41	-0.45
GPLDL10	-0.53	0.30
GPLDL11	-0.78	-0.69
GPLDL12	-0.28	-0.44
GPLDL13	0.59	0.66
GPLDL14	-0.17	0.14
GPLDL15	0.80	0.30
GPLDL16	0.69	0.88
GPLDL17	0.75	0.28
GPLDL18	0.66	0.47

Significant correlations are shown in bold;
p<0.05

DISCUSSION AND CONCLUSIONS

By combining multiple omics analyses with biological tests it was possible to pave the first steps in the path of understanding the role of the lipidome and the glycome in structure-function relationships across lipoprotein particles.

1. Lipidome of normolipidemic HDL particles

Lipidome of normolipidemic HDL revealed a high level of heterogeneity across human plasma HDL subpopulations as was reported by us earlier [85]. The abundance of LPC, PI, PS, and PA was elevated in small, dense relative to large, light HDL, whereas the inverse was observed for SM and Cer. Furthermore, multiple components of the HDL phosphosphingolipidome were strongly correlated with biological activities of HDL, including cholesterol efflux capacity from THP-1 cells and antioxidative activity toward LDL thereby suggesting that the HDL lipidome may affect particle functionality.

Different lipid classes play distinct roles in HDL metabolism. LPC is the product of PC hydrolysis in the LCAT reaction, a key step of HDL maturation from small pre- β to large α -particles, which involves transfer of an acyl residue from PC to FC with a formation of CEs. Preferential association of LCAT with small, dense HDL can account for LPC enrichment in this fraction [291]. PS, a negatively charged minor PL, was reported to be enriched in small discoid pre- β -HDL relative to large spherical α -particles [308]. Mechanistically, this observation may derive from ABCA1-mediated translocation of PS through the plasma membrane to participate in the formation of nascent HDL by apoA-I [309]. Another pathway underlying PS enrichment in small HDL may involve preferential uptake of PS from HDL on interaction with SR-B1 as compared with PC and SM [310]. PI and PA are two other negatively charged minor PL enriched

in small, dense vs large, light HDL. PA is a lipid second messenger with multiple binding partners that can be produced in platelets by the action of phospholipase D [311]. The preferential association of PA with small, dense HDLs may reflect their enrichment in apoL-I [312], a lipid-binding protein with high affinity for PA [313].

By contrast, SM and Cer, two SL subclasses present in HDL, were enriched in large, light HDL, in parallel to FC. These data are consistent with our earlier findings [85, 291]. As metabolism of SM is closely linked to that of Cer, the observed distributions may reflect common metabolic pathways for these lipid subclasses. The low SM content of small, dense HDL may, in part, result from the depletion of SM in nascent HDL, a metabolic precursor of small, dense HDL3, which is derived from the exofacial leaflet of the plasma membrane [314]. These data suggest that marked heterogeneity in the phosphosphingolipidome of individual HDL subpopulations may reflect their distinct metabolic origins, which are not normalized by intravascular remodeling processes.

Our structure–function analysis revealed that the heterogeneity in the HDL lipidome was linked to HDL function. Both biological activities evaluated in HDL subpopulations were elevated in small, dense, protein-rich HDL3 as reported earlier [85]. Such superior functional properties of small vs large particles were previously reported for cholesterol efflux via ABCA1 [85, 315, 316], a major efflux pathway operating in human macrophages, for protection of LDL from oxidation [85, 296], and for protection of endothelial cells from apoptosis [85, 117, 317]. In these studies, the conclusion on functional superiority of small vs large HDLs did not depend on the concentration basis used to normalize their concentrations, thereby documenting superior intrinsic functionality of small, protein-rich particles.

Mechanisms underlying these biological activities of HDL differ considerably, involving interactions with distinct cellular proteins, such as ABCA1 [294] and SR-B1 [317]. Strong

intercorrelations of such diverse activities are, therefore, particularly striking, potentially reflecting distinct proteome [312] and lipidome [291] in small, dense HDL3. Indeed, small, dense HDL3 is not only quantitatively enriched in protein but equally contains a much higher number of distinct, functional proteins as compared with large, light HDL2 [312]. Importantly, HDL content of some of these proteins correlates with HDL function [312].

In the present study, all evaluated metrics of HDL functionality exhibited significant correlations with the phosphosphingolipidome of HDL. Several phospholipids and sphingolipids can directly affect biological activities of HDL. Thus, both LPC and PI [318-320], two PL subclasses regulating intracellular signaling cascades, enhance cholesterol efflux capacity of HDL via ABCA1. Similarly, PS seems to activate ABCA1-dependent cellular cholesterol efflux as suggested by experiments with apoptotic cells [321] and with PS-phospholipase A1-overexpressing mice [322]. In addition, PA is a downstream mediator of protein kinase C-stimulated cholesterol efflux from fibroblasts [323]. The potent cholesterol efflux capacity of small, dense HDLs may, therefore, reflect their elevated content of PC, LPC, PS, and PA.

Fluid physical state of PLs represents another important determinant of the ability of HDL to accept cellular cholesterol [150]. Indeed, high SM content decreases both the fluidity of surrounding liquid-crystal lipids and cellular cholesterol efflux to HDL containing such lipids [324]. Similarly, FC reduces fluidity of surface PLs in the liquid-crystal phase. The low abundance of SM and FC in small, dense HDL may, therefore, result in elevated fluidity of surface lipids in this subpopulation, potentially enhancing functionality [291]. In a similar fashion, HDL surface lipids can markedly influence antioxidative [158] effects of HDL, acting in part via modulation of physical properties.

Other biologically active lipids linked to HDL function include lysosphingolipids, exemplified by S1P, which contribute to HDL-mediated protection from apoptosis [325, 326]. S1P enrichment in HDL3 may, therefore, play a role in the potent cytoprotection provided by this HDL subfraction [291, 317, 327]. In contrast to S1P, Cer act as stress-signaling molecules and are proapoptotic in several cell types [328].

2. Lipidome of HDL particles in CMD

2.1 Lipidome of HDL particles isolated from apoA-I-deficient patients

HDL lipidome in FAID revealed a markedly altered profile of molecular lipid species characterized by multiple perturbations in the phosphosphingolipidome, adding to the deficient biological activities of HDL. Importantly, the analysis of abundances of lipid species uncovered numerous alterations in apoA-I-deficient HDLs, which remained hidden in the analysis of abundances of lipid classes performed by us earlier [279].

The perturbations of the phosphosphingolipidome of HDL affected species from all lipid classes. Among highly to moderately abundant classes of PC, SM, and PI, the pattern was complex, with some species featuring elevated abundances in apoA-I-deficient HDLs, whereas abundances of other species were reduced. Remarkably, apoA-I-deficient HDLs lacked numerous polyunsaturated lipid species, including PC 34:2 and PC 40:8, while possessing increased amounts of saturated species, including PC 32:0 and PC 34:0. It is generally accepted that saturated fatty acids exert proinflammatory actions, whereas the opposite can be said about polyunsaturated fatty acids, which possess anti-inflammatory properties [290]. The imbalance of polyunsaturated relative to saturated species found in the present study may have contributed to elevated low-grade inflammation as observed by us in the apoA-I deficiency [279].

When plotted as a part of a correlational network map, PC, PE, and PI species were scattered, adjacent to three clusters separately formed by SM, Cer, and PS species, as well as to another cluster formed by LPC and PA species. Such distribution can be attributed to LPC, PS, and PA species predominantly present in small HDL3 particles, whereas SM and Cer species are known to be concentrated in large HDL2 as discussed above. Combining with functional characteristics of HDL, the network analysis demonstrated that multiple moderately to highly abundant PC and SM species were related to cholesterol efflux capacity and antioxidative activity of HDL. Unsurprisingly, abundances of the species that were decreased in apoA-I-deficient HDL subpopulations displayed positive correlations with the HDL functional metrics, whereas negative correlations were observed for the species whose HDL content was increased. Notwithstanding, all the species linked to functional properties of HDL carried one or more double bonds in their fatty acid moieties.

The clustering patterns revealed that cholesterol efflux capacity of HDL was located, at the network map, between the PS and PE clusters, in the vicinity of a single PC species of PC 34:2. The highly abundant PC 34:2, moderately abundant SM 42:1 and PC 40:4, as well as less abundant PC 40:8 species were all significantly associated with the both biological activities, and their HDL abundances were significantly different between the patient and control groups. Of particular interest, while SM lipid species revealed a number of correlations with biological functions of HDL, total SM was not correlated with HDL functional metrics in our previous study [279]. The associations with the HDL function were thus masked by summarizing abundances of all the SM species in the previous study [279], emphasizing the strength of our present in-depth approach.

Major alterations were present in polyunsaturated lipid species of LPC, Cer, PA, and PG classes, manifesting themselves as their increased abundances in apoA-I-deficient vs control HDL subpopulations. Although, as described above, LPC is involved in a key step of HDL maturation from small pre- β to large α -particles, LPC is also well-known to possess proinflammatory properties [103] and to display a high affinity for G-protein-coupled receptors, thereby playing a signaling role [104-106]. PA, as said earlier, participates in the regulation of inflammation [107] and intracellular signaling [108] as well, while ceramides possess proapoptotic activity, as mentioned earlier [109]. Although a whole array of LPC, Cer, PA, and PG species was significantly enriched in apoA-I-deficient HDLs, the structure-function analysis revealed direct links with biological function of HDL only for Cer lipids. The species of the proatherogenic trio of LPC, PA, and Cer may therefore have acted indirectly by promoting formation of a proinflammatory milieu, further deteriorating HDL function already hampered by the altered particle composition. In a similar fashion, PG species revealed significant between-group differences in their HDL content but their abundances were not associated with the HDL function.

Between-group differences in PE species were complex, with some apoA-I-deficient HDL subpopulations (HDL2b and 2a) displaying decreased PE content, while others (HDL3c) being enriched in PE. In particular, the content of the saturated species of PE 34:0 was significantly elevated in apoA-I-deficient HDL, adding up to the set of saturated species of PC 32:0 and PC 34:0 with increased HDL content described above. As in the correlation network map, PE species were located closely to cholesterol efflux capacity of HDL and there were several PE species whose HDL content was correlated with the HDL function. Among them, abundances of the

species of PE 38:6 and PE 40:7 were significantly decreased in apoA-I-deficient HDL2b and 2a relative to control HDLs, consistent with their beneficial functional role.

Interestingly, altered biological functions of HDL in apoA-I-deficient subjects were confined to cholesterol efflux capacity and antioxidative activity and did not include antiapoptotic properties. This result probably reflects the protein concentration basis used for the measurements of antiapoptotic activity of HDL. Indeed, apoA-I-deficient HDLs were not deficient in S1P when the latter was expressed per unit protein mass, consistent with their normal capacity to reduce apoptosis.

We used metabolic pathway ab initio analysis to identify pathways affected in the metabolism of apoA-I-deficient HDL. Our approach revealed that GP, SL, and LA metabolism were significantly altered in apoA-I deficiency. GP and SL metabolism are reportedly associated with atherosclerosis progression in apoE-deficient mice, with distinct plasma metabolomic profiles differentiating between the different stages of atherosclerosis progression [329].

Glycerophospholipids represent a common class of lipids critically important for the integrity of cellular membranes; oxidation of esterified unsaturated fatty acid moieties dramatically alters biological activities of phospholipids [330]. ApoA-I-deficient HDL particles can be prone to oxidation due to increased amounts of proinflammatory and prooxidative lipids LPC and PA as mentioned above. Finally, LA metabolism is tightly linked to atherogenesis. Indeed, it is well documented that LA exerts multiple antiatherogenic activities. Conjugated LAs can reduce the concentration of atherogenic lipoproteins and the intensity of inflammatory processes [331]. LA exerts protective effects against cholesterol accumulation in THP-1-derived macrophages [332]. Dietary supplementation of LA-rich fat, compared with a saturated fatty acid-rich fat in apoE-

deficient mice, delayed atherosclerosis, reduced serum total cholesterol levels, increased HDL-C and lowered hepatic cholesterol [333].

Genes potentially playing a role in the observed alterations of the HDL lipidome and function in the apoA-I deficiency were identified using MetaboAnalyst's network analysis. Validating our approach, we found that the *APOA1* gene was involved as it directly follows from the study design. This result is consistent with our earlier demonstration of perturbed HDL proteome in heterozygous apoA-I deficiency, primarily involving reduced content of apoA-I as well as that of apoA-II [279], which might both contribute to the defective HDL function. Other affected genes included *LCAT*, *CDS1* and *2*, *GLTP*, *PLA2G1B*, and *PCSK7*. The presence of the *LCAT* gene in this list additionally supports our earlier observation of the dysregulation of *LCAT* in apoA-I deficiency [279]. Both *CDS1* and *CDS2* genes are known to regulate PI production [334], and thus, may contribute to the observed alterations of PI content. The *GLTP* gene is tightly linked to Cer biosynthesis [335], which was also disturbed in the apoA-I deficiency. The enzyme encoded by *PLA2G1B* gene is responsible for hydrolysis of PLs to LPC in the intestine⁴¹ and may be related to increased LPC and decreased PC contents of HDL in the apoA-I deficiency. *PCSK7* gene was reportedly associated with lipid metabolism [336], consistent with its association with the alterations found in the HDL lipidome in our study.

Expectedly, we observed that apoA-I and, as a consequence, HDL-C concentrations were significantly reduced in the patient group relative to controls, reflecting hampered apoA-I production in the patients [186]. In parallel, TG levels were significantly elevated in the patient group as much as one-third from the control group level. Interestingly, this value can reach a much higher magnitude—available literature describes a case of a patient with apoA-I deficiency involving TG concentration as high as 417 mg/dl, which is more than three times of what we

observed in our study, despite intensive treatment with statins, ezetimibe, fenofibrate, and niacin [337]. These observations additionally emphasize the absence of efficient therapeutic strategy to treat this metabolic condition. Our present data may therefore have clinical implication. Indeed, they suggest that a proven therapy involving plasma transfusions in apoA-I-deficient patients [221, 338, 339] can be enhanced by HDL enriched in vitro with the lipids we found in this study to be positively associated with antiatherogenic function of HDL and to be reduced in apoA-I deficiency. The most obvious candidate for this approach represents such a major lipid of HDL as palmitoyl linoleoyl PC, a major isomer of PC 34:2.

2.2. Lipidome of HDL particles isolated from STEMI patients

In this study, HDL particles isolated from STEMI patients revealed markedly altered phosphosphingolipidome, adding to decreased plasma HDL concentrations. It is worth noting here, though, that diminished HDL concentrations alone may not be a reliable estimate for HDL dysfunction and cholesterol efflux impairment [340]. Abundances of minor proinflammatory lysophospholipid species of LPC and PA were increased in STEMI HDL, while abundances of minor species of PC, PG, PI, PE and SM were decreased. As already observed in apoA-I deficiency, the analysis of the abundances of lipid species uncovered distinct patterns in STEMI HDLs, which remained hidden in the analysis of the abundances of lipid classes performed by us earlier [102].

The perturbations of phosphosphingolipidome of HDL affected multiple species from all lipid classes, except for PS and PG classes, which possessed only one or two species whose abundances were significantly different between the groups. Among the species whose HDL content differed between the groups, the content of PC, SM and PI species was predominantly decreased, while that of LPC and PA species was typically increased in STEMI patients. PE, PS

and Cer species revealed complex patterns, with some species featuring elevated abundances, while other species featured decreased abundances in STEMI HDLs.

Interestingly, abundances of species from PC, SM and Cer classes were positively correlated with their between-group fold differences throughout all HDL subpopulations. Furthermore, negative correlations between the abundances of LPC and PA lipids with their between-group differences were observed in HDL2b, HDL3a and HDL3b subpopulations. The first relationship indicates that the higher between-group differences for certain PC, SM or Cer species, the lower their abundance in the whole lipidome. The relationship observed for the LPC and PA species, though possessing the opposite sign, can be interpreted in a similar way as the positive trend was found for the PC, SM and Cer species. This phenomenon can be termed as “backbone effect”: major, in terms of overall abundance, species can be too vital for homeostasis to be significantly altered, while quantitatively minor species, though being far from minor in their biological role, are subject to volatility with, probably, long-lasting deleterious effects on HDL function.

Alternatively, their reduced content in HDL may constitute a consequence, rather than a cause of HDL dysfunction; the causality here cannot be clearly established.

In addition, we observed two other interesting trends involving the relationships of HDL lipidomic alterations in STEMI with carbon chain length and double bond number of the affected species. The first trend was represented by intermediate- and long-chain species of PC, PI and PG displaying positive correlations between their fold decrease in STEMI and the carbon chain length, while the second relationship included positive correlations between fold decrease in the abundances of PE, PG and PI species with the number of double bonds. In conjunction with the backbone effect, its definition can be expanded to specifically include alterations in minor long-chained species possessing at least one double bond in their fatty acid moieties.

Remarkably, STEMI HDLs lacked numerous (relatively) abundant polyunsaturated lipid species, including PC 36:2 and PC 38:5, while possessing increased amounts of (less abundant) LPC 16:0, LPC 18:0 and PA 32:0. It has been mentioned several times above that saturated fatty acids exert proinflammatory actions [341]; so did we mention that, LPC is well-known to possess proinflammatory properties [103] We may assume that increased oxidation of polyunsaturated fatty acids in STEMI condition is at least partially responsible to their decreased content in STEMI HDL. Oxidative stress may play a direct role in the impairment of HDL functionality [342]. PA, as mentioned previously, participates in the regulation of inflammation [107] and intracellular signaling [108], while ceramides, as we know it already from the past, possess proapoptotic activity [109]. Although a whole array of LPC and PA species was significantly enriched in STEMI HDLs, the structure-function analysis did not reveal their direct links with biological function of HDL evaluated as cholesterol efflux capacity and antioxidative activity. The species of the proatherogenic duo of LPC and PA may therefore have acted indirectly by promoting formation of a pro-inflammatory milieu and further deteriorating HDL function already hampered by the altered particle composition. The imbalance of polyunsaturated relative to saturated species found in the present study may have contributed to already significantly elevated inflammation naturally occurring in STEMI as we observed in the patients.

Using a network analysis we attempted to elucidate structure-function relationships across HDL particles in MI and normolipidemic HDL. When plotted as a part of a correlation network map PC and PS species formed two distinct clusters, while a separate cluster involving Cer and SM lipids, as well as a distinct cluster of LPC and PA lipids intermingled together were observed. PE species presented a cluster between the hodgepodge clusters and PI species formed a cluster placed between the PC and PS clusters. This clustering pattern might be attributed to similar

differences in the phosphosphingolipidome between the groups observed across different HDL subpopulations. The heatmaps revealed that PC, for example, was predominantly represented by reddish-coloured bars for all PC species in all five HDL subpopulations, indicating that there was not only an agreement between the lipid species of the same class in terms of the direction of the between-group differences in their abundances, but also an agreement in terms of the direction of the between-group differences across the HDL subpopulations. Similar relationships were observed for lipid species of SM, PI, PS and Cer in their respective classes and across the HDL subpopulations.

Combined with functional characteristics of HDL, the network analysis demonstrated that cholesterol efflux capacity was located in the center of the PI cluster, while antioxidative activity was found in the middle of the LPC cluster. These data suggest that both PI and LPC species contribute to functional deficiency of HDL in STEMI. Unsurprisingly, abundances of the species that were decreased in STEMI HDL subpopulations displayed positive correlations with the HDL functional metrics. Strikingly, all the species whose HDL content was linked to functional properties of HDL carried one or more double bonds in their fatty acid moieties. The moderately abundant PC 38:5 and low-abundant PI 36:1 and PS 38:1 species were all significantly associated with the both biological activities measured, and their HDL abundances were significantly different between the patient and control groups.

As with the FAID, we employed *ab initio* metabolic pathway analysis to identify pathways affected in the metabolism of STEMI HDL. Our approach revealed that after Benjamini-Hochberg correction for multiple comparisons, glycerophospholipid and linoleic acid (LA) metabolism were both significantly altered in STEMI. We discussed possible implications of both pathways above in the section of the discussion devoted to FAID, because metabolic pathways,

affected in FAID included both of the pathways found to be disturbed in STEMI HDL, so we will not talk about this in detail now and refer the reader to the appropriate subsection of the manuscript. What we could add here, however, is an observation in our *in vitro* experiments that STEMI HDL particles display reduced antioxidative activity [102], which potentially may reflect their increased content of pro-inflammatory lipids LPC and PA.

Previously it was demonstrated that HDL from CAD patients cannot activate endothelial antiapoptotic pathways, and rather stimulates proapoptotic pathways [343]. Our current findings on the subject of altered metabolic pathways in STEMI add up to that information.

3. Glycome of normolipidemic HDL and LDL

The N-glycome of both HDL and LDL revealed a high level of diversity, reflected in the presence of complex, high-mannose and hybrid N-glycans. We showed that HDL and LDL are highly sialylated particles, consistent with earlier reports [111, 344].

In our study, the most abundant HDL N-glycans were biantennary complex type N-glycans with one and two sialic acid residues. In this regard, HDL is similar to other glycoproteins of human plasma, which are rich in biantennary complex type N-glycans [345]. In a similar fashion, a biantennary complex type glycan A2G2S2 containing two sialic acid residues was recently reported to represent the most abundant glycan in HDL, followed by a glycan with a single sialic acid residue [111]. While our present studies identified A2G2S1 as the major HDL glycan, this subtle difference may reflect different methodologies employed to isolate HDL or variations in analytical and/or experimental conditions [346].

Similarly to HDL, the most abundant LDL N-glycan was A2G2S1 but in contrast to HDL, the LDL N-glycome was also found to be rich in high-mannose (M5-M9) structures. Consistent with

this data, a high level of high-mannose N-glycans was reported for apoB [347], a primary protein component of LDL. After the treatment of HDL and LDL with neuraminidase, the proportions of individual N-glycans were altered, reflecting removal of sialic acids.

The majority of proteins secreted in the circulation are glycosylated. Sialic acids are N- and O-acyl derivatives of neuraminic acid that are typically found at the terminus of N- and O-glycans [348]. Sialic acids increase electronegativity of glycoproteins [349] and display a number of biological activities, acting as a ligand [350], as a biological mask that covers sub-terminal galactose residues [349], and as a regulator of protein retention in the circulation [351]. Increased levels of free sialic acid are observed in the circulation of patients with atherosclerosis and T2D relative to controls, consistent with the role of sialic acid as a biomarker for cardiometabolic diseases [352, 353]. A recent study showed that sialylation of total plasma proteins is increased in patients with diabetes, even before the onset of the disease [354].

We found that removal of sialic acid residues from native HDL significantly diminished its efficacy in effluxing cellular cholesterol from THP-1 macrophages. The distinct role of sialylation for this key biological activity was highlighted by the experiments with the removal of other glycan moieties from HDL. Indeed, while the cleavage of galactose residues following that of sialic acids was without effect, complete removal of glycans by PNGase F reduced HDL-mediated cholesterol efflux to an extent similar to that of the treatment with neuraminidase.

Cells possess several pathways to efflux cholesterol [355]. Cholesterol removal occurs according to cholesterol concentration gradient and is mediated by SR-B1 encoded by the *SCARB1* gene. Active pathways are mediated by ABCA1 and ABCG1 transporters, which are membrane lipid translocases [355]. We did not observe any differences in cholesterol efflux capacity of native and desialylated HDL from human THP-1 cells in which *SCARB1* or *ABCA1* expression were knocked-

down. These data suggest that sialylation is required for optimal binding of HDL to SR-B1 and ABCA1 [205].

Up to date, there is no evidence regarding the importance of sialylation for binding of HDL to macrophages. Since negatively charged acetylated HDL [356] and oxidized HDL [357] are recognized by scavenger receptors from rat hepatocytes and mouse peritoneal macrophages, it appears reasonable to suggest that sialylation of HDLs is important for interaction with scavenger receptors. The differential cholesterol efflux capacity of desialylated and native HDL can also be linked to ABCA1 but not to other, than ABCA1, transporters, such as ABCG1. It should be noted, however, that we achieved in our experiments approximately 80% silencing of mRNA production for *SCARB1* and *ABCA1* relative to controls and cannot therefore ensure that the residual activity was not sufficient to maintain the efflux; these results should therefore be interpreted with caution.

In addition to cellular cholesterol efflux, HDL desialylation may diminish cholesteryl esterification rate mediated by LCAT which is heavily N-glycosylated [204]. Consistent with these data, LCAT activity was markedly reduced following HDL desialylation in our present study. In addition, desialylation decreases HDL electronegativity [206]; as HDL charge exerts specific effects on lipolysis, decreasing the negative charge of HDL by desialylation might impact the association of lipases with HDL [358]. As N- and O-glycosylation of human apoA-I was recently reported [114, 359], desialylation might equally alter interactions of apoA-I with cellular proteins, including ABCA1. The question of apoA-I glycosylation remains controversial though as apoA-I-associated glycans were not detected in several studies employing LC/MS/MS [112, 113, 115].

It is interesting that we observed a slight decrease in the mean HDL size following desialylation. Given that ABCA1 preferentially effluxes cholesterol to small relative to large HDL [316], such

effect should have resulted in the elevated cholesterol efflux capacity of the desialylated particles, which was not the case, suggesting that other factors, including HDL charge, were more important for this functional alteration. We interpret these data to hypothesise that the N-glycome of HDL proteins, including fetuin A, A1AT, angiotensinogen [112, 113, 115], LCAT [204] and possibly apoA-I [114, 359], can be affected by neuraminidase-induced desialylation and that these modifications bear a potential to reduce electronegativity and LCAT activity of HDL to concomitantly contribute to the diminished capacity of HDL to efflux cellular cholesterol via ABCA1, counteracting potentially beneficial effects of the diminished HDL size.

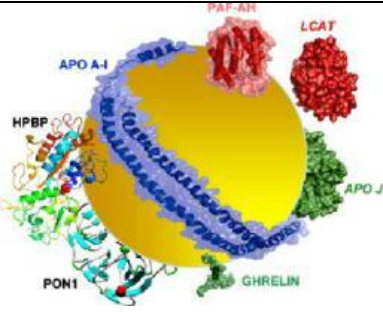
LDL desialylation may equally have negative consequences in the metabolic context of atherosclerosis. Thus, LDL particles isolated from plasma of patients with coronary atherosclerosis are atherogenic, as they induce accumulation of cholesteryl esters in macrophages upon *in vitro* incubation, while LDL samples obtained from healthy donors are without effect [360-362]. Such atherogenic LDLs contained less sialic acid relative to their counterparts from healthy controls [262]. Consistent with these data and with an earlier report [205], we observed that desialylated LDL particles provoked cellular cholesteryl ester accumulation. In such desialylated LDL, a galactose residue preceding those of sialic acid in the carbohydrate chain becomes a terminal and externally exposed residue. In macrophages, desialylated LDL can be internalised via galactose-specific lectin receptors and/or the LDL receptor [274]. Interestingly, treatment with LPS up-regulates expression of galactose-specific lectins in macrophages that in turn increases cholesteryl ester accumulation after incubation of macrophages with desialylated LDL [269]. In addition, lipoprotein desialylation may elicit a faster CETP-mediated CE transfer from HDL to LDL, thereby augmenting LDL cholesterol content [205].

It is well known that different techniques of *in vitro* LDL modification, including acetylation, methylation and oxidation, lead to the formation of electronegative LDL, which induce cellular cholesterol accumulation [363]. Importantly, electronegative LDL can form aggregates [364] that do not interact with scavenger receptors, including CD36 and SR-A, nor with the LDL receptor and associate with macrophages in a high- capacity, receptor-independent manner [365]. Unlike desialylated LDL, oxidized LDL are known to interact with cells via CD36, SR-AI, SR-AII and LOX-1 scavenger receptors [366]. Pathologically, desialylation of LDL might represent an early atherogenic modification *in vivo* that does not lead to LDL interaction with scavenger receptors but may still cause a domino effect of further alterations, amplifying the atherogenicity of the particles [261, 367]. At the end, LDL which underwent such multiple modifications enters the cells through scavenger receptors, signifying the climax of a perfect storm of atherogenic modifications.

4. General conclusions

Analysis of normolipidemic human HDL particles identified negatively charged PS and PA together with LPC, SM, and Cer as potential contributors to HDL functionality. In order to discover atheroprotective components of HDL lipidome which are clinically relevant both under chronic and acute proatherogenic conditions, we conducted two separate structure–function studies of the lipidome of HDL particles in two metabolic states associated with compromised atheroprotective function of HDL, specifically FAID and STEMI. In addition, as a first step in the discovery of glycomic determinants of HDL functionality, we characterized the N-glycome of normolipidemic HDL and its relationships with cholesterol efflux capacity of HDL. Major results of these studies are summarized in Table 20.

Table 20. Major results of this thesis summarized in a single table

		CMD		
		FAID (chronic form of CMD)	STEMI (acute form of CMD)	
	<p>Lipidomic species whose abundances correlate with biological functions of HDL, impaired in CMD</p>	<p>PC 34:2 ↓</p> <p>PC 40:4 ↑</p> <p>PC 40:8 ↓</p> <p>SM 41:1 ↑</p> <p>SM 42:1 ↑</p> <p>PS 38:4 ↑</p>	<p>PC 38:5 ↓</p> <p>PI 36:1 ↓</p> <p>PS 38:1 ↓</p>	
	<p>Glycomic species whose abundances correlate with biological functions of HDL in controls, which can be impaired in CMD*</p>		<p>Sialylated glycans ↓</p>	
	<p>Affected metabolic pathways</p>	<p>SL, GP and LA metabolism</p>	<p>GP and LA metabolism</p>	

Red and green arrows denote decreased and increased in the disease vs controls, respectively. The depiction of HDL is from [368]. *Unpublished data obtained in T2D.

Analysis of the lipidome of HDL isolated from apoA-I-deficient subjects revealed multiple alterations in the molecular composition of the HDL lipidome and their links to HDL

functionality. The list of species linked to HDL functionality included 24 items, of which only abundances of 13 showed significant between-groups differences in HDL subpopulation. The most prominent of these species was PC 34:2, a major (20-22 wt%) HDL PL that was decreased in apoA-I-deficient subjects throughout all five HDL subpopulations. Alterations of HDL lipidome were linked to GP, LA and SL metabolic pathways, as well as to *CDS1*, *CDS2*, *GLTP*, *LCAT*, *PCSK7* and *PLA2G1B* genes. Thus, normalization of HDL phospholipid and/or sphingolipid composition (i.e., via HDL enrichment in a functional phospholipid and/or a sphingolipid through a diet or medical intervention) might represent promising therapeutic strategy in genetic apoA-I deficiency.

Alterations in the molecular composition of HDL lipidome and their links to HDL functionality in STEMI included three species (PC 38:5, PI 36:1, PS 38:1), linked to abnormalities in GP and LA metabolic pathways. Multiplied by low circulating HDL concentrations, such deficiency in HDL composition and function can be expected to contribute to enhanced CV risk observed in this clinical condition. Again, normalization of HDL lipid composition may represent promising therapeutic strategy to reduce cardiovascular risk in STEMI.

The proteome of HDL and LDL is fairly well studied, so I felt no obligation to dive into this field in the course of our research, although one may argue that this is a limitation of this study. I also feel the necessity to acknowledge that my study did not investigate the causality of the alterations in the HDL lipidome. It is not clear whether the dysfunction of HDL causes its lipidome to accumulate lipids that promote degeneration of its antiatherogenic properties, or whether such compositional alterations occur before the onset of the disease that provokes eventual deficiency of HDL in its antiatherogenic properties. Another limitation was that my analysis did not allow us

to distinguish between individual molecular species of phospholipids but rather between isobaric structural isomers instead.

The N-glycomes of human plasma HDL and LDL revealed a high level of diversity, which directly impacted their biological properties in cellular cholesterol metabolism. Our data indicated that sialylation of human plasma HDL and LDL represents an important determinant of their biological function. We further propose that analysis of N-glycomic profiles of lipoproteins bears a potential to be used in clinical practice to detect the presence of desialylated LDL and HDL, which can serve as biomarkers of CVD risk. Together, these studies highlight the power of omics approaches in the field of lipoprotein metabolism; perspectives of this methodology are undoubtedly wide.

REFERENCES

1. Zakiev, E., et al., *Distinct phospholipid and sphingolipid species are linked to altered HDL function in apolipoprotein A-I deficiency*. J Clin Lipidol, 2019.
2. Sukhorukov, V., et al., *Glycosylation of human plasma lipoproteins reveals a high level of diversity, which directly impacts their functional properties*. Biochim Biophys Acta Mol Cell Biol Lipids, 2019. **1864**(5): p. 643-653.
3. Lagrost, L., D. Masson, and J. Chapman, *Lipoprotéines et métabolisme lipidique*, in *L'athérosclérose - Physiologie, diagnostics, thérapeutiques* D. Masson, Editor. 2003. p. 59-74.
4. Havel, R.J. and J.P. Kane, *Introduction : Structure and Metabolism of plasma lipoproteins.*, in *The metabolic and molecular bases of inherited disease.*, C.R. Scriver, et al., Editors. 2001, McGraw-Hill. p. 1841-1853.
5. Berg, K., *A NEW SERUM TYPE SYSTEM IN MAN--THE LP SYSTEM*. Acta Pathol Microbiol Scand, 1963. **59**: p. 369-82.
6. Tang, W.H.W. and S.L. Hazen, *Microbiome, trimethylamine N-oxide, and cardiometabolic disease*. Translational research : the journal of laboratory and clinical medicine, 2017. **179**: p. 108-115.
7. Sigurdsson, A.F., *VLDL – The Role of Triglyceride-Rich Lipoproteins and Remnant Cholesterol*. Available from: <https://www.docsoption.com/2017/01/30/vldl-triglyceride-remnant-cholesterol/>. 2017.
8. Segrest, J.P., et al., *Structure of apolipoprotein B-100 in low density lipoproteins*. J Lipid Res, 2001. **42**(9): p. 1346-67.
9. Dashti, M., et al., *A phospholipidomic analysis of all defined human plasma lipoproteins*. Sci Rep, 2011. **1**: p. 139.
10. Dashti, M., et al., *Proteome of human plasma very low-density lipoprotein and low-density lipoprotein exhibits a link with coagulation and lipid metabolism*. Thromb Haemost, 2014. **111**(3): p. 518-30.
11. GA, F., *High-Density Lipoproteins*, in *Biochemistry of Lipids, Lipoproteins and Membranes*. 2016, Elsevier. p. 437–457.
12. Asztalos BF, T.M., Ishida B, *The Complexity of High-Density Lipoproteins*, in *The HDL Handbook*. 2014: Elsevier. p. 37–64.
13. Rosenson, R.S., et al., *HDL measures, particle heterogeneity, proposed nomenclature, and relation to atherosclerotic cardiovascular events*. Clin Chem, 2011. **57**(3): p. 392-410.
14. Anderson, L.J., J.K. Boyles, and M.M. Hussain, *A rapid method for staining large chylomicrons*. J Lipid Res, 1989. **30**(11): p. 1819-24.
15. Gantz, D., et al., *Size and shape determination of fixed chylomicrons and emulsions with fluid or solid surfaces by three-dimensional analysis of shadows*. J Lipid Res, 1990. **31**(1): p. 163-71.
16. Davidson, N.O., M.E. Kollmer, and R.M. Glickman, *Apolipoprotein B synthesis in rat small intestine: regulation by dietary triglyceride and biliary lipid*. J Lipid Res, 1986. **27**(1): p. 30-9.
17. Green, P.H. and R.M. Glickman, *Intestinal lipoprotein metabolism*. J Lipid Res, 1981. **22**(8): p. 1153-73.
18. Zilversmit, D.B., *Formation and transport of chylomicrons*. Fed Proc, 1967. **26**(6): p. 1599-605.
19. Zilversmit, D.B., *The composition and structure of lymph chylomicrons in dog, rat, and man*. J Clin Invest, 1965. **44**(10): p. 1610-22.
20. Miller, K.W. and D.M. Small, *Surface-to-core and interparticle equilibrium distributions of triglyceride-rich lipoprotein lipids*. J Biol Chem, 1983. **258**(22): p. 13772-84.
21. Brussaard, J.H., et al., *Effects of amount and type of dietary fat on serum lipids, lipoproteins and apolipoproteins in man. A controlled 8-week trial*. Atherosclerosis, 1980. **36**(4): p. 515-27.

22. Hay, R. and G.S. Getz, *Translation in vivo and in vitro of proteins resembling apoproteins of rat plasma very low density lipoprotein*. J Lipid Res, 1979. **20**(3): p. 334-48.
23. Robertson, M.D., et al., *Mobilisation of enterocyte fat stores by oral glucose in humans*. Gut, 2003. **52**(6): p. 834-9.
24. Xiao, C., et al., *Gut-liver interaction in triglyceride-rich lipoprotein metabolism*. Am J Physiol Endocrinol Metab, 2011. **301**(3): p. E429-46.
25. Gibbons, G.F., et al., *Synthesis and function of hepatic very-low-density lipoprotein*. Biochem Soc Trans, 2004. **32**(Pt 1): p. 59-64.
26. Kane, J.P., et al., *Apoprotein composition of very low density lipoproteins of human serum*. J Clin Invest, 1975. **56**(6): p. 1622-34.
27. Shelness, G.S. and J.A. Sellers, *Very-low-density lipoprotein assembly and secretion*. Curr Opin Lipidol, 2001. **12**(2): p. 151-7.
28. Rapp, J.H., et al., *Triglyceride-rich lipoproteins isolated by selected-affinity anti-apolipoprotein B immunosorption from human atherosclerotic plaque*. Arterioscler Thromb, 1994. **14**(11): p. 1767-74.
29. Tomkin, G.H. and D. Owens, *Abnormalities in apo B-containing lipoproteins in diabetes and atherosclerosis*. Diabetes Metab Res Rev, 2001. **17**(1): p. 27-43.
30. Vine, D.F., D.R. Glimm, and S.D. Proctor, *Intestinal lipid transport and chylomicron production: possible links to exacerbated atherogenesis in a rodent model of the metabolic syndrome*. Atheroscler Suppl, 2008. **9**(2): p. 69-76.
31. Wilson, P.W.F., et al., *Prediction of Coronary Heart Disease Using Risk Factor Categories*. Circulation, 1998. **97**(18): p. 1837-1847.
32. Sharrett, A.R., et al., *Coronary Heart Disease Prediction From Lipoprotein Cholesterol Levels, Triglycerides, Lipoprotein(a), Apolipoproteins A-I and B, and HDL Density Subfractions*. Circulation, 2001. **104**(10): p. 1108-1113.
33. Willer, C.J., et al., *Newly identified loci that influence lipid concentrations and risk of coronary artery disease*. Nature genetics, 2008. **40**(2): p. 161-169.
34. Stitzel, N.O., et al., *Inactivating mutations in NPC1L1 and protection from coronary heart disease*. N Engl J Med, 2014. **371**(22): p. 2072-82.
35. Linsel-Nitschke, P., et al., *Lifelong reduction of LDL-cholesterol related to a common variant in the LDL-receptor gene decreases the risk of coronary artery disease--a Mendelian Randomisation study*. PLoS One, 2008. **3**(8): p. e2986.
36. Stender, S., et al., *The ABCG5/8 cholesterol transporter and myocardial infarction versus gallstone disease*. J Am Coll Cardiol, 2014. **63**(20): p. 2121-2128.
37. Crosby, J., et al., *Loss-of-function mutations in APOC3, triglycerides, and coronary disease*. N Engl J Med, 2014. **371**(1): p. 22-31.
38. Ference, B.A., et al., *Effect of long-term exposure to lower low-density lipoprotein cholesterol beginning early in life on the risk of coronary heart disease: a Mendelian randomization analysis*. J Am Coll Cardiol, 2012. **60**(25): p. 2631-9.
39. Navar-Boggan, A.M., et al., *Hyperlipidemia in early adulthood increases long-term risk of coronary heart disease*. Circulation, 2015. **131**(5): p. 451-8.
40. Mihaylova, B., et al., *The effects of lowering LDL cholesterol with statin therapy in people at low risk of vascular disease: meta-analysis of individual data from 27 randomised trials*. Lancet, 2012. **380**(9841): p. 581-90.
41. Barr, D.P., E.M. Russ, and H.A. Eder, *Protein-lipid relationships in human plasma. II. In atherosclerosis and related conditions*. Am J Med, 1951. **11**(4): p. 480-93.
42. Nikkila, E., *Studies on the lipid-protein relationship in normal and pathological sera and the effect of heparin on serum lipoproteins*. Scand J Clin Lab Invest, 1953. **5 Suppl. 8**: p. 9-100.

43. Glomset, J.A., et al., *Role of plasma lecithin:cholesterol acyltransferase in the metabolism of high density lipoproteins*. J Lipid Res, 1966. **7**(5): p. 638-48.
44. Miller, G.J. and N.E. Miller, *Plasma-high-density-lipoprotein concentration and development of ischaemic heart-disease*. Lancet, 1975. **1**(7897): p. 16-9.
45. Gordon, D.J., et al., *High-density lipoprotein cholesterol and cardiovascular disease. Four prospective American studies*. Circulation, 1989. **79**(1): p. 8-15.
46. Jacobs, D.R., Jr., et al., *High density lipoprotein cholesterol as a predictor of cardiovascular disease mortality in men and women: the follow-up study of the Lipid Research Clinics Prevalence Study*. Am J Epidemiol, 1990. **131**(1): p. 32-47.
47. Toth, P.P., et al., *High-density lipoproteins: a consensus statement from the National Lipid Association*. J Clin Lipidol, 2013. **7**(5): p. 484-525.
48. Gofman, J.W., W. Young, and R. Tandy, *Ischemic heart disease, atherosclerosis, and longevity*. Circulation, 1966. **34**(4): p. 679-97.
49. Rhoads, G.G., C.L. Gulbrandsen, and A. Kagan, *Serum lipoproteins and coronary heart disease in a population study of Hawaii Japanese men*. N Engl J Med, 1976. **294**(6): p. 293-8.
50. Miller, N.E., et al., *The Tromso heart-study. High-density lipoprotein and coronary heart-disease: a prospective case-control study*. Lancet, 1977. **1**(8019): p. 965-8.
51. Assmann, G., et al., *High-density lipoprotein cholesterol as a predictor of coronary heart disease risk. The PROCAM experience and pathophysiological implications for reverse cholesterol transport*. Atherosclerosis, 1996. **124 Suppl**: p. S11-20.
52. Goldbourt, U., S. Yaari, and J.H. Medalie, *Isolated low HDL cholesterol as a risk factor for coronary heart disease mortality. A 21-year follow-up of 8000 men*. Arterioscler Thromb Vasc Biol, 1997. **17**(1): p. 107-13.
53. Heiss, G., et al., *Black-white differences in plasma levels of apolipoproteins: the Evans County Heart Study*. Am Heart J, 1984. **108**(3 Pt 2): p. 807-14.
54. Haffner, S.M., et al., *The role of behavioral variables and fat patterning in explaining ethnic differences in serum lipids and lipoproteins*. Am J Epidemiol, 1986. **123**(5): p. 830-9.
55. Saha, N., *Serum high density lipoprotein cholesterol, apolipoprotein A-I, A-II and B levels in Singapore ethnic groups*. Atherosclerosis, 1987. **68**(1-2): p. 117-21.
56. Heiss, G., et al., *The epidemiology of plasma high-density lipoprotein cholesterol levels. The Lipid Research Clinics Program Prevalence Study. Summary*. Circulation, 1980. **62**(4 Pt 2): p. Iv116-36.
57. Seidell, J.C., et al., *Fat distribution in European men: a comparison of anthropometric measurements in relation to cardiovascular risk factors*. Int J Obes Relat Metab Disord, 1992. **16**(1): p. 17-22.
58. Santos, R.D., et al., *Characterization of high density lipoprotein particles in familial apolipoprotein A-I deficiency*. J Lipid Res, 2008. **49**(2): p. 349-57.
59. Chehade, J.M., M. Gladysz, and A.D. Mooradian, *Dyslipidemia in type 2 diabetes: prevalence, pathophysiology, and management*. Drugs, 2013. **73**(4): p. 327-39.
60. Morgantini, C., et al., *HDL lipid composition is profoundly altered in patients with type 2 diabetes and atherosclerotic vascular disease*. Nutr Metab Cardiovasc Dis, 2014. **24**(6): p. 594-9.
61. Superko, H.R., et al., *High-density lipoprotein subclasses and their relationship to cardiovascular disease*. J Clin Lipidol, 2012. **6**(6): p. 496-523.
62. Pirillo, A., G.D. Norata, and A.L. Catapano, *High-density lipoprotein subfractions--what the clinicians need to know*. Cardiology, 2013. **124**(2): p. 116-25.
63. Rached, F.H., M.J. Chapman, and A. Kontush, *HDL particle subpopulations: Focus on biological function*. BioFactors, 2015. **41**(2): p. 67-77.
64. Brown, J.L.G.H.H.M.S., *Familial Hypercholesterolemia*, in *The Online Metabolic and Molecular Bases of Inherited Disease*, D. Valle, Editor. 2001: New York: McGraw-Hill. p. 2863–913.

65. Brunzell JD, D.S., *Familial lipoprotein lipase deficiency, Apo C-II deficiency, and hepatic lipase Deficiency*, in *The Metabolic & Molecular Bases of Inherited Disease*, B.A. Scriver CR, Sly WS, Valle D, Editor. 2001: New York: McGraw-Hill. p. 2789–816.
66. Nordestgaard, B.G., S. Stender, and K. Kjeldsen, *Reduced atherogenesis in cholesterol-fed diabetic rabbits. Giant lipoproteins do not enter the arterial wall*. *Arteriosclerosis*, 1988. **8**(4): p. 421-8.
67. Nordestgaard, B.G. and D.B. Zilversmit, *Large lipoproteins are excluded from the arterial wall in diabetic cholesterol-fed rabbits*. *J Lipid Res*, 1988. **29**(11): p. 1491-500.
68. Shaikh, M., et al., *Quantitative studies of transfer in vivo of low density, Sf 12-60, and Sf 60-400 lipoproteins between plasma and arterial intima in humans*. *Arterioscler Thromb*, 1991. **11**(3): p. 569-77.
69. Nordestgaard, B.G., A. Tybjaerg-Hansen, and B. Lewis, *Influx in vivo of low density, intermediate density, and very low density lipoproteins into aortic intimas of genetically hyperlipidemic rabbits. Roles of plasma concentrations, extent of aortic lesion, and lipoprotein particle size as determinants*. *Arterioscler Thromb*, 1992. **12**(1): p. 6-18.
70. Nordestgaard, B.G., R. Wootton, and B. Lewis, *Selective retention of VLDL, IDL, and LDL in the arterial intima of genetically hyperlipidemic rabbits in vivo. Molecular size as a determinant of fractional loss from the intima-inner media*. *Arterioscler Thromb Vasc Biol*, 1995. **15**(4): p. 534-42.
71. Nordestgaard, B.G., et al., *Nonfasting triglycerides and risk of myocardial infarction, ischemic heart disease, and death in men and women*. *Jama*, 2007. **298**(3): p. 299-308.
72. Bansal, S., et al., *Fasting compared with nonfasting triglycerides and risk of cardiovascular events in women*. *Jama*, 2007. **298**(3): p. 309-16.
73. Freiberg, J.J., et al., *Nonfasting triglycerides and risk of ischemic stroke in the general population*. *Jama*, 2008. **300**(18): p. 2142-52.
74. Di Angelantonio, E., et al., *Major lipids, apolipoproteins, and risk of vascular disease*. *Jama*, 2009. **302**(18): p. 1993-2000.
75. Varbo, A., et al., *Remnant cholesterol as a causal risk factor for ischemic heart disease*. *J Am Coll Cardiol*, 2013. **61**(4): p. 427-36.
76. Chapman, M.J., et al., *Triglyceride-rich lipoproteins and high-density lipoprotein cholesterol in patients at high risk of cardiovascular disease: evidence and guidance for management*. *Eur Heart J*, 2011. **32**(11): p. 1345-61.
77. Varbo, A., M. Benn, and B.G. Nordestgaard, *Remnant cholesterol as a cause of ischemic heart disease: evidence, definition, measurement, atherogenicity, high risk patients, and present and future treatment*. *Pharmacol Ther*, 2014. **141**(3): p. 358-67.
78. Davidson, W.S. and T.B. Thompson, *The structure of apolipoprotein A-I in high density lipoproteins*. *J Biol Chem*, 2007. **282**(31): p. 22249-53.
79. Wlodawer, A., et al., *High-density lipoprotein recombinants: evidence for a bicycle tire micelle structure obtained by neutron scattering and electron microscopy*. *FEBS Lett*, 1979. **104**(2): p. 231-5.
80. Segrest, J.P., et al., *A detailed molecular belt model for apolipoprotein A-I in discoidal high density lipoprotein*. *J Biol Chem*, 1999. **274**(45): p. 31755-8.
81. Silva, R.A.G.D., et al., *Structure of apolipoprotein A-I in spherical high density lipoproteins of different sizes*. *Proceedings of the National Academy of Sciences*, 2008. **105**(34): p. 12176-12181.
82. Gogonea, V., *Structural Insights into High Density Lipoprotein: Old Models and New Facts*. *Frontiers in Pharmacology*, 2016. **6**(318).
83. Rye, K.-A., et al., *The metabolism and anti-atherogenic properties of HDL*. *J. Lipid Res.*, 2009. **50**(Supplement): p. S195-200.

84. Schaefer, E.J., R.D. Santos, and B.F. Asztalos, *Marked HDL deficiency and premature coronary heart disease*. *Curr Opin Lipidol*, 2010. **21**(4): p. 289-97.
85. Camont, L., et al., *Small, Dense High-Density Lipoprotein-3 Particles Are Enriched in Negatively Charged Phospholipids*. *Arteriosclerosis, Thrombosis, and Vascular Biology*, 2013. **33**(12): p. 2715-2723.
86. Duriez, P. and J.C. Fruchart, *High-density lipoprotein subclasses and apolipoprotein A-I*. *Clin Chim Acta*, 1999. **286**(1-2): p. 97-114.
87. Miller, N.E., *HDL metabolism and its role in lipid transport*. *Eur Heart J*, 1990. **11 Suppl H**: p. 1-3.
88. Cheung, M.C., et al., *Distribution and localization of lecithin:cholesterol acyltransferase and cholesteryl ester transfer activity in A-I-containing lipoproteins*. *J Lipid Res*, 1986. **27**(11): p. 1135-44.
89. Lund-Katz, S., et al., *High density lipoprotein structure*. *Front Biosci*, 2003. **8**: p. d1044-54.
90. Vaisar, T., et al., *Shotgun proteomics implicates protease inhibition and complement activation in the antiinflammatory properties of HDL*. *J Clin Invest*, 2007. **117**(3): p. 746-56.
91. Tselepis, A.D. and M. John Chapman, *Inflammation, bioactive lipids and atherosclerosis: potential roles of a lipoprotein-associated phospholipase A2, platelet activating factor-acetylhydrolase*. *Atheroscler Suppl*, 2002. **3**(4): p. 57-68.
92. Li, L., et al., *Mass Spectrometry Methodology in Lipid Analysis*. *International Journal of Molecular Sciences*, 2014. **15**(6): p. 10492-10507.
93. Scanu, A., *Forms of human serum high density lipoprotein protein*. *J Lipid Res*, 1966. **7**(2): p. 295-306.
94. Edman, P. and G. Begg, *A Protein Sequenator*. *European Journal of Biochemistry*, 1967. **1**(1): p. 80-91.
95. Davidson, W.S., et al., *Proteomic Analysis of Defined HDL Subpopulations Reveals Particle-Specific Protein Clusters: Relevance to Antioxidative Function*. *Arterioscler Thromb Vasc Biol*, 2009. **29**(6): p. 870-876.
96. McClements, J., *5. Analysis of Lipids*, in *ANALYSIS OF FOOD PRODUCTS*.
97. Camont, L., et al., *Small, dense high-density lipoprotein-3 particles are enriched in negatively charged phospholipids: relevance to cellular cholesterol efflux, antioxidative, antithrombotic, anti-inflammatory, and antiapoptotic functionalities*. *Arterioscler Thromb Vasc Biol*, 2013. **33**(12): p. 2715-23.
98. Kontush, A., M. Lhomme, and M.J. Chapman, *Unraveling the complexities of the HDL lipidome*. *J Lipid Res*, 2013. **54**(11): p. 2950-63.
99. Lucke, S. and B. Levkau, *Endothelial functions of sphingosine-1-phosphate*. *Cell Physiol Biochem*, 2010. **26**(1): p. 87-96.
100. Christensen, P.M., et al., *Apolipoprotein M mediates sphingosine-1-phosphate efflux from erythrocytes*. *Scientific Reports*, 2017. **7**(1): p. 14983.
101. Kontush, A., et al., *Structure of HDL: particle subclasses and molecular components*. *Handb Exp Pharmacol*, 2015. **224**: p. 3-51.
102. Rached, F., et al., *Defective functionality of small, dense HDL3 subpopulations in ST segment elevation myocardial infarction: Relevance of enrichment in lysophosphatidylcholine, phosphatidic acid and serum amyloid A*. *Biochim Biophys Acta*, 2015. **1851**(9): p. 1254-61.
103. Marathe, G.K., et al., *To hydrolyze or not to hydrolyze: the dilemma of platelet-activating factor acetylhydrolase*. *J Lipid Res*, 2014. **55**(9): p. 1847-54.
104. Xu, H., et al., *Targeted lipidomics - advances in profiling lysophosphocholine and platelet-activating factor second messengers*. *Febs j*, 2013. **280**(22): p. 5652-67.
105. Zmijewski, J.W., et al., *Cell signalling by oxidized lipids and the role of reactive oxygen species in the endothelium*. *Biochem Soc Trans*, 2005. **33**(Pt 6): p. 1385-9.

106. Litvack, M.L. and N. Palaniyar, *Review: Soluble innate immune pattern-recognition proteins for clearing dying cells and cellular components: implications on exacerbating or resolving inflammation*. *Innate Immun*, 2010. **16**(3): p. 191-200.
107. Lim, H.K., et al., *Phosphatidic acid regulates systemic inflammatory responses by modulating the Akt-mammalian target of rapamycin-p70 S6 kinase 1 pathway*. *J Biol Chem*, 2003. **278**(46): p. 45117-27.
108. Delon, C., et al., *Sphingosine kinase 1 is an intracellular effector of phosphatidic acid*. *J Biol Chem*, 2004. **279**(43): p. 44763-74.
109. Green, D.R., *Apoptosis and sphingomyelin hydrolysis. The flip side*. *J Cell Biol*, 2000. **150**(1): p. F5-7.
110. Wiesner, P., et al., *Lipid profiling of FPLC-separated lipoprotein fractions by electrospray ionization tandem mass spectrometry*. *J. Lipid Res.*, 2009. **50**(3): p. 574-585.
111. Huang, J., et al., *Glycomic analysis of high density lipoprotein shows a highly sialylated particle*. *J Proteome Res*, 2014. **13**(2): p. 681-91.
112. Krishnan, S., et al., *Combined High-Density Lipoprotein Proteomic and Glycomic Profiles in Patients at Risk for Coronary Artery Disease*. *J Proteome Res*, 2015. **14**(12): p. 5109-18.
113. Krishnan, S., et al., *HDL Glycoprotein Composition and Site-Specific Glycosylation Differentiates Between Clinical Groups and Affects IL-6 Secretion in Lipopolysaccharide-Stimulated Monocytes*. *Sci Rep*, 2017. **7**: p. 43728.
114. Majek, P., et al., *N-Glycosylation of apolipoprotein A1 in cardiovascular diseases*. *Transl Res*, 2015. **165**(2): p. 360-2.
115. Kailemia, M.J., et al., *Targeted measurements of O- and N-glycopeptides show that proteins in HDL particles are enriched with specific glycosylation compared to plasma*. *J Proteome Res*, 2017.
116. Millar, J.S., *The sialylation of plasma lipoproteins*. *Atherosclerosis*, 2001. **154**(1): p. 1-13.
117. Camont, L., M.J. Chapman, and A. Kontush, *Biological activities of HDL subpopulations and their relevance to cardiovascular disease*. *Trends Mol Med*, 2011. **17**(10): p. 594-603.
118. Goulinet, S. and M.J. Chapman, *Plasma LDL and HDL subspecies are heterogenous in particle content of tocopherols and oxygenated and hydrocarbon carotenoids. Relevance to oxidative resistance and atherogenesis*. *Arterioscler Thromb Vasc Biol*, 1997. **17**(4): p. 786-96.
119. Asztalos, B.F., et al., *Distribution of ApoA-I-containing HDL subpopulations in patients with coronary heart disease*. *Arterioscler Thromb Vasc Biol*, 2000. **20**(12): p. 2670-6.
120. Kontush, A. and M.J. Chapman, *Functionally defective high-density lipoprotein: a new therapeutic target at the crossroads of dyslipidemia, inflammation, and atherosclerosis*. *Pharmacol Rev*, 2006. **58**(3): p. 342-74.
121. Tsompanidi, E.M., et al., *HDL biogenesis and functions: role of HDL quality and quantity in atherosclerosis*. *Atherosclerosis*, 2010. **208**(1): p. 3-9.
122. Lewis, G.F. and D.J. Rader, *New insights into the regulation of HDL metabolism and reverse cholesterol transport*. *Circ Res*, 2005. **96**(12): p. 1221-32.
123. Rothblat, G.H. and M.C. Phillips, *High-density lipoprotein heterogeneity and function in reverse cholesterol transport*. *Curr Opin Lipidol*, 2010. **21**(3): p. 229-38.
124. Yvan-Charvet, L., N. Wang, and A.R. Tall, *Role of HDL, ABCA1, and ABCG1 transporters in cholesterol efflux and immune responses*. *Arterioscler Thromb Vasc Biol*, 2010. **30**(2): p. 139-43.
125. Rader, D.J., *Molecular regulation of HDL metabolism and function: implications for novel therapies*. *J Clin Invest*, 2006. **116**(12): p. 3090-100.
126. Santos-Gallego, C.G., B. Ibanez, and J.J. Badimon, *HDL-cholesterol: is it really good? Differences between apoA-I and HDL*. *Biochem Pharmacol*, 2008. **76**(4): p. 443-52.

127. Chapman, M.J., et al., *Cholesteryl ester transfer protein: at the heart of the action of lipid-modulating therapy with statins, fibrates, niacin, and cholesteryl ester transfer protein inhibitors.* Eur Heart J, 2010. **31**(2): p. 149-64.
128. Curtiss, L.K., et al., *What is so special about apolipoprotein AI in reverse cholesterol transport?* Arterioscler Thromb Vasc Biol, 2006. **26**(1): p. 12-9.
129. Rohrl, C., et al., *Characterization of endocytic compartments after holo-high density lipoprotein particle uptake in HepG2 cells.* Histochem Cell Biol, 2010. **133**(3): p. 261-72.
130. Röhrl, C. and H. Stangl, *HDL endocytosis and resecretion.* Biochimica et biophysica acta, 2013. **1831**(11): p. 1626-1633.
131. Kontush, A. and M.J. Chapman, *Antiatherogenic small, dense HDL--guardian angel of the arterial wall?* Nat Clin Pract Cardiovasc Med, 2006. **3**(3): p. 144-53.
132. Ganjali, S., et al., *HDL functionality in type 1 diabetes.* Atherosclerosis, 2017. **267**: p. 99-109.
133. Besler, C., T.F. Luscher, and U. Landmesser, *Molecular mechanisms of vascular effects of High-density lipoprotein: alterations in cardiovascular disease.* EMBO Mol Med, 2012. **4**(4): p. 251-68.
134. Glomset, J.A. and J.L. Wright, *SOME PROPERTIES OF A CHOLESTEROL ESTERIFYING ENZYME IN HUMAN PLASMA.* Biochim Biophys Acta, 1964. **89**: p. 266-76.
135. Tall, A.R., *Cholesterol efflux pathways and other potential mechanisms involved in the athero-protective effect of high density lipoproteins.* J Intern Med, 2008. **263**(3): p. 256-73.
136. Adorni, M.P., et al., *The roles of different pathways in the release of cholesterol from macrophages.* J Lipid Res, 2007. **48**(11): p. 2453-62.
137. Hayden, M.R., et al., *Cholesterol efflux regulatory protein, Tangier disease and familial high-density lipoprotein deficiency.* Curr Opin Lipidol, 2000. **11**(2): p. 117-22.
138. Oram, J.F., *Molecular basis of cholesterol homeostasis: lessons from Tangier disease and ABCA1.* Trends Mol Med, 2002. **8**(4): p. 168-73.
139. Repa, J.J. and D.J. Mangelsdorf, *The liver X receptor gene team: potential new players in atherosclerosis.* Nat Med, 2002. **8**(11): p. 1243-8.
140. Wang, N., et al., *ATP-binding cassette transporters G1 and G4 mediate cellular cholesterol efflux to high-density lipoproteins.* Proc Natl Acad Sci U S A, 2004. **101**(26): p. 9774-9.
141. Kennedy, M.A., et al., *ABCG1 has a critical role in mediating cholesterol efflux to HDL and preventing cellular lipid accumulation.* Cell Metab, 2005. **1**(2): p. 121-31.
142. Rothblat, G.H., et al., *Cell cholesterol efflux: integration of old and new observations provides new insights.* J Lipid Res, 1999. **40**(5): p. 781-96.
143. Covey, S.D., et al., *Scavenger receptor class B type I-mediated protection against atherosclerosis in LDL receptor-negative mice involves its expression in bone marrow-derived cells.* Arterioscler Thromb Vasc Biol, 2003. **23**(9): p. 1589-94.
144. Zhang, W., et al., *Inactivation of macrophage scavenger receptor class B type I promotes atherosclerotic lesion development in apolipoprotein E-deficient mice.* Circulation, 2003. **108**(18): p. 2258-63. Epub 2003 Oct 27.
145. Zhang, Y., et al., *Overexpression of apolipoprotein A-I promotes reverse transport of cholesterol from macrophages to feces in vivo.* Circulation, 2003. **108**(6): p. 661-3.
146. von Eckardstein, A., J.R. Nofer, and G. Assmann, *High density lipoproteins and arteriosclerosis. Role of cholesterol efflux and reverse cholesterol transport.* Arterioscler Thromb Vasc Biol, 2001. **21**(1): p. 13-27.
147. Westerterp, M., et al., *Apolipoprotein CI aggravates atherosclerosis development in ApoE-knockout mice despite mediating cholesterol efflux from macrophages.* Atherosclerosis, 2007. **195**(1): p. e9-16.

148. Rotllan, N., et al., *Overexpression of Human Apolipoprotein A-II in Transgenic Mice Does Not Impair Macrophage-Specific Reverse Cholesterol Transport In Vivo*. *Arterioscler Thromb Vasc Biol*, 2005. **25**(9): p. e128-32.
149. Yancey, P.G., et al., *High density lipoprotein phospholipid composition is a major determinant of the bi-directional flux and net movement of cellular free cholesterol mediated by scavenger receptor BI*. *J Biol Chem*, 2000. **275**(47): p. 36596-604.
150. Davidson, W.S., et al., *The effect of high density lipoprotein phospholipid acyl chain composition on the efflux of cellular free cholesterol*. *J Biol Chem*, 1995. **270**(11): p. 5882-90.
151. Nofer, J.-R. and G. Assmann, *Atheroprotective Effects of High-Density Lipoprotein-Associated Lysosphingolipids*. *Trends Cardiovasc Med.*, 2005. **15**(7): p. 265-271.
152. Zhou, L., et al., *High-density lipoprotein synthesis and metabolism (Review)*. *Mol Med Rep*, 2015. **12**(3): p. 4015-4021.
153. Assmann, G. and A.M. Gotto, Jr., *HDL cholesterol and protective factors in atherosclerosis*. *Circulation*, 2004. **109**(23 Suppl 1): p. Iii8-14.
154. Nicholls, S.J., et al., *Reconstituted high-density lipoproteins inhibit the acute pro-oxidant and proinflammatory vascular changes induced by a periarterial collar in normocholesterolemic rabbits*. *Circulation*, 2005. **111**(12): p. 1543-50.
155. Van Lenten, B.J., et al., *The role of high-density lipoproteins in oxidation and inflammation*. *Trends Cardiovasc Med*, 2001. **11**(3-4): p. 155-161.
156. Navab, M., et al., *The oxidation hypothesis of atherogenesis: the role of oxidized phospholipids and HDL*. *J Lipid Res*, 2004. **45**(6): p. 993-1007.
157. Kontush, A. and M.J. Chapman, *Antiatherogenic function of HDL particle subpopulations: focus on antioxidative activities*. *Curr Opin Lipidol*, 2010. **21**(4): p. 312-8.
158. Zerrad-Saadi, A., et al., *HDL3-mediated inactivation of LDL-associated phospholipid hydroperoxides is determined by the redox status of apolipoprotein A-I and HDL particle surface lipid rigidity: relevance to inflammation and atherogenesis*. *Arterioscler Thromb Vasc Biol*, 2009. **29**(12): p. 2169-75.
159. Chantepie, S., et al., *Distinct HDL subclasses present similar intrinsic susceptibility to oxidation by HOCl*. *Arch Biochem Biophys*, 2009. **487**(1): p. 28-35.
160. Navab, M., et al., *HDL and the inflammatory response induced by LDL-derived oxidized phospholipids*. *Arterioscler Thromb Vasc Biol*, 2001. **21**(4): p. 481-8.
161. Boisfer, E., et al., *Antioxidant properties of HDL in transgenic mice overexpressing human apolipoprotein A-II*. *J Lipid Res*, 2002. **43**(5): p. 732-41.
162. Ribas, V., et al., *Human apolipoprotein A-II enrichment displaces paraoxonase from HDL and impairs its antioxidant properties: a new mechanism linking HDL protein composition and antiatherogenic potential*. *Circ Res*, 2004. **95**(8): p. 789-97.
163. Ostos, M.A., et al., *Antioxidative and antiatherosclerotic effects of human apolipoprotein A-IV in apolipoprotein E-deficient mice*. *Arterioscler Thromb Vasc Biol*, 2001. **21**(6): p. 1023-8.
164. Davignon, J., *Apolipoprotein E and atherosclerosis: beyond lipid effect*. *Arterioscler Thromb Vasc Biol*, 2005. **25**(2): p. 267-9.
165. Navab, M., et al., *Mildly oxidized LDL induces an increased apolipoprotein J/paraoxonase ratio*. *J Clin Invest*, 1997. **99**(8): p. 2005-19.
166. Trougakos, I.P., et al., *Differential effects of clusterin/apolipoprotein J on cellular growth and survival*. *Free Radic Biol Med*, 2005. **38**(4): p. 436-49.
167. Dahlback, B. and L.B. Nielsen, *Apolipoprotein M affecting lipid metabolism or just catching a ride with lipoproteins in the circulation?* *Cell Mol Life Sci*, 2009. **66**(4): p. 559-64.

168. Kontush, A., S. Chantepie, and M.J. Chapman, *Small, dense HDL particles exert potent protection of atherogenic LDL against oxidative stress*. *Arterioscler Thromb Vasc Biol*, 2003. **23**(10): p. 1881-1888.
169. Calabresi, L., M. Gomaschi, and G. Franceschini, *Endothelial protection by high-density lipoproteins: from bench to bedside*. *Arterioscler Thromb Vasc Biol*, 2003. **23**(10): p. 1724-31.
170. Besler, C., et al., *Mechanisms underlying adverse effects of HDL on eNOS-activating pathways in patients with coronary artery disease*. *J Clin Invest*, 2011. **121**(7): p. 2693-708.
171. Kuvin, J.T., et al., *A novel mechanism for the beneficial vascular effects of high-density lipoprotein cholesterol: enhanced vasorelaxation and increased endothelial nitric oxide synthase expression*. *Am Heart J*, 2002. **144**(1): p. 165-72.
172. Mineo, C., et al., *High density lipoprotein-induced endothelial nitric-oxide synthase activation is mediated by Akt and MAP kinases*. *J Biol Chem*, 2003. **278**(11): p. 9142-9.
173. Nofer, J.R., et al., *HDL induces NO-dependent vasorelaxation via the lysophospholipid receptor S1P3*. *J Clin Invest*, 2004. **113**(4): p. 569-81.
174. Drew, B.G., et al., *High-density lipoprotein and apolipoprotein AI increase endothelial NO synthase activity by protein association and multisite phosphorylation*. *Proc Natl Acad Sci U S A*, 2004. **101**(18): p. 6999-7004.
175. Calkin, A.C., et al., *Reconstituted High-Density Lipoprotein Attenuates Platelet Function in Individuals With Type 2 Diabetes Mellitus by Promoting Cholesterol Efflux*. *Circulation*, 2009. **120**(21): p. 2095-2104.
176. Nofer, J.R., et al., *HDL and arteriosclerosis: beyond reverse cholesterol transport*. *Atherosclerosis*, 2002. **161**(1): p. 1-16.
177. Li, Y., J.B. Dong, and M.P. Wu, *Human ApoA-I overexpression diminishes LPS-induced systemic inflammation and multiple organ damage in mice*. *Eur J Pharmacol*, 2008. **590**(1-3): p. 417-22.
178. Argraves, K.M., et al., *S1P, dihydro-S1P and C24:1-ceramide levels in the HDL-containing fraction of serum inversely correlate with occurrence of ischemic heart disease*. *Lipids Health Dis*, 2011. **10**: p. 70.
179. Brodde, M.F., et al., *Native high-density lipoproteins inhibit platelet activation via scavenger receptor BI: role of negatively charged phospholipids*. *Atherosclerosis*, 2011. **215**(2): p. 374-82.
180. Darabi, M. and A. Kontush, *Phosphatidylserine in atherosclerosis*. *Curr Opin Lipidol*, 2016. **27**(4): p. 414-20.
181. Fichtlscherer, S., A.M. Zeiher, and S. Dimmeler, *Circulating microRNAs: biomarkers or mediators of cardiovascular diseases?* *Arterioscler Thromb Vasc Biol*, 2011. **31**(11): p. 2383-90.
182. De Rosa, S., et al., *Transcoronary concentration gradients of circulating microRNAs*. *Circulation*, 2011. **124**(18): p. 1936-44.
183. Wagner, J., et al., *Characterization of levels and cellular transfer of circulating lipoprotein-bound microRNAs*. *Arterioscler Thromb Vasc Biol*, 2013. **33**(6): p. 1392-400.
184. Mackness, M., P. Durrington, and B. Mackness, *Paraoxonase 1 activity, concentration and genotype in cardiovascular disease*. *Curr Opin Lipidol*, 2004. **15**(4): p. 399-404.
185. Aviram, M. and J. Vaya, *Paraoxonase 1 activities, regulation, and interactions with atherosclerotic lesion*. *Curr Opin Lipidol*, 2013. **24**(4): p. 339-44.
186. Schaefer, E.J., P. Anthanont, and B.F. Asztalos, *High-density lipoprotein metabolism, composition, function, and deficiency*. *Curr Opin Lipidol*, 2014. **25**(3): p. 194-9.
187. Khera, A.V., et al., *Cholesterol efflux capacity, high-density lipoprotein function, and atherosclerosis*. *N Engl J Med*, 2011. **364**(2): p. 127-35.
188. Li, X.M., et al., *Paradoxical association of enhanced cholesterol efflux with increased incident cardiovascular risks*. *Arterioscler Thromb Vasc Biol*, 2013. **33**(7): p. 1696-705.

189. Kontush, A. and M.J. Chapman, *Functionally defective HDL: A new therapeutic target at the crossroads of dyslipidemia, inflammation and atherosclerosis*. *Pharmacol. Rev.*, 2006. **3**(58): p. 342-374.
190. von Eckardstein, A., *Differential diagnosis of familial high density lipoprotein deficiency syndromes*. *Atherosclerosis*, 2006. **186**(2): p. 231-9.
191. Chiesa, G. and C.R. Sirtori, *Apolipoprotein A-I Milano: current perspectives*. *Curr Opin Lipidol*, 2003. **14**(2): p. 159-63.
192. Oram, J.F. and A.M. Vaughan, *ATP-Binding cassette cholesterol transporters and cardiovascular disease*. *Circ Res*, 2006. **99**(10): p. 1031-43.
193. Ossoli, A., et al., *Role of LCAT in Atherosclerosis*. *Journal of Atherosclerosis and Thrombosis*, 2016. **23**(2): p. 119-127.
194. Oldoni, F., et al., *Complete and Partial Lecithin:Cholesterol Acyltransferase Deficiency Is Differentially Associated With Atherosclerosis*. *Circulation*, 2018. **138**(10): p. 1000-1007.
195. Weissglas-Volkov, D. and P. Pajukanta, *Genetic causes of high and low serum HDL-cholesterol*. *J Lipid Res*, 2010. **51**(8): p. 2032-57.
196. Lamarche, B., S. Rashid, and G.F. Lewis, *HDL metabolism in hypertriglyceridemic states: an overview*. *Clin Chim Acta*, 1999. **286**(1-2): p. 145-61.
197. Thompson, J.F., et al., *High-density genotyping and functional SNP localization in the CETP gene*. *J. Lipid Res.*, 2007. **48**(2): p. 434-443.
198. Khovidhunkit, W., et al., *Effects of infection and inflammation on lipid and lipoprotein metabolism: mechanisms and consequences to the host*. *J Lipid Res*, 2004. **45**(7): p. 1169-96.
199. Rohatgi, A., et al., *HDL cholesterol efflux capacity and incident cardiovascular events*. *N Engl J Med*, 2014. **371**(25): p. 2383-93.
200. Kontush, A. and M.J. Chapman, *Antiatherogenic function of HDL particle subpopulations: focus on antioxidative activities*. *Curr Opin Lipidol*, 2010. **21**: p. 312-318.
201. Kontush, A. and M.J. Chapman, *High-Density Lipoproteins: Structure, Metabolism, Function and Therapeutics*. 2012, New York: Wiley & Sons. 648.
202. Gordon, S.M., et al., *High density lipoprotein proteome is associated with cardiovascular risk factors and atherosclerosis burden as evaluated by coronary CT angiography*. *Atherosclerosis*, 2018. **278**: p. 278-285.
203. Van Lenten, B.J., et al., *Anti-inflammatory HDL becomes pro-inflammatory during the acute phase response. Loss of protective effect of HDL against LDL oxidation in aortic wall cell cocultures*. *J Clin Invest*, 1995. **96**(6): p. 2758-67.
204. Dobiasova, M., *Lecithin: cholesterol acyltransferase and the regulation of endogenous cholesterol transport*. *Adv Lipid Res*, 1983. **20**: p. 107-94.
205. Harada, L.M., et al., *Lipoprotein desialylation simultaneously enhances the cell cholesterol uptake and impairs the reverse cholesterol transport system: in vitro evidences utilizing neuraminidase-treated lipoproteins and mouse peritoneal macrophages*. *Atherosclerosis*, 1998. **139**(1): p. 65-75.
206. Marmillot, P., et al., *Desialylation of human apolipoprotein E decreases its binding to human high-density lipoprotein and its ability to deliver esterified cholesterol to the liver*. *Metabolism*, 1999. **48**(9): p. 1184-92.
207. Savinova, O.V., et al., *Reduced apolipoprotein glycosylation in patients with the metabolic syndrome*. *PLoS One*, 2014. **9**(8): p. e104833.
208. Barter, P.J., et al., *Effects of torcetrapib in patients at high risk for coronary events*. *N Engl J Med*, 2007. **357**(21): p. 2109-22.
209. Connelly, M.A., et al., *Torcetrapib produces endothelial dysfunction independent of cholesterol ester transfer protein inhibition*. *J Cardiovasc Pharmacol*, 2010. **55**(5): p. 459-68.

210. Schwartz, G.G., et al., *Effects of dalcetrapib in patients with a recent acute coronary syndrome*. N Engl J Med, 2012. **367**(22): p. 2089-99.
211. Lincoff, A.M., et al., *Evacetrapib and Cardiovascular Outcomes in High-Risk Vascular Disease*. N Engl J Med, 2017. **376**(20): p. 1933-1942.
212. Group, H.T.R.C., et al., *Effects of Anacetrapib in Patients with Atherosclerotic Vascular Disease*. N Engl J Med, 2017. **377**(13): p. 1217-1227.
213. Armitage, J., M.V. Holmes, and D. Preiss, *Cholesteryl Ester Transfer Protein Inhibition for Preventing Cardiovascular Events JACC Review Topic of the Week*. Journal of the American College of Cardiology, 2019. **73**(4): p. 477-487.
214. Nissen, S.E., et al., *Effect of recombinant ApoA-I Milano on coronary atherosclerosis in patients with acute coronary syndromes: a randomized controlled trial*. Jama, 2003. **290**(17): p. 2292-300.
215. Reijers, J.A.A., et al., *MDCO-216 Does Not Induce Adverse Immunostimulation, in Contrast to Its Predecessor ETC-216*. Cardiovasc Drugs Ther, 2017. **31**(4): p. 381-389.
216. Kempen, H.J., et al., *Incubation of MDCO-216 (ApoA-IMilano/POPC) with Human Serum Potentiates ABCA1-Mediated Cholesterol Efflux Capacity, Generates New Prebeta-1 HDL, and Causes an Increase in HDL Size*. J Lipids, 2014. **2014**: p. 923903.
217. Nicholls, S.J., et al., *Effect of Infusion of High-Density Lipoprotein Mimetic Containing Recombinant Apolipoprotein A-I Milano on Coronary Disease in Patients With an Acute Coronary Syndrome in the MILANO-PILOT Trial A Randomized Clinical Trial*. Jama Cardiology, 2018. **3**(9): p. 806-814.
218. Tardif, J.C., et al., *Effects of reconstituted high-density lipoprotein infusions on coronary atherosclerosis: a randomized controlled trial*. Jama, 2007. **297**(15): p. 1675-82.
219. Michael Gibson, C., et al., *Safety and Tolerability of CSL112, a Reconstituted, Infusible, Plasma-Derived Apolipoprotein A-I, After Acute Myocardial Infarction: The AEGIS-I Trial (ApoA-I Event Reducing in Ischemic Syndromes I)*. Circulation, 2016. **134**(24): p. 1918-1930.
220. Didichenko, S.A., et al., *Enhanced HDL Functionality in Small HDL Species Produced Upon Remodeling of HDL by Reconstituted HDL, CSL112: Effects on Cholesterol Efflux, Anti-Inflammatory and Antioxidative Activity*. Circ Res, 2016.
221. Kootte, R.S., et al., *Effect of open-label infusion of an apoA-I-containing particle (CER-001) on RCT and artery wall thickness in patients with FHA*. J Lipid Res, 2015. **56**(3): p. 703-12.
222. Kataoka, Y., et al., *Regression of coronary atherosclerosis with infusions of the high-density lipoprotein mimetic CER-001 in patients with more extensive plaque burden*. Cardiovascular Diagnosis and Therapy, 2017. **7**(3): p. 252-263.
223. Tardif, J.C., et al., *Effects of the high-density lipoprotein mimetic agent CER-001 on coronary atherosclerosis in patients with acute coronary syndromes: a randomized trial*. Eur Heart J, 2014. **35**(46): p. 3277-86.
224. Nicholls, S.J., et al., *Effect of Serial Infusions of CER-001, a Pre-beta High-Density Lipoprotein Mimetic, on Coronary Atherosclerosis in Patients Following Acute Coronary Syndromes in the CER-001 Atherosclerosis Regression Acute Coronary Syndrome Trial A Randomized Clinical Trial*. Jama Cardiology, 2018. **3**(9): p. 815-822.
225. Waksman, R., et al., *A first-in-man, randomized, placebo-controlled study to evaluate the safety and feasibility of autologous delipidated high-density lipoprotein plasma infusions in patients with acute coronary syndrome*. J Am Coll Cardiol, 2010. **55**(24): p. 2727-35.
226. Navab, M., et al., *Structure and function of HDL mimetics*. Arterioscler Thromb Vasc Biol, 2010. **30**(2): p. 164-8.
227. Bloedon, L.T., et al., *Safety, pharmacokinetics, and pharmacodynamics of oral apoA-I mimetic peptide D-4F in high-risk cardiovascular patients*. J. Lipid Res., 2008. **49**(6): p. 1344-1352.

228. Ditiatkovski, M., et al., *Apolipoprotein A-I Mimetic Peptides: Discordance Between In Vitro and In Vivo Properties-Brief Report*. *Arterioscler Thromb Vasc Biol*, 2017. **37**(7): p. 1301-1306.
229. Shamburek, R.D., et al., *Safety and Tolerability of ACP-501, a Recombinant Human Lecithin:Cholesterol Acyltransferase, in a Phase 1 Single-Dose Escalation Study*. *Circ Res*, 2016. **118**(1): p. 73-82.
230. Graham, M.J., et al., *Antisense oligonucleotide inhibition of apolipoprotein C-III reduces plasma triglycerides in rodents, nonhuman primates, and humans*. *Circ Res*, 2013. **112**(11): p. 1479-90.
231. Yang, X.H., et al., *Reduction in lipoprotein-associated apoC-III levels following volanesorsen therapy: phase 2 randomized trial results*. *Journal of Lipid Research*, 2016. **57**(4): p. 706-713.
232. Chapman, M.J., et al., *Niacin and fibrates in atherogenic dyslipidemia: pharmacotherapy to reduce cardiovascular risk*. *Pharmacol Ther*, 2010. **126**(3): p. 314-45.
233. Millan, J., et al., *Fibrates in the secondary prevention of cardiovascular disease (infarction and stroke). Results of a systematic review and meta-analysis of the Cochrane collaboration*. *Clinica E Investigacion En Arteriosclerosis*, 2018. **30**(1): p. 30-35.
234. Araki, E., et al., *Effects of Pemafibrate, a Novel Selective PPAR alpha Modulator, on Lipid and Glucose Metabolism in Patients With Type 2 Diabetes and Hypertriglyceridemia: A Randomized, Double-Blind, Placebo-Controlled, Phase 3 Trial*. *Diabetes Care*, 2018. **41**(3): p. 538-546.
235. Scott, L.J., *Alipogene tiparvovec: a review of its use in adults with familial lipoprotein lipase deficiency*. *Drugs*, 2015. **75**(2): p. 175-82.
236. Boden, W.E., et al., *Niacin in patients with low HDL cholesterol levels receiving intensive statin therapy*. *N Engl J Med*, 2011. **365**(24): p. 2255-67.
237. Group, H.T.C., et al., *Effects of extended-release niacin with laropiprant in high-risk patients*. *N Engl J Med*, 2014. **371**(3): p. 203-12.
238. Schandelmaier, S., et al., *Niacin for primary and secondary prevention of cardiovascular events*. *Cochrane Database of Systematic Reviews*, 2017(6).
239. Keene, D., et al., *Effect on cardiovascular risk of high density lipoprotein targeted drug treatments niacin, fibrates, and CETP inhibitors: meta-analysis of randomised controlled trials including 117,411 patients*. *Bmj*, 2014. **349**: p. g4379.
240. Nicholls, S.J., et al., *Efficacy and safety of a novel oral inducer of apolipoprotein a-I synthesis in statin-treated patients with stable coronary artery disease a randomized controlled trial*. *J Am Coll Cardiol*, 2011. **57**(9): p. 1111-9.
241. Nicholls, S.J., et al., *Effect of the BET Protein Inhibitor, RVX-208, on Progression of Coronary Atherosclerosis: Results of the Phase 2b, Randomized, Double-Blind, Multicenter, ASSURE Trial*. *Am J Cardiovasc Drugs*, 2016. **16**(1): p. 55-65.
242. Shishikura, D., et al., *The Effect of Bromodomain and Extra-Terminal Inhibitor Apabetalone on Attenuated Coronary Atherosclerotic Plaque: Insights from the ASSURE Trial*. *American Journal of Cardiovascular Drugs*, 2019. **19**(1): p. 49-57.
243. Nicholls, S.J., et al., *Selective BET Protein Inhibition with Apabetalone and Cardiovascular Events: A Pooled Analysis of Trials in Patients with Coronary Artery Disease*. *American Journal of Cardiovascular Drugs*, 2018. **18**(2): p. 109-115.
244. Nomiyama, T. and D. Bruemmer, *Liver X receptors as therapeutic targets in metabolism and atherosclerosis*. *Curr Atheroscler Rep*, 2008. **10**(1): p. 88-95.
245. Katz, A., et al., *Safety, pharmacokinetics, and pharmacodynamics of single doses of LXR-623, a novel liver X-receptor agonist, in healthy participants*. *J Clin Pharmacol*, 2009. **49**(6): p. 643-9.
246. Yonezawa, S., et al., *Each liver X receptor (LXR) type has a different purpose in different situations*. *Biochemical and Biophysical Research Communications*, 2019. **508**(1): p. 92-96.
247. Najafi-Shoushtari, S.H., et al., *MicroRNA-33 and the SREBP host genes cooperate to control cholesterol homeostasis*. *Science*, 2010. **328**(5985): p. 1566-9.

248. Rayner, K.J., et al., *MiR-33 contributes to the regulation of cholesterol homeostasis*. Science, 2010. **328**(5985): p. 1570-3.
249. Diffenderfer, M.R. and E.J. Schaefer, *The composition and metabolism of large and small LDL*. Curr Opin Lipidol, 2014. **25**(3): p. 221-6.
250. Wiesner, P., et al., *Lipid profiling of FPLC-separated lipoprotein fractions by electrospray ionization tandem mass spectrometry*. J Lipid Res, 2009. **50**(3): p. 574-85.
251. Vauhkonen, M., et al., *High-mannose structure of apolipoprotein-B from low-density lipoproteins of human plasma*. Eur J Biochem, 1985. **152**(1): p. 43-50.
252. Tertov, V.V., et al., *Carbohydrate composition of protein and lipid components in sialic acid-rich and -poor low density lipoproteins from subjects with and without coronary artery disease*. J Lipid Res, 1993. **34**(3): p. 365-75.
253. Swaminathan, N. and F. Aladjem, *The monosaccharide composition and sequence of the carbohydrate moiety of human serum low density lipoproteins*. Biochemistry, 1976. **15**(7): p. 1516-22.
254. Khosravi, M., R. Hosseini-Fard, and M. Najafi, *Circulating low density lipoprotein (LDL)*. Horm Mol Biol Clin Investig, 2018. **35**(2).
255. Packard, C.J., et al., *Apolipoprotein B metabolism and the distribution of VLDL and LDL subfractions*. J Lipid Res, 2000. **41**(2): p. 305-18.
256. Aguilar-Salinas, C.A., et al., *A Familial Combined Hyperlipidemic Kindred With Impaired Apolipoprotein B Catabolism*. Arteriosclerosis, Thrombosis, and Vascular Biology, 1997. **17**(1): p. 72-82.
257. Geiss, H.C., et al., *In vivo metabolism of LDL subfractions in patients with heterozygous FH on statin therapy: rebound analysis of LDL subfractions after LDL apheresis*. Journal of Lipid Research, 2004. **45**(8): p. 1459-1467.
258. Zheng, C., et al., *Apolipoprotein C-III and the metabolic basis for hypertriglyceridemia and the dense low-density lipoprotein phenotype*. Circulation, 2010. **121**(15): p. 1722-34.
259. Bouhairie, V.E. and A.C. Goldberg, *Familial hypercholesterolemia*. Cardiology clinics, 2015. **33**(2): p. 169-179.
260. Davidsson, P., et al., *A proteomic study of the apolipoproteins in LDL subclasses in patients with the metabolic syndrome and type 2 diabetes*. J Lipid Res, 2005. **46**(9): p. 1999-2006.
261. Orekhov, A.N., et al., *Modified Low Density Lipoprotein and Lipoprotein-Containing Circulating Immune Complexes as Diagnostic and Prognostic Biomarkers of Atherosclerosis and Type 1 Diabetes Macrovascular Disease*. International Journal of Molecular Sciences, 2014. **15**(7): p. 12807-12841.
262. Orekhov, A.N., et al., *Modification of low density lipoprotein by desialylation causes lipid accumulation in cultured cells: discovery of desialylated lipoprotein with altered cellular metabolism in the blood of atherosclerotic patients*. Biochem Biophys Res Commun, 1989. **162**(1): p. 206-11.
263. Sobenin, I.A., et al., *Modified low density lipoprotein from diabetic patients causes cholesterol accumulation in human intimal aortic cells*. Atherosclerosis, 1993. **100**(1): p. 41-54.
264. Tertov, V.V., et al., *Isolation of atherogenic modified (desialylated) low density lipoprotein from blood of atherosclerotic patients: separation from native lipoprotein by affinity chromatography*. Biochem Biophys Res Commun, 1990. **167**(3): p. 1122-7.
265. Orekhov, A.N., et al., *Sialic acid content of human low density lipoproteins affects their interaction with cell receptors and intracellular lipid accumulation*. J Lipid Res, 1992. **33**(6): p. 805-17.
266. Tertov, V.V., et al., *Characteristics of low density lipoprotein isolated from circulating immune complexes*. Atherosclerosis, 1996. **122**(2): p. 191-9.

267. Orekhov, A.N., V.V. Tertov, and D.N. Mukhin, *Desialylated low density lipoprotein--naturally occurring modified lipoprotein with atherogenic potency*. *Atherosclerosis*, 1991. **86**(2-3): p. 153-61.
268. Tertov, V.V., et al., *Lipoprotein aggregation as an essential condition of intracellular lipid accumulation caused by modified low density lipoproteins*. *Biochem Biophys Res Commun*, 1989. **163**(1): p. 489-94.
269. Bartlett, A.L., et al., *Role of the macrophage galactose lectin in the uptake of desialylated LDL*. *Atherosclerosis*, 2000. **153**(1): p. 219-30.
270. Hunt, J.V., et al., *Glucose oxidation and low-density lipoprotein-induced macrophage ceroid accumulation: possible implications for diabetic atherosclerosis*. *Biochemical Journal*, 1994. **300**(Pt 1): p. 243-249.
271. Brown, B.E., et al., *Glycation of low-density lipoprotein results in the time-dependent accumulation of cholesteryl esters and apolipoprotein B-100 protein in primary human monocyte-derived macrophages*. *Febs j*, 2007. **274**(6): p. 1530-41.
272. Chisolm, G.M. and D. Steinberg, *The oxidative modification hypothesis of atherogenesis: an overview*. *Free Radic Biol Med*, 2000. **28**(12): p. 1815-26.
273. Orekhov, A.N., V.V. Tertov, and D.N. Mukhin, *Desialylated low density lipoprotein - naturally occurring modified lipoprotein with atherogenic potency*. *Atherosclerosis*, 1991. **86**(2): p. 153-161.
274. Grewal, T., et al., *Desialylated LDL uptake in human and mouse macrophages can be mediated by a lectin receptor*. *Atherosclerosis*, 1996. **121**(1): p. 151-63.
275. Oesterle, A., U. Laufs, and J.K. Liao, *Pleiotropic Effects of Statins on the Cardiovascular System*. *Circulation research*, 2017. **120**(1): p. 229-243.
276. Mager, D.R., *Statins: The Good, the Bad, and the Unexpected*. *Home Healthc Now*, 2016. **34**(7): p. 388-93.
277. Ferreira, A.M. and P. Marques da Silva, *Defining the Place of Ezetimibe/Atorvastatin in the Management of Hyperlipidemia*. *Am J Cardiovasc Drugs*, 2017. **17**(3): p. 169-181.
278. Karatasakis, A., et al., *Effect of PCSK9 Inhibitors on Clinical Outcomes in Patients With Hypercholesterolemia: A Meta-Analysis of 35 Randomized Controlled Trials*. *J Am Heart Assoc*, 2017. **6**(12).
279. Rached, F., et al., *Defective functionality of HDL particles in familial apoA-I deficiency: relevance of alterations in HDL lipidome and proteome*. *Journal of Lipid Research*, 2014. **55**(12): p. 2509-2520.
280. Hamm, C.W. and E. Braunwald, *A classification of unstable angina revisited*. *Circulation*, 2000. **102**(1): p. 118-22.
281. Rumsey, S.C., et al., *Human plasma LDL cryopreserved with sucrose maintains in vivo kinetics indistinguishable from freshly isolated human LDL in cynomolgus monkeys*. *J Lipid Res*, 1994. **35**(9): p. 1592-8.
282. Lefevre, G., et al., *Effect of sucrose/ -80 degrees C storage of plasma on between-site values of low-density lipoprotein susceptibility to copper-induced oxidation*. *GERBAP Section Lipoproteines. Groupe d'Evaluation et de Recherche des Biologistes de l'Assistance Publique*. *Clin Chim Acta*, 1997. **258**(2): p. 249-55.
283. Guérin, M., et al., *Fenofibrate Reduces Plasma Cholesteryl Ester Transfer From HDL to VLDL and Normalizes the Atherogenic, Dense LDL Profile in Combined Hyperlipidemia*. *Arteriosclerosis, Thrombosis, and Vascular Biology*, 1996. **16**(6): p. 763-772.
284. Chapman, M.J., et al., *A density gradient ultracentrifugal procedure for the isolation of the major lipoprotein classes from human serum*. *J Lipid Res*, 1981. **22**(2): p. 339-58.

285. Chapman, M.J., et al., *A density gradient ultracentrifugal procedure for the isolation of the major lipoprotein classes from human serum*. J Lipid Res., 1981. **22**(2): p. 339-358.
286. Guerin, M., et al., *Atorvastatin reduces postprandial accumulation and cholesteryl ester transfer protein-mediated remodeling of triglyceride-rich lipoprotein subspecies in type IIb hyperlipidemia*. J Clin Endocrinol Metab, 2002. **87**(11): p. 4991-5000.
287. Kontush, A., et al., *Antioxidative activity of HDL particle subspecies is impaired in hyperalphalipoproteinemia: relevance of enzymatic and physicochemical properties*. Arterioscler Thromb Vasc Biol, 2004. **24**(3): p. 526-33.
288. Larijani, B., D.L. Poccia, and L.C. Dickinson, *Phospholipid identification and quantification of membrane vesicle subfractions by ³¹P-1H two-dimensional nuclear magnetic resonance*. Lipids, 2000. **35**(11): p. 1289-1297.
289. Quehenberger, O., et al., *Lipidomics reveals a remarkable diversity of lipids in human plasma*. Journal of Lipid Research, 2010. **51**(11): p. 3299-3305.
290. Quehenberger, O. and E.A. Dennis, *The Human Plasma Lipidome*. New England Journal of Medicine, 2011. **365**(19): p. 1812-1823.
291. Kontush, A., et al., *Preferential sphingosine-1-phosphate enrichment and sphingomyelin depletion are key features of small dense HDL3 particles: relevance to antiapoptotic and antioxidative activities*. Arterioscler Thromb Vasc Biol, 2007. **27**(8): p. 1843-9.
292. Akmacic, I.T., et al., *High-throughput glycomics: optimization of sample preparation*. Biochemistry (Mosc), 2015. **80**(7): p. 934-42.
293. Reiding, K.R., et al., *High-Throughput Profiling of Protein N-Glycosylation by MALDI-TOF-MS Employing Linkage-Specific Sialic Acid Esterification*. Analytical Chemistry, 2014. **86**(12): p. 5784-5793.
294. Larrede, S., et al., *Stimulation of cholesterol efflux by LXR agonists in cholesterol-loaded human macrophages is ABCA1-dependent but ABCG1-independent*. Arterioscler Thromb Vasc Biol, 2009. **29**(11): p. 1930-6.
295. Fournier, N., et al., *Analysis of the relationship between triglyceridemia and HDL-phospholipid concentrations: consequences on the efflux capacity of serum in the Fu5AH system*. Atherosclerosis, 2001. **157**(2): p. 315-23.
296. Kontush, A., S. Chantepie, and M.J. Chapman, *Small, Dense HDL Particles Exert Potent Protection of Atherogenic LDL Against Oxidative Stress*. Arteriosclerosis, Thrombosis, and Vascular Biology, 2003. **23**(10): p. 1881-1888.
297. Nobecourt, E., et al., *Defective antioxidative activity of small dense HDL3 particles in type 2 diabetes: relationship to elevated oxidative stress and hyperglycaemia*. Diabetologia, 2005. **48**(3): p. 529-38.
298. Hansel, B., A. Kontush, and M.T. Twickler, *High-density lipoprotein as a key component in the prevention of premature atherosclerotic disease in the insulin resistance syndrome*. Semin Vasc Med, 2004. **4**(2): p. 215-23.
299. Stocker, R., *Lipoprotein oxidation: mechanistic aspects, methodological approaches and clinical relevance*. Curr Opin Lipidol, 1994. **5**(6): p. 422-33.
300. Abbott, C.A., et al., *Serum paraoxonase activity, concentration, and phenotype distribution in diabetes mellitus and its relationship to serum lipids and lipoproteins*. Arterioscler Thromb Vasc Biol, 1995. **15**(11): p. 1812-8.
301. Nofer, J.-R., et al., *Suppression of Endothelial Cell Apoptosis by High Density Lipoproteins (HDL) and HDL-associated Lysosphingolipids*. Journal of Biological Chemistry, 2001. **276**(37): p. 34480-34485.
302. Jourdan, F., et al., *Use of reconstituted metabolic networks to assist in metabolomic data visualization and mining*. Metabolomics, 2010. **6**(2): p. 312-321.

303. Kanehisa, M., et al., *Data, information, knowledge and principle: back to metabolism in KEGG*. Nucleic Acids Res, 2014. **42**(Database issue): p. D199-205.
304. Xia, J. and D.S. Wishart, *Using MetaboAnalyst 3.0 for Comprehensive Metabolomics Data Analysis*, in *Current Protocols in Bioinformatics*. 2002, John Wiley & Sons, Inc.
305. Goeman, J.J., et al., *A global test for groups of genes: testing association with a clinical outcome*. Bioinformatics, 2004. **20**(1): p. 93-9.
306. Hummel, M., R. Meister, and U. Mansmann, *GlobalANCOVA: exploration and assessment of gene group effects*. Bioinformatics, 2008. **24**(1): p. 78-85.
307. Kontush, A. and M.J. Chapman, *High-density lipoproteins*. Hoboken, NJ: John Wiley & Sons, 2012.
308. Jaspard, B., et al., *Biochemical characterization of pre-beta 1 high-density lipoprotein from human ovarian follicular fluid: evidence for the presence of a lipid core*. Biochemistry, 1996. **35**(5): p. 1352-7.
309. Hamon, Y., et al., *ABC1 promotes engulfment of apoptotic cells and transbilayer redistribution of phosphatidylserine*. Nat Cell Biol, 2000. **2**(7): p. 399-406.
310. Rodriguez, W.V., et al., *Mechanism of scavenger receptor class B type I-mediated selective uptake of cholesteryl esters from high density lipoprotein to adrenal cells*. J Biol Chem, 1999. **274**(29): p. 20344-50.
311. Jang, J.H., et al., *Understanding of the roles of phospholipase D and phosphatidic acid through their binding partners*. Prog Lipid Res, 2012. **51**(2): p. 71-81.
312. Davidson, W.S., et al., *Proteomic analysis of defined HDL subpopulations reveals particle-specific protein clusters: relevance to antioxidative function*. Arterioscler Thromb Vasc Biol, 2009. **29**(6): p. 870-6.
313. Wan, G., et al., *Apolipoprotein L1, a novel Bcl-2 homology domain 3-only lipid-binding protein, induces autophagic cell death*. J Biol Chem, 2008. **283**(31): p. 21540-9.
314. Duong, P.T., et al., *Characterization of nascent HDL particles and microparticles formed by ABCA1-mediated efflux of cellular lipids to apoA-I*. J Lipid Res, 2006. **47**(4): p. 832-43.
315. Favari, E., et al., *Small discoidal pre-beta1 HDL particles are efficient acceptors of cell cholesterol via ABCA1 and ABCG1*. Biochemistry, 2009. **48**(46): p. 11067-74.
316. Du, X.M., et al., *HDL particle size is a critical determinant of ABCA1-mediated macrophage cellular cholesterol export*. Circ Res, 2015. **116**(7): p. 1133-42.
317. de Souza, J.A., et al., *Small, dense HDL 3 particles attenuate apoptosis in endothelial cells: pivotal role of apolipoprotein A-I*. J Cell Mol Med, 2010. **14**(3): p. 608-20.
318. Zhao, Y., D.L. Sparks, and Y.L. Marcel, *Effect of the apolipoprotein A-I and surface lipid composition of reconstituted discoidal HDL on cholesterol efflux from cultured fibroblasts*. Biochemistry, 1996. **35**(51): p. 16510-8.
319. Hara, S., et al., *Lysophosphatidylcholine promotes cholesterol efflux from mouse macrophage foam cells*. Arterioscler Thromb Vasc Biol, 1997. **17**(7): p. 1258-66.
320. Rosenblat, M., et al., *Paraoxonase 1 (PON1) enhances HDL-mediated macrophage cholesterol efflux via the ABCA1 transporter in association with increased HDL binding to the cells: a possible role for lysophosphatidylcholine*. Atherosclerosis, 2005. **179**(1): p. 69-77.
321. Aslanian, A.M. and I.F. Charo, *Targeted disruption of the scavenger receptor and chemokine CXCL16 accelerates atherosclerosis*. Circulation, 2006. **114**(6): p. 583-90.
322. Yancey, P.G., et al., *In vivo modulation of HDL phospholipid has opposing effects on SR-BI- and ABCA1-mediated cholesterol efflux*. J Lipid Res, 2004. **45**(2): p. 337-46.
323. Haidar, B., et al., *Cellular cholesterol efflux is modulated by phospholipid-derived signaling molecules in familial HDL deficiency/Tangier disease fibroblasts*. J Lipid Res, 2001. **42**(2): p. 249-57.

324. Marmillot, P., S. Patel, and M.R. Lakshman, *Reverse cholesterol transport is regulated by varying fatty acyl chain saturation and sphingomyelin content in reconstituted high-density lipoproteins*. *Metabolism*, 2007. **56**(2): p. 251-9.
325. Kimura, T., et al., *Sphingosine 1-phosphate may be a major component of plasma lipoproteins responsible for the cytoprotective actions in human umbilical vein endothelial cells*. *J Biol Chem*, 2001. **276**(34): p. 31780-5.
326. Nofer, J.R. and G. Assmann, *Atheroprotective effects of high-density lipoprotein-associated lysosphingolipids*. *Trends Cardiovasc Med*, 2005. **15**(7): p. 265-71.
327. de Souza, J.A., et al., *Metabolic syndrome features small, apolipoprotein A-I-poor, triglyceride-rich HDL3 particles with defective anti-apoptotic activity*. *Atherosclerosis*, 2008. **197**(1): p. 84-94.
328. Taha, T.A., T.D. Mullen, and L.M. Obeid, *A house divided: ceramide, sphingosine, and sphingosine-1-phosphate in programmed cell death*. *Biochim Biophys Acta*, 2006. **1758**(12): p. 2027-36.
329. Dang, V.T., et al., *Comprehensive Plasma Metabolomic Analyses of Atherosclerotic Progression Reveal Alterations in Glycerophospholipid and Sphingolipid Metabolism in Apolipoprotein E-deficient Mice*. *Sci Rep*, 2016. **6**: p. 35037.
330. Bochkov, V.N., et al., *Generation and biological activities of oxidized phospholipids*. *Antioxid Redox Signal*, 2010. **12**(8): p. 1009-59.
331. Stachowska, E., et al., *Conjugated linoleic acid isomers may diminish human macrophages adhesion to endothelial surface*. *Int J Food Sci Nutr*, 2012. **63**(1): p. 30-5.
332. Song, Y., et al., *Polyunsaturated fatty acid relatively decreases cholesterol content in THP-1 macrophage-derived foam cell: partly correlates with expression profile of CIDE and PAT members*. *Lipids Health Dis*, 2013. **12**: p. 111.
333. Sato, M., et al., *Linoleic acid-rich fats reduce atherosclerosis development beyond its oxidative and inflammatory stress-increasing effect in apolipoprotein E-deficient mice in comparison with saturated fatty acid-rich fats*. *Br J Nutr*, 2005. **94**(6): p. 896-901.
334. Lykidis, A., et al., *The role of CDP-diacylglycerol synthetase and phosphatidylinositol synthase activity levels in the regulation of cellular phosphatidylinositol content*. *J Biol Chem*, 1997. **272**(52): p. 33402-9.
335. Malinina, L., et al., *Sphingolipid transfer proteins defined by the GLTP-fold*. *Q Rev Biophys*, 2015. **48**(3): p. 281-322.
336. Kurano, M., et al., *Genome-wide association study of serum lipids confirms previously reported associations as well as new associations of common SNPs within PCSK7 gene with triglyceride*. *J Hum Genet*, 2016. **61**(5): p. 427-33.
337. Lee, E.Y., et al., *HDL Deficiency due to a New Insertion Mutation (ApoA-I(Nashua)) and Review of the Literature*. *Journal of clinical lipidology*, 2013. **7**(2): p. 169-173.
338. MURAYAMA, N., et al., *Effects of plasma infusion on plasma lipids, apoproteins and plasma enzyme activities in familial lecithin: cholesterol acyltransferase deficiency*. *European Journal of Clinical Investigation*, 1984. **14**(2): p. 122-129.
339. Shamburek, R.D., et al., *Familial lecithin:cholesterol acyltransferase deficiency: First-in-human treatment with enzyme replacement*. *Journal of clinical lipidology*, 2016. **10**(2): p. 356-367.
340. Hafiane, A., et al., *High-density lipoprotein mediated cellular cholesterol efflux in acute coronary syndromes*. *Am J Cardiol*, 2014. **113**(2): p. 249-55.
341. Quehenberger, O. and E.A. Dennis, *The human plasma lipidome*. *N Engl J Med*, 2011. **365**(19): p. 1812-23.
342. Bounafaa, A., et al., *Alteration of HDL functionality and PON1 activities in acute coronary syndrome patients*. *Clin Biochem*, 2014. **47**(18): p. 318-25.

343. Riwanto, M., et al., *Altered activation of endothelial anti- and proapoptotic pathways by high-density lipoprotein from patients with coronary artery disease: role of high-density lipoprotein-proteome remodeling*. *Circulation*, 2013. **127**(8): p. 891-904.
344. Lindbohm, N., H. Gylling, and T.A. Miettinen, *Sialic acid content of low density lipoprotein and its relation to lipid concentrations and metabolism of low density lipoprotein and cholesterol*. *J Lipid Res*, 2000. **41**(7): p. 1110-7.
345. Ruhaak, L.R., et al., *Hydrophilic interaction chromatography-based high-throughput sample preparation method for N-glycan analysis from total human plasma glycoproteins*. *Anal Chem*, 2008. **80**(15): p. 6119-26.
346. Vaisar, T., *Proteomics investigations of HDL: challenges and promise*. *Curr Vasc Pharmacol*, 2012. **10**(4): p. 410-21.
347. Vauhkonen, M., et al., *High-mannose structure of apolipoprotein-B from low-density lipoproteins of human plasma*. *European Journal of Biochemistry*, 1985. **152**(1): p. 43-50.
348. Varki, A., *Sialic acids in human health and disease*. *Trends Mol Med*, 2008. **14**(8): p. 351-60.
349. Schauer, R., *Sialic acids as regulators of molecular and cellular interactions*. *Curr Opin Struct Biol*, 2009. **19**(5): p. 507-14.
350. Lehmann, F., E. Tiralongo, and J. Tiralongo, *Sialic acid-specific lectins: occurrence, specificity and function*. *Cell Mol Life Sci*, 2006. **63**(12): p. 1331-54.
351. Weigel, P.H. and J.H. Yik, *Glycans as endocytosis signals: the cases of the asialoglycoprotein and hyaluronan/chondroitin sulfate receptors*. *Biochim Biophys Acta*, 2002. **1572**(2-3): p. 341-63.
352. Lindberg, G., et al., *Serum sialic acid concentration and cardiovascular mortality*. *Bmj*, 1991. **302**(6769): p. 143-6.
353. Yokoyama, H., et al., *Serum sialic acid concentration is elevated in IDDM especially in early diabetic nephropathy*. *J Intern Med*, 1995. **237**(5): p. 519-23.
354. Keser, T., et al., *Increased plasma N-glycome complexity is associated with higher risk of type 2 diabetes*. *Diabetologia*, 2017. **60**(12): p. 2352-2360.
355. Phillips, M.C., *Molecular Mechanisms of Cellular Cholesterol Efflux*. *J Biol Chem*, 2014. **289**(35): p. 24020-9.
356. Murakami, M., et al., *Distinction in the mode of receptor-mediated endocytosis between high density lipoprotein and acetylated high density lipoprotein: evidence for high density lipoprotein receptor-mediated cholesterol transfer*. *J Biochem*, 1987. **101**(3): p. 729-41.
357. La Ville, A.E., et al., *In vitro oxidised HDL is recognised by the scavenger receptor of macrophages: implications for its protective role in vivo*. *Atherosclerosis*. **105**(2): p. 179-189.
358. Boucher, J.G., T. Nguyen, and D.L. Sparks, *Lipoprotein electrostatic properties regulate hepatic lipase association and activity*. *Biochem Cell Biol*, 2007. **85**(6): p. 696-708.
359. Cubedo, J., T. Padro, and L. Badimon, *Glycoproteome of human apolipoprotein A-I: N- and O-glycosylated forms are increased in patients with acute myocardial infarction*. *Transl Res*, 2014. **164**(3): p. 209-22.
360. Orekhov, A.N., et al., *Blood serum atherogenicity associated with coronary atherosclerosis. Evidence for nonlipid factor providing atherogenicity of low-density lipoproteins and an approach to its elimination*. *Circ Res*, 1988. **62**(3): p. 421-9.
361. Tertov, V.V., et al., *Low-density lipoproteins isolated from the blood of patients with coronary heart disease induce the accumulation of lipids in human aortic cells*. *Exp Mol Pathol*, 1989. **50**(3): p. 337-47.
362. Chazov, E.I., et al., *Atherogenicity of blood serum from patients with coronary heart disease*. *Lancet*, 1986. **2**(8507): p. 595-8.
363. Liu, Y. and D. Atkinson, *Enhancing the contrast of ApoB to locate the surface components in the 3D density map of human LDL*. *J Mol Biol*, 2011. **405**(1): p. 274-83.

364. Sanchez-Quesada, J.L., S. Villegas, and J. Ordonez-Llanos, *Electronegative low-density lipoprotein. A link between apolipoprotein B misfolding, lipoprotein aggregation and proteoglycan binding*. *Curr Opin Lipidol*, 2012. **23**(5): p. 479-86.
365. Boyanovsky, B.B., D.R. van der Westhuyzen, and N.R. Webb, *Group V secretory phospholipase A2-modified low density lipoprotein promotes foam cell formation by a SR-A- and CD36-independent process that involves cellular proteoglycans*. *J Biol Chem*, 2005. **280**(38): p. 32746-52.
366. Moore, K.J. and M.W. Freeman, *Scavenger receptors in atherosclerosis: beyond lipid uptake*. *Arterioscler Thromb Vasc Biol*, 2006. **26**(8): p. 1702-11.
367. Tertov, V.V., et al., *Antioxidant content in low density lipoprotein and lipoprotein oxidation in vivo and in vitro*. *Free Radic Res*, 1998. **29**(2): p. 165-73.
368. Kowalska, K., E. Socha, and H. Milnerowicz, *Review: The role of paraoxonase in cardiovascular diseases*. *Ann Clin Lab Sci*, 2015. **45**(2): p. 226-33.